University of Alberta

In Situ Hybridization for Decorin and Transforming Growth Factor-ß1 mRNA in Hypertrophic Scar

by

Karim Nurali Sayani ©

A thesis submitted to the Faculty of Graduate Studies and Research in partial fulfillment
of the requirements for the degree of Master of Science

in

Experimental Surgery

Department of Surgery

Edmonton, Alberta
Fall 1997

National Library
of Canada

Acquisitions and
Bibliographic Services

395 Wellington Street
Ottawa ON K1A 0N4
Canada

Bibliothèque nationale
du Canada

Acquisitions et
services bibliographiques

395, rue Wellington
Ottawa ON K1A 0N4
Canada

Your file Votre référence

Our file Notre référence

The author has granted a non-exclusive licence allowing the National Library of Canada to reproduce, loan, distribute or sell copies of this thesis in microform, paper or electronic formats.

The author retains ownership of the copyright in this thesis. Neither the thesis nor substantial extracts from it may be printed or otherwise reproduced without the author's permission.

L'auteur a accordé une licence non exclusive permettant à la Bibliothèque nationale du Canada de reproduire, prêter, distribuer ou vendre des copies de cette thèse sous la forme de microfiche/film, de reproduction sur papier ou sur format électronique.

L'auteur conserve la propriété du droit d'auteur qui protège cette thèse. Ni la thèse ni des extraits substantiels de celle-ci ne doivent être imprimés ou autrement reproduits sans son autorisation.

0-612-22668-9

Canada

University of Alberta

Library Release Form

Name of Author: Karim Nurali Sayani

Title of Thesis: In Situ Hybridization for Decorin and Transforming Growth Factor-ß1 mRNA in Hypertrophic Scar

Degree: Master of Science

Year this Degree Granted: 1997

Permission is hereby granted to the University of Alberta Library to reproduce single copies of this thesis and to lend or sell such copies for private, scholarly, or scientific research purposes only.

The author reserves all other publication and other rights in association with the copyright in the thesis, and except as hereinbefore provided, neither the thesis nor any substantial portion thereof may be printed or otherwise reproduced in any material form whatever without the author's prior written permission.

#217, 5125 Riverbend Road
Edmonton, Alberta T6H 5K5

September 29, 1997.

University of Alberta

Faculty of Graduate Studies and Research

The undersigned certify that they have read, and recommend to the Faculty of Graduate Studies and Research for acceptance, a thesis entitled In Situ Hybridization for Decorin and Transforming Growth Factor-ß1 mRNA in Hypertrophic Scar submitted by Karim Sayani in partial fulfillment of the requirements for the degree of Master of Science in Experimental Surgery.

Dr. P. G. Scott

Dr. E. E. Tredget

Dr. A. Ghahary

Dr. L. D. Jewell

In the name of Allah, the most beneficent, the most merciful.

Allah is the light of the heavens and the earth.
The parable of His Light is as if there were a niche and within it a lamp; the lamp
enclosed in glass; the glass as it were a brilliant star.
It is lit from a blessed tree,
An olive, neither of the east, nor of the west.
Whose oil is well-nigh luminous, though fire scarce touched it.
Light upon light.
Allah doth guide whom He will to His light.
Allah doth set forth parables for men.
And Allah all things doth know.

The Holy Quran
Surah Nur (24:35)

Praise be to Allah, the maintainer of all beings.

To my beloved father, Nurali Dhanji Sayani

ABSTRACT

Hypertrophic scar (HSc) is a fibroproliferative disorder which occurs after thermal and other injuries which penetrate the dermis. It is characterized by a perturbation in the balance of extracellular matrix components and thus an abnormal composition and organization of the matrix.

The proteoglycan decorin is found abundantly in normal skin and is believed to be necessary for the proper morphology of collagen fibers. Its impact in wound healing may be considerable because of its ability to bind to and neutralize the cytokine transforming growth factor-beta 1 (TGF-ß1). Biochemical and immunohistochemical studies of HSc have shown decorin to be virtually absent.

In contrast, systemic and local levels of TGF-ß1 increase after wounding in patients who develop HSc. TGF-ß1 is an inflammatory and fibrogenic cytokine which upregulates the production of many extracellular matrix components and inhibits the degradation of others. It can also inhibit the production of decorin through a TGF-ß1 negative regulatory element in the promoter of the decorin gene.

The altered amounts of decorin and TGF-ß1 in HSc have not been explained. In this study, therefore, the patterns of expression of decorin and TGF-ß1 mRNAs were investigated in post-burn hypertrophic scar, post-burn mature scar and normal skin by *in situ* hybridization using cRNA probes labeled with digoxigenin-11-UTP.

Decorin mRNA was virtually absent in scars obtained less than 12 months after injury. A significantly higher percentage of cells expressed this mRNA between 12 and 36 months. This level of staining showed a notable reduction in specimens obtained after 36 months. All samples of normal skin studied had a very small percentage of positive cells.

The results of probing for TGF-ß1 were inconclusive due to staining with both sense and antisense probes. Preliminary analysis suggests the existence of an endogenous TGF-ß1 antisense transcript which may play a role in the regulation of this cytokine.

ACKNOWLEDGMENTS

The completion of this work was possible because of the support that I received from my family, colleagues, and friends. Although I will make a sincere attempt to acknowledge all of them, I request, in advance, the forgiveness of those whose names I might have overlooked.

I am grateful to my family for their support throughout my life, especially, during the course of my degree program. Firstly, I would like to recognize my late father, Nurali Sayani, to whom I attribute the origin of my drive and perserverence. I thank my mother, Parin Sayani, for her concern, love, and hard work which have contributed not only to the success in this Masters program but, more importantly, to the survival of our family since my father's demise. I thank my sister, Nashifa Sayani, for her warmth and kind-heartedness and for always being a source of inspiration and good cheer to me.

I am grateful to my dear friend, and now my wife, Almina Pardhan, for believing in me. I would not have survived the many challenges I faced during this program, especially the long months of despair when experiments failed one after the other, had it not been for the unrelenting source of encouragement, advice, and love that I received from Almina. My marriage to her on July 19, 1997 was the start of the happiest era of my life.

I thank my friend Almin Surani for being my comrade, my confidante, and my brother for what has seemed a lifetime. Almin's devout friendship has been a source of immense strength. He has lent me everything from his ear to his apartment whenever I was in need.

I am grateful to Dr. Tredget for allowing me the opportunity to be involved in the research endeavours of the University of Alberta Hospitals Firefighters' Burn Treatment Unit. I thank Dr. Ghahary for initially recognizing my talents and offering me a graduate position; thereafter, I thank him for his kind support. I am especially grateful to Dr. Scott for his patient, analytical, open-minded, and thorough approach to my work and to science in general. Dr. Scott's continuous and perservering belief in my efforts and results paved a prosperous path which otherwise would never have been found.

Ah yes, and the merry accompaniment of my colleagues and friends who I met through my stay in the laboratory but with whom I have made life-long friendships. Without them, my last four years would have been dry and meaningless. Thank you Rajeet Pannu, Bernadette Nedelec, Neda Asadi, Fan Dong, Itaru Mizoguchi, Rijian Wang, Kalal Derhami and Christopher Telasky for intellectual discourse, technical help, humour, and most of all, continued friendships.

Throughout my program, I have received invaluable assistance from three very talented individuals: Carole Dodd, You Jun Shen, and Dennis Carmel. I thank Dennis for his tireless efforts at processing and sectioning all the parrafin-embedded tissues used in this study. I thank You Jun for sharing so willingly her exceptional talents in many areas of molecular biology. And I thank Carole for her daily cooperation and support, company, technical assistance and tolerance of my bizzare and unreliable work schedules. Carole's technical expertise as well as her drive and meticulous work ethic set an example which I hope to follow in the future.

I am especially grateful to the two jewels of the University of Alberta Hospitals Firefighters' Burn Treatment Unit: Heather Shankowsky and Tracey Dean. I consider the contributions of these individuals as vital to the daily operations of this Unit, and more so, to the success of all of the students who come through this Unit. I thank them especially for their tolerance of our 'last-minute' requests, for their continual cooperation and help, and for their smiles.

I thank Karl Fischer for remaining in close contact with me for the last eight years. I have undoubtedly been able to rely on him continually for accurate and thorough theoretical and technical assistance as well as interesting midnight chats outside the doors of the Heritage Medical Research Center.

I am grateful for the friendship, support, and encouragement provided for by the many companions who stood close to me during my program and helped me directly and indirectly with completing my MSc. To list all of these individuals would probably require more pages than the thesis itself. I will only list a few with the hope that anyone I have missed will accept my appreciation, nonetheless. Salima Mulji, Alshad Lalani, Amaan Pardhan, Azhar Pardhan, Zahra Somani, Faizal Hasham, Altaf Kassam, Monica Valsangar, Nadir Hirji and Ezmina Surani.

I am also grateful to my friend Aly Valli for saving my life one day during my program when I choked over dinner. Without Aly's assistance, I definitely would not have reached this moment.

I thank the Ismaili community and faith for providing to me the peace and fortitude which were so vital in maintaining balance in my life.

I thank the Medical Research Council and the University of Alberta Hospitals Firefighters' Burn Treatment Fund for supporting my study.

Above all, I thank Allah.

TABLE OF CONTENTS

Page #

Chapter 1: Literature Review 1

Part 1. Proteoglycan Expression, Regulation and Functional Significance 1

I. Introduction 1

II. Biology 1

A. Protein Cores 1
  1. Large Proteoglycans 2
  2. Small Proteoglycans 4

B. Glycosaminoglycan Chains 5
  1. Chemical Composition 5
  2. Specificity of Attachment to Protein Cores 6
    a) Aggrecan 6
    b) Versican 7
    c) Perlecan 7
    d) Small Proteoglycans 8

C. Molecular Organization

  1. Perlecan 8
  2. Decorin 10

III. Differential Expression - Function and Regulation 11

A. Glycosaminoglycans 11
  1. General 11
  2. Heparan Sulfate 12

B. Aggrecan 12

C. Perlecan 13

D. Syndecans 15

E. Versican 16

F. Small PGs: Decorin, Biglycan, Fibromodulin 18
  1. Differential Expression 18
  2. Interactions with Collagen 19
  3. Interactions with Growth Factors 20
  4. Expression During Fibrosis and Other Disorders 24
    a) Fibrotic Disorders 24
      i) Liver Fibrosis 24
      ii) Hypertrophic Scar 27
    b) Progeria 27
    c) Osteogenesis Imperfecta 28
    d) Colon Carcinoma 29

Part 2. Decorin, TGF-ß1, and Hypertrophic Scar 31

I. Hypertrophic Scar 31

A. The Clinical Problem 31

B. The Architectural Problem/Chemical Imbalance 32

C. Proteoglycan Expression 33

D. Cytokine Expression 34

II. Transforming Growth Factor Beta 1 35

A. Protein Characteristics 35

B. Latent vs. Active TGF-ß 36

C. TGF-ß Receptors 36

D. Distribution and Functions 37

E. Regulation 39

F. Expression in Hypertrophic Scar 44

III. Decorin 44

A. Role in Collagen Assembly/Architecture 44

B. A Sink for Growth Factors 45

C. Regulation of Expression 45

D. Expression in Hypertrophic Scar 48

IV. Thesis Rationale 48

Chapter 2: Methods and Materials 50

A. Tissue Samples 50

B. Cell Cultures 50

C. APTEX Coating Glass Slides 52

D. Controlling Ribonuclease Activity 52

E. Probes 54
  1. Decorin 54
  2. TGF-ß1 55

F. Probe Labeling and Quantitation 56
    1. Labeling 56
    2. Quantitation 58

G. Determining Functionality of Probes 59
    1. Dot Blot Hybridization 59

H. In Situ Hybridization 59
    1. Protocol #1 60
    2. Protocol #2 62
    3. Protocol #3 63
    4. Protocol #4 64
    5. Protocol #5 66

I. Quantitating In Situ Hybridization Results 68

J. RNA Extraction; Probe Preparation; Northern Analysis 68
    1. RNA Extraction 68
    2. Probe Preparation for Northern Analysis 69
    3. Northern Analysis 71

K. RNase Protection Assay 72

L. Immunohistochemistry 73

Chapter 3: Results 75

I. Decorin Expression Correlates with the Progressive Maturation of Hypertrophic Scar 75

A. Establishing D150 Probes 75

B. Establishing D600 Probes 76

C. Optimizing In Situ Hybridization with D600 Probes 77

D. In Situ Hybridization on Hypertrophic Scar, Mature Scar, and Normal Skin with D600 Probes 78

E. Possible Nonspecificity of D600 Probes 79

F. Establishing D620 Probes 79

G. Optimizing In Situ Hybridization with D620 Probes 80

H. In Situ Hybridization on Hypertrophic Scar, Mature Scar, and Normal Skin with D620 Probes 82

I. Decorin mRNA expression shows a time course of appearance during hypertrophic scar 82

J. Immunohistochemical staining levels correlate with decorin mRNA expression except in late hypertrophic scar 84

K. Decorin expression displays regional variation during the course of hypertrophic scar 84

II. TGF-ß1 Expression in Hypertrophic Scar 85

A. Rat TGF-ß1(287)/pGEM 3Z as a Template for cRNA Probes 86
  1. Establishing cRNA Probes From Rat TGF-ß1(287)/pGEM 3Z 86
  2. Optimizing *in situ hybridization* protocol with TGF-ß1(287)/pGEM 3Z cRNA Probes 86
  3. Re-evaluating cRNA Probes Produced From TGF-ß1(287)/pGEM 3Z 88
  4. In Situ Hybridization on Human Dermal Fibroblasts with TGF-ß1(287)/pGEM 3Z cRNA Probes 89
  5. In Situ Hybridization on Hypertrophic Scar,Mature Scar, and Normal Skin with TGF-ß1(287)/pGEM 3Z cRNA Probes 91
  6. In Situ Hybridization Using TGF-ß1(287)/pGEM 3Z cRNA Probes on Hypertrophic Scar From Patients Treated with IFN-α2b 94

B. Rat TGF-ß1(287)/pT7T3 as a Template for cRNA Probes 96
  1. Establishing cRNA Probes From Rat TGF-ß1(287)/pT7T3 96
  2. In Situ Hybridization on Human Dermal Fibroblasts with rTGF-ß1(287)/pT7T3 cRNA Probes 97
  3. In Situ Hybridization on Hypertrophic Scar Used to Optimize Variables of the Protocol 99
  4. Regional Variation in the Expression of TGF-ß1 mRNA in Hypertrophic Scar 101
  5. In Situ Hybridization on Normal Skin with rTGF-ß1(287)/pT7T3 cRNA Probes 101
  6. In Situ Hybridization on Other Samples of Hypertrophic Scar, Mature Scar, and Normal Skin with rTGF-ß1(287)/pT7T3 cRNA Probes 102
  7. In Situ Hybridization on Hypertrophic Scar From Patients Treated with IFN-α2b with rTGF-ß1(287)/pT7T3 cRNA Probes 103

C. Human TGF-ß1 cDNA as a Template for cRNA Probes 104
  1. Establishing cRNA Probes Using a 420bp Portion of Human TGF-ß1 cDNA 104
  2. Establishing T112 Probes 105
  3. In Situ Hybridization on Human Dermal Fibroblasts with T112 Probes 105
  4. In Situ Hybridization on Hypertrophic Scar, Mature Scar, and Normal Skin with T112 Probes 106

D. The Possibility of an Antisense TGF-ß1 Transcript 107
  1. Northern Analysis Using T112 Probes 107
  2. Attempted Ribonuclease Protection Assay Using T112 Probes 110

Figures 1 - 42 112-169

Tables 1 - 4 170-173

Chapter 4: Discussion 174

I. Establishing an *in situ* hybridization protocol to study scar and normal skin tissue 174

II. The Time Course Expression of Decorin mRNA During Hypertrophic Scar 176

III. The Regulation of TGF-ß1 Expression in Hypertrophic Scar is Complex 182

Bibliography 188

LIST OF TABLES

Page #

Table 1. Source of Burn Tissues 170

Table 2. Average Number of Cells Expressing Decorin mRNA in Early, Intermediate, and Late Hypertrophic Scars and in Normal Skin 171

Table 3. Average Number of Connective Tissue Cells in Early, Intermediate, and Late Hypertrophic Scars and in Normal Skin 172

Table 4. Average Percentage of Cells Expressing Decorin mRNA in Early, Intermediate, and Late Hypertrophic Scars and in Normal Skin 173

LIST OF FIGURES

Page #

Figure 1A. Gel electrophoresis of pD150 113
Figure 1B. Dot blot quantitation of D150 probes 113
Figure 1C. Dot blot hybridization of D150 probes to serially diluted pD150 113
Figure 2A. Gel electrophoresis of linearized pD600 115
Figure 2B. Gel electrophoresis of double digested pD600 115
Figure 2C. Pseudonorthern analysis of D600 transcripts 115
Figure 2D. Dot blot quantitation of D600 probes 115
Figure 2E. Dot blot hybridization of D600 probes to serially diluted pD600 115
Figure 3. In situ hybridization with antisense D600 on H16/N16 117
Figure 4. In situ hybridization on H2 with antisense D600 118
Figure 5. In situ hybridization with D600 probes on HSc from PT#8 119
Figure 6. In situ hybridization with antisense D600 on HSc from PT#8 120
Figure 7. In situ hybridization with antisense D600 on HSc from PT#15 121
Figure 8. In situ hybridization with antisense D600 on MSc (PT#27) and NSk 122
Figure 9. In situ hybridization with antisense D600 on HSc from PT#12 123
Figure 10A. Gel electrophoresis of pD620 125
Figure 10B. Dot blot quantitation of D620 probes 125
Figure 10C. Dot blot hybridization of D620 probes to serially diluted pD620 125
Figure 10D. Pseudonorthern analysis of D620 and T112 probes 125
Figure 10E. Pseudonorthern analysis of D620 and T112 probes 125
Figure 11. In situ hybridization with antisense D620 on H8/N8 127
Figure 12. In situ hybridization with D620 probes on Hsc (PT#s 5, 12, and 30) 129
Figure 13. Explanation of quantitation of *in situ* hybridization results 130
Figure 14. Scatter plot of decorin expression with time after injury 132
Figure 15. Grouped scatter plot of decorin expression with time after injury 134
Figure 16. Scatter plot of cell number with time after injury 136
Figure 17. Scatter plot of percent decorin expression with time after injury 138
Figure 18. Grouped scatter plot of percent decorin expression with time after injury 139
Figure 19. Immunolocalization of decorin in HSc (PT#s 5, 12, and 30) and NSk 141
Figure 20. Regional variation in decorin expression in Hsc (PT#19) 142
Figure 21A. Gel electrophoresis of double digested rat TGF-ß1(287)/pGEM 144
Figure 21B. Gel electrophoresis of linearized rat TGF-ß1(287)/pGEM 144
Figure 21C. Dot blot quantitation of rTGF-ß1/pGEM 3Z probes 144
Figure 21D. Dot blot hybridization of rTGF-ß1/pGEM 3Z probes to serially diluted unlabeled rTGF-ß1/pGEM 3Z 144
Figure 22. Dot blot quantitation of rTGF-ß1/pGEM 3Z probes 145
Figure 23. In situ hybridization with antisense rTGF-ß1/pGEM 3Z on H15/N15 146
Figure 24. In situ hybridization with different batches of rTGF-ß1/pGEM 3Z probes on serial sections of HSc from PT#8 148
Figure 25. Hematoxylin and eosin or hematoxylin only staining of HSc (PT#8) 149
Figure 26. In situ hybridization with antisense rTGF-ß1/pGEM 3Z on HSc from PT#15 150
Figure 27. In situ hybridization for TGF-ß1 in mature scar (PT#26) 151
Figure 28. In situ hybridization with antisense rTGF-ß1/pGEM 3Z on HSc and NSk from PT#7 during the course of treatment with IFN-α2b 153
Figure 29. Gel electrophoresis of linearized and double digested rTGF-ß1/pT7T3 154
Figure 30. In situ hybridization with rTGF-ß1/pT7T3 probes on H16/N16 155
Figure 31. In situ hybridization with rTGF-ß1/pT7T3 probes on H15/N15 156
Figure 32. In situ hybridization with rTGF-ß1/pT7T3 probes on HSc (PT#8) and NSk 157

Figure 33. Regional expression of staining with rTGF-ß1/pT7T3 probes by *in situ* hybridization on HSc from PT#8 158
Figure 34. In situ hybridization with sense rTGF-ß1/pT7T3 on MSc from PT#s 26 and 27 159
Figure 35. In situ hybridization with antisense rTGF-ß1/pT7T3 on HSc from PT#4 during the course of treatment with IFN-α2b 161
Figure 36. In situ hybridization with sense rTGF-ß1/pT7T3 on HSc from PT#4 during the course of treatment with IFN-α2b 162
Figure 37A. Gel electrophoresis of double digested pT420 164
Figure 37B. Gel electrophoresis of linearized pT420 164
Figure 37C. Dot blot quantitation of T420 probes 164
Figure 37D. Sequencing of TGF-ß1(420)/pT7T3 164
Figure 38. Gel electrophoresis of linearized and double digested pT112 165
Figure 39. Northern blot hybridization of total and poly (A)$^+$-enriched RNA from H20/N20 using ^{32}P-labeled T112 probes 166
Figure 40. Analysis of total RNA from H4/N4, H11/N11, and H20/N20 by northern blot hybridization using gel purified ^{32}P-labeled T112 probes 167
Figure 41. Polyacrylamide gel electrophoresis of ^{32}P-labeled T112 probes 168
Figure 42. Ribonuclease protection assay of total RNA from H20 and N20 with ^{32}P-labeled T112 probes 169

CHAPTER 1. LITERATURE REVIEW

Part 1. Proteoglycan Expression, Regulation and Functional Significance

I. Introduction

The development of proteoglycan research is intriguing. Its beginnings can be traced back to the late 19th century when chondroitin sulfate was first isolated from cartilage (Fischer et al., 1861 from Yanagishita, 1994). The early half of the 20th century saw the discovery of many glycosaminoglycans (GAGs) as well as the elucidation of their chemical characteristics. An example of such research was performed by Karl Meyer and his co-workers who discovered hyaluronan (Meyer and Palmer, 1934), dermatan sulfate (Meyer and Chaffee, 1941), keratan sulfate I and II (Meyer et al., 1953) and hyaluronidase (Meyer et al., 1937) as well as differentiated between chondroitin sulfate A and C (Meyer et al., 1956).

Throughout this era, GAGs were thought to function mainly as inert "ground substance" which filled the extracellular space of connective tissues. No fundamental associations were recognized between GAGs and proteins until the 1950s when Shatton and Schubert (1954) established the covalent linkage of GAG chains to protein cores while working with extracts from native cartilage. They isolated a polysaccharide-protein product which they called mucoprotein or mucoid. These mucoproteins, however, were still considered as inert scaffolding in ground substance which allowed cellular organization in extracellular matrices.

The advent of the molecular biology era reshaped the progress of proteoglycan (PG) research and reidentified the functional significance of PGs. The extracellular matrix is no longer the only environment where PGs are found. They have been found as integral membrane proteins which act as receptors, ie. betaglycan and as signaling molecules, ie. macrophage colony stimulating factor (M-CSF) (Price et al., 1992 and Suzu et al., 1992). They can interact with growth substances and can play critical roles in signal transduction. Shatton and Shubert's mucoids are now considered to be bioactive molecules with integral roles in development and maintenance of tissue integrity.

II. Biology

A. Protein Cores

Proteoglycans are a large and diverse group of glycosylated proteins. They are defined as proteins to which are covalently linked at least one GAG chain. Glycosaminoglycan chains are always found covalently associated with a polypeptide chain with the sole exception of hyaluronic acid (Hascall, 1986). Their diversity is a product of differences in their core proteins as well as the number and type of GAGs attached. Proteoglycans are classified into two broad groups - large and small PGs - depending on the size of their core proteins. Numerous studies have characterized core proteins to be modular in sequence and function. These modules or domains have characteristic protein motifs that are responsible for the functions of the proteoglycans.

1. Large Proteoglycans

An example of a large proteoglycan is the large aggregating chondroitin sulfate proteoglycan of cartilage, aggrecan. Its core protein is about 200 kDa and is substituted with chondroitin sulfate and keratan sulfate chains which amount to about ten times this mass (Hascall, 1986). Its core protein has three globular domains - G1, 2, and 3. G1 and 2 are proximal to each other toward the N-terminus whereas G3 lies toward the C-terminal end (Hardingham and Fosang, 1992). The G1 domain gives aggrecan its aggregating properties since this is the portion which contains a binding site for hyaluronic acid (HA) and one HA chain can bind many aggrecan monomers. The G3 domain contains EGF-like sequences which contribute a fundamental structural motif to many proteins in which they are found and may serve in protein-protein interactions. This region may also have growth factor activities. The non-globular region between G2 and G3 is where GAG attachment is found (Hardingham and Fosang, 1992).

Another example of a large PG is versican from '*versatile proteoglycan*' (Zimmermann and Ruoslahti, 1989). There are seven distinct domains proposed for its protein core (Zimmermann and Ruoslahti, 1989). Starting at the N-terminus, the first domain contains sequences that are similar to the link protein-like sequences in aggrecan and mediate binding to hyaluronic acid.

On the carboxy-terminal side of this link protein-like sequence is a 200 amino acid domain which contains two cysteines and many glutamic acid residues in tandem (Zimmermann and Ruoslahti, 1989). The function of this domain is not yet elucidated.

The next domain (amino acid residues 559 - 1654) is where GAG attachment occurs. This domain contains around twelve to fifteen Ser-Gly or Gly-Ser sequences that show similarity to previously reported attachment sites for chondroitin sulfate in collagen type IX (Huber et al., 1988). This domain also harbors seventeen Ser-Thr clusters and ten potential N-glycosylation sites. As well, two sites which display similarity to the SGXG, or the concensus GAG attachment sequence in some small PGs, are located in this domain.

Near its carboxy terminus, the versican core protein contains two EGF-like repeats and a lectin-like domain (Krusius et al., 1987). Another domain was found (Zimmermann and Ruoslahti, 1989) which displays varying degrees of similarity to the repeats in complement regulatory proteins such as human C4 binding protein (Chung et al., 1985).

Another large, well-characterized proteoglycan is perlecan which is distributed primarily in basement membranes. Hassell and coworkers (Noonan et al., 1991) coined this mnemonic from *perl* (bead or gem) and *can* (proteoglycan) to symbolize the 'beads-on-a-string' appearance of perlecan from rotary shadowing. The core protein of this PG is about 470 kDa and is characterized by five domains. These domains are shaped into specific protein motifs that have similarities to regions of known polypeptides which are used in binding and delivering nutrients and lipids, cellular growth, and in intercellular signalling pathways (Iozzo et al., 1994). These regions of the human perlecan protein are well-conserved across different species as perlecan from mouse and the nematode *C. elegans* display similar domain characteristics to human perlecan (Iozzo et al., 1994).

At the N-terminus of the polypeptide, following the signal peptide, there are three consecutive Ser-Gly-Asp (SGD) repeats which are the proposed sites for attachment of heparan sulfate side chains (Noonan et al., 1991). Whether these are the sole sites of attachment of GAG side chains is not yet fully determined.

The second domain of perlecan is a region homologous to the ligand-binding portion of the LDL receptor (Sudhof et al., 1985) and contains four cysteine-rich motifs.

The third domain of perlecan displays considerable homology with the short arm of the laminin A chain (Haaparanta et al., 1991). It contains three globular subdomains devoid of cysteine residues but flanked by cysteine-rich domains.

Domain IV of perlecan is its largest and most repetitious domain. It shares homology with the immunoglobulin (Ig) superfamily in that it contains 21 consecutive Ig repeats which are organized in a manner very similar to N-CAM, a member of the Ig superfamily (Cunningham et al., 1987). Comparisons with other molecules with similar domains suggests functions for this domain such as stabilizing homophilic protein-protein interactions, promoting perlecan dimerization in the basement membrane which increases the stability of this matrix, and increasing intercellular adhesion (Iozzo et al., 1994).

At the C-terminus of perlecan three globular and four epidermal growth factor (EGF)-like motifs display structural similarity to the C-terminus of the laminin A chain (Haaparanta et al., 1991). Molecules harboring this structure have been implicated in cell adhesion and growth (Iozzo et al., 1994). Also identified in this domain are two SGXG tetrapeptides, which may be sites of attachment of GAG chains other than heparan sulfate (Iozzo et al., 1994), and two conserved LRE (Leu-Arg-Glu) tripeptides, which have been identified as the sequence responsible for the binding of motor neurons to s-laminin in synaptic basement membranes and hence possibly perlecan-dependent neurite outgrowth (Hunter et al., 1989).

2. Small Proteoglycans

The small PGs can be grouped into two main families but all have much smaller core proteins compared to those PGs mentioned above with sizes down to 10 kDa. One family of small PGs are the serglycin PGs which are largely intracellular PGs and are named as such because of the many Ser-Gly repeat sequences in its protein core to which can be attached many CS and/or heparin chains. Serglycins are found in secretory vesicles in cells of hematopoietic lineage (Kresse et al., 1994) and are implicated in functions such as enzyme inactivation, maintenance of electrical neutrality as well as proper osmostic pressure in histamine-rich vacuoles, and prevention of autolysis through their interaction with perforins in natural killer lymphocytes.

Members of the second family of small PGs are the leucine-rich PGs of the extracellular matrix which, as their name suggests, are comprised of leucine-rich motifs. These motifs are usually an amphipathic sequence of 24 amino acids that appear to form structures that expose critical areas of the protein so they may interact with other macromolecules. Such interactions may facilitate the interaction of these PGs with other proteins and lipids.

The leucine-rich PGs include biglycan, decorin, fibromodulin, and lumican. Biglycan and decorin are interstitial chondroitin/dermatan sulfate proteoglycans with globular core proteins (Morgelin et al., 1989), substituted with two and one GAG chain(s) respectively. Fibromodulin is a keratan sulfate PG (Plaas et al., 1990) and its name was derived from its inhibitory effect on collagen fibril formation. Lumican, also a keratan sulfate PG, was named for its presumed role in corneal transparency (Blochberger et al., 1992).

The core proteins for these small PGs are also arranged in a modular fashion with different domains existing with their own specific characteristics and hence function. The main regions of these core proteins in the mature PGs include a GAG attachment site near to the N-terminus which is surrounded by sequences that display low interspecies homology. Following this site is a cysteine-rich region which appears to be well conserved across species (Kresse et al., 1994).

The central portion of the core proteins contains ten repeats of a well-conserved, fourteen amino acid long, leucine-rich sequence (Kresse et al., 1994). Each fourteen amino acid block is followed by proline residues 41% of the time. This high frequency of proline residues may offer rigidity to the protein and hence maintain its structure. The significance of the leucine-rich segments is apparent in the secondary structure assumed by these core proteins. This domain is mainly amphipathic and therefore will usually contribute a bipolar surface orientation to the protein. At the C-terminus, no repeat structures are found but there is a conserved disulfide loop.

In addition to the GAG chains, decorin and biglycan are also substituted with *N*-linked oligosaccharides, three for decorin (Scott and Dodd, 1990) and two for biglycan (Fisher et al., 1989; Neame et al., 1989). In decorin, three tryptic peptides were isolated which displayed asparagine-linked complex-type oligosaccharides (Scott and Dodd, 1989). Therefore, these oligosaccharides are mostly of the complex type, however, high mannose types have been observed in the decorin secreted by cultured fibroblasts (Kresse et al., 1994).

When these oligosaccharides were removed from the protein core of bovine skin decorin *in vitro*, self-aggregation occured (Scott and Dodd, 1990). Also, biglycan has a greater tendancy to self-aggregate and, as mentioned above, has fewer oligosaccharides attached (Scott, PG., 1993). These few pieces of data suggest that the oligosaccharides may retard self-aggregation *in vivo* and therefore allow decorin to perform its many duties, most importantly, to associate with collagen and maintain the proper architecture of the extracellular matrix (Scott, PG., 1993).

B. Glycosaminoglycan Chains

All proteoglycans have a common feature and that is a post-translational attachment of at least one glycosaminoglycan chain. The number of GAG chains attached as well as the type of GAG associated with any PG are sources of variation between PGs and contribute to the functional significance of the PGs.

1. Chemical Composition

Glycosaminoglycan chains are polymers of disaccharides and each disaccharide has one amino sugar, either glucosamine or galactosamine, and at least one sugar in the disaccharide has a negatively charged carboxylate or sulfate group (Stryer, 1981). Glycosaminoglycans differ in the configuration of their carboxylate groups, the number and position of sulfate groups, and the attachment between two sugars which make one disaccharide unit. Furthermore, GAG composition is influenced by the type of tissue producing it (Kresse et al., 1994). For example, small PGs from skin contain the highest proportion of L-iduronic acid residues when compared to similar PGs from other tissues (Choi et al., 1989). Different disaccharides are found in dermatan sulfate (DS), chondroitin sulfate (CS), keratan sulfate (KS), heparin, heparan sulfate (HS), and hyaluronic acid (HA).

Dermatan sulfate is nearly identical to, and is actually derived from, chondroitin 4-sulfate (C 4-S) . Chondroitin 4-sulfate is modified to DS by epimerisation of the carboxylate group on carbon 5 in D-glucuronic acid forming L-iduronic acid (Stryer, 1981). This does not occur for all disaccharides; therefore DS is a copolymer. Chondroitin 4-sulfate and C 6-S differ only in the position of the sulfate group on N-acetylgalactosamine. Keratan sulfate consists of repeating disaccharides made up of a D-galactose, instead of a uronic acid, attached to N-acetyl-D-glucosamine (Stryer, 1981). Heparan sulfate and heparin are like DS in that they both contain D-glucuronic acid and L-iduronic acid residues. Both HS and heparin disaccharides contain N-acetyl-or N-sulfo-D-glucosamine (Stryer, 1981).

2. Specificity of Attachment to Protein Cores

The specificity of GAG attachment has been extensively studied both at the molecular and protein levels. Glycosaminoglycan chains are attached to serine residues, especially when they occur in Ser-Gly dipeptides and less commonly in Ser-Ala dipeptides (Scott, 1993). The serine residue has been identified as the site where xylosytransferase attaches a xylose residue which then initiates the polymerization of the GAG chain on the core protein.

a) Aggrecan

In aggrecan, the attachment region is encoded by exon 10 which has high inter-species variability in size and sequence (Upholt et al., 1994). The reasoning used to identify the region in aggrecan core protein encoded by exon 10 as the CS attachment site is two-fold. First, it occurs in the core protein at a location where there is a high frequency of Ser-Gly repeats (Upholt et al., 1994). Secondly, when GAG-substituted peptides from this region of chicken aggrecan were deglycosylated, the residues which were substituted were all identified as serines and this was confirmed by DNA sequence analysis (Krueger et al., 1990).

Based on a comparison of aggrecan amino acid sequences from various species using dot plot analysis and on patterns of repeated sequences thereof, the attachment for CS chains in rat aggrecan was divided into two regions - CS-1 and CS-2 (Upholt et al., 1994). Further analyses identified two other domains with tandem repeats, all encoded by exon 10. The first domain was identified in bovine aggrecan and was found to be encoded by the 5' end of the exon where there was a high density of KS chains; the second was identified in chicken aggrecan as the CS-3 domain (Upholt et al., 1994). The extent of each region varies among species as all repeat sequences are not completely conserved.

When the Ser-Gly repeats were studied more in context of their surrounding residues, Krueger et al. (1990) recognized a pattern with the Ser-Gly doublets: the Ser-Gly pairs are always interrupted by two amino acids. Furthermore, a consensus sequence was found which consists of 10 amino acids that includes two Ser-Gly pairs separated by two amino acids which all follow an acidic amino acid and a nonpolar amino acid (D/E-X-S-G-L/D/E-P/X-S-G-X-P/X or more simply S-G-X-X-S-G; summarized in Upholt et al., 1994). An exception to this finding may be serglycin which contains in its core protein a central region of alternating Ser and Gly residues with no other intervening amino acids (Angerth et al., 1990).

When using this 10 amino acid repeat to search aggrecan sequences of other species (chicken, rat, human, and cow), a related repeat sequence was found in all species and, furthermore, these repeats included the majority of the Ser-Gly doublets found in the CS region. Comparisons have been done of the 10 amino acid repeat sequences from the different species noted above to check for degree of conservation of each residue. The sequences appear to have evolved independently of each other and therefore indicate that the frequency of any particular amino acid at any of the positions in this sequence may be just a species specific phenomenon and not a structural or functional requirement of the proteoglycan (Upholt et al., 1994).

b) Versican

Versican contains between twelve and fifteen Ser-Gly and/or Gly-Ser dipeptides which are contained within a consensus sequence which is thought to be the site responsible for CS attachment. This sequence, E/DGSGE/D, is also found in collagen type IX (Huber et al., 1988) and in a CS/HS proteoglycan syndecan (Saunders et al., 1989) as sites of GAG attachment. As well, another two sites of GAG attachment in versican belong to the consensus sequence for GAG attachment in small PGs, SGXG (Zimmermann and Ruoslahti, 1989).

c) Perlecan

Within the modular structure of the core protein of perlecan, the site of attachment of the heparan sulfate side chains is proposed in the small domain which follows the signal peptide at the N-terminus of the protein (Noonan et al., 1991). Three consecutive Ser-Gly-Asp (SGD) repeats are found in this domain and this sequence has been demonstrated in other studies to occur with high frequency in regions of core proteins where GAG chains are attached including heparan sulfate. Whether this is the sole domain responsible for GAG attachment is not known and perlecan contains more than fifty Ser-Gly repeats in its protein core, some of which may be surrounded by acidic amino acids and therefore would be potential sites of attachment of GAG chains (Iozzo et al., 1994).

Interestingly, there have been reports of perlecan species with no associated GAGs (Iozzo and Hassell, 1989). This is explained at the molecular level since SGD sequences in perlecan get encoded by different exons and some may get spliced out.

d) Small Proteoglycans

The sites for GAG attachment on protein cores of small PGs display consensus sequences with characteristics similar to those of the large PGs. For example, most decorin isolated from bovine skin contained only one DS chain and this was attached to Ser 4 in the sequence Asp-Glu-Ala-Ser-Gly-Ile-Gly- (Chopra et al., 1985). The sequence SGXG is apparent but more importantly the Ser-Gly dipeptide is conserved in this GAG attachment site. It is important to note, however, that this sequence, SGXG, is absent in biglycan (Kresse et al., 1994). As more members are added to the list of PGs whose protein cores are compared for their attachment sites, this dipeptide appears to be the minimum signal requirement for glycosylation of the core protein.

The presence of more than one Ser-Gly pair in decorin core protein (Scott, 1993) as well as the presence of Gly-Ser pairs, but the attachment of a GAG chain to only one specific site, indicates other characteristics of GAG attachment sites that need to be understood. Site-directed mutagenesis of Ser 4 to a Thr caused a decrease in the amount of GAG attachment to decorin (Mann et al., 1990). However, the mutation of Gly 5 and 7 to Ala had little, if any, effect.

The structure of the protein in the region of these Ser-Gly pairs may lend the specificity required for glycosylation. In fact, it has been suggested that the location of a Ser on a ß-turn can be a signal for GAG attachment and this type of structure is predicted for the first five residues of bovine decorin (Scott, 1993).

Biglycan shares many similarities with decorin but the number of CS/DS chains attached is usually two.

C. Molecular Organization

1. Perlecan

The genetic organization of various proteoglycans and their promoters have been characterized revealing interesting features. The domain-specific organization of the perlecan gene was elucidated by Cohen and coworkers in 1993. Using genomic clones from cosmid or phage libraries, they conservatively estimated the gene to be comprised of 94 exons which span more than 120 kbp of genomic DNA. They found that the modular domains were conserved across homologous genes and therefore the organization of the domains are always presented in relation to homologous protein domains. The coupling of functional domains is thought to have arisen from the homogeneity in codon phasing, ie. the modules are usually found to comprise exons that are flanked by introns in the same phase (Cohen et al., 1993).

The leader exon of perlecan codes for the 5' untranslated region as well as the signal peptide of the protein (Cohen et al., 1993). Following this exon, the first domain, encoded by five exons, displays no homology with any other protein it was compared to and is therefore the only unique region of perlecan (Cohen et al., 1993). Within this region, three SGD sequences are encoded between two exons, 2 and 3. These sites serve as the attachment sites for the heparan sulfate side chains. One SGD triplet is divided between exons 2 and 3 whereas the other two are contained in exon 3. Therefore, all SGD triplets, or parts thereof, fall in exon 3. Therefore, if exon 3 is deleted by alternative splicing, the result would be perlecan protein with no GAG chains and this species of perlecan has been reported to be secreted by colon carcinoma cells (Iozzo and Hassell, 1989).

The second domain of perlecan is divided into two parts, II and IIa, which together are encoded by three exons. Domains III and IV are the largest in perlecan and are encoded by 27 and 40 exons, respectively. The fifth domain is encoded by 16 exons and contains the largest exon of perlecan, 1.2 kbp in size, which consists of the entire 3' untranslated region (Cohen et al., 1993).

The 5' flanking region of the human perlecan gene was also sequenced and was found to contain no TATA or CAAT boxes (Cohen et al., 1993) which are common to eukaryotic gene promoters that are transcribed by RNA polymerase II. These sequences can also be found in the decorin gene promoter in a region which displays the strongest promoter activity of different promoter regions studied for decorin. The perlecan promoter, however, contains binding sites for the transcription factor SP1, specifically four GC boxes and three GGGCGG hexanucleotides (Mitchell and Tjian, 1989). SP1 is one type of zinc finger-containing transcription factor that is involved in transcription mediated by RNA polymerase II. Specifically, SP1 contains TFIIIA-like zinc fingers each of which is about 30 amino acids long, containing two cysteine and two histidine residues that stabilize the domain by incoorporating a tetrahedrally-coordinated zinc ion (Mitchell and Tjian, 1989). SP1 factors that recognize GC box cis elements contain three tandem zinc fingers at their carboxy terminus which mediate binding.

An additional striking feature of the perlecan promoter is the high G+C content: more than 80% of the 500bp upstream to exon 1 is G+C. And interestingly, the CpG/GpC ratio is about 0.9. This high G+C content (over 50%), nearly equal amounts of CpG as GpC, and a lack of methylation identify this region to be a CpG island or a HpaII tiny fragment (HTF) island (Bird, 1986). The presence of CpG-rich regions is due to a lack of CpG suppression by methylation in an HTF island as well as a G+C richness in this region (more than 65% compared to 40% in bulk DNA) (Bird, 1986). Implications of these islands have been studied in transcriptional regulation especially for oncoproteins, growth factors, transcription factors and housekeeping proteins where HTF islands have been found in their transcriptional control regions (Iozzo et al., 1994). Transcription has been shown to be inhibited by HTF islands when they are methylated (Bird, 1986). As well, CpG islands are found associated mainly with genes that are not tissue specific, ie. housekeeping genes (Bird, 1986). Therefore, the CpG island may explain how the expression of the perlecan gene in the basement membranes of most tissues is regulated.

2. Decorin

The human decorin gene has only eight exons (Santra et al., 1994). Exons Ia and Ib lie in the 5' untranslated region of the gene and were found to be alternatively spliced leader exons. The functional activity of the regions upstream to these exons was assessed using transient transfection assays and stepwise 5' deletion analysis (Santra et al., 1994).

Analysis of promoter Ia revealed no CAAT or TATA boxes and few cis-acting regulatory elements (Danielson, et al., 1993). A construct of exon Ia including its 2.1 kb 5'-flanking sequence subcloned upstream to a CAT-containing plasmid showed no transcriptional activity in transient transfection assays (Santra et al., 1994). This 2.1 kb region proximal to exon Ia is not considered to function, therefore, as part of the decorin promoter.

The 5'-flanking sequence of exon Ib, however, contains two TATA-like motifs and a CAAT box (Santra et al., 1994). The TATA motifs may be involved in fixing the start site for transcription. Other cis-acting regulatory elements were found in this region including AP5 and AP1 sequences which were originally described as SV 40 enhancer sequences (Santra et al., 1994). Two direct repeats in close proximity to each other were found upstream to the AP5 sequence. They have been identified as consensus sites for NF-kB and have previously been shown to take part in transcriptional activation of a variety of genes via IL-1 (Santra et al., 1994). These genes may include those for CS/DS PGs in human synovial fibroblasts and decorin in human skin fibroblasts.

Another sequence found upstream to the two NF-kB sequences has implications for expression of decorin mRNA in proliferative situations and in the wound environment. This consensus sequence GnnTTGGtGa is also found in the promoter for transin/stromelysin and is expressed with the help of the c-fos proto-oncogene (Kerr et al., 1990). It has been identified as a putative TGF-ß negative element and may serve as a transcriptional silencer of decorin gene expression in TGF-ß-sensitive cells.

The final 5' region of the promoter Ib to be discussed is a 150 bp stretch of homopyrimidine residues (CT). Two direct 18 bp repeats were contained within this region as well as other mirror repeats. This region was also found to be sensitive to S1 nuclease digestion. Such a stretch of homopyrimidine residues and hence a double stranded fragment of a homopurine/ homopyrimidine stretch favors formation of a triplex structure or H-forms of DNA (Santra et al., 1994). This occurs as a result of the unpairing and folding back of the pyrimidine strand which then forms Hoogsteen hydrogen bonds with the complementary purine strand in a parallel orientation. This creates CGC and TAT triplet repeats. The significance of such pur/pyr stretches may be to activate chromatin by binding specific protein motifs.

III. Differential Expression - Function and Regulation

In the last ten years, the perception of the role of the proteoglycans has evolved from one of just inert support, ie. scaffolding for tissue development and maintenance, to one where they are considered the bioactive molecules ultimately involved in cellular growth and differentiation. Proteoglycans are being found in all tissues but their patterns of expression are increasingly seen to be tissue-specific.

The different PGs expressed, their abundance, the amount of their glycosylation, the type and ratio of GAGs, their temporal and spatial regulation, and their dynamic structural characteristics are just some of the ways in which they exert their different, yet specific functions in different tissue types. Age-related differences in PG expression have also been observed as well as a dynamic expression pattern during fibrotic conditions, wound healing, and tumor development and metastasis.

A. Glycosaminoglycans

1. General

The importance of GAG side chains in the function of PGs can vary from being the main functional constituent to being completely dispensible. Glycosaminoglycans in the extracellular matrix are relatively large molecules which harbor a high density of negative charge. This in turn attracts many counter ions which then creates an osmotic imbalance that further attracts water from surrounding areas. The result is a hydrated matrix. Another implication of large aggregating GAG chains is the exclusion of other macromolecules from the water-filled compartment they create (Hardingham and Fosang, 1992). This increases the concentration of these macromolecules available for specific reactions and may increase the probability and rates of such reactions that may be concentration dependent.

2. Heparan Sulfate

The role of heparan sulfate in growth factor signalling has been studied extensively, especially with fibroblast growth factor (FGF). Membrane bound heparan sulfate chains have been found to associate with FGF and increase its activity possibly by binding FGF and presenting it in an altered and more optimal configuration to the FGF receptors (Rapraeger et al., 1991). This activity disappeared when chlorate was used to inhibit sulfation of PGs in culture but was restored when sulfate was provided again. Interestingly, the minimal sequence required for binding FGF is not sufficient for FGF activity. Although hexasaccharides bind FGF-2, a decasaccharide is needed for activity (Rapraeger, 1993). Other growth factors which need heparan sulfate for signaling include vascular endothelial cell growth factor and heparin-binding epidermal growth factor.

B. Aggrecan

Aggrecan was originally known as the large CSPG of cartilage. It is found in the extracellular matrix usually as large molecular aggregates noncovalently bound to hyaluronan through its G1 domain. Aggrecan attracts large amounts of water due to the high density of GAGs bound to it. This allows for aggrecan to increase the resiliency of cartilage and accounts for the main physical effect of this PG (Hardingham and Fosang, 1992). As well, its role in distributing load in weight-bearing joints has been studied (Hardingham and Bayliss, 1990). The predicted secondary structure of its amino terminus implies ß-sheets similar to the putative immunoglobulin folds (Hardingham and Fosang, 1992). Proteins harboring this motif are usually found on the cell surface and mediate cell recognition, cell adhesion, or immune function. These functions are due partly to the ability of different members of the immunoglobulin superfamily to interact with each other. Therefore, aggrecan probably interacts with link protein through homologous Ig-fold regions and this increases the amount of aggregation since both aggrecan and link protein bind to hyaluronan through their homologous proteoglycan tandem repeat regions (Hardingham and Fosang, 1992). Toward its carboxy terminus, in its G3 domain, aggrecan contains three structural motifs that resemble other protein families. These three motifs qualify aggrecan as a selectin, mainly due to the lectin domain which has been demonstrated to mediate cell-cell recognition processes during extravasation and inflammation. Interestingly, versican also contains these three domains towards its carboxy terminus (Hardingham and Fosang, 1992). The lectin domain has demonstrated low-affinity selectivity for fucose and galactose ligands (Halberg et al., 1988). Therefore, in type II collagen, the hydroxylysine-linked galactose units may serve as ligands for the G3 domain of aggrecan in cartilage.

The EGF-like sequences have been shown in other proteins to possess growth factor activity. Considering the widespread occurence of this motif in different proteins, it may function simply as a structural motif or in protein-protein interactions such as binding to other matrix proteins.

C. Perlecan

Perlecan is ubiquitously expressed in basement membranes. Its importance in establishing structural and functional integrity of tissue is emphasized by its early detection in mouse embryos, specifically at the 2 - 4 cell stage, and its detection in the dermo-epidermal basement membrane of human fetal skin (Iozzo et al., 1994). This is followed by its later detection in all basement membranes. Monoclonal antibodies against domain III as part of a fusion protein have localized perlecan in the basement membrane of every vascularized organ studied and in the tumor stroma of several human cancers (Iozzo et al., 1994).

Perlecan expression, however, is not confined to basement membranes as many studies have indicated. Perlecan has been localized to the pericellular matrices of many organs. As well, fibroblasts which do not assemble basement membranes are found to be a major producer of perlecan. For example, in human skin, perlecan mRNA was found in fibroblasts of the upper dermis and not in keratinocytes (Murdoch et al., 1994). Many cell types, independent of their ability to express a basement membrane, have demonstrated mRNA for perlecan; examples include colon carcinoma, osteosarcoma, fetal lung and skin fibroblasts, and prostate carcinoma cells (Iozzo et al., 1994). In addition, the perisinusoidal space of liver and the sinusoidal space of many lymphoreticular and endocrine organs were found to express perlecan (Murdoch et al., 1994). As well, epithelial cells of the developing intestine produce perlecan which is later assembled into a basement membrane.

Studies using monoclonal antibodies indicate a vectorial orientation of individual perlecan molecules (Iozzo et al., 1994). These studies show the N-terminus of perlecan near the plasma membrane whereas domain V extends across the basement membrane and interacts with other extracellular matrix components. This specific orientation may be made possible by a post-translational modification which attaches long-chain fatty acids such as myristate or palmitate to perlecan allowing it to attach to the cell surface, as has been found in human colon carcinoma cells.

Perlecan's vital role in cellular survival and growth is demonstrated by its expression in hepatocytes only in vitro in a cell culture system (Iozzo et al., 1994). Otherwise, in the liver, sinusoidal endothelial cells, and not hepatocytes, produce this PG.

Perlecan's expression in articular cartilage and human chondrosarcomas is an intriguing observation since these systems are avascular and lack any basement structures. However, perlecan does not necessarily go through all post-translational modifications and therefore may lack heparan sulfate side chains. This has been confirmed in rat chondrosarcoma where perlecan core protein has been found without any GAG chains attached and was localized to the pericellular environment where it most likely mediates attachment of these cells to their substratum.

Perlecan has been shown to display homotypic and heterotypic interactions (Iozzo et al., 1994). Experiments have demonstrated dimeric and multimeric forms of perlecan and have suggested that these interactions are mediated by the carboxyl end of the protein core. The ability to aggregate into large multimeric structures implies perlecan's direct involvement in basement membrane formation. Heterotypic interactions of perlecan have been found with extracellular components like laminin, nidogen, and fibronectin (Iozzo et al., 1994). Using the EHS tumor as an example, perlecan was found tightly bound to other matrix molecules as stringent conditions such as the use of denaturing solvents and chaotropic agents were needed to release it. Nidogen binding to perlecan is via perlecan's core protein and the G2 domain of nidogen which also contains binding sites for collagen type IV. Nidogen is expected to participate in a supromolecular complex with perlecan, collagen type IV, and laminin since nidogen also contains a laminin-binding region in its G3 domain.

Perlecan's association with cell surfaces is well-documented. Recent studies have demonstrated that tumor cells can spread on and attach to a perlecan substratum via ß1 integrins (Battaglia et at., 1993 from Iozzo et al., 1994). The core protein has been found to interact with perlecan-producing endothelial cells of aorta via ß1 and ß3 integrins. The region of perlecan which is responsible for cell surface binding was narrowed down to a 160 kDa fragment at the C-terminus in the N-CAM repeats and domain V (Hayashi et al., 1992 from Iozzo et al., 1994).

D. Syndecans

Another group of proteoglycans can be found on cell surfaces. This category of PGs are very significant to communications between cells and their surroundings. Cell surface PGs have been implied in functions like binding of growth factors followed by their activation or inactivation, presentation of growth factors to their receptors, intercellular adhesion, and in signal transduction activities.

The majority of cell surface proteoglycans known and studied to date are the transmembrane heparan sulfate proteoglycans known as the syndecans. At least four members have been identified in this family of PGs (Rapraeger, 1993). Their amino acid sequences demonstrate highly conserved transmembrane regions as well as cytoplasmic domains. Four tyrosines are present in the cytoplasmic domains of these syndecans at exactly the same position with the first tyrosine occuring at the boundary between the transmembrane and cytoplasmic domains (Rapraeger, 1993). This first tyrosine is followed by 10 more amino acids that are also invariant between the other syndecans. This highly conserved pattern of amino acids implies their significant role perhaps in interactions with the cytoskeleton and hence in influencing some aspect of cell behavior. As well, the four conserved tyrosine residues might serve as phosphorylation sites for tyrosine kinases in a signal transduction cascade.

The ectodomains of these syndecans are nowhere nearly as conserved as their cytoplasmic domains, however two areas display some conservation. The sites of attachment of heparan sulfate chains seem to be similar in different species although different syndecan types can vary in this regard. As well, a short sequence of basic amino acids close to the transmembrane domain is well conserved across species and syndecan types. This sequence is sensitive to proteinases and may be the target for plasmin-like proteases which cause the shedding of PGs from the cell surface.

Syndecan-1 has been co-localized with the intracellular cytoskeleton at the basolateral cell surface of mouse mammary epithelial cells which suggests its role as a supporting anchor in the continuum between the intracellular network and the extracellular matrix.

The expression of syndecan is highly tissue-specific but also overlaps as many cell types express more than one type of syndecan. Rat microvascular endothelial cells express syndecan-1 and -4; human epidermal and dermal cells express syndecan-1, -2, and -4. The expression of different types of syndecan can also be specific for the stage of differentiation of the expressing cell. Circulating B-lymphocytes do not express any of this PG. However, within lymph nodes, plasma cells display message and protein for different syndecans. Mature human myeloma cells use only syndecan as a receptor for collagen type

I. By removing the heparan sulfate chains or blocking sulfation of the PG, cells no longer bind to collagen. Therefore, the anchoring role of syndecan is further emphasized here and this role then explains the need for syndecan in other developing environments where cell-matrix adhesions must occur, for example, in mesenchymal aggregation in the developing tooth and kidney tubulogenesis during metanephric kidney induction. Increased syndecan-1 expression in these situations correlates with enhanced cell proliferation and therefore implies a role in growth regulation.

E. Versican

The expression and function of versican has not been as intensely studied as some of the other PGs discussed here. From its primary structure, elucidated by Zimmermann and Ruoslahti in 1989, many inferences can be made about its potential role. Seven distinct domains were identified in its core protein. Four of these domains, the link protein-like sequence at the amino terminal end, the EGF-like, lectin-like, and the complementary regulatory protein-like (CRPL) domains toward the carboxy terminal, are all implied in interactions within the extracellular matrix as well as in interactions between cells and their surrounding matrix.

The glycosaminoglycan attachment sites occur interspersed along the largest domain of the core protein. This arrangement is thought to keep versican in an extended conformation so as to keep the specific functional domains at the two ends of the protein accessible (Zimmermann and Ruoslahti, 1989).

The EGF-like repeats and the CRPL domain toward the carboxy terminal of versican core protein are implied in protein-protein interactions as they have served similar functions in other proteins where they are found. EGF-like sequences in laminin have been reported to promote cell growth which may be another possible function for this domain in versican (Zimmermann and Ruoslahti, 1989).

The three structural motifs at the carboxy terminal of versican are also found in a group of cell adhesion molecules called LEC-CAMs. They also appear in the lymphocyte homing and adhesion molecules ELAM-1, MEL-14 and GMP-140 (Zimmermann and Ruoslahti, 1989). This strongly implies a role for versican in cell adhesion to other cells and to matrix molecules. A related function would be cell recognition where such adhesion domains may confer specific attachment of cells to their environment.

A recent study by Zimmermann and co-workers (1994) was conducted to localize versican in specific regions of adult human skin. Bacterial fusion proteins containing unique regions of versican core protein were prepared to which polyclonal antibodies were raised. These antibodies when used in immunohistochemical studies demonstrated differential staining patterns in human skin. In the epidermis, staining was confined to the basal keratinocyte layers and absent from the suprabasal keratinocytes where terminally differentiated cells are found. In the dermis, both the papillary and reticular layers were stained and versican was found to colocalize with different fibrillar structures of the elastic network which suggests an association of versican with microfibrils.

Cultured keratinocytes and dermal fibroblasts were also stained and expressed versican mainly during active cell proliferation. A down-regulation of versican expression was observed in cells that were cultured in conditions which promoted keratinocyte differentiation. A comparison of versican mRNA abundance in RNA preparations of semi-confluent and confluent fibroblast cultures yielded lowered amounts of versican mRNA at higher cell densities.

This localization of versican in the proliferating zone of the epidermis as well as the density dependent expression of versican in cultured cells suggest a role in cell proliferation in tissues not necessarily confined to the skin. As well, versican seems to be involved in the growth and differentiation of epidermal cells.

In a comparative immunohistochemical study of human post-burn hypertrophic scar, mature scar, and normal adult skin (Scott et. al., 1995), versican was absent from the dermis of normal skin but presented itself very weakly in the epidermis. In mature scar, a few areas of the dermis stained very weakly but the epidermis displayed a high concentration of versican. In hypertrophic scar, versican appeared throughout the dermis but was absent from the epidermis as well as a layer of dermis just beneath the epidermis and from the deepest dermis. Although, in this study, the interpretation of this finding is made in relation to the distribution of two other PGs and TGF-ß, the increase in expression of such a large CS-bearing PG such as versican in hypertrophic scar may be one causal factor for the deranged collagen fibril assembly seen in the scar.

Versican binds hyaluronan with high affinity. Hyaluronan (HA) has been suggested to play a role in the detachment and rounding of fibroblasts and keratinocytes during mitosis. Interestingly, versican antibodies have strongly stained rounded fibroblasts and keratinocytes in mitosis. The secretion of HA and versican into the proliferating epidermis by keratinocytes may form a highly hydrated matrix in which the movement of dividing cells into the suprabasal layers is facilitated. Subsequent differentiation of keratinocytes may result in a down-regulation of versican expression which then may accomodate tighter cell surface HS PG- and integrin-mediated cell-cell contacts.

F. Small PGs: Decorin, Biglycan, Fibromodulin

The small chondroitin/dermatan sulfate proteoglycans decorin and biglycan as well as the small keratan sulfate PG fibromodulin all share similarities in structure but can vary considerably as to their localization, regulation of expression, and functional implications.

1. Differential Expression

The pattern of expression of decorin in adult human skin was studied by Schonherr and coworkers (1993). They found that different cells in different layers of the dermis express different patterns of CS/DS PGs and this is maintained in culture conditions. Immunohistochemical staining of this PG in intact skin resulted in staining throughout the dermis but not in the epidermis, and more specifically, a higher density of staining was found in the papillary (next to the epidermis) dermis as compared to the reticular layer (lower dermis). These results were complemented by in situ hybridization and northern analysis results which localized more mRNA for decorin to fibroblasts of the papillary layer of the dermis. Immunohistochemical staining for biglycan localized it to the dermo-epidermal border.

Upon culturing papillary and reticular fibroblasts separately and comparing their PG synthesis patterns, up to 5.9 times more decorin was released by the papillary fibroblasts. Interestingly, the amount of cell-associated decorin was similar for both types of fibroblasts. The amount of biglycan synthesis in culture was found to be ten times less than decorin but no difference was seen between cell types.

For cell culture, cells were obtained from donors of a large range of age groups and the expression pattern of decorin and biglycan was not found to be age-dependent as there was no difference seen between cells from these groups. These results contrast with other studies conducted on human bone cells (Kresse et al., 1994) which revealed high biglycan levels in fetal cells and cells from pubescent donors. Decorin, however, was found at maximal levels in cells from adolescent donors but at lower levels in osteoblasts from newborns.

The higher concentration of decorin found in papillary fibroblasts was suggested to lead to a higher cell density in papillary cultures but no mechanism was suggested. The results from this study typify the heterogeneity of expression of PGs from one tissue source. This type of information is very significant in pathologies that are specific to particular regions of a tissue or organ or specific cell types in one tissue. Such information would especially be useful if tissue is obtained from a donor with such a pathology.

The expression of biglycan is more restricted when compared to decorin. It has not been demonstrated to bind to collagen and thus has different functions than decorin. In a study by Bianco and co-workers (1990) biglycan was found to have a spatially restricted pattern of expression in developing bone indicating an association with specific developmental events at specific sites. In non-skeletal tissue, biglycan was also localized to specific cell types such as skeletal myofibers and endothelial cells of connective tissue, and differentiating keratinocytes in epithelial cells. A role for biglycan in cell and tissue proliferation has been suggested but more definitive data are required.

2. Interactions with Collagen

Decorin is found naturally bound to collagen and this interaction has been studied and found to affect the kinetics and formation of collagen fibrils. Vogel and co-workers in 1984 found, while studying the precipitation of collagen in vitro, that a small dermatan sulfate PG isolated from bovine tendon inhibited fibrillogenesis of collagen types I and II from bovine tendon and cartilage, respectively. This effect was specific as PGs from cartilage, tendon, and aorta did not display this function. Alkali treatment of this PG, which digests the GAG chains as well as the protein core, abolished this function; however, chondroitinase treatment, which is supposed to specifically digest the GAG chains of this PG, had no effect. This suggested that decorin conveyed its effects on collagen by direct interaction with its core protein. When the telopeptides of the collagen were digested away by pepsin as well in this study, decorins effect on the fibrillogenesis of collagen was not affected. The tissue specificity of decorin and collagen for this study was also recognized as they used PG and collagen types I and II from the same source.

A study that shortly followed this one by the same group confirmed their previous results and recognized the effects of decorin on the structure of collagen fibrils. They studied the morphology of collagen fibrils by negative staining and scanning electron microscopy (sem) at various times during its polymerization in vitro (Vogel and Trotter, 1987). When collagen alone was observed in solution during polymerization by heat, its light scattering ability rose as insoluble collagen formed. As well, a rapid rise in the absorbance of collagen was observed. In the presence of the PG, the development of light scattering decreased and no rapid rise is absorbance was observed. However, the change in light scattering reached the same levels as pure collagen after 24 hours. Using sem, collagen fibrils appeared thinner with the addition of the small PG and this effect seemed to continue over time with a decrease in diameter of 31% in the presence of this PG; however, there was no effect on the banding periodicity of collagen fibrils. Negative staining allowed the observation of collagen fibrils joining laterally to produce larger fibrils in the absence of the small PG. With its addition, the frequency of this lateral aggregation decreased.

Therefore, the addition of the small dermatan sulfate PG from bovine tendon caused the resulting collagen fibrils to be thinner and also slowed the rate of increase in fibril diameter. This PG was suggested to inhibit lateral aggregation of forming collagen fibrils. The large PGs from cartilage, in contrast, had no similar effects.

Recently, the binding of fibromodulin and decorin to collagen was compared and separate sites on fibrillar collagens were found to be responsible for this binding (Hedbom and Heinegard, 1993). In this study, the binding of metabolically-labeled decorin and fibromodulin from fibroblast cultures to collagen type I was measured in an assay based on the precipitation of collagen fibrils in vitro.

The binding of either radiolabeled PG was competed out by only the corresponding non-labeled PG. As well, the binding of either PG to collagen was saturatable and the binding saturation of one of the PGs did not affect the other. This study concluded, therefore, that the binding sites for fibromodulin and decorin on collagen are distinct, specific, and limited in number. Interestingly, neither of these PGs interacted with denatured collagen; both required intact triple helical molecules.

An average of one binding site was suggested per collagen I molecule for fibromodulin whereas more than one interaction site was suggested for decorin with some involvement from the dermatan sulfate chains. The influence of the DS chains imply that decorin may serve to connect collagen fibrils in the extracellular matrix. The differing sites of attachment of fibromodulin and decorin to collagen emphasizes the distinct significant roles that different small proteoglycans may have in similar locations.

3. Interactions with Growth Factors

The interaction of proteoglycans with growth factors and cytokines is an area of research which is receiving increasing attention. Specifically, the effects of transforming growth factor-beta (TGF-ß) and FGF on the patterns of expression of proteoglycans are being studied. However, their mechanisms of action are not known and more work is needed in this area.

Kahari and co-workers made some observations in 1991 that were crucial to identifying specific effects of TGF-ß1 on the expression of biglycan, versican, and decorin. They found that when cultured fibroblasts from normal human skin and gingiva were exposed to TGF-ß1, message for biglycan and versican increased up to 24-fold and 6-fold, respectively. As well, the increase in biglycan was coordinate with an elevation of message for type I procollagen. In contrast, decorin mRNA decreased up to 70%. Their entire study, however, was conducted *in vitro* on cultured cells which made extrapolating their data to the *in vivo* situation difficult.

Similar responses were also seen in cultured fibroblasts that were metabolically labeled with ^{35}S. Quantitation of ^{35}S-sulfate- and ^{3}H-leucine-labeled decorin in culture media by immunoprecipitation displayed a 50% reduction in decorin in cultures treated with TGF-ß1. But, interestingly, this cytokine caused an increase in the size of decorin molecules but not in the size of the core proteins which indicates a longer GAG chain on decorin in the presence of TGF-ß1.

Many interesting speculations can be made about the effects of TGF-ß1 on the expression of these PGs. For example, decreased levels of decorin in the tissue may allow for increased rates of fibrillogenesis of collagen types I and II during development and repair of injured tissue, two environments where elevated levels of TGF-ß are found.

The coordinate decrease in decorin expression with an increase in collagen type I implies a functional role of TGF-ß1 in matrix remodeling. This has become more apparent through studies which have demonstrated the interaction of PGs such as decorin with growth factors like TGF-ß1 in the ECM. Conversely, these studies also helped to elucidate more of the biological roles of PGs.

Yamaguchi and Ruoslahti (in 1988) found that CHO cells that were stably transfected with decorin grew in a more orderly monolayer and to a lower saturation density than cells with no decorin. The extent of change in their morphology correlated with the amount of decorin expressed and their saturation density was inversely proportional to the level of decorin. Therefore, decorin displayed an ability to inhibit growth in these cells.

This effect of decorin was later attributed to the ability of decorin core protein to bind TGF-ß which normally stimulates growth of CHO cells (Yamaguchi et al., 1990). This binding was thought to neutralize or inactivate the effects of TGF-ß. These results may demonstrate a control system where PGs act as negative feedback regulators of TGF-ß activity. Therefore, with a decrease in decorin expression in the presence of TGF-ß1, more of this cytokine exists in its activated or activatable form which can, in turn, produce more dramatic effects such as an increase in collagen type I production.

To further establish the effects of the interaction between growth factors and proteoglycans in vivo, Border and co-workers (1992) reported on the effects of decorin in glomerulonephritis in an animal model. This experimental kidney disease is induced by administration of antithymocyte serum (Border et al. 1990) which results in an inflammation of the kidney characterized by the accumulation of ECM containing decorin and biglycan. Anti-TGF-ß antibodies suppressed this excessive matrix production down to near normal levels (Border et al. 1990). Therefore, the effects observed with this experimental disease were attributed to excessive TGF-ß levels.

Decorin administration (Border et al., 1992) resulted in an inhibition of the increased production of the ECM in glomerulonephritis and therefore an attenuation of the disease. Furthermore, decorin was found to interfere with the growth inhibiting action of all three isoforms of TGF-ß, TGF-ßs 1, 2, and 3, on mink lung epithelial cells. Whereas anti-TGF-ß1 antibodies can affect only the activity of TGF-ß1, the scope of activity of decorin is broader. As well, since excessive levels of TGF-ß have been found in other fibrotic disorders like liver fibrosis (Krull et al., 1993), proliferative vitreoretinopathy (MacDonald et al., 1995), and systemic sclerosis (Kulozik et al., 1990), decorin may have potential as a therapeutic agent in such environments.

Hildebrand and coworkers (1994) recently reported on the interaction of decorin, biglycan, and fibromodulin with TGF-ß using radiolabeled core proteins expressed as fusion proteins with *E. coli* maltose binding protein. They found that all of the core proteins bound to solid phase-associated TGF-ß1 in a concentration-dependent manner. Maximum binding was 50%, 20%, and 55% respectively for biglycan, decorin, and fibromodulin. Interestingly, fibromodulin showed higher competition for TGF-ß bound to biglycan than biglycan or decorin. Little or no binding was observed to NGF, EGF, insulin, or platelet factor 4 which indicates the specificity of binding. Also, intact PGs from bovine tissues competed with the fusion proteins for binding.

Affinity labeling experiments showed that the binding of TGF-ß to its types I and III receptors was decreased in the presence of the fusion proteins. But the effect on the binding to the type I receptor should be interpreted with caution as a 60 kDa TGF-ß-binding protein has been observed that appears to resemble the type I receptor but is found bound to the cell surface via glycosaminoglycans (Butzow et al., 1993). The affinity labeling experiments support other studies which found that these core proteins also compete with a TGF-ß-binding fragment of betaglycan for TGF-ß binding in microtitre assays (Fukushima et al., 1993) Interestingly, the removal of GAG chains from decorin and biglycan increased their activity indicating that they may interfere with the binding of the PGs to growth factors.

Another note of caution to be observed regards the interpretation of these results considering that PG-TGF-ß interactions in vivo, and for that matter interactions of any ECM PG with growth factors in vivo, is not likely to occur in the fluid phase. For example, decorin and fibromodulin would most likely be bound to collagen fibrils. Future studies need to address the interactions between growth factors and PGs in an environment that approximates more closely the in vivo situation. The effect of decorin or fibromodulin bound to collagen on the activity of TGF-ß is an example. It is possible that the PGs mentioned here when bound to ECM components may compete with receptors for growth factors or cytokines and thereby sequester them in the ECM, away from their receptors. This sequestration may improve the half-life of such growth substances and make them available at a more opportune time.

The effect of TGF-ß1 on CS/DS PG expression in human embryonic skin fibroblasts was studied by Westergren-Thorsson and coworkers (1992). They found that TGF-ß1 increased the production of biglycan by three- to four-fold. As well, large CS/DS PG synthesis was increased by five- to seven-fold. This large PG had a core protein about 4-500 kDa in size and they presumably identify it as versican. An increase was also observed in the synthesis of a major cell surface heparan sulfate PG which they think is a syndecan (core protein about 350 kDa in size). In contrast, very minimal changes were observed in decorin expression.

Glycosaminoglycan synthesis was also found to be affected by TGF-ß1 in this study. Although no increase in size of GAGs associated with these PGs was observed, a higher proportion of D-glucuronosyl residues was found with treatment. Therefore, the ratio of glucuronic acid to iduronic acid increased in xyloside-primed chains produced by TGF-ß-treated cells. This could alter the structure of DS chains and possibly affect their self-association. Other reports have emphasized the effects of the ratio of glucuronic acid to iduronic acid residues on secondary structure of PGs and on the regulation of cellular growth. A high proportion of iduronic acid has been found to have an inhibitory effect on cell proliferation compared to glucuronic acid-rich PGs (Westergren-Thorsson et al., 1993). This complies with the results stated above since TGF-ß has been found to cause cell proliferation and this may be partly due to its effects on GAG chains.

TGF-ß, therefore, has both qualitative and quantitative effects on PG synthesis. It changes the copolymeric structure of DS chains by affecting GAG-synthesizing machinery. This can then affect cell growth and migration as well as the organization of matrix fibres.

TGF-ß is only one of the growth substances studied in relation to the regulation of PG expression. Other growth substances studied include bFGF (Tan et al., 1993), IGF-1 (Roughley et al., 1994), interleukins, dexamethasone (Nakayama et al., 1994), and more. Results of studies with TGF-ß and PGs, however, are examples of the importance of the association PGs have with the enormous array of factors present in the pericellular environment and the ECM. The effects of the interaction between PGs and these substances on the regulation of expression and function of both will hopefully provide us with necessary clues in evaluating many human pathologies for treatment.

4. Expression During Fibrosis and Other Disorders

The important role that small leucine-rich proteoglycans plays in maintaining structural integrity as well as in controlling cell proliferation in connective tissue becomes more and more apparent through studies of different pathologies where the expression of such proteoglycans is found to be altered or dysregulated. Fibrotic disorders are one example of a type of pathology in which an altered expression of extracellular matrix proteins occur. The overall outcome of such conditions is the production of excessive connective tissue that disrupts the normal function of the afflicted organ(s) . Other conditions, not necessarily considered fibrotic, in which excessive connective tissue is produced result in environments which facilitate the invasive properties of cells that have lost growth control. Examples of such pathologies include carcinomas or metastatic tumors. The growing list of pathologies, whatever they may be, where the expression of PGs is identified to be dysregulated provide an increasingly diverse and convincing collection of evidence to establish the multifunctional character of small PGs.

a) Fibrotic Disorders

Fibrotic disorders which display an alteration in the expression of small PGs include liver cirrhosis and hypertrophic scar.

i. Liver Fibrosis

Liver fibrosis was experimentally induced in rats by prolonged bile-duct ligation which led to secondary biliary cirrhosis or by thioacetamide (TAA) poisoning which led to toxic liver fibrosis (Meyer et al., 1992). The result of these two treatments was a specific rate of progression, depending on the type of treatment, of fibrosis of the liver until the cirrhotic stage where septal fibrosis and cirrhotic nodules were observed. Other results that were studied were the changes in expression of decorin and biglycan during the progression of the disorders as well as the cell types responsible for the production of these proteoglycans. Total RNA was extracted from liver tissue of normal rats and of rats at various time intervals during the progression of fibrosis inflicted by bile-duct ligation and TAA administration, separated by gel electrophoresis, transferred by northern blotting and probed for decorin and biglycan transcripts. Very little message was detectable in the early stages of fibrosis but increased dramatically until strong expression of transcripts for both of the PGs was detected during advanced cirrhosis. In comparison, un-operated rats as well as sham operated animals had barely detectable mRNA levels for the PGs studied.

Also of interest in this study was that these PGs were being produced primarily by one cell type, the fat-storing cells (FSCs). After probing total RNA that was extracted from liver tissue of normal and fibrotic rats, parenchymal and nonparenchymal cells were isolated from normal livers and analyzed for the production of decorin and biglycan over time in culture. Freshly isolated hepatocytes and Kupffer cells demonstrated barely any detectable mRNA for these PGs by northern and slot-blot analyses. Intriguingly, myofibroblast-like cells, which were generated by passaging primary cultures of FSCs twice to yield fully transformed tertiary cultures, demonstrated a significant reduction of mRNA for the two PGs studied, especially decorin. In an attempt to correlate this data to rate of synthesis of secreted sulfated PGs of the FSCs, the rate of incorporation of $^{35}SO_4$ into GAG chains of PGs that are secreted into the medium of the FSCs was measured for the primary as well as the tertiary cultures (myofibroblast-like cells). The rate of synthesis of sulfated PGs per cell increased with time in culture and further made a dramatic rise in myofibroblast-like cells. Additionally, the proportion of chondroitin sulfate increased in FSCs about four-fold from primary to tertiary cultures. These results did not correlate with the steady-state levels of mRNA maintained for the decorin and biglycan in FSCs and in myofibroblast-like cells and with the reduced mRNA levels of the PGs in myofibroblast-like cells. Explanations for this phenomenon include a possible increase in the sulfation and chain length of GAG chains as well as a possible reduction in the degradation of the PGs produced by the cells.

In this study, Meyer and co-workers also studied the effect of TGF-ß1 on mRNA levels of decorin and biglycan in primary and tertiary cultures of FSCs and found that this cytokine significantly increased the transcription of these PGs only in the primary cultures with no effect on the myofibroblast-like cells. Myofibroblast-like cells have previously been described as a terminally transformed phenotype of fibroblasts (Schmitt-Graff et al., 1994). They have also been the focus of study in other fibrotic disorders such as HSc where some investigators consider them to be responsible for the severe contraction experienced in this disorder (Scott et al., 1994).

This study clearly demonstrates a coordinate increase in biglycan and decorin gene expression by rat FSCs during the progression of experimentally-induced fibrosis. Furthermore, exogenous TGF-ß increased the gene expression of both of these PGs by primary FSCs in culture. An attempt by the authors to reproduce a differential effect by TGF-ß on the expression of decorin (down-regulation) and biglycan (up-regulation) as has previously been reported, was not successful. This they attribute to the possible difference in cell-type-specific regulatory mechanisms, such as different combinations and quantities of TGF-ß receptor types, that may be present in the diffent models in which the expression of these PGs are studied. Another possible explanation of the results could involve the role that these PGs play in the accumulation and assembly of the extracellular matrix as well as in the regulation of cytokine activity. The increased expression of biglycan and decorin by the liver during fibrosis and by FSCs during treatment with TGF-ß may simply be a response to control the activity of such cytokines and thereby bring the fibrotic response under control. Additionally, considering that decorin is found at regular intervals along collagen fibrils and is believed to play a role in collagen fiber assembly, the increase in decorin expression during fibrosis may simply be a response to the increase in collagen production.

In a follow-up study conducted by Krull and co-workers (1993), the expression of biglycan and decorin as well as TGF-ß1 were studied by *in situ* hybridization during the progression of experimentally induced liver fibrosis in the rat. In this study, fibrosis was induced only by one method which was thioacetamide poisoning. This method of investigation was very interesting since it simultaneously revealed the spatial and temporal expression of the genes for these PGs and TGF-ß1. While the expression of biglycan appeared to be constitutive in normal liver, the expression of decorin and TGF-ß1 were very sparse if not absent. During the acute and subacute stages of TAA-induced fibrosis (0-4weeks), these expression patterns remained the same. During the transition to the chronic stage (4-8 weeks), there was a dramatic increase in the expression of decorin which was primarily seen along the advancing fibrotic septa. In correlation to this observation, the expression of TGF-ß1 also increased in the same time frame with its expression in the chronic stage being seen exclusively in the septa. Decorin and TGF-ß1 continued to be expressed during the cirrhotic stage (8-12 weeks) at relatively high levels. The expression of biglycan also increased in the chronic stage parallel to the formation of the fibrotic septa, where there was an increase in the number of cells expressing biglycan as well as an increase of positive signal per cell. In the cirrhotic stage, the expression per cell decreased slightly but the number of positive cells was found to increase and this was attributed to the substantial increase in the fraction of nonparenchymal cells.

Biglycan mRNA levels, therefore, correlated closely with the progression of fibrosis and increased alongside the intensity of proliferation. The mRNA levels for decorin and TGF-ß1, however, appeared more toward the chronic stage and showed a tight correlation in their spatial and temporal expression. Since decorin has been shown to have antiproliferative activity (Yamaguchi and Ruoslahti, 1988), its increased expression alongside the increase seen in the expression of TGF-ß1 may be a response to control the extent of fibrosis. Also of importance to consider is the type of model of fibrosis studied. When comparing TAA induced fibrosis to the bile-duct ligation model, there is a higher expression of decorin earlier in the latter where symptoms of fibrosis such as cholangioproliferation are seen earlier. Considered together, this evidence supports the up-regulation of decorin as a response to control the extent of fibrosis.

ii. Hypertrophic Scar

Another fibrotic disorder in which the expression pattern of the small PGs was found to differ from the normal state is hypertrophic scar. In such a condition, which will be reviewed below, the inflammatory phase of wound healing is prolonged which leads to a fibroproliferative situation in which there is an excessive production of extracellular matrix components. Interestingly, however, while the expression of biglycan protein, which was found to be undetectable in normal skin, was found to be abundant throughout hypertrophic scars, decorin protein, which was found abundantly in normal skin, was expressed very sparsely and often was entirely absent in some areas of the scars studied (Scott et al., 1995). The localization of decorin in the scar was restricted to the deep dermis and a zone just beneath the epidermis. In this same study, TGF-ß1 was found to be absent in normal skin. Its expression increased in HSc sections but was mainly restricted to nodular areas of the scar as well as the deep dermis. Both decorin and TGF-ß1 levels were found to be higher in mature scars than in HSc whereas the level of biglycan decreased considerably.

The altered expression patterns of the small PGs biglycan and decorin in hypertrophic scar are quite striking. Biglycan and decorin appear to be regulated in opposite ways as the first is abundant in the scar whereas the second appears quite scarce. Considering what is known about decorin as an antiproliferative agent as well as a matrix organizer, its absence during wound healing logically leads one to predict an uncontrolled environment such as that found in hypertrophic scar where fibroproliferation exists as well as a disorganized matrix.

b) Progeria

The expression pattern of biglycan and decorin described for hypertrophic scar was also observed in infantile progeroid patients (Beavan et al., 1993). Skin fibroblasts that were grown from biopsies taken from two patients who were diagnosed with neonatal progeroid or Wiedemann-Rautenstrauch syndrome were metabolically labeled with ^{35}S-methionine after which secreted macromolecules were immunoprecipitated with antibodies against biglycan and decorin. The products were directly analyzed by SDS PAGE and fluorography. Compared to fibroblasts from a control person, those from the two patients produced hardly any mature decorin. Digestion of the products with chondroitin ABC lyase before analysis revealed a 70-90% reduction in the amount of radioactivity incoorporated into the core proteins. Analysis of the products obtained by immunoprecipitation using an antibody to biglycan revealed at least a two-fold increase in the amount of this PG secreted by fibroblasts of the progeroid patients compared to the control.

The deficiency in decorin production was not due to a problem with the secretion of the PG as a pulse-chase experiment showed functional transport kinetics for both decorin and biglycan. Northern blot analyses indicated that the altered expression of these PGs occured at the transcriptional level since the amount of decorin mRNA isolated from the patients fibroblasts was only 6-20% of that observed for normal fibroblasts; for biglycan, the opposite occured where substantially more biglycan mRNA was observed in total RNA from patients' fibroblasts than from normal controls. Another interesting difference found between the expression of these PGs by the patients' fibroblasts as compared to normal fibroblasts was that the mature decorin isolated from the patients' cells had a slower electrophoretic mobility on the SDS PAGE. This was attributed to a possible increase in the size of the GAG chains. Finally, with respect to this study, a second skin biopsy was obtained from one of these patients 12 years later from which fibroblasts seemed to express normal levels of decorin protein and mRNA. During this study, fibroblast cultures from two other patients who were diagnosed with neonatal progeria as well as from a patient with classical progeria (or Hutchinson-Gilford syndrome) and from two patients with Marfan's syndrome were obtained and exhibited decorin deficiency at the protein and mRNA levels as well.

c) Osteogenesis Imperfecta

A recent report on a case of osteogenesis imperfecta (OI) reveals yet another disorder in which the deficient expression of decorin may influence the pathological outcome (Dyne et al., 1996). Osteogenesis imperfecta is caused by mutations in type I collagen genes with the result being abnormal secretion, assembly and function of type I collagen. Mutations that lead to OI are usually unique to the individual affected and his/her family. However, there is a growing number of cases where identical mutations have been found in unrelated individuals who display the same phenotype. Of even greater interest is the finding of unrelated individuals with identical mutations but with different phenotypes. Recently, such individuals have been studied by evaluating the decorin expression of their skin fibroblasts at the protein and mRNA levels. The main individual focused on in this report (P1) had an $\alpha1$(I)Gly415Ser mutation and suffered from severe/lethal OI. Thirteen other unrelated cases of OI were also studied of which particular interest was paid to an individual with a mutation in the same position of the type I collagen triple helix, 415, but the mutation was from a Gly to a Cys (P2). Another individual with an identical mutation as the individual described above with the severe/lethal OI was not studied here but this case as well as the α1(I)Gly415Cys mutation mentioned above both resulted in only moderate cases of OI. Also of interest is that the mutation at position 415 occurs at the d band of collagen fibrils which is primarily where decorin is found.

Fibroblasts from the patients studied were metabolically labeled with ^{35}S-sulfate and the PGs secreted into the medium were isolated and analyzed by SDS-PAGE. Cultured fibroblasts from P1 were found to secrete barely any mature decorin whereas all other subjects studied demonstrated normal levels of decorin secretion. Medium PGs were further digested with chondroitin ABC lyase and subjected to Western blot analysis after which P1 demonstrated undetectable levels of decorin core protein whereas all other subjects studied expressed normal amounts of core protein. Northern blot analysis showed that decorin mRNA was below the detectable limit in P1, however, all other OI patients studied had decorin mRNA expression that was comparable to normal individuals. The patient P2 who has a mutation in the same location as P1 but who expresses a less severe phenotype than P1 expresses decorin at the mRNA and protein levels, even though the expression is a little lower than normal. It was therefore concluded that the absence of decorin in P1 may have aggravated her condition which is why she possibly displayed a more severe phenotype of OI.

The dysregulation or altered expression of small proteoglycans during such disorders as those discussed above can have a number of different effects which provide us with clues as to the possible roles of these PGs in the normal condition. Structural integrity of connective tissue as well as the control of cell proliferation are two main areas within which the roles of these PGs are being elucidated. The study of PGs in the matrix of the human colon and colon carcinoma gives further insight into their roles in cell proliferation and, furthermore, cell invasiveness.

d) Colon Carcinoma

A significantly higher amount of C4S and C6S was produced by cells of the connective tissue stroma in colonic tumors when compared to normal human colon (Iozzo et al., 1982). This increase in GAG content was later connected to an increased expression of decorin (Adany et al., 1990). Immunohistochemically, C6S was found predominantly in the stroma of malignant cells whereas C4S displayed equal distribution in normal and malignant tissue. The distribution of decorin protein core was later found to be similar to that of C6S. Analysis of mRNA by northern blot revealed a dramatic increase in the two transcripts encoding decorin in the carcinoma. The relative increase in the mRNA for decorin was estimated to be three fold when analyzed by slot blot hybridization and normalized on one milligram of total RNA. However, when corrected for changes in the total RNA content and expressed as relative hybridization per gram of tissue, there was a 7.4 fold increase in decorin mRNA expression in the tumor as compared to normal colon. Therefore, the increase in chondroitin sulfate was linked to the increased steady state levels of decorin mRNA in colon carcinoma. As well, enhanced decorin expression was believed to be important to the invasive ability of neoplastic cells in the tumor.

Genomic DNA was also isolated from cells of normal colon and from those of the carcinoma and subjected to digestion by methylation-sensitive restriction endonucleases (Adany et al., 1990). Such enzymes would only recognize and digest their target if the internal cytosine in their target sequence is unmethylated. Upon Southern blot analysis of the products of digestion which involved probing with a probe specific for decorin, genomic DNA from the tumor contained smaller fragments than that of normal colon tissue. This suggested that certain cytosines were hypomethylated in the tumor tissue but not in the normal tissue. The degree of hypomethylation of the decorin gene was estimated to be three-fold higher in the carcinoma tissue than in normal colon. This finding was very important since the degree of methylation of some genes has been previously linked to the degree of their expression (Bird, 1986)

A subsequent study to localize the site of hypomethylation of the decorin gene in human colon carcinoma tissue revealed that there was specific hypomethylation of the internal cytosine of the 5'-CCGG-3' sequence (Hpa II restriction site) encompassing codons 360-361 of the decorin gene (Adany and Iozzo, 1991). This occurs at the 3' end of the gene whereas three other Hpa II sites in the untranslated region were found to be fully methylated as is the case in normal colon tissue. This hypomethylation was also found in samples of colonic polyps but not in ulcerative colitis which was taken to indicate that the inflammation process alone was not responsible for this alteration.

The hypomethylation of the decorin gene in a malignant environment such as the one described here may be a response, as previously described, to the lack of control over cellular proliferation. Such an alteration of the decorin gene would lend itself to increased expression which may subsequently help to control the malignancy. This hypothesis is supported by the recent study which involved stably transfecting human colon cancer cells with decorin cDNA which markedly suppressed their transformed phenotype (Santra et al., 1995). The cells were found to arrest in the G1 phase of the cell cycle and this growth suppression was reversed by antisense oligonucleotides to decorin mRNA.

The differential expression of the small proteoglycans, of which only a small number were considered here, in normal connective tissue together with evidence of their altered expression in different pathologies provide us with valuable clues as to their possible functions. Moreover, this collection of evidence has enlightened us considerably about the biological activity of these molecules.

Part 2: Decorin, TGF-ß1, and Hypertrophic Scar

I. Hypertropic Scar

A. The Clinical Problem

Hypertrophic scar is a complication sometimes experienced in the wound healing of patients, especially children, who have suffered thermal and other injuries which penetrate the dermis. The wound healing process involves a number of overlapping stages which start with hemostasis. This is followed by inflammation and fibroproliferation in which cells belonging to the immune system exert their control over infection; also, tissue components needed for the regenerative process, for example extracellular matrix components of dermis, are produced; and finally, mechanical continuity is restored. The final stage of the healing process is remodeling in which the normal tissue or organ contours are restored. The damaged tissue is usually replaced by fibrous scar which is mechanically strong but is not as compliant as the original tissue and therefore may compromise normal function.

Hypertrophic scar (HSc) (reviewed in Scott et al., 1994) results from a combined prolongation of the inflammatory phase of wound healing and a high rate of fibroproliferative activity which lead to a perturbation in the balance of components in the extracellular matrix (ECM) of the dermis, possibly influenced by the excessive levels of fibrogenic cytokines such as TGF-ß (Ghahary et al., 1993). This condition is characterized by exuberant amounts of firm scar tissue that is erythematous, itchy, and intolerant to heat. The bulky and inelastic qualities of the scar as well as the frequent occurrence of contractures can severly restrict the mobility of joints and extremities, constrict orifices, and immobilize structures such as eyelids. As well, it can drastically compromise cosmetic appearance (Scott et al., 1994). Risk factors which have been identified include sex, age, race, genetic factors (Castagnoli et al., 1990), and location of the wound (Rockwell et al., 1989). However, it has also been observed that slowly healing burn wounds with prolonged inflammation develop HSc with high frequency regardless of any association with these risk factors (Deitch et al., 1983).

Hypertrophic scar and keloids are two different types of overhealing whose terms are commonly used interchangeably to refer to both conditions. However, the two pathologies which can both occur in healing burn wounds are clearly different in that HSc stays confined to the injured area whereas keloids extend beyond these boundaries. Hypertrophic scar is spontaneously resolved, either partially or completely, within several months to several years from the time of initial injury. This resolution cannot be predicted and is highly variable between patients who are inflicted. Therefore, a better chemical and molecular understanding of the disorder is warranted to help improve methods of treatment both subsequent to the occurence of HSc and hopefully, prior to the initiation of the scar process which would thereby help to avoid the onset of HSc.

B. The Architectural Problem/Chemical Imbalance

The ECM components in HSc appear different in composition and organization from normal skin and normal scar. The first macroscopic observation which clearly demarcates HSc is the significantly thicker dermis and epidermis compared to normal skin. Histological observations within the dermis reveal abnormal qualities of the collagen. Whereas in normal skin the collagen is found organized into fibres and fibre-bundles that run parallel to the surface, these structures are absent in the whorls and nodules of hypertrophic scar in which the collagen is arranged into narrow and widely-spaced fibrils. As well, the center of such nodules appear avascular, whereas networks of small blood vessels can be seen along the outside of these structures. Electron microscopic observations of cross sections of collagen fibrils of normal dermis present round or ovoid structures whereas those of HSc appear irregular and angular (Kischer, 1974). In addition to the qualitative abnormalities observed in the dermal matrix of HSc, quantitative aberrations have also been reported and moreover in the noncollagen component rather than in the collagen itself.

Early chemical characterizations of HSc revealed increased amounts of hexoses, hexosamines, uronic acid, and sialic acid compared to normal skin and normal scar (Shetlar et al., 1971). The total collagen concentration, calculated on a dry weight basis, however, was not found to be significantly different. These pieces of evidence led to the supposition that there are increased proportions of GAGs and glycoproteins in HSc. This was supported by the finding of an 11% increase in the water content of HSc compared to normal skin and normal scar (Bailey et al., 1975). More recent chemical studies on post-burn HSc and mature scars reveal a 12% increase in water content in HSc over normal skin (Scott et al., 1996). As well, the hydroxyproline (and therefore collagen) content was lower by 30% and the uronic acid (found in all GAGs) content was 2.4-fold higher in HSc compared to normal skin. Differences between normal skin and mature post-burn scar were insignificant.

Another component of the ECM whose distribution and abundance is altered in the scar is the glycosaminoglycans (GAGs). These macromolecules (reviewed in Part 1 above) are large polyanionic carbohydrates which contain a high charge density, and therefore, may influence considerably the organization and the functional behavior of different components of the dermal matrix. The principle GAGs found in normal dermis are dermatan sulfate (DS) and hyaluronic acid (HA) with small amounts of chondroitin sulfate (CS) (Shetlar et al., 1981). An altered pattern of GAG distribution was found in HSc where DS was almost absent except in the parallel-fibered areas (Alexander and Donoff, 1980); the quantity of HA was significantly lower (Shetlar et al., 1977, 1981); and higher amounts of CS, particularly C4S, were detected (Shetlar et al., 1972) especially in the nodules (Shetlar et al., 1977).

C. Proteoglycan Expression

More recent reports have focused on the PGs to which these GAGs are attached (except, of course, HA). Immunohistochemical localization of decorin, biglycan, and versican in human post-burn hypertrophic scars, mature scars, and normal skin revealed interesting differences in the patterns between the tissue types studied (Scott et al., 1995). Decorin was the only PG of these three that was detected abundantly in normal dermis, with no detectable staining for biglycan or versican. Some versican was seen in the epidermis. In HSc tissue samples, biglycan and versican seemed to be much more abundant; decorin, however, was almost absent from the dermis of HSc with only some detectable in a narrow region below the epidermis and in the deep dermis. Interestingly, staining for versican showed a reciprocal pattern compared to that for decorin with staining throughout the dermis except in the regions where decorin appeared. In the mature scar, both biglycan and versican stained very sparsely except for abundant amounts of versican in the epidermis. In contrast, decorin was visible throughout the dermis at levels which appeared to approach that of normal skin.

An intensive chemical characterization of samples of HSc, mature scar, and normal skin provided a quantitative measure of the differences in expression of these three PGs between these tissue types (Scott et al., 1996). Biglycan and versican were purified from a biopsy of HSc, and decorin from a biopsy of normal skin. These samples were then used in an inhibition ELISA to quantify the amounts of these PGs isolated in the total PG pools by DEAE-Sephacel chromatography. The decorin contents of HSc samples were found to be a striking 25% of that of normal skin. The amounts of biglycan and versican, however, were each found to be about 6-fold higher in HSc samples. The differences found between mature scar and normal skin were insignificant.

D. Cytokine Expression

The matrix of hypertrophic scar is an active, healing environment in which the production of connective tissue components differs from that in normal wound healing environments. The signals that lead to such an irregular pattern of events need elucidation to better understand the etiology of this disorder. These signals are mainly provided by a group of molecules called growth factors or cytokines. Particularly important to fibrotic disorders are those growth factors which affect the growth and behavior of fibroblasts. Growth factors that may be mitogenic or chemotactic for fibroblasts and, through these actions or other pathways, stimulate the production of ECM components, have been termed fibrogenic cytokines (Kovacs, 1991). These include platelet-derived growth factor (PDGF), the fibroblast growth factors (FGFs), epidermal growth factor (EGF), interleukin 1 (IL-1), the insulin-like growth factors (IGFs), and the transforming growth factors (TGFs). The interferons (IFNs), on the other hand, are anti-fibrogenic in that they inhibit the proliferation of fibroblasts and connective tissue production and therefore have been utilized as therapeutic agents.

PDGF is a mitogen and a chemoattractant for fibroblasts (Antoniades et al., 1982). It is produced primarily by platelets (Ross et al., 1974; Kohler and Lipton, 1974) although other sources include activated macrophages (Shimokado et al., 1985) and endothelial cells (DiCorleto and Bowen-Pope, 1983). Normal fibroblasts express only receptors for PDGF but are stimulated to produce PDGF as well during injury (Antoniades et al., 1991). PDGF is known to accelerate wound healing in animal models (Scott et al., 1994) but the effects of this cytokine have not been studied extensively in relation to HSc.

FGFs are of two kinds: acidic and basic (Esch et al, 1985). Basic FGF is the form which is more widely distributed but they were both found to be mitogens for fibroblasts (Gospodarowicz et al., 1986). It is produced by activated macrophages (Baird et al., 1985) and endothelial cells (Vlodavsky et al., 1987) which indicate its importance in stimulating the formation of granulation tissue and in neovascularization of normal healing wounds (Scott et al., 1994). However, there are no studies of the importance of this cytokine in HSc.

EGF is a potent mitogen for fibroblasts but displays no chemoattractive properties for these cells (Seppa et al., 1982). It is known to be a strong inducer of neovascularization as well as to cause fibroblast proliferation and collagen accumulation in rats (Buckley et al., 1985). Later studies, however, found that in cultured human skin fibroblasts, EGF inhibited collagen production in a dose-dependent manner (Hata et al., 1988). The ability of EGF to stimulate connective tissue accumulation is, therefore, thought to be secondary to its fibroproliferative potential. No studies have implicated EGF in the development of HSc.

IGFs are also of two known forms: IGF-1 and IGF-2. IGF-1 is mitogenic and has been demonstrated to increase the synthesis of certain PGs by chondrocytes (Makower et al., 1988) and collagen by fibroblasts (Spencer et al., 1988). Its effects on wound healing appear to be the result of the simultaneous presence of PDGF (Lynch et al., 1987). Although research into the role of IGFs in HSc is not extensive, a recent report indicates that fibroblasts explanted from HSc tissue appear to contain more mRNA for IGF-1 transcript than those of normal skin (Ghahary et al., 1995).

TGFs are again, also, of two known forms, namely TGF-α and TGF-ß. TGF-ß is a potent chemoattractant for fibroblasts and has been shown to be powerful fibroproliferative agent. TGF-ß, in its three main isoforms, have been studied more extensively compared to the above mentioned cytokines in the wound healing environment and in HSc. A separate, yet brief, overview of this cytokine, its distribution and functions, and the regulation of its expression is offered below.

II. Transforming Growth Factor Beta 1

A. Protein Characteristics

TGF-ß belongs to a superfamily of signalling peptides that includes Mullerian inhibiting substance, the *decapentaplegic* gene product in *Drosophila* (DPP-C), the bone morphogenic proteins, and a family of proteins which include the developmental regulators activin and inhibin. These proteins do not display any sequence homology to any other known growth factors. However, they share between 23% and 40% sequence identity in their C-terminal portions which includes seven conserved cysteine residues. They also all occur as 25kDa disulfide-linked dimers (reviewed in Ghahary et al., 1996).

There are five known isoforms of TGF-ß, TGF-ß1-5, of which only TGF-ß1, 2, and 3 are found in mammals. These polypeptides share between 70% and 80% sequence identity and the mature form of each member is highly conserved among species. TGF-ß isoforms are synthesized as a precursor protein which is about 390-412 amino acids in length. A 4-5 amino acid processing site as well as a 20-23 amino acid signal peptide occur at its N-terminus (Derynck et al., 1985). Signal peptidase and proteolytic cleavage are responsible for processing this precursor peptide down to its mature monomeric form of 112 amino acids (Wakefield et al., 1988). The biologically active form of TGF-ß occurs as a dimer of two monomeric molecules linked by a single disulfide bond at Cys 77 of both monomers.

B. Latent vs. Active TGF-ß

TGF-ß is secreted as a large, latent molecule of about 75kDa consisting of the disulfide-linked dimer and a dimeric N-terminal peptide or latency associated peptide (LAP). The TGF-ß dimer and the LAP are translated together as a precursor peptide (Tsuji et al., 1990). Certain cell types, for example fibroblasts, platelets, and bone cells, secrete a TGF-ß-LAP complex which is also associated covalently with another large protein called the latent TGF-ß binding protein (LTBP) which can be between 125kDa to 205kDa depending on where it is found (Dallas et al., 1994; Moren et al., 1994). The LTBP is not involved in maintaining the latency of TGF-ß; this function is reserved for the LAP. Although its function is yet to be elucidated, the LTBP is thought to help target the latent complex to structures responsible for its activation.

The activation of TGF-ß has been shown to occur by a number of different mechanisms including the complete dissociation of the LAP or a conformational change of the latent complex to reveal the binding site of TGF-ß for its receptor(s).

C. TGF-ß Receptors

Six receptors have been identified for TGF-ß: TGF-ß receptor types I - VI. Types I - III are most widely distributed and are found on most cells which appear to respond in some way to TGF-ß (Segarini et al., 1989). Studies using iodinated TGF-ß1 have shown high affinities for these receptors with dissociation constants of 5-25 picomolar for the types I and II receptors and 200 picomolar for type III. The affinity of each isoform for each receptor types is different with TGF-ß1 having a higher affinity for receptor types I and II than TGF-ß2 and all isoforms displaying similar affinities for receptor type III.

The type I and II receptors are transmembrane proteins which are members of the serine/threonine receptor-kinase family. The type II receptor has a short, N-terminal, cysteine-rich extracellular domain with a long, C-terminal cytoplasmic region which harbors its serine/threonine kinase domain (Ebner et al., 1993). The type I receptor is different from type II in that its cytoplasmic domain is shorter and contains in its juxtamembrane position a GS domain (Ser-Gly-Ser-Gly-Ser-Gly-Leu-Pro motif). As well, the extracellular domain of the type I receptor is short and contains a short cysteine cluster in its juxtamembrane domain. The type III receptor is a heparan sulfate/chondroitin sulfate proteoglycan also called betaglycan. It is found in both soluble and cell membrane associated forms (Andres et al., 1989). Its large extracellular domain contains its N-terminus and harbors one GAG attachment site. Its C-terminus is inserted in the cell membrane and it has a very short cytoplasmic domain of only 41 amino acids with no known signalling function (Gougos et al., 1992).

The TGF-ß receptors have been reported to associate with one another in biological membranes and certain interactions have been found to be necessary for signal transduction. Whereas the type II receptor binds ligand independently, the type I receptor needs coexpression with II in order to bind TGF-ß (Wrana et al., 1994). Other studies revealed that types I and II can form stable heterooligomers, whereas types I, II and III can all form stable homooligomers in cell membranes in the presence or absence of biologically active ligand (Chen and Derynck, 1994; Franzen et al., 1993).

Experiments conducted with chimeric constructs containing different combinations of the internal and external domains of types I and II receptors expressed in mutant Mu1Lv cells revealed that direct interactions between the intracellular domains of I and II were necessary for signal transduction (Okadome et al., 1994). The homomeric associations of type I receptors or of the intracellular domains of type II receptors were incapable of transducing any signal in the presence of active ligand.

Betaglycan is hypothesized to present ligand to signaling receptors and may also serve as a reservoir for the ligand on the cell membrane. This suggestion comes in the light of evidence which shows a higher affinity of the type II receptor for TGF-ß when types II and III are co-expressed than when type II is alone (Lopez-Casillas et al., 1991). An interesting possibility is that betaglycan may bind to, and alter the configuration of, latent TGF-ß. This may result in the activation of TGF-ß before its presentation to its receptors.

D. Distribution and Functions

TGF-ß has a widespread distribution throughout the body with effects on many different cell types and many different physiological processes. To appreciate its multitudinous effects, a number of factors need to be addressed including the type and state of differentiation of the affected cell types, the presence and local concentration of activators and inhibitors including ECM components, receptor types and concentrations, its structure in the latency complex, and the presence of other growth factors (Pannu, 1995). Its most significant effects *in vitro* are on mesenchymal cells, epithelial cells, and hematopoetic cells. Through its effects on mesenchymal cells TGF-ß is a significant contributor to the regulation of ECM production (Roberts and Sporn, 1990).

TGF-ß increases transcription of mRNAs for matrix components and proteinase inhibitors such as plasminogen activator inhibitor and tissue inhibitor of metalloproteinases (TIMP) (Edwards et al., 1987). Conversely, it down-regulates the synthesis of proteolytic enzymes such as cysteine protease, serine proteinases, plasminogen activator, collagenase, elastase, cathepsin L, and transin/stromelysin which degrade ECM elements and increase the production of cellular receptors for matrix proteins (Chiang and Nilsen-Hamilton, 1986; Laiho et al., 1990; Lund et al., 1986; Overall et al., 1989; Matrisian et al., 1986). TGF-ß has been found to increase the production of collagens types I, III, IV, and V as well as thrombospondin, certain DS- and CS-PGS, and the secreted protein acidic and rich in cysteine (SPARC) glycoprotein (Rossi et al., 1988; Madri et al., 1988; Pentinnen et al., 1988; Westergren-Thorsson et al., 1991; Reed et al., 1994). It has also been found to decrease the production of decorin (Kahari et al., 1991). TGF-ß also exerts its effects sometimes with the help of other growth factors and this was observed with the reciprocal effect of TGF-ß on collagenase and TIMP which needs the presence of bFGF and EGF. As well, other growth factors such as angiotensin II use TGF-ß to perform their functions.

Therefore, TGF-ß has considerable effects on the regulation of the biosynthesis and the degradation of many matrix and matrix-associated components with the overall result of accumulation of extracellular matrix.

Different regulatory mechanisms are affected by TGF-ß, in addition to increasing transcription, to achieve these effects. TGF-ß has been reported to enhance the activity of the mouse a2(1) collagen promoter and the fibronectin promoter, possibly through the nuclear factor-1 (NF-1) transcription factor (Rossi et al., 1988; Dean et al., 1988). Other mechanisms include the stabilization of transcript as is seen for the effect of TGF-ß on collagen I, III, and V and fibronectin mRNA expression (Ignotz et al., 1987).

The general outcome of the effects of TGF-ß in connective tissues, then, is the accumulation of matrix components and hence scar production. This is accomplished through the induction of fibroblast production of collagen, fibronectin, and PG synthesis (Sporn et al., 1987); as well, it enhances neovascularization (Allen et al., 1991) and modulates the production of some proteases and their inhibitors (Overall et al., 1989; Edwards et al., 1987). Collagen type I upregulation by TGF-ß has been demonstrated in normal fibroblasts (Ignotz et al., 1987); as well, this effect has been demonstrated in fibrotic disorders of the liver and in fibroproliferative disorders such as scleroderma, myelofibrosis, intraocular and pulmonary fibrosis. Additionally, cross sections of hypertrophic scars were found, immunohistochemically, to contain more TGF-ß protein than normal skin and the scar tissue was found to contain a higher level of transcipt as well (Ghahary, et al., 1993). Interestingly, most of the TGF-ß protein was localized to the perivascular and nodular areas of the scar.

The effects of TGF-ß were further realized through studies which used specific antibodies to this cytokine to antagonize its functions. This tool was used to block the progression of arthritis, glomerulonephritis, and pulmonary fibrosis in animal models. Isoform specific neutralizing antibodies to TGF-ß1 and TGF-ß2 were administered to dermal wounds in Sprague-Dawley rats during the healing process which resulted in a reduced level of collagen deposition; however, the tensile strength of the reconstituted tissue was unaffected and the healing process was more regenerative than fibrotic (Shah et al., 1992). In the rats with the anti-TGF-ß antibodies, the neodermal architecture was more like that of normal dermis. This is also the case in fetal or embryonic wounds in which are found higher amounts of TGF-ß than adult healing wounds (Longaker et al., 1994), but which heal with no scars unless supplied with exogenous TGF-ß. It is probable, and therefore tempting to suggest, that in fetal tissue there must be a higher concentration of neutralizing molecules for TGF-ß expressed.

Studies which have focused on localizing specific isoforms of TGF-ß have provided evidence for a functional significance for the differential regulation of the different isoforms of this cytokine. TGF-ß1 appears to be expressed in constant quantities regardless of the outcome of a healing wound; however, TGF-ß2 levels change and appear highest in those wounds that heal with no scar (Longaker et al., 1994). Such studies suggest the important role of TGF-ß in controlling cell proliferation and function. As well, they call attention to the mechanisms which regulate this growth factor. In a normal, static environment as well in a normal wound healing situation, the expression and activity of the different isoforms of TGF-ß must be highly regulated involving proteins which bind and alter its activity as well as factors which control transcription and translation. One can appreciate that dysregulation of specific isoforms of TGF-ß could result in many pathologies characterized by excessive matrix production. Therefore, a brief overview of the transcriptional regulation of TGF-ß, especially TGF-ß1, will be considered below.

E. Regulation

Since the initial identification of transforming growth factors as substances that promote anchorage-independent growth of normal rat kidney (NRK) fibroblasts (DeLarco and Todaro, 1978), research flourished to reveal the different kinds of TGFs that exist, in which environments they are found, their effects on different cell types and different physiological systems, and factors which affect their activity. These studies mainly attempted to elucidate the mechanisms of action and regulation of TGFs, particularly TGF-ß, at the protein level. TGF-ß1 was eventually discovered, however, to increase the steady-state level of its own message in different normal and transformed cultured cells (Van Obberghen-Schilling, et al., 1988); therefore, it could autoinduce its own expression. Additionally, viral transformation was accompanied by increased expression of transcript

(Jakolew, et al., 1988) and protein (Anzano, et al., 1985) for TGF-ß1. Studies in the developing mouse embryo demonstrated a type of regulation for TGF-ß1 that was developmental in nature considering that the cytokine showed a tissue-specific and time-dependent localization.

Characterization of the promoter region of the human TGF-ß1 gene (Kim et al., 1989) has provided a deeper understanding of the regulation of TGF-ß. A human leukocyte genomic DNA library was used to isolate the 5' end of the human TGF-ß1 gene. Using S1 nuclease protection assay with an end-labeled probe extending from nucleotide -453 to nucleotide +727 of the TGF-ß1 gene, at least five S1 nuclease-resistant fragments were found. Of these, two were most prominent and they were 727bp and 457bp long. This indicated that one major site of transcript initiation occurred at the 5'-most end of the TGF-ß1 cDNA whereas the other major site occurred about 270bp downstream from the first site. These sites were confirmed using primer extension analysis.

Many interesting observations were made of the sequences 5' to the two major transcription initiation sites designated as +1 and +271. Firstly, there are no conventional "TATA" or "CAAT" boxes contained in these regions. Secondly, the sequence between nucleotides -262 and -1, which contains the putative promoter, are extremely G+C rich (80%); furthermore, nine hexanucleotide repeats (CCGCCC or GGGCGG) were found 5' to the first initiation site and two more in the region between the two initiation sites. Sequences such as these have been found in viral promoters and in promoters of cellular housekeeping genes. Additionally, seven putative binding sites for the SP1 transcription factor (GGGGCGG and its reverse complement) were identified between nucleotides -236 and +175. Thirdly, a sequence homologous to the fat-specific element (FSE2), which has been reported to act as a negative regulatory element in preadipocyes, was found twice, and its reverse complement once, 5' to the first initiation site. Its activity as a negative element was confirmed by assaying for CAT activity using a TGF-ß1-CAT chimera containing this region fused to the coding region of the CAT gene (see below for explanation). Its actual function in the TGF-ß1 promoter has yet to be determined. The reverse complement of the putative sequence for the nuclear factor 1 (NF-1) was also found 5' to the first initiation site. As mentioned above, NF-1 has been found to be involved in the transcriptional activation of mouse a2(I) collagen promoter by TGF-ß1 and therefore its presence in the TGF-ß1 promoter may indicate a mechanism by which TGF-ß1 upregulates itself. Finally, the consensus sequence for the AP-1 transcription factor was also found twice 5' to the first initiation site. The significance of this will be discussed below.

A deletion analysis was also carried out in this study to decipher which regions of the promoter were absolutely essential for transcription. Chimeric gene constructs were made by fusing varying lengths of the 5'-flanking regions of both of the transcription initiation sites to the coding region of the bacterial chloramphenicol acetyltransferase (CAT) gene in an expression vector. These chimeras were then transfected into different cell types and relative CAT activities were measured as an indication of the level of promoter activity in the different regions of the TGF-ß1promoter. The results revealed, with respect to the region 5' to the first initiation site, two negative regulatory regions which efficiently repress transcriptional activity. Furthermore, an enhancer-like element was found between the two negative regulatory regions. As well, the authors of the study identify the DNA sequences responsible for the cell-specific expression of the TGF-ß1 to be between -483 and -175. With respect to the region 5' to the second intitiation site, one portion was found to have as strong a promoter activity as the strongest portion 5' to the first initiation site. This confirms the presence of two major sites of transcript initiation in the TGF-ß1 gene each with their separate promoters which may then be regulated differently and therefore contribute to the complex pattern of regulation of TGF-ß1 expression.

The AP-1 site was later found to be of fundamental importance to the regulation of TGF-ß1. In a very thorough study conducted by Kim and co-workers (1990) using the chimeric constructs previously established, the autoinduction of TGF-ß1 was found to involve the AP-1 complex. The CAT constructs were transfected into human lung adenocarcinoma cells and grown with and without added TGF-ß1; as well the constructs were cotransfected into embryonal carcinoma cells (which produce Fos only when induced and produce no Jun) together with an expression vector that produced either wild-type Jun/AP-1 protein or a mutated form that cannot bind DNA. The promoter regions which appeared to be induced by TGF-ß1 were also transactivated by Jun. As well, both TGF-ß1 inducibility and Jun transactivation disappeared together due to the presence of a negative regulator in some promoter regions. Analysis by RNase protection of the mRNA produced by the embryonal carcinoma cells when cotransfected with wild-type Jun/AP-1 expression vector together with TGF-ß1-CAT constructs containing active promoter regions from areas 5' to both initiation sites, revealed that CAT expression increased only when wild-type Jun/AP-1 was expressed. Interestingly, when the TGF-ß1-CAT chimeric genes were cotransfected with vectors expressing either antisense c-*jun* or antisense c-*fos*, the CAT activity, which was induced by the two putative promoter regions under the influence of TGF-ß1, was abrogated. The promoter regions studied which were sensitive to autoinduction and transactivation by AP-1 components were verified to be AP-1 binding sites by DNase I footprinting. This analysis revealed one high-affinity AP-1 binding site 5' to the first initiation site and two low-affinity sites in the second promoter. Taken together, these data provide strong evidence to suggest that the autoinduction of TGF-ß1 is mediated by AP-1 binding sites in the TGF-ß1 promoters.

The importance of the AP-1 site in the regulation of TGF-ß1 expression was further appreciated in a later study which found a role for the src protein in the transcriptional regulation of the TGF-ß1 gene (Birchenall-Roberts, et. al., 1990). Plasmids containing various regions of the two putative promoters of TGF-ß1 fused to the CAT gene were cotransfected with expression vectors containing the genes c-*src* or v-*src*. Only cotransfection with v-*src* resulted in a dramatic increase in TGF-ß1 expression. Therefore, pp60$^{v\text{-}src}$ can regulate TGF-ß1 expression and this was demonstrated in various cell types. As well, this effect was mediated by regions of both of the promoters of the TGF-ß1 gene. In an attempt to elucidate the specific promoter regions responsible for the transactivation by pp60$^{v\text{-}src}$, deletion plasmids containing sequences 5' to both promoters were cotransfected with an expression vector for v-*src*. The region from the first promoter which showed the highest induction of CAT activity contained an AP-1 site, indicating the involvement of AP-1 in the transactivation regulation of TGF-ß1 expression by v-*src*. However, those regions not containing an AP-1 site still induced some CAT activity, indicating that other elements were also involved in this regulation. For the second promoter, constructs containing no AP-1 sites induced CAT activity very close to basal levels whereas those containing AP-1 sites showed a drastic increase in induction indicating that v-*src* regulation of this TGF-ß1 promoter has to be mediated through the AP-1 site.

The functions of TGF-ß also include control over cell cycle progression. TGF-ß isoforms have been implicated in arresting growth at late G$_1$ phase of the cell cycle (Silberstein and Daniel, 1987). Therefore, it is likely that other cell-cycle regulatory factors contribute to the overall regulation of TGF-ß expression. The retinoblastoma gene product (RB) was found to do just that. RB remains mainly underphosphorylated during G$_0$ and G$_1$ phases of the cell cycle but undergoes phosphorylation at several sites as cells progress to the S phase from G$_1$ (Mihara et al., 1989). TGF-ß was shown to influence this process as it was able to inhibit phosphorylation of RB and keep it in its growth-suppressive state (Laiho et al, 1990). The relationship between these two factors became even more interesting when RB was demonstrated to down-regulate the activity of AP-1 (Robbins et al., 1990) and this was found to occur through a cis-acting element, the RB control element (RCE), found in the c-*fos* promoter. This RCE is also found in the TGF-ß1 gene and its potency was verified by deletion anaysis in which various regions of the TGF-ß1 promoter fused to the CAT gene were cotransfected with an expression plasmid for RB into mink lung epithelial cells (CCL-64) (Kim et al., 1991). The presence of RB was found to induce promoter activity except when a certain region became deleted and this region harbored sequences similar to RCEs found in the c-*fos* promoter. In fact multiple copies of these RCE-like sequences were found in the TGF-ß1 gene in both direct and inverted forms.

The induction of c-*fos* transcription by RB was also demonstrated in the same cell type (Kim et al., 1991) but these results were opposite to those reported in NIH-3T3 cells (Robbins et al., 1990). This cell-type specific behavior was demonstrated to occur with the effects of RB on TGF-ß1 promoter activity as CAT constructs containing the TGF-ß1 promoter harboring RCEs cotransfected with an RB expression plasmid demonstrated the induction of TGF-ß1 promoter activity in CCL-64 and A-549 cells but a repression in NIH-3T3 and AKR-2B cells. Therefore, it appears that in cell types where RB downregulates c-*fos* transcription, it also does the same to TGF-ß1 transcription and *vice versa*. A regulatory loop is apparent here in which TGF-ß1 keeps RB in its underphosphorylated state and underphosphorylated RB (Kim et al., 1991) influences the activity of the TGF-ß1 promoter. Of interest also is that in cell types in which this regulatory loop produces more TGF-ß1, namely CCL-64 and A-549, TGF-ß1 is also known to strongly inhibit growth. Therefore, together, RB and TGF-ß1 may play a role in the suppression of tumorigenesis.

TGF-ß1 gene expression was also studied in response to the effects of the transcriptional factor SP1 (Geiser et al., 1993). This study was conducted in a cell culture system in which background SP1 expression was negligible. When the complete mouse TGF-ß1 promoter region fused to CAT gene was cotransfected with an expression plasmid for human SP1, CAT activity was induced by SP1. Furthermore, when deletion constructs of this TGF-ß1 promoter were tested, SP1 was found to stimulate transcription with increasing effectiveness as the promoter regions increased to include more SP1 sites. Therefore, synergistic activation of the TGF-ß1 promoter using different SP1 sites is a possibility. Interestingly, CAT constructs containing promoter regions from TGF-ß2 and TGF-ß3 were also tested for their responsiveness to SP1; only the -ß3 promoter responded to SP1 expression. This is understandable considering that only TGF-ß2 does not contain the consensus sequence for SP1. Such a study sheds light on one possible mechanism by which differential regulation of the three isoforms of TGF-ß occurs.

Hitherto, regulatory factors affecting TGF-ß expression which have been elucidated present mainly potential mechanisms to upregulate TGF-ß expression. RB is one of only a few factors which affect expression in the opposite manner but even this factor has not been demonstrated to obliterate TGF-ß expression. With such a potent cytokine whose function is so widespread and whose disregulation leads to devastating pathologies, the elucidation of mechanisms which control the expression of this cytokine is of vital importance.

Another interesting mechanism which has not been very widely studied but, nonetheless, has been reported on involves antisense transcript. Although broadly accepted as a mode of gene regulation in prokaryotic systems, its importance in eukaryotes is only beginning to emerge. Two very interesting studies in this regard involve the observation of antisense transcripts for the bFGF gene and for the TGF-ß3 gene. Considering the actions of regulatory factors which differentially affect only -ß1 and -ß3 expression such as SP1, it is tempting to suggest that the control mechanism responsible for production of the reported TGF-ß3 antisense transcript might produce antisense to TGF-ß1 as well.

F. Expression in HSc

The expression of TGF-ß1 in hypertrophic scar seems to be disregulated, possibly involving one of the mechanisms mentioned above. Its expression was studied immunohistochemically in HSc sections and compared to mature scar and normal skin (Scott et al., 1995). No staining for TGF-ß1 was detected in normal skin and this was slightly altered in HSc with only minimal expression in the nodular areas and in the deep dermis. Mature scar, however, stained strongly for TGF-ß1 throughout the dermis except for a thin zone in the papillary dermis adjacent to the epidermis. Interestingly, staining for the PG decorin in sections of the same scars showed a similar pattern. This apparent codistribution of TGF-ß1 and decorin could implicate the interaction of the two proteins in HSc tissue, considering previous reports of this type of association, as a method for regulating the activity of TGF-ß1.

III. Decorin

A. Role in Collagen Assembly/Architecture

The association between collagen and proteoglycans has been examined in fibrous connective tissues of many vertebrate and invertebrate species (Scott, JE., et al., 1981; Scott, JE., 1988; Van Kuppevelt et al., 1987; Trotter and Koob, 1989). This evolutionarily conserved phenomenon demonstrates the importance of PGs in the collagen network. Decorin, in particular, through previous studies, has been demonstrated to be an important contributor to the proper organization of collagen fibers. Electron microscopy studies have shown the presence of dermatan sulphate chains in regular orthogonal arrays on collagen fibrils (Scott and Haigh, 1985); moreover, it has been proposed from such studies that antiparallel dermatan sulphate duplexes may form between pairs of protein cores on adjacent fibrils to strengthen the interaction between fibrils (Scott, JE., 1993). As well, binding studies have revealed specific binding sites on fibrillar collagens for decorin (Hedbom and Heinegard, 1993). Furthermore, studies which examined fibrillogenesis of collagen, *in vitro*, by measuring the turbidity of soluble collagen upon warming found an inhibition of fibrillogenesis in the presence of decorin (Vogel et al., 1984); however, turbidity levels in the presence of this PG did eventually reach the same levels as the controls (Vogel and Trotter, 1987). This result was found with collagen that was isolated from different species. And recently, a binding site for type I collagen was mapped to leucine-rich repeats 4-5 of the core protein of decorin (Svensson et al., 1995). The presence of decorin early in the wound healing process, therefore, seems vitally important to establish the proper conditions for collagen fiber regeneration. When bound to the fibrils during fiber growth and assembly, decorin may establish and sustain the proper spacing and regular interaction of collagen fibrils through protein-protein and GAG-GAG interactions. These interactions may also regulate the extent of contraction that collagen fibrils are involved in during the wound healing process. The absence of this PG, therefore, early after severe burn injury may result in the abnormal arrangement of collagen fibrils into the whorls and nodules seen in HSc.

B. A Sink for Growth Factors

In addition to its hypothesized function in collagen architecture, decorin has also been reported to bind to and regulate the activity of TGF-ß (refer to Part 1). Considering that excessive levels of TGF-ß1 have been found in a number of fibrotic disorders, the expression of decorin may be critical to control excessive levels of active TGF-ß. Decorin may even bind to abundant amounts of this cytokine and keep it in a matrix reservoir. In this case, one would expect to find these two proteins colocalizing in tissue, especially during the wound healing process where TGF-ß plays a vital fibroregenerative role. This is true for post-burn mature scars in which immunohistochemical staining for TGF-ß1 and decorin revealed colocalization for the two proteins (Scott et al., 1995) as well as for tissue from cirrhotic liver (Krull et al., 1993). Whereas decorin demonstrates control over the activity of TGF-ß, TGF-ß in turn appears to exert transcriptional control over the expression of decorin. This will be discussed in more detail below when we address the regulation of the expression of the decorin gene.

C. Regulation of Expression

Early reports of the effects of TGF-ß on decorin expression appear to be inconsistent. Bassols and Massague (1988) reported an apparent upregulation in the expression of decorin in response to TGF-ß. However, their identification of decorin is questionable. Contrary to this, Kahari and coworkers (1991) reported an inhibitory effect of TGF-ß1 on the production of decorin by human dermal fibroblasts. Since then many reports have revealed a stimulatory as well as an inhibitory effect of TGF-ß on the expression of this PG (Westergren-Thorsson et al.,1992); it appears that the regulation of decorin expression by TGF-ß is dependent on the cell type affected as well as the local milieu.

The human decorin gene promoter was later characterized (Santra et al., 1994) and found to contain a TGF-ß-negative element, the sequence of which corresponded to a consensus sequence found in the promoter region of transin/stromelysin (GnnTTGGtGa) and whose expression was mediated by the proto-oncogene product c-Fos (Kerr et al., 1990). Several other regions were also identified in the promoter with putative binding sites for transcription factors as well as consensus sequences for promoter activity (Santra et al., 1994). Whereas two promoter regions, Ia and Ib, were originally identified in the decorin gene (Danielson et al., 1993); later evidence demonstrated that promoter activity resides only in Ib (Santra et al., 1994).

Computer-assisted analysis of the sequence of Ib presented many interesting findings including two TATA-like motifs (TATAAT and TTTAAA) and a CAAT box very close to the transcriptional initiation site. More distal to these regions were found two cis-acting motifs, AP5 and AP1. Two direct repeats, in tandem, were found just upstream of the AP5 site; this sequence harbored the consensus site recognized by NF-kB (GGGACT) which is suggested by the authors to be a possible mechanism by which interleukin-1 enhances transcription of decorin (Heino et al., 1988).

In the most distal 5' portion of the promoter a 150bp region was identified which consisted entirely of homopyrimidine residues (CT) within which was found two direct repeats. This region was shown to be sensitive to S1 nuclease digestion. This stretch of pyrimidine residues in the coding strand means that in the noncoding strand there must be a complementary stretch of purine residues (GA). The significance of this pyr/pur stretch lies in the hairpin triplex structure that they form which is referred to as the H form of DNA (Mirkin et al., 1987; Wells et al., 1988). This form of DNA involves a strand of pyrimidine residues some of which forms normal Watson-Crick pairs with a stretch of purine residues but the rest of which folds back on the purine strand resulting in a triplex stem of CGC and TAT triplets, a loop of pyrimidine residues, and a stretch of purine residues that are not paired. This stretch of unpaired purine residues is the region which is most likely the target of the S1 nuclease. The authors suggest that this pyr/pur stretch in the decorin gene could be involved in making the chromatin "active" for transcriptional activity by acting as cis-active motifs which bind specific DNA-binding proteins involved in transcription. When the activity of different regions of the promoter was analyzed by deletion analysis utilizing various decorin promoter-CAT fusion constructs, promoter regions containing more of the pyr/pur stretch were found to induce more activity. Interestingly enough, when promoter constructs were extended to include the TGF-ß-negative element, promoter activity decreased.

Another regulatory mechanism may play a critical role in the abundant expression of decorin in human colon cancer (Adany et al., 1990) (refer to Part 1). In this study, genomic DNA of normal colon and colon carcinoma tissue which was digested with methylation-sensitive restriction endonucleases and probed with a probe for decorin revealed that certain cytosines were hypomethylated in the tumor tissue but not in the normal tissue. The degree of hypomethylation of the decorin gene was estimated to be three-fold higher in the carcinoma tissue than in normal colon. This finding was very important since the degree of methylation of some genes has been previously linked to their expression (Bird, 1986).

The growth phase of a cell was recently found to be another factor affecting the level of decorin gene expression (Mauviel et al., 1995). Total RNA extracted from normal human fibroblasts at various time points before and after reaching confluency was analyzed by northern blotting and a cDNA probe for decorin and revealed a significant increase in decorin expression (about 8-fold) 8 days after reaching confluency. This effect continued at 16 days postconfluency. Nuclear proteins were then extracted from fibroblasts and tested for their ability to drive transcription off the decorin gene using plasmid constructs containing various regions of the decorin promoter. The amount of transcript generated was significantly elevated with nuclear extracts obtained from confluent cells compared to that from proliferating cells. This result was not dependent on which deletion construct of the decorin promoter was used and therefore the smallest region used (-140bp to +1bp) was considered to be involved in a phenomenon that was described as a transcriptionally up-regulated expression of the decorin gene during quiescence. To further correlate the elevated gene expression with growth arrest, a decorin promoter-CAT construct containing only the 140bp of the promoter (as mentioned above) was transfected into proliferating and confluent fibroblast cultures; CAT activity was significantly higher in the confluent cells.

The effects of TNF-α and TGF-ß on the up-regulation of decorin expression during quiescence was further revealed in the same study. By northern analysis of total RNA extracted from proliferating and normal fibroblasts grown in the absence and presence of TNF-α, this cytokine was shown to inhibit decorin expression by up to 60% in confluent cells with no effect on proliferating cells. This inhibition was confirmed to occur at the transcriptional level as nuclear extracts from confluent cells grown in the absence of this cytokine were found to drive transcription off a decorin promoter at significantly elevated levels compared to that from cells grown in the presence of TNF-α. By northern analysis, TGF-ß was found to similarly reduce decorin expression by up to 60%; there was, however, an additive effect of both cytokines used together where decorin mRNA levels were found to be only 10% of control values. In this study, the response element that was responsible for mediating the effects of TNF-α-induced inhibition of decorin expression, the TNFRE, was mapped to a region in the first exon of the 5'-untranslated region of the decorin gene.

D. Expression in HSc

The altered levels of decorin in hypertrophic scar, compared to normal scar and normal skin, have been well established. Previous immunohistochemical (Scott, PG., 1995) and biochemical (Scott, PG., 1996) analyses of hypertrophic scar, mature scar, and normal skin have demonstrated lower levels of decorin protein in the former as compared to normal skin and mature scar. Except for the deep dermis and a small region below the epidermis, decorin is virtually absent in the dermis of HSc but reappears in mature scars. In contrast, decorin is found abundantly in normal skin. The relative amount of decorin in hypertrophic scar tissue, which was quantitated by inhibition ELISA, was found to be only 25% of that found in normal skin. What exactly regulates the expression of decorin in hypertrophic scar has not been discerned and any one or a combination of any of the regulatory mechanisms discussed above may be involved. This requires further investigation so as to better understand the uncontrolled signals in the wound healing process which lead to the perturbation in the balance of ECM components in HSc.

IV. Thesis Rationale

In the dermis of skin, decorin may be able to bind TGF-ß1 and selectively inactivate it (Hausser et al., 1994). As well, this PG may act as a reservoir for this growth factor in the extracellular matrix. Excessive amounts of TGF-ß1 in hypertrophic scar (Ghahary et al., 1993), however, may serve to inhibit the production of decorin which then results in the excessive and uncontrolled activity of this growth factor in HSc. A negative regulatory loop is apparent where TGF-ß inhibits decorin production and low levels of decorin allow for more uncontrolled activity of TGF-ß. The combination of the absence of decorin to integrate into newly forming collagen fibrils and the excessive levels of TGF-ß which can upregulate the production of many ECM components and inhibit the degradation of others, leads to an uncontrolled environment such as the fibrotic condition of hypertrophic scar.

It is not known whether the altered expression of decorin in HSc is due to regulation at the transcriptional, translational, or post-translational levels, ie. whether there is deficient production, incomplete production, or enhanced degradation of the PG. As discussed above, decorin has been localized in the scar primarily to the deep dermis with a striking absence from the nodular and whorl-like areas of the dermis (Scott et al., 1995). In contrast, decorin is found abundantly throughout the dermis of normal skin. TGF-ß1 has similarly been colocalized to the same region of the deep dermis in the scar as well as minor amounts in other regions of the dermis. Although increased mRNA levels have been previously reported for TGF-ß1 in HSc (Ghahary et al., 1993), the expression of this cytokine has not been localized to any particular area of the dermal component of the scar. As well, it is not known whether fibroblasts in the local milieu of the scar are the major source of this cytokine or whether another cell type or sytemic sources (Pannu, 1995) are major contributors. If this cytokine is not produced locally, it may be delivered to the wound site and stored in a reservoir in the matrix until required. In the absence of sufficient levels of this reservoir, the activity of TGF-ß1 could become unregulated leading to the uncontrolled environment of the scar.

In this study, the pattern of expression of decorin and TGF-ß1 mRNA was studied in post-burn hypertrophic scar, post-burn mature scar, and normal skin by*in situ* hybridization using cRNA probes labeled with digoxigenin-11-UTP. It is hoped that the findings of this study will provide convincing evidence with which to start addressing the issues discussed above.

CHAPTER 2. METHODS AND MATERIALS

A. Tissue Samples

Scar samples were obtained during reconstructive surgery, between two months and 18 years after thermal injury, from patients who were being treated at the University of Alberta Hospitals Firefighters' Burn Treatment Unit. Normal skin was usually acquired during procedures such as breast reductions and panniculectomies. Normal skin was also obtained during reconstructive surgery from hypertrophic scar patients. After surgery, samples were cut to $0.5cm^2$ - $1.0cm^2$ and immediately immersed in 4% paraformaldehyde in PBS for paraffin embedding. Alternatively, samples were immersed in Dulbecco's Modified Eagle Medium (DMEM; GIBCO BRL) and fibroblasts were explanted from them as explained in *Cell Cultures.*

Paraffin embedding was by an automated process. Briefly, samples were fixed in 4% paraformaldehyde in PBS for 6 to 48 hours and then dehydrated in a series of graded ethanols which increase in concentration until nearly absolute ethanol. Samples were then cleared in xylene and immersed in molten wax (about 53°C). This was followed by perfusion of the samples with molten wax under vacuum after which tissue pieces were oriented in moulds in molten wax before being left to attach and solidify under a tissue cassette.

Paraffin-embedded samples were cut into 4-5um-thick sections with a microtome and then placed on glass slides previously coated with 3-aminopropyl-triethoxy-silane (Sigma) according to the protocol described below. The sections were incubated at 53-55°C overnight after which they were ready for *in situ* hybridization and immunoperoxidase staining. Sections were stored in a box at room temperature until they were used. A list of tissue samples together with the details of their sources is provided in Table 1.

All samples used in this study were processed and cut by Dennis Carmel in the Oral Pathology Laboratory at the University of Alberta.

B. Cell Cultures

Human dermal fibroblasts were explanted from scar samples and normal skin by the following method which was developed in the Division of Plastic Surgery at the University of Alberta. Each scar sample was collected with a normal skin sample from the same patient and preferably from a region near to the scar. These paired samples were sequentially numbered such that the first pair collected would be H1/N1 (where H means hypertrophic and N means normal), the second would be H2/N2, and so on.

Skin samples were collected during reconstructive surgery in Dulbecco's Modified Eagle Medium (DMEM; GIBCO BRL) supplemented with antibiotic-antimycotic mixture (100units/mL penicillin G sodium, 100μg/mL streptomycin sulfate, 250ng/mL amphotericin B; GIBCO BRL; hereafter referred to as A_b) and 10% fetal bovine serum (GIBCO BRL). Samples were cut to $1mm^3$ pieces while being kept wet with DMEM/A_b. Thereafter, the pieces were immersed in DMEM/A_b in a 50mL sterile polypropylene centrifuge tube (Fisher Scientific) and washed repeatedly by inversion. The DMEM/A_b was changed after the pieces settled and the washing was continued by inversion. This procedure was repeated 4 - 6 times.

Tissue pieces were then individually laid out in $25cm^2$ tissue culture flasks (6 pieces per flask) after which one drop of fetal bovine serum (FBS; GIBCO BRL) was applied to each piece. The pieces were then allowed to attach to their plastic substrate under FBS for up to 0.5 hour at room temperature. One drop of DMEM/A_b was then added to each piece (therefore, final concentration of FBS was 50%) and the flasks were incubated at 37°C with 5% CO_2. Each day, thereafter, for three days, 1mL of DMEM/A_b was added to each flask. Flasks were monitored for emerging fibroblasts. Medium (DMEM + A_b + FBS) was changed weekly until 50 - 75% confluence was reached (usually about 4 - 6 weeks). At this time, tissue pieces were removed to a fresh flask to allow for fibroblasts to keep emerging from them. These pieces were treated just as they were when initially plated in the flasks.

The 50 - 75% confluent, attached fibroblasts were subcultured 1:3 (therefore, all fibroblasts from one $25cm^2$ flask were subcultured into one $75cm^2$ flask) by adding 1mL of 0.1% trypsin, 0.02% EDTA, which had been prewarmed to 37°C, to each flask and incubating for 1 minute at room temperature. Cells were then removed and poured into a centrifuge tube. Each flask was washed once with 1mL fresh DMEM/A_b/FBS which was then added to the centrifuge tube. Cells were centrifuged at 1500rpm for 8 minutes; each pellet was resuspended in 10mL of fresh DMEM/A_b/FBS which was added to one $75cm^2$ tissue culture flask.

When these cells reached confluence, they were similarly withdrawn from the flasks using trypsin/EDTA, pelleted using centrifugation at 1500rpm for 8 minutes, resuspended in an appropriate volume of DMEM/A_b/FBS such that 1mL would contain 1-3 million cells. Dimethyl sulfoxide (DMSO; Sigma) was added to 5% (v/v) and the cells were frozen down in 2.0mL-cryogenic vials (Corning) at -80°C overnight after which they were stored under liquid nitrogen. These cells were now in their second passage since cells are considered to have undergone an additional passage every time they are exposed to trypsin/EDTA.

The fibroblasts which were used for *in situ* hybridization were in their 3rd to 8th passages. These cells were thawed from liquid nitrogen, grown to confluence in a 75cm^2 tissue culture flask, subcultured to expand the cells to more flasks, and grown again to confluence. Cells were then treated with trypsin/EDTA and pelleted as described above. Pellets were resuspended in DMEM/A$_b$ to 20000 cells/mL and 0.5mL of this resuspension was dropped into a marked area on glass slides coated with 2% 3-aminopropyl-triethoxy-silane (APTEX; Sigma). Each marked area (1cm^2 to 2.25cm^2) was bordered with a wax pen (ImmunoPen; Calbiochem) mark. Cells were incubated for 60 to 72 hours after subculturing, washed with PBS and fixed under 4% paraformaldehyde for 10 minutes at 4°C. The cells were then stored under 70% ethanol at 4°C.

C. APTEX Coating Glass Slides

Before glass slides were used for growing cells or mounting tissue sections, they were coated with 3- aminopropyltriethoxysilane to increase the adherence to the slides as well as to decrease background staining in different applications (Maddox and Jenkins, 1987; Henderson, 1989). An abridged method was developed from the various suggestions offered in previous reports (Maddox and Jenkins, 1987; Henderson, 1989).

Briefly, glass slides were placed in racks and soaked in 10% Decon 75 (BDH) overnight. Slides were then washed in hot tap water for 1-2 hours such that the water was fed directly into the bottom of the beaker harboring the slides with the aid of a 10mL pipet. Slides were then rinsed briefly in distilled water and then dried at 60°C. Slides were then cooled to room temperature and incubated for 2 minutes each in acetone, acetone containing 2% APTEX, acetone twice, and distilled water twice. Slides were then dried overnight at 37°C. APTEX-coated slides were stored in a box at room temperature for several months until needed.

D. Controlling Ribonuclease Activity

To preserve RNA target and probes, it was necessary to inhibit as much as possible the activity of ribonucleases (RNases). RNases are notorious for their ability to contaminate solutions and hardware; their sources include cultured cells during lysis, human contamination during laboratory manipulations and other laboratory sources.

Controlling their activity can be achieved by agents that inhibit them, by treatments that destroy or inactivate them, or simply by prevention.

The most common source of contamination is human touch. Wearing disposable gloves is the first basic preventive measure to take against this form of contamination. If the gloves come into contact with dirty sufaces, they must be changed regularly.

Hardware that is used in the laboratory is usually comprised of glassware and plasticware. As far as disposable plasticware is concerned, for example, pipet tips and microfuge tubes, they are considered relatively RNase-free as supplied. However, microfuge tubes were still immersed in Millipore purified water containing 0.1% diethylpyrocarbonate (DEPC), which is a strong inhibitor of RNases, at 37°C for at least 12 hours after which the water was drained and the tubes autoclaved for 1 hour at 15lb/sq. in. to destroy the DEPC. Other disposable items such as pipet tips were autoclaved and stored separately for use only with RNA to ensure that only gloved hands were in contact with them and the containers they were in. Plasticware which was supplied as sterile was used directly.

Nondisposable plasticware was rinsed with chloroform before use. For example, the Tissue-Tek staining containers (Baxter Canlab), in which most of the reactions for *in situ* hybridization were carried out, were each filled with 250mL of chloroform, one after the next. After all of the chloroform was removed and trace amounts had evaporated, the containers were rinsed with DEPC-treated water.

Glassware such as beakers, graduated cylinders, Erlenmeyer flasks, and solution bottles was baked at 180 - 200°C for at least 12 hours. These were marked and stored separately from other glassware.

Working solutions were all made up in baked glassware and then stored in baked bottles. Stock solutions which could be autoclaved were made up using normal glassware after which the solutions were treated with 0.1% DEPC in the bottles they were to be stored in for at least 12 hours at 37°C. Thereafter, solutions were autoclaved at 15lb/sq. in. for 45 minutes to 1 hour . Solutions such as Tris buffers, which contain amines, react rapidly with DEPC and therefore cannot be treated. Such buffers must be prepared using RNase-free glassware and plasticware and DEPC-treated water; as well, powder stocks of these reagents such as Tris crystals must be kept clean and separate for preparation of RNase-free solutions.

One more reagent that was used in the battle against RNases was RNase Inhibitor from human placenta (Boehringer Mannheim), a protein inhibitor of RNases. This reagent was used in labeling reactions to protect the newly transcribed RNA from degradation by

RNases. This inhibitor inactivates RNases by non-covalently binding to the enzyme in an equimolar fashion.

E. Probes

1. Decorin:

The first probes that were used for decorin mRNA were transcribed off a 150bp cDNA fragment corresponding to a region in exon 8 of human decorin which was cloned into pGEM 4Z (Promega). This construct was referred to as pD150 and the labeled transcipts generated from it as D150. This vector contains a T7 and an SP6 promoter region, one on each side of its polycloning site (PCS). When this plasmid was sequenced (Sanger method; Biochemistry Sequencing Lab, University of Alberta) using the T7 primer, a sequence that was complementary to the mRNA sequence listed in Genbank (accession #L01131) for exon 8 of decorin was found indicating that the strand from which this sequence was generated was sense and the riboprobe synthesized from it using T7 RNA polymerase, antisense (data not shown). Consequently, SP6 polymerase should yield a sense riboprobe.

The second set of probes used to search for decorin mRNA were transcribed off a 622bp cDNA fragment corresponding to nucleotides 727 to 1348 of human decorin cDNA (Krusius and Ruoslahti, 1986) which was cloned into the Hinc II site of the PCS of pBluescript KS+ (Stratagene). This fragment includes parts of exons 7 and 8 of human decorin (Genbank accession #L01130 and L01131) and is least identical to biglycan cDNA when compared to other similarly sized regions in the cDNA. This contruct was referred to as pD600 and the labeled riboprobes transcribed from it as D600. The PCS in this vector is flanked on either side by RNA polymerase promoters T3 or T7 .

Sequencing of the insert (Sanger method; Biochemistry Sequencing Lab, University of Alberta) was conducted at both ends of the insert, therefore, using both T3 and T7 primers; the results verified the accuracy of the insert sequence as well as its orientation in the plasmid (data not shown). The sequence obtained using the T7 primer matched exactly with portions of sequences provided for exons 7 and 8 in Genbank indicating that the transcript produced off the same promoter should be sense. The plasmid pD600 was linearized with the restriction enzymes *Apa*I or *Cla*I to prepare it for *in vitro* transcription labeling using either T7 or T3 RNA polymerase, respectively (Figure 2a).

The third batch of probes used to search for decorin mRNA was transcribed off a 622bp cDNA fragment corresponding to part of exon 7 and exon 8 of decorin contained in the pT7/T3α-18 transcription vector (GIBCO BRL). This fragment was digested out of pD600 with *Kpn* I and *Pst* I and ligated into pT7/T3 at the same sites. Sequencing (Sanger method; Biochemistry Sequencing Lab, University of Alberta) verified the construct and identified the sense and antisense strands of the cDNA when compared to decorin sequences in Genbank (Accession #s: L01130 and L01131). Since sequencing was performed using the Sanger method, it verified that using T7 polymerase, the resulting cRNA would be sense; hence, using T3 polymerase and transcribing off the opposite strand would yield an antisense cRNA probe. This contruct was referred to as pD620 and the labeled riboprobes transcribed off it as D620.

2. TGF-ß1:

The first template that was used to generate cRNA probes for TGF-ß1 consisted of a 286bp cDNA fragment corresponding to nucleotides 601 to 886 of rat TGF-ß1 (rTGF-ß1) (Genbank accession #X52498) cDNA contained within the plasmid vector pGEM 3Z (Promega) at restriction sites *Pst* I and *Bam* H I. The polycloning site of this vector is flanked by a T7 promoter at one side and by an SP6 promoter at the other. Sequencing (Sanger method; Biochemistry Sequencing Lab, University of Alberta) with the T7 primer revealed the rTGF-ß1 sequence in the sense orientation. Therefore, a cRNA probe generated off this template using T7 RNA polymerase had the same sequence as rat TGF-ß1 mRNA and would be sense. For labeling, the template was linearized with the restriction enzymes *Pst* I or *Bam* H I which digested the template DNA on either side of the insert cDNA (Figure 14b). The *Pst* I digest was then used in the labeling reaction with the T7 polymerase and the *Bam* H I digest with SP6 polymerase.

The persistently poor labeling efficiency obtained using SP6 RNA polymerase eventually led to subcloning of the 287bp rTGF-ß1 cDNA fragment from pGEM 3Z into the PCS of pT7/T3 (GIBCO BRL) between the restriction sites *Hind* III and *Eco* RI . This was the second template constructed to generate cRNA probes to TGF-ß1. Using either the restriction enzyme *Hind* III or *Eco* RI to linearize this recombinant vector (Figure 22), the use of either T7 or T3 RNA polymerase respectively, led to the production of either sense or antisense probes respectively.

The third template that was used to generate cRNA probes to TGF-ß1 was prepared before my arrival to the department and consisted of a 420bp cDNA fragment of human TGF-ß1 cloned into the *Bam* HI and *Eco* RI sites of pGEM 3 (Promega) plasmid vector DNA. This construct was referred to as pT420 and any probes transcribed off it as T420. Sequencing of this plasmid using the T7 primer revealed a 47bp poly(A)$^+$ stretch in the insert cDNA. This invalidated the use of this plasmid in any further experiments (refer to Results).

The fourth template generated harbored a 112bp fragment from the 5' end of the cDNA insert of T420/pT7/T3 which was digested out of this plasmid using *Sma* I and *Xba* I and cloned into these sites in pT7/T3. Sequencing using the T7 primer yielded a product that was complementary to TGF-ß1 mRNA; therefore, the use of T7 polymerase to transcribe off this template yielded antisense probe. The template, when linearized with *Pst* I, was used with T7 polymerase to generate the antisense probe. Conversely, *Eco* R I was used to generate a linearized template which could be used with T3 polymerase to produce sense probes (Figure 30). These linearized templates were purified by phenol/chloroform (1:1) extraction followed by precipitation with 1/10 v/v sodium acetate (pH 5.2; 3M) and 3 v/v of 99% ethanol. Double digestion with both *Pst* I and *Eco* R I liberated the 112bp cDNA fragment from its vector (Figure 30). This construct is henceforth referred to as pT112, and all probes transcribed off it as T112 probes.

Except for the initial use of the first TGF-ß1 template, all of the linearized vectors mentioned above were cleaned up before being used as templates for *in vitro* transcription. This clean up took the form of an extraction of the solution of linearized DNA with phenol/chloroform (1:1) followed by chloroform alone and precipitation as described above with sodium acetate and ethanol.

F. Probe Labeling and Quantitation

1. Labeling:

DNA templates used as substrates for the labeling reactions were subcloned into the PCS of appropriate plasmid vectors which contain RNA polymerase promoter sites (see *Probes*). Restriction enzymes were used to linearize the plasmids at either end of the PCS just adjacent to the end of the insert DNA fragment (see *Probes*). Hence, the use of an RNA polymerase, either T3, T7, or SP6, and its respective promoter in an *in vitro* transcription reaction yielded probes exactly or very close to the exact length of the insert DNA template.

Linearized templates were purified by phenol/chloroform extraction and precipitation. A volume of phenol/chloroform (1:1; adjusted to pH 8 using 1M Tris HCl, pH8; stored under 0.1M Tris HCl, pH8) and equal to the volume of DNA solution was added. This mixture was vortexed and spun down for 1 minute at 12,000 x *g*. The supernatant was removed to another tube and similarly treated with chloroform alone (equal volume). After centrifugation for 1 minute at 12,000 x *g*, the supernatant was removed again to a new tube to which was subsequently added sodium acetate (0.1v/v, pH 5.2) and ethanol (3 v/v, 99%, -20°C). The contents were mixed and incubated at -80°C for at least 30 minutes. The DNA was then pelleted at 12,000 x *g* for 20 minutes at 4°C. The pellet was washed with 70% ethanol (-20°C) and centrifuged again at the same speed for 5 minutes. The pellet was then dried and resuspended in 0.01M Tris (pH 8), 0.001M EDTA such that the final concentration of DNA was between 0.1 and 1.0 ug/uL.

Digoxigenin-11-UTP labeled cRNA probes were prepared by *in vitro* transcription using the Genius 4 RNA Labeling Kit and the RNA Labeling protocol on pages 30-32 of The Genius System User's Guide for Filter Hybridization (henceforth referred to as The User's Guide) (Boehringer Mannheim, 1992). The kit was purchased only once; individual components were replaced as necessary through purchases from Boehringer Mannheim; exceptions include additional 10X transcription buffer which was made as described on page 69 of The User's Guide and RNA polymerases which were purchased from GIBCO BRL.

Briefly, to an RNase-free microcentrifuge tube which was on ice, the following components were added in order: purified DNA template (0.5mg to 2.5mg; this amount was optimized as described in Chapter 4); 1/10 volume 10X NTP labeling mixture; 1/10 volume 10X transcription buffer; DEPC-treated water to make up to desired volume minus the polymerases; and the RNA polymerase to 2.5 units/uL. The total volume was usually 20uL; however, this varied in reactions which were scaled-up (refer to Results). In such cases, the amount of template DNA in the reaction was kept constant while the amounts of the other components were increased by a standard ratio. The labeling mixture was mixed gently by pipetting and incubated at 37°C for 2 hours or more (see Results).

Labeling mixtures were centrifuged briefly (for less than one minute at 12,000 x *g*). RNase-free DNase I was added to each reaction; solutions were mixed by pipetting and then incubated at 37°C for 15 minutes. Originally, 2uL of the DNase I from the RNA Labeling kit was used; the concentration of this stock was 10 units/uL. This product was later replaced with a similar product from GIBCO BRL which was supplied at 10mg/uL; 0.5uL to 1.0uL of this product was used. Solutions were, once again, centrifuged briefly after which 2uL of 0.2M EDTA (pH8.0) was added to stop the reaction. This was followed by 1uL of glycogen (20ug/uL). Once again, the volumes of the EDTA and the glycogen were based on a standard 20uL labeling reaction; they were increased accordingly in the scaled-up reactions. Finally, labeled RNA was precipitated by adding 0.1 volume of 4M LiCl and 3.0 volumes of 99% ethanol (-20°C), mixing by vortexing, and incubation at -80°C for 30 minutes or longer.

Solutions were then centrifuged at 12,000 x *g* for 15 minutes at 4°C. Pellets were washed with 100uL of 70% ethanol and centrifuged again at the same relative centrifugal force for 5 minutes. The ethanol was removed and pellets were allowed to dry at room temperature after which they were resuspended in 100uL of DEPC-treated water. Dissolution was carried out at 37°C for 15 minutes with regular vortexing. Labeled probe was stored in 10uL aliquots at -80°C.

2. Quantitation:

Ten-fold serial dilutions of the probe were made in DEPC-treated water. Therefore, 1uL of probe was added to 9uL of water and mixed by vortexing. Then, 1uL of this mixture was added to to 9uL of water and mixed by vortexing. This was continued until 7 such dilutions were made. Each time a dilution was made, a fresh pipette tip was used; as well, pipette tips were rinsed out well each time a delivery was made. Labeled control RNA from the RNA Labeling kit was also serially diluted in the same way, by 10-fold serial dilutions, until the final concentration was 10fg/uL.

Thereafter, on a piece of nylon membrane (Hybond N; Amersham) that was prewetted in 10X SSC and setup on a dot blotting apparatus under vacuum, 1uL of each of the dilutions of the Labeled Control RNA (from 1ng to 10fg) and the labeled probes (from $1/10$ to $1/10^7$) was dotted. RNA was then bound to the membrane, while still wet, by exposure to 120 000uJ/cm^2 of ultraviolet light at 254nm in a UVC 515 Ultraviolet Multilinker. Thereafter, membranes underwent a standard colorimetric detection procedure as outlined in the User's Guide (page 63-64).

Briefly, membranes were equilibrated in buffer 1 (100mM Tris HCl, 150mM NaCl; pH 7.5) for 1 minute after which they were agitated for 0.5 hours - 3 hours in buffer 2 (2% (w/v) Blocking reagent dissolved in buffer 1) at room temperature. Membranes were then gently agitated in anti-DIG-alkaline phosphatase (1:5000 in buffer 2; Boehringer Mannheim) for at least 0.5 hours and up to 1 hour at room temperature. Membranes were then washed twice in buffer 1, 15 minutes per wash, with rigorous shaking. Membranes were then equilibrated in a small amount of buffer 3 (100mM Tris HCl, 100mM NaCl, 50mM $MgCl_2$; pH 9.5) for about 2 to 5 minutes. Color solution (0.34ug/uL nitroblue tetrazolium chloride and 0.18ug/uL 5-bromo-4-chloro-3-indolylphosphate in buffer 3; Boehringer Mannheim) was then added to the membranes in a fresh plastic bag which was sealed and left to incubate overnight in the dark at room temperature.

Membranes were then washed in buffer 4 (10mM Tris HCl, 1mM EDTA; pH 8.0) twice with at least 15 minutes per wash and with rigorous shaking. Membranes were now photographed or dried for storage. The amount of labeled RNA was calculated by comparing its color intensity with those of the labeled control RNA dots. Therefore, if the intensity of the color in the dot represented by the $1/10^4$ dilution of the probe matches the color intensity of the dot represented by 10pg of control labeled RNA, we assume that there is about 10pg of labeled RNA in the probe when it is diluted 10000 times.

G. Determining Functionality of Probes

1. Dot Blot Hybridization:

This procedure was carried out based on the protocol outlined for DNA dot blotting in The User's Guide (page 47). It was used to determine the sensitivity and specificity of the labeled probes. The template plasmid from which a particular set of sense and antisense probes was generated was diluted using 10-fold serial dilutions (as described in Quantitation above) in DNA dilution buffer (50μg/mL salmon sperm DNA, in 10mM Tris HCl, 1mM EDTA; pH 8.0) such that concentrations between 1.0ng/uL and 10fg/uL were achieved. DNA was then denatured in boiling water for 10 minutes after which the solutions were immersed in ice/NaCl for at least 3 minutes. One microliter from each dilution was dotted onto a piece of Hybond-N nylon membrane (Amersham), previously wetted with 10X SSC, which was on a dot blotting apparatus under vacuum. The DNA was then crosslinked to the membranes with U.V. irradiation as described above in Quantitation.

Membranes were then prehybridized in prehybridization solution (50% formamide, 5X SSC, 2% Blocking reagent, 0.1% N-lauroylsarcosine, 0.02% sodium dodecyl sulfate (SDS)) for 1 to 3 hours at 50°C. Thereafter, probe was denatured in a small volume of the same prehybridization mixture at 70°C for 5 minutes and added to the membranes which had fresh prehybridization solution added to them. The concentration of the probe during hybridization was between 30 and 50ng/uL. Hybridization was carried out overnight (12-18 hours) at 50°C with agitation.

After hybridization, the membranes were washed twice in 2X wash solution (2X SSC, 0.1% SDS) at room temperature, 5 minutes each time. Then, the membranes were washed twice in 0.5X wash solution (0.5X SSC, 0.1% SDS) at 60-65°C, 15 minutes each time. Thereafter, membranes were equilibrated in buffer 1 and subjected to the standard detection procedure as outlined above in Quantitation.

H. In Situ Hybridization

The protocols followed for *in situ* hybridization in this study evolved as different conditions were optimized. As well, conditions needed to be altered with the use of different probes, ie. the stringency of hybridization and post-hybridization was altered depending on the length and the GC content of the probes.

The original method of *in situ* hybridization used and built upon for this study was established by Angerer and coworkers (1984). Modifications were made to simplify the method in the beginning, after which the controlled addition of different steps was performed as needed. The result was the development of five different protocols which are summarized below, and which will be referred to throughout the thesis, as protocols 1 to 5.

The most critical condition to determine for any hybridization is the T_m, or the melting temperature, of the expected duplex structure or hybrid between the probe and its target. The T_m of a duplex is usually referred to as the temperature at which there are equal amounts of native duplex and their denatured form. Alternatively, it is the mid-point in the transition of a duplex from the native form to the fully denatured form. Initially, the formula used to derive the T_m of the expected hybrid in our reactions was:

$$T_m = 81.5 + 41\ F_{GC} + 16.6\ \log[Na^+] - 0.35\ [\%\ \text{formamide}]$$

(equation 1; Hames and Higgins, 1988)

where T_m is the melting temperature of the expected hybrid and F_{GC} is the fraction of guanosine and cytosine residues in the expected hybrid.

The hybridization reaction was carried out at less stringent conditions than the post-hybridization washes. In this way, we ensure maximum hybridization to the target while the excess, non-specific binding is washed away in subsequent, more stringent washes. Therefore, the hybridization was usually carried out at T_m - 25°C to T_m - 35°C and the most stringent post-hybridization washes were usually conducted at T_m - 15°C to T_m - 25°C.

1. Protocol #1:

This study started with the use of the following protocol for *in situ* hybridization. Unless specified, incubations were carried out at room temperature. Paraffin-embedded tissue sections were heated to 60°C for 10 minutes after which the hot slides were immersed twice in xylene for deparaffinization, 5 minutes each. Tissue was then hydrated through graded ethanols, ie. 99% (twice), 70%, 50%, 30% for 5 minutes each and then immersed in phosphate buffered saline (PBS) containing 5mM $MgCl_2$ twice for 10 minutes each.

Tissue was then immersed in 0.2M NaCl for 10 minutes after which they were transferred to 2X SSC, 5mM EDTA at 50°C twice for 20 minutes each. The tissue was now prepared for treatment with proteinase K (Boehringer Mannheim) which was used at 100μg/mL in PBS at 37°C for 30 minutes. The concentration of proteinase K must be optimized with each new batch of enzyme; as well, different tissue types which have been fixed differently require different proteinase K conditions. Therefore, this variable was changed often for optimization (refer to Chapter 4). This solution was dropped onto the tissue sections and the slides were incubated in a humid chamber that was prewarmed at 37°C. This reaction was terminated with 0.2% glycine in PBS for 10 minutes after which the tissues were post-fixed in 4% paraformaldehyde (PFA) in PBS for 20 minutes.

The PFA was washed off with 2 changes of PBS containing 5mM $MgCl_2$ for 10 minutes each. Free amino groups were then acetylated using 0.1M triethanolamine containing freshly added 0.25% (v/v) acetic anhydride for 10 minutes. The acetic anhydride was added just before the solution was needed; this was followed by vigorous stirring to dissolve the acetic anhydride after which the slides were immersed immediately. Tissue was washed in 2X SSC twice for 10 minutes each before being treated with prehybridization mixture (50% formamide, 5X Denhardts' solution [0.1% each of bovine serum albumin, Ficoll (Sigma), and polyvinylpyrollidone (Sigma)], 4X SSC, 600ng/uL of salmon sperm DNA). Liquid was wiped off around tissue sections before prehybridization mixture was dropped on; sections were not allowed to dry. The incubation continued for 1 hour at about 60°C.

Hybridization followed in the same mixture as the pre-hybridization mixture except that the salmon sperm DNA was replaced with 10% dextran sulfate (Sigma) and that labeled probe (predenatured at 95°C for 10 minutes) was added at a concentration such that each slide would receive 20 to 50ng of probe. Hybridization mixture (50uL per slide) was applied to each slide after which slides received a coverslip which was sealed on with LePages rubber cement. Hybridization was carried out at 65°C (T_m - 25°C based on a GC content of 60%) overnight or for 12 - 18 hours.

After hybridization, coverslips were removed and post-hybridization washes started with 0.1X SSC, 50% formamide (T_m - 15°C based on 60% GC) twice for 15 minutes each followed by two 5 minute rinses in 1X SSC. This was followed by two 15 minute washes in 0.1X SSC at 56°C (T_m - 20°C based on a GC content of 60%). Tissue was then equilibrated in buffer 1 to start the detection procedure which is very similar to that described in Quantitation (above).

Briefly, slides were incubated in buffer 2 (2.0% Blocking Reagent in buffer 1) for 30 minutes and then rinsed in buffer 1 for about 1 minute. Anti-DIG-alkaline phosphatase was diluted 1:5000 in buffer 2 and dropped onto tissue sections and allowed to incubate for 30 minutes. Sections were then washed twice in buffer 1 for 15 minutes each after which they were equilibrated in buffer 3 for about 5 minutes. Excess liquid was wiped off the tissue sections after which color solution made in buffer 3 was dropped on and the slides were allowed to incubate at room temperature in the dark for 6 to 18 hours or until color appeared fully developed. After color development, tissue was washed in 2 changes of buffer 4 for at least 15 minutes each, dehydrated in graded ethanols for 2 minutes each, and cleared in 2 changes of xylene for 5 minutes each before being mounted with S/P Accu Mount 280 Mounting Medium (Baxter).

2. Protocol #2:

Alterations were made to Protocol #1 in an attempt to optimize conditions to get specific results with antisense probes only and to minimize background staining in the extracellular matrix in the dermis. Many of these changes were made at the start of the study while working with probes for TGF-ß1.

The most significant change in Protocol #1 which affected all subsequent *in situ* hybridizations was the change in the formula used to determine T_m. The formula used above was later found to apply to natural DNA polymers. Due to the nature of the sugar, RNA duplexes are more stable than DNA; this is true at moderate salt concentrations and for duplexes with a moderate-to-high GC content. Therefore, the T_m of high molecular weight, duplex RNA molecules with a GC content between 30 and 70% was predicted by the following formula:

$$T_m = 67.62 + 93\, F_{GC} + 14.88 \log[Na^+] - 0.35\,[\%\ \text{formamide}]$$

(equation 2; Paetkau, 1994)

It is important to consider that this equation shows a higher dependence on GC content than the previous formula.

There were also a few other changes made in the Protocol #1. The post-hybridization washes begin with an incubation in 2X SSC, 50% formamide at 55°C (T_m - 37.5°C based on 60% GC content in the duplex). This was followed by a wash in 3 different solutions at different stringencies to optimize conditions. It was found that 0.01X SSC at 57°C (T_m - 18°C based on 60% GC) washed the tissues well and left staining only with antisense probes which localized to the cytoplasm. The first wash after hybridization was also soon changed to just 0.2X SSC at 57°C; this was found to have the same stringency as the first wash described above and no formamide was needed.

In the detection procedure, buffer 1 was replaced by maleate buffer (100mM sodium maleate, pH 7.5; 150mM NaCl; The User's Guide, 1992); consequently, buffer 2 was made up in maleate buffer and the anti-DIG complex was diluted in this new mixture of buffer 2.

3. Protocol #3:

After testing many parameters of the above protocol, a simpler procedure was developed in which individual incubation times were reduced and in which fewer steps were involved. Since RNA is highly susceptible to degradation, a shorter protocol exposes both target and probe for less time to degradative enzymes.

The paraffin-embedded tissues are still heated to 60°C for 10 minutes to start the procedure; this step adheres the tissues well to the slides and melts the wax which makes its dissolution in xylene easier. Next, the washes in xylene were kept in this protocol as well as the hydration in graded ethanols. The sections are then immersed in PBS, 5mM $MgCl_2$ for 5 minutes after which they were 'pre-fixed' in cold (4°C) 4% PFA for 10 minutes.

Sections were then washed in PBS, 5mM $MgCl_2$ twice, for 5 minutes each, followed by one 5 minute incubation in 0.5X SSC. Cultured cells were introduced at this time and immersed in 0.5X SSC from the 70% ethanol which they were stored in. Proteinase K digestion was carried out next in 0.5M NaCl, 0.01M Tris HCl, pH 8.0 for 10 minutes at room temperature. The concentration of enzyme used was still being optimized but the limit now was 50µg/mL and a range down to 5µg/mL was tested. Tissues were washed next in 0.5X SSC for 10 minutes followed by an incubation in 0.2% glycine in PBS for 10 minutes. Tissues were then washed in PBS, 5mM $MgCl_2$ for 5 minutes. This was followed by acetylation in 0.1M triethanolamine, 0.25% acetic anhydride for 10 minutes and two washes in 2X SSC for 5 minutes each.

Prehybridization was carried out next during which excess liquid was wiped off from around the tissues before prehybridization mixture (2X SSC, 50% formamide, 0.1mg/mL salmon sperm DNA, 5X Denhardts' solution) was dropped onto each section. Prehybridization was carried out for 1 to 3 hours followed by hybridization overnight in the same mixture as the prehybridization with the addition of probe to 0.4ng/uL; usually, 50uL of hybridization mixture was used per slide equating to 20ng of probe. The temperature of the prehybridization and hybridization varied depending on the probe used but was usually around 50°C to 53°C.

The temperature of posthybridization washes also varied depending on the probe. The appropriate stringency of these washes depends heavily on the GC concentration of the expected duplex. Therefore, with the TGF-ß1 probes which had GC concentrations around 60-65%, the washes were 0.2X SSC at 53°C twice for 15 minutes each followed by 0.01X SSC at 55°C twice for 10 minutes each. However, with the decorin probes which typically had GC concentrations less than 50%, the most stringent wash was with 0.1X SSC at 50-55°C.

Following these washes, tissues were equilibrated in maleate buffer for 1 - 5 minutes. Cultured cells were transferred directly to buffer 2 or 2% Blocking Reagent (made in maleate buffer) for 1 - 3 hours. For paraffin-embedded tissue, Casein Blocking Buffer (Cambridge Research Biochemicals; 1:5 in PBS) was dropped onto the tissue and allowed to incubate for 30 minutes in a humid chamber at room temperature. These tissues were then drained and immersed in buffer 2 with the cultured cells for 1 - 3 hours. Anti-DIG antibody conjugate (1:5000 in buffer 2) was then dropped onto the tissues and allowed to incubate at room temperature for 30 minutes in a humid chamber. Antibody was washed off using 2 washes of maleate buffer for 10 minutes each. Slides were then immersed in buffer 3 for about 5 minutes after which color solution was dropped onto the tissue and cells and allowed to incubate for 6 - 18 hours at room temperature in the dark. Color solution was drained and washed off using buffer 4 after which sections were dehydrated in graded ethanols and cleared in 2 incubations of xylene, 5 minutes each. Sections were then mounted with S/P Accu Mount 280 Mounting Medium (Baxter).

One variable which was tested in only 3 experiments which used Protocol #3 was digestion of the tissues with bovine testicular hyaluronidase (Sigma; see Results). This enzyme was used at 1mg/mL in hyaluronidase buffer (0.1M sodium acetate, 0.15M NaCl, pH 5.5) at 37C for 30 minutes. Hyaluronidase was applied to the slides before proteinase K digestion and after incubations with PFA and PBS. After hyaluronidase, slides followed the rest of the protocol starting with immersion in 0.5X SSC followed by proteinase K digestion.

4. Protocol #4:

The continual appearance of staining with the sense probes for TGF-ß1 as well as high background levels led to yet another significant change in the protocol used for *in situ* hybridization. The major change in this protocol, compared to Protocols 1 through 3, is its simplified approach. There are fewer steps and the incubation times are shorter. Other changes include the change in proteinase K and buffer, the elimination of acetylation, the elimination of fixation, a different recipe for the prehybridization mixture, and the dehydration of tissue before prehybridization.

Protocol #4 starts with the same steps as the other protocols. Tissue sections are heated to 60°C after which they are deparaffinized in two changes of xylene for 5 minutes each. Sections were then hydrated through graded ethanols, specifically, 99%, 95%, 70%, and 50% ethanols for 2 to 5 minutes each after which they were immersed in PBS for 5 minutes. Cultured cells, which were stored in 70% ethanol, were introduced at this step after immersion in 50% ethanol.

Proteinase K digestion was then conducted in 50mM Tris HCl, 10mM EDTA, 10mM NaCl, pH 7.4. The enzyme was diluted to 20µg/mL in this buffer and then dropped onto the sections after the excess liquid had been wiped off. Sections were then incubated for 20 minutes at room temperature in a humid chamber. Proteinase K digestion was stopped by immersing the slides in 2mg/mL glycine in 0.1M Tris HCl (pH 7.5), 0.1M NaCl for 10 minutes. The sections were then washed once in PBS for 5 minutes after which they were dehydrated through graded ethanols from 50% to 99% for 2 to 5 minutes each.

Sections were then air dried for 5 minutes after which prehybridization solution (50% formamide, 5X SSC, 0.02% SDS, 0.1% N-lauroylsarcosine, 2% Blocking Reagent) was dropped onto the sections and they were allowed to incubate in a humidified chamber at 53-55°C for 1 hour. Prehybridization solution was then drained off the slides and hybridization solution (same as prehybridization solution but with probe added to 0.5ng/mL) was added to the slides. Coverslips were applied to the sections and sealed using LePages rubber cement. Slides were incubated at 53-55°C in a humid chamber overnight or for 12 - 18 hours.

Posthybridization washes were started with two washes in 5X SSC for 15 minutes each at room temperature followed by two washes in 2X SSC for 15 minutes each at room temperature. The stringent wash was performed next in 0.1X SSC twice for 15 minutes each at 53-55°C. This wash was at T_m - 40 to T_m - 42°C according to equation 2 (calculated for a hybrid with an expected [GC] of 60%). Sections were then equilibrated in maleate buffer after which they went through the same detection procedure as described for Protocol #3. After this procedure, however, a change was introduced in the mounting medium used to preserve the slides. An aqueous mounting medium (Aquaperm™ Mounting Medium; Lipshaw Immunon) was applied. The change in the mounting medium was made as a result of crystal formation seen in archived slides which was thought to have been caused by the nonaqueous mounting medium reacting with the color development products.

The most valuable addition in this protocol was the dehydration of the sections before prehybridization and hybridization which seemed to clear up background levels considerably.

Controlled studies were performed with Protocol #4 in which different variables were added to test their effects (see Chapter 4). It was found that acetylation, fixation, and proteinase K digestion with higher concentrations of the enzyme had merit. Additionally, RNase A digestion after hybridization also helped reduce background levels. Therefore, these variables were reintroduced to establish a more robust protocol. Also, a different hybridization mixture was used. This new protocol (Protocol #5) was based on other previously established methods (Lehnert and Akhurst, 1988; Schmid et al., 1991; Pelton et al., 1989).

5. Protocol #5:

Paraffin-embedded sections were heated to 60°C for 10 minutes. Hot slides were immersed in xylene for 10 minutes followed by another 10 minute incubation in fresh xylene. Sections were then hydrated in graded ethanols, ie. 99% (twice), 95%, 70%, 50%, 30% for 2 to 5 minutes each. This was followed by washing in PBS for 5 minutes. Sections were then immersed in 4% (PFA) for 20 minutes to provide an even fixation through the tissue sections. This was followed by 2 washes in PBS, 5 minutes each, in which the slides were entirely covered in PBS to rinse off as much of the PFA as possible. At this point, human dermal fibroblasts which were cultured on slides (see B above) were introduced into the experiment by immersing them in PBS.

Proteinase K digestion was carried out next. Excess liquid was wiped off the tissue sections and proteinase K (Boehringer Mannheim) at 40μg/mL in 50mM Tris HCl (pH 8.0), 5mM EDTA (0.5μg/mL for cultured fibroblasts) was dropped onto the sections and allowed to incubate for 10 minutes at room temperature. The proteinase K digestion was stopped by immersing the sections in 0.2% glycine in PBS. The sections and cells were then 'post-fixed' by immersion in 4% PFA for 5 minutes after which they were washed thoroughly in PBS.

Free amino groups were treated by acetylation to reduce electrostatic binding of the probes particularly to the tissues and the slides. This was done by immersing sections and cells in 0.1M triethanolamine containing 0.25% acetic anhydride for 10 minutes at room temperature. This was followed by washing in PBS. Tissue sections were then dehydrated in graded ethanols, the same as those used for the hydration except that they were used in the opposite order and the final 99% ethanol was fresh. Sections were then air dried for 5 minutes. The cells were never dried but were covered with prehybridization mix immediately after washing in PBS.

After sections were completely dry they were covered with prehybridization solution (60% formamide (Fluka), 0.3M NaCl, 10mM Tris HCl (pH 8), 5mM EDTA, 10%

dextran sulfate, 1X Denhardts' solution, 0.5mg/mL *E. coli* tRNA, 0.02% SDS, 0.1% N-lauroylsarcosine). Prehybridization was carried out at 50°C for 3 hours in a chamber humidified with 50% formamide and 0.3M NaCl. Hybridization was carried out in the same chamber; the prehybridization mixture was drained off the slides and the sections and cells were covered with hybridization mixture (50μL of prehybridization solution containing labeled riboprobe at 1ng/μL; this mixture was heated to 75°C for 5 minutes to denature the probes and then placed on ice prior to use), coverslipped, and sealed with LePages rubber cement. Hybridization was carried out for 15 - 18 hours at 50°C.

The coverslips were removed by carefully sliding them just 1-2mm over the slides to create an edge which was used to peel them off. This was done very slowly. The slides were then washed twice in 50% formamide, 2X SSC for 15 minutes each at room temperature followed by 2 changes of 2X SSC for 10 minutes each also at room temperature. RNase A treatment was then carried out by immersing slides in 2X SSC containing RNase A at 2μg/mL at 37°C for 15 minutes. Sections and cells were washed in 3 changes of 2X SSC at 37°C for 10 minutes each and then immersed twice, 15 minutes each, into 0.1X SSC at 55°C.

To begin the immunological detection procedure, the slides were immersed briefly in maleate buffer (0.1M maleic acid, 0.15M NaCl). Thereafter, Casein Blocking Buffer, which was diluted 1:5 in PBS , was dropped onto the paraffin sections and allowed to incubate for one hour at room temperature in a humid chamber (closed chamber containing liquid). The Blocking Buffer was then poured off and the sections were immersed into 4% Blocking Reagent (Boehringer Mannheim), dissolved in maleate buffer, for 2 hours. The cells were not treated with Casein Blocking Buffer but immersed into the 4% Blocking Reagent immediately after the maleate buffer. Anti-DIG-alkaline phosphatase antibody (Boehringer Mannheim), diluted 1:5000 was dropped onto the tissue sections and the cells which had had excess liquid wiped off from around them. Antibody incubation was then carried out overnight or for 12 - 18 hours at 4°C.

Excess antibody was washed off using 6 washes of maleate buffer over 1 hour. Sections and cells were then equilibrated in buffer 3 for 5 minutes after which color solution was dropped on. They remained in the dark at room temperature for 6 hours for color development. Color solution was then drained off the slides which were then washed twice in buffer 4 for at least 15 minutes each time. Slides were drained and excess liquid was wiped off around sections and cells. Aquaperm™ Mounting Medium was then applied and allowed 6 hours to completely dry.

I. Quantitating In Situ Hybridization Results

The depths of the sections were measured under 400x magnification from epidermis to dermis using a marked ocular lens (Figure 10). The marking on the lens was a box and the area within the box was termed one "field". The total number of fields from the epidermis to the bottom of the deep dermis was labeled as "x". Sections were then divided into thirds and this was done by simply dividing the total number of fields in x by 3. The resulting value was referred to as "y". The one-third segment closest to the epidermis was termed the papillary dermis; below that the next one-third of the dermis was called the middle dermis and the lowest third was called the reticular dermis.

In each third of the dermis, the number of fields across its width was referred to as "z". Multiplying y and z resulted in the total number of fields in that third of the dermis. This number was referred to as "f". Using a table of 1000 random digits (Rosner, 1990, pg. 540) 10 numbers were selected which were lower than f. These numbers then corresponded to ten randomly chosen fields within that third of the dermis. This was done for every third of every section quantitated. The number of positively stained cells was counted in each of the randomly chosen fields and then summed for each third of each section.

The same strategy was used to quantitate the total number of connective tissue cells in each third of each section studied. These sections were either stained with hematoxylin/eosin or just hematoxylin. A fraction or percent of the number of positive cells in each third of each section was then derived by dividing the summed number of positive cells for decorin in a particular region of a section by its corresponding total number of cells.

Averages of sums and percentages from tissues that were grouped together were analyzed for significant differences using a one-way analysis of variance (ANOVA).

J. RNA Extraction; Probe Preparation; Northern Analysis

1. RNA Extraction:

Total RNA was isolated from human dermal fibroblasts using the methods described previously which depend on guanidinium isothiocyanate (GITC) to lyse the cells and CsCl to purify the RNA (Chirgwin et al., 1979; Chomczynski, 1989; Chomczynski and Sacchi, 1978). Briefly, cultured cells grown in 75cm^2 flasks were washed twice with 10mL of cold (0°C) PBS. The last wash was left in the set of flasks being worked on. The PBS from one flask was removed completely by suctioning and was replaced with 6mL of GITC which was pipetted over the cells repeatedly until all cells lost adherence.

The removal of all the PBS before adding GITC was important to ensure that the volume of the final collected solution did not exceed 7mL.

The same aliquot of GITC was used in all flasks of one series. Therefore, the GITC, after being pipetted over one flask, was kept in there for 2 minutes as it rested on ice at an angle. This was done to ensure that as much of the GITC as possible had been collected before being transferred to another flask in the same series. This was continued until all flasks in the same series had been treated. The resulting viscous lysate was transferred to a sterile 50mL polypropylene tube. The GITC was kept cold throughout the procedure to minimize degradation of the RNA.

Chromosomal DNA was sheared next to reduce its viscosity. This was done by adding 3 - 5 drops of antifoam A (Sigma) to each sample and aspirating it through an 18-G needle attached to a 10mL syringe. Each sample was aspirated 20 - 30 times. Thereafter, samples were slowly added to 3mL of CsCl (1.71 - 1.76 g/mL) in an ultracentrifuge tube. Care was taken to add the samples to the CsCl such that the samples would layer themselves on the bottom of the tubes and the samples and the CsCl would not mix. The polypropylene tube and the syringe and needle were washed with a small volume of fresh GITC which was added to the CsCl. Tubes were balanced with GITC, capped and centrifuged at 25,000 rpm (in a Beckman Ti 70 rotor) for 16 - 18 hours at 22°C.

Centrifuge tubes were cut and supernatants were discarded with care taken to not disturb the RNA pellets. The mouths of the tubes were wiped with Q-tips. Prewarmed TE (10mM Tris HCl, 1mM EDTA, pH 8.0; 0.5mL) at 65°C was added to the RNA pellets and pipetted repeatedly along the walls of the tube to dissolve the RNA. This TE was transferred to a precooled (ice) 15mL sterile polystyrene centrifuge tube. The ultracentrifuge tube was washed out with an additional 0.5mL of prewarmed TE which was added to the other TE in the 15mL centrifuge tube on ice.

The RNA was then precipitated using 0.1volumes of 3M sodium acetate (pH 5.2) and 3 volumes of 99% ethanol (-20°C). After adding these reagents to the resuspended RNA, the mixtures were stored at -80°C. When needed, an aliquot of this mixture was transferred to a 1.5mL polypropylene centrifuge tube and centrifuged at 12,000 xg for 30 minutes at 4°C. Supernatants were removed and the pellets were dissolved in warm (37 - 45°C) TE by pipetting repeatedly.

2. Probe Preparation for Northern Analysis:

The template pT112 was prepared with a fragment of TGF-ß1 cDNA as described above. This template was linearized on either side of its PCS (also described above) and these linearized plasmid DNAs were used in *in vitro* transcription reactions, as described previously to generate sense and antisense probes labeled with ^{32}P-CTP. Briefly, the following (from Promega except for the radioisotope and the polymerases) were added to a microfuge tube on ice, in this order: 100 uCi ^{32}P-CTP (DuPont), all four NTPs (rCTP, rATP, rGTP, rUTP) to a final concentration of 1mM, transcription buffer to a final concentration of 1X, dithiothreitol (DTT) to a final concentration of 10mM, 1ug of BSA (RNase-free), 1uL ribonuclease inhibitor (RNasin), and 50 units of RNA polymerase (either T3 or T7; GIBCO BRL). The mixture was mixed by pipetting repeatedly and then incubated at 37°C for 2 hours.

The template DNA was then removed using deoxyribonuclease I (DNase I) from GIBCO BRL. The enzyme buffer (1M NaAc; pH 5.2, 50mM $MgCl_2$; this mixture is referred to as 10X DNase I buffer) was first added to a final concentration of 1X; this was followed by DNase I. This mixture was incubated at 37°C for a further 15 minutes after which the probes were precipitated in 0.1 volume NaAc (pH 5.2; 3M), 3 volumes ethanol (99%, -20C) at -80°C for at least 30 minutes. Probes were then centrifuged at 12,000 x*g* for 30 minutes at 4°C. RNA pellets were washed with 70% ethanol (-20°C) and centrifuged again at 12,000 x*g* for 5 - 10 minutes at 4°C. Pellets were air dried and resuspended each in 10µL RNA loading buffer (80% formamide (Fluka), 1mM EDTA, 0.1% bromophenol blue (Sigma), 0.1% xylene cyanol FF (Sigma)).

Samples were denatured for 5 minutes at 85°C after which they were loaded onto a 8% polyacrylamide gel (19 acrylamide:1 bisacrylamide) containing 7M urea and 1X TBE buffer. The gel was pre-run for 0.5 - 1 hour at 300V after which the wells were rinsed out and the samples loaded. The gel was then exposed for about 30 seconds to 1 minute to autoradiographic film. The film was developed and revealed the bands corresponding to labeled RNA in the probes. The autoradiogram was then laid under the gel to locate the areas in the gel with labeled RNA fragments. These areas of the gel were cut out, minced into small pieces, collected in microfuge tubes and then eluted using 400uL elution buffer (2M ammonium acetate, 1% SDS, 25µg/mL *E. coli* tRNA) and regular mixing at 37 to 50°C for at least 2 hours. The gel pieces were spun down briefly and the supernatants transferred to separate tubes to which 1mL of ethanol was added to precipitate the RNA. These samples were then mixed and incubated at -80°C for at least 30 minutes.

Gel purified probes were centrifuged at 12,000 x*g* for 20 - 30 minutes at 4°C. Pellets were dried and then dissolved in 50µL of northern hybridization mixture. The radioactivity was measured in 1uL of each sample using a liquid scintillation counter (Beckman).

3. Northern Analysis:

A 1% gel was prepared first in a fumehood by dissolving 1.5g of agarose powder (GIBCO BRL) in 108mL of DEPC-treated water on a heat plate. The solution was brought to a gentle boil after which the mixture was allowed to cool while stirring. Formaldehyde (26.7mL), 10X MOPPS (15mL), and 10mg/mL ethidium bromide (10uL) were added and the gel was poured, after it had cooled to below 50°C, into its mould. A comb for the wells was inserted. After solidifying, the gel was placed in a gel box and 1X MOPPS was added to the surface of the gel.

RNA samples to be electrophoresed were first read spectrophotometrically for their concentrations. Usually, they were diluted 200 times (5uL in 1mL) in water for their concentrations to be determined. Thereafter, the necessary quantities were denatured in 50% formamide, 1X MOPPS, 2.2M formaldehyde for 30 minutes at 65°C. Loading buffer (20% w/v Ficoll 400, 0.1M EDTA, 1.0% w/v SDS, 0.25% w/v bromophenol blue, 0.25% w/v xylene cyanol FF) was added at 1/10 v/v and the samples were loaded onto the gel. The gel was run at 100 volts for about 15 minutes after which it was turned down to 30 volts and left overnight or for about 12 to 18 hours under 1 inch of 1X MOPPS.

RNA was then transferred to nitocellulose membrane (Micron Separations Inc.) in 20X SSC buffer in the following manner. A wick was set up by prewetting 3MM chromatography paper (Whatman) in 20X SSC and laying it over a glass sheet with the ends hanging into a reservoir of 20X SSC (usually in a pyrex dish). The gel was trimmed to retain only the essential areas after which it was laid down on the wick. A piece of nitrocellulose membrane, which is exactly the same size as the gel, was pretreated by immersing it in cold DEPC-treated water followed by boiling DEPC-treated water and then laid onto the gel. Two dry sheets of 3MM Whatman paper cut to the exact size of the gel were laid on top of the nitrocellulose after which a 2 - 3 inch thick stack of paper towels was placed on top. A glass sheet was then laid on top of the paper towels followed by a one pound weight. This assembly was left overnight (12 - 18 hours) so that the RNA could transfer by capillary action onto the nitrocellulose membrane.

The nitrocellulose blot was first washed in 6X SSC and then baked between two pieces of 3MM Whatman paper at 80°C for 2 hours under vacuum to cross link the transferred RNA to the membrane. The membrane was then prehybridized at 45°C for 48 hours (only 1 - 3 hours is necessary) in 60% formamide (Fluka), 0.3M NaCl, 10mM Tris

HCl (pH 8), 5mM EDTA, 10mM $NaPO_4$ (pH 6.8), 10% dextran sulfate, 1X Denhardts' solution (0.02% BSA; 0.02% Ficoll; 0.02% polyvinlylpyrolidone), 0.5mg/mL *E. coli* tRNA, 50mM dithiothrietol or DTT). The prehybridization was conducted in a plastic bag which was placed in a shaking incubator.

Hybridization was subsequently conducted in the same bag as the prehybridization, with the same solution, except that ^{32}P-CTP-labeled T112 probes (gel purified; see below) were added such that the sense probe (T_3) was at 1.2 X 10^6 cpm/mL and the antisense (T_7) was at 2.7 X 10^5 cpm/mL. Optimally, the probe concentration used was 1.0 X 10^6 cpm/mL, however, probe quantities were limited in this instance. Hybridization was conducted for about 18 hours at 48°C.

Blots were washed 3 times, for about 1 - 2 minutes each time, in 2X SSC, 0.1% SDS at room temperature after which they were immersed into 0.1X SSC, 0.1% SDS at 55 - 65°C twice for 15 minutes each time. The blots were then placed in a cassette with an autoradiographic film and exposed for 48 hours.

K. RNase Protection Assay

The protocol used for RNase protection assay (RPA) was obtained from the Third Edition of *Short Protocols in Molecular Biology* (1995). Briefly, gel-purified ^{32}P-CTP-labeled T112 probes were prepared as described above. It was very important to purify labeled probe of uniform size. Therefore, when the acrylamide gel containing probe alone for purification was exposed and revealed smears, only a narrow region was isolated to ensure a homogenous probe sample. This is important since if the probe is protected, then the gel which demonstrates this will show a smear if the initial probe sample is not homogenous with respect to size.

Total RNA extracted from human dermal fibroblasts and precipitated and stored under ethanol at -80°C was centrifuged at 12,000 x*g* for 30 minutes at 4°C. The amount of RNA centrifuged was approximately 50µg to 70µg. The pellets were washed with 70% ethanol (-20°C) and centrifuged again for 10 minutes. Pellets were air dried and resuspended each in 60µL of hybridization mixture (0.2M PIPES, 2M NaCl, 5mM EDTA). These samples were then divided in two to allow each sample to be equally exposed to sense and antisense probes. At this time, no probe control tubes were also setup in which only hybridization mixture was added. These tubes would either receive only probe during the whole procedure or probe and RNase cocktail (see below); however, none of these controls would receive any total cell-extracted RNA. A negative control was also setup in which we expect no protection. This control consisted of substituting the total RNA from fibroblasts with *E. coli* tRNA (Boehringer Mannheim).

Sense and antisense probes were added to their respective target samples and control tubes such that each reaction received 5 X 10^5 cpm. Mixtures containing probes were denatured at 85°C for 5 minutes. Thereafter, hybridization was carried out at 45°C overnight or for 12 to 18 hours.

Samples were centrifuged briefly to bring down condensate after which each received 350µL of ribonuclease digestion cocktail (10mM Tris HCl, pH7.5, 300mM NaCl, 5mM EDTA, 40µg/mL RNase A, 2µg/mL RNase T1). Samples were mixed and incubated for 30 - 60 minutes at 30 minutes. Each sample then received 20µL of 10% SDS and 5µL of proteinase K (10mg/mL) and was then incubated at 37°C for 15 minutes. Samples were then extracted with phenol/chloroform/isoamyl alcohol (25:24:1) by adding 400µL of a phenol/chloroform/isoamyl alcohol mixture to each reaction and vortexing followed by centrfuging for 2 minutes at 12,000 x*g*. The aqueous phase was removed to another tube and treated with an equal volume of chloroform after which samples were centrifuged briefly again. Supernatants were transferred to fresh tubes containing 1µL of 10mg/mL *E. coli* tRNA and to these was added 1mL of ethanol. Samples were incubated at -80°C for at least 30 minutes.

Samples were centrifuged at 12,000 x*g* for 30 minutes at 4°C. Pellets were washed with 70% ethanol and centrifuged again for 10 minutes. Pellets were then resuspended in 10µL of RNA loading buffer and run on an 8% acrylamide/7M urea gel as described above under Probe Preparation. Also included on this gel were two labeled molecular weight markers. One was a 100bp DNA ladder (GIBCO BRL) which was end-labeled using a-^{32}P-dCTP and the T4 DNA polymerase labeling protocol which is supplied with the DNA ladder. The other marker was lambda/HindIII (GIBCO BRL) which was labeled in the same way.

The gel was run for 2 hours at 300V at which time the bromophenol blue had just started to run off the gel. The gel was then dried using a gel drier under vacuum and exposed to autoradiographic film for 2.5 hours after which the autoradiogram was developed.

L. Immunohistochemistry

Decorin was detected using a mouse IgG monoclonal antibody known as 6D6 (Pringle et. al., 1985). The antibody 6D6 has been previously determined to be specific for the C-terminal portion of the protein core (Scott et. al., 1993). The staining was conducted as previously described (Scott et. al., 1995). Briefly, tissues were deparaffinized in xylene then hydrated through decreasing concentrations of ethanols. Tissues were then immersed in 2% H_2O_2 in methanol to inactivate endogenous peroxidases. Thereafter, blocking non-specific sites was performed in blocking agent (20% v/v normal goat serum/0.2% w/v dry non-fat milk/0.1% v/v Tween 20/10% v/v Cambridge Research Biochemicals 'Blocking Reagent' in PBS) followed by overnight incubation at 4°C with 6D6.

Antibody was detected using a peroxidase-antiperoxidase system. The colorimetric reagent was diaminobenzidine/hydrogen peroxide; sections were counterstained with haematoxylin.

CHAPTER 3. RESULTS

I. Decorin Expression Correlates with the Progressive Maturation of Hypertrophic Scar

The expression of decorin mRNA in post-burn hypertrophic skin was investigated by *in situ* hybridization using a riboprobe that was generated by *in vitro* transcription off a decorin cDNA template that was inserted into a bacterial plasmid DNA vector.

A. Establishing D150 Probes

The first cDNA clone that was tested for this purpose was a 150bp fragment corresponding to a region in exon 8 of human decorin that was previously cloned into the polycloning site (PCS) of pGEM 4Z (henceforth, this construct will be referred to as pD150 and the labeled transcipts generated from it as D150). This vector harbors a T7 and an SP6 promoter region, one on each side of its PCS. The size of the fragment was confirmed by restriction digestion with *Pst*I and *Eco*R1. The resulting fragments were compared for size against the DNA molecular weight marker lambda DNA digested with *Hind*III (λ/*Hind*III) which gives eight DNA fragments ranging in size from 125 to 23,130 base pairs. Upon digestion a small fragment is liberated from pD150 that corresponds to the expected size of the cDNA fragment (Figure 1A).

Sequencing of the plasmid using the T7 primer yielded a sequence that was complementary to the mRNA sequence listed in Genbank (accession #L01131) for exon 8 of decorin, indicating that the strand from which this sequence was generated was sense and the riboprobe synthesized from it using T7 RNA polymerase, antisense. Consequently, SP6 polymerase should yield a sense riboprobe. Two attempts were made to label riboprobes transcribed off this template with digoxigenin-11-UTP as the label. In both attempts the SP6 polymerase yielded substantially less probe, five times less in the first reaction and 20 times less in the second reaction, than the T7 polymerase (Figure 1B). Interestingly, when spectrophotometry was used to quantitate the total amount of RNA transcribed in an *in vitro* transcription reaction using rat TGF-ß1 cDNA (discussed in more detail below) as the template, SP6 polymerase was found to produce six times less RNA than T7 polymerase. The low yield of cRNA probes synthesized by SP6 polymerase has been reported by others (Logel, et al., 1992) and some investigation into the problem has led some to believe that premature transcript termination (Roitsch and Lehle, 1989) may be a cause.

Dot blot hybridizations of the probes to serially diluted pD150 bound to nylon displayed a sensitivity of only 50pg in two experiments (Figure 1C); the aim of the dot blot hybridizations was to detect down to between 0.1pg and 10pg of target DNA which would be sufficiently sensitive. Six attempts at performing *in situ* hybridization on cultured human dermal fibroblasts and on sections of hypertrophic scar failed; problems included staining with both sense and antisense probes as well as excessive background levels.

B. Establishing D600 Probes

Such problems led to choosing a different template construct from which to generate riboprobes. The next template tested was a 622bp fragment corresponding to nucleotides 727 to 1348 of human decorin cDNA (Krusius and Ruoslahti, 1986). This fragment includes regions from exons 7 and 8 of human decorin (Genbank accession #L01130 and L01131) and is least identical to biglycan cDNA when compared to other similarly sized regions in the cDNA. This fragment was cloned into pBluescript KS+ vector at the *Hinc II* site in its PCS (henceforth, this construct will be referred to as pD600 and the labeled riboprobes transcribed from it as D600) . The PCS in this vector is flanked on either side by RNA polymerase T3 or T7 promoters. Sequencing of the insert was conducted from both ends using both T3 and T7 primers; the results verified the accuracy of the insert sequence as well as its orientation in the plasmid. The sequence obtained using the T7 primer matched exactly with portions of sequences provided for exons 7 and 8 in Genbank indicating that the transcript produced off the same promoter should be sense. The plasmid pD600 was digested with the restriction enzymes *Apa*I or *Cla*I (Figure 2A) to linearize it for use as a template for *in vitro* transcription labeling using either T7 or T3 RNA polymerase, respectively; digestion with *Apa* I and *Cla* I was used to liberate the 600bp fragment for verification of the clone (Figure 2B).

The labeled riboprobes were run on a 1% denaturing agarose gel containing formaldehyde and subsequently transferred to nitrocellulose by northern blotting and fixed to the membrane by baking. The RNA was then subject to the standard colorimetric detection procedure for digoxigenin-labeled probes (Boehringer Mannheim) (Figure 2C). This procedure is referred to as a pseudonorthern analysis and was conducted to check the efficiency of transcription, the integrity of the probes, and the level of degradation. The results indicate efficient transcription since uniform sized bands were detected for both the T7- and T3-labeled products. As well, the amount of degradation seemed low since there did not appear to be many bands smaller than the prominent, intense bands. Unfortunately, however, the digoxigenin-labeled RNA molecular weight marker III (Boehringer Mannheim) that was run in lane 2 did not appear after developing and therefore, it was not possible to verify the size of these transcripts. For reference purposes, though, the digoxigenin-labeled transcripts which were generated earlier from pD150 ran faster than those of pD600 (lanes 3 and 4 compared to lanes 5 to 8) as expected. Another reference which was later incorporated into the gel was the digoxigenin-labeled control RNA from Boehringer Mannheim which is 760 bases in length and labeled using the same protocol.

All D600 probes that were synthesized were subject to quantitation and dot blot hybridization. Probes were only used if the amounts of both sense and antisense transcripts were within one order of magnitude (Figure 2D). Usually, the quantities were much closer than this. Another criterion for the use of the probes was that they had to perform specifically by dot blot hybridization, ie. when all dots appeared on a dot blot hybridization or when the dots corresponding to salmon sperm DNA or yeast/*E. coli* tRNA appeared then the probes were not used (Figure 2E). Since the target was applied in serial dilution, the resulting signal after hybridization should be graded according to dilution. A final criterion applied to the screening of probes was their sensitivity. Using dot blot hybridizations, the probes were tested for the least amount of target DNA they could detect. Only those probes showing a sensitivity equal to or less than 10pg of DNA were used for *in situ* hybridizations.

C. Optimizing In Situ Hybridization with D600 Probes

In situ hybridization, using sense and antisense probes, was attempted on H16/N16 fibroblasts which were cultured on APTEX-coated slides using protocol #3. Cultured fibroblasts were chosen as a positive control on which to test the decorin probes because these cells are reported to produce decorin abundantly. From the sequencing results, it was determined that T3 polymerase should generate an antisense probe and conversely, T7 polymerase should generate a sense probe. Conditions which were tested were stringency of hybridization and of the post-hybridization washes as well as a monoclonal antibody against digoxigenin (the polyclonal antibody from Boehringer Mannheim is their prescribed antibody for the standard detection procedure). When hybridization was conducted at T_m-10°C, the signal detected in the fibroblasts was very weak; the signal appeared as faint dots instead of the expected clear blue staining. When the stringency of hybridization was lowered, by decreasing the temperature of hybridization to 21°C below T_m, strong cytoplasmic staining appeared. At this hybridization stringency, when the stringent post-hybridization wash was conducted at 19°C below T_m (Figure 3A,B), the staining was lighter compared to lower stringency conditions (T_m-28°C; Figure 3C,D). When the stringency of hybridization was lowered using higher salt concentrations in the hybridization buffer, nuclear staining appeared more intense (Figure 4). Use of the monoclonal antibody against digoxigenin resulted in no staining at all.

The use of D600 probes in paraffin-embedded skin tissue required the optimization of additional variables in the *in situ* hybridization protocol. This included finding the optimal concentration of proteinase K which would enhance the accessibility of the target to the probe and thereby enhance the final staining without compromising tissue morphology. As well, acetylation of free amino groups was tested to minimize background binding of the probe. The hybridization mix was also altered to include a higher concentration of formamide for higher stringency, dextran sulfate to improve the probe-to-target ratio, and tRNA to bind nonspecific sites which the probe may attach to. Post-hybridization washes later incorporated RNase A to minimize any signal contributed by nonhybridized probe. And finally, in the detection procedure, casein blocking buffer (Cambridge Research Biochemicals) was used to minimize background binding of the anti-digoxigenin antibody. This series of changes resulted in the development of protocol #5. When this protocol was used with the sense D600 probe, it yielded negligible amounts of cellular staining whereas the antisense probe demonstrated mainly cytoplasmic staining of cells in the matrix believed to be mostly fibroblasts.

D. In Situ Hybridization on Hypertrophic Scar, Mature Scar, and Normal Skin with D600 Probes

Nine sections of hypertrophic scar, four sections of mature scar, and eight sections of normal skin were probed with D600 probes (both sense and antisense) using protocol #5. Varying numbers of positive cells were found in the sections of HSc (Figure 5 - 7) and MSc (Figure 8); more interesting, however, was the observation that in regions where the collagen fibrils appeared to be thin, loosely packed, and arranged in whorls, decorin expression appeared very faint or absent. Where the collagen architecture appeared to be gaining a more normal appearance such that the collagen appeared more organized, which sometimes was within the whorls, decorin expression was more prevalent. Normal skin (Figure 8), in contrast, displayed very few positive cells. Background was minimal. However, some problems which persisted were staining in the keratinocytes of the epithelium, which are not expected to produce decorin, and frequent occurrence of staining in nuclei where we do not expect to find any mRNA.

Some background problems were alleviated by incubating tissue sections under cold antibody solution at 4°C overnight instead of at room temperature for 0.5 hours during the detection procedure. One particular *in situ* hybridization experiment was used to test this variable. Serial sections of one block of HSc tissue were probed using the D600 probes and, during detection, were subject to polyclonal anti-digoxigenin antibody at three temperatures for different lengths of time: at room temperature for 30 minutes (Figure 9A), at 4°C for 7.5 hours, and at 4°C for 20 hours (Figure 9B). Incubation at 4°C greatly reduced the background staining associated with the matrix and made the positive cells more easily detectable. The longer period of incubation seemed to intensify the specific signal but did not increase the background to any obvious extent.

E. Possible Nonspecificity of D600 Probes

A report by Saunders and co-workers (1994) provided a reason to investigate further the specificity of the staining obtained with the D600 probes. In this report, a well-planned and comprehensive study showed that previous studies which localized mRNAs for seminiferous tubule proteins to the basal portions of stage IX and X tubules in rat testis were not accurate. This was believed to be due to artefactual binding of probes produced from a pBluescript vector. Furthermore, a GC-rich region in the pcs of the vector was implicated as the region most likely to be responsible for this nonspecific binding. From a battery of riboprobes used, only those which were produced from pBluescript by T7 polymerase appeared to hybridize to a target in residual bodies which were basally located in stage IX and X tubules. Using a cRNA probe generated by pBluescript vector alone using T7 polymerase and a 27mer oligonucleotide probe corresponding to the polycloning site of pBluescript adjacent to the T7 promoter, hybridization was found to localize to basal residual bodies. Antisense D600 probes, in contrast, were generated using T3 polymerase. Nonetheless, this data renders suspicious results generated by probes that were made from pBluescript vectors especially with T7 polymerase. For this reason, the decorin fragment in pD600 was digested out of pBluescript and cloned into the pT7/T3(α-18) vector.

F. Establishing D620 Probes

The plasmid pD600 was digested with *Kpn* I and *Pst* I to liberate the decorin cDNA fragment along with small regions of the pBluescript PCS flanking it on either side. This fragment was then ligated into pT7/T3α-18 and the resulting clone was amplified. The new construct (henceforth referred to as pD620 and the labeled riboprobes transcribed from it as D620) had two *Eco*R I sites, one on either side of the decorin insert. One *Eco* RI site came from the pBluescript vector that the insert came from and the other was part of the pT7/T3 vector. Linearizing with *Kpn* I or *Pst* I resulted in a single plasmid DNA band of approximately 3.58kb which is the predicted length (Figure 10A). Digesting with *Eco*R I resulted in a shorter plasmid fragment with an additional band of about 620bp as expected

(Figure 10A). These results confirm the structure of the new construct. To verify the integrity of this construct and the orientation of the decorin insert in the plasmid, sequencing was performed using the T7 primer. This resulted in a sequence that displayed regions of identity to exons 7 and 8 of human decorin mRNA as reported in Genbank (Accession #s L01130 and L01131). Since sequencing was performed using the Sanger method, this also confirmed that using T7 polymerase, the resulting cRNA would be sense; hence, using T3 polymerase and transcribing off the opposite strand would yield an antisense cRNA probe.

Labeled probe was produced using pD620 as template and digoxigenin-11-UTP as the label. Probes which displayed a sensitivity of 50pg or less, by dot blot hybridization against serially diluted pD620 (Figure 10C), were used for *in situ* hybridization. Quantitation was performed by dot blot and the amounts of T3 and T7 probes transcribed were always within one order of magnitude (Figure 10B). Labeled D620 was examined by pseudonorthern analysis and compared to a 760bp digoxigenin-labeled control RNA transcript provided by Boehringer Mannheim (Figure 10D). Initial results displayed one strong band for the T3 probe in the same area as the 760bp control in addition to two other high molecular weight bands. The T7 probe also gave a band in the same area as the 760bp control; however, it appeared less intense even though five times more of it was run than the T3 probe and two other more intense higher molecular weight bands appeared. When these probes were denatured under more stringent conditions, ie. 80% formamide instead of 50% and 85°C instead of 65°C, only single bands appeared for both the T3 and T7 probes and the T7 band appeared more intense, as expected considering that more of it was loaded on the gel than the T3 probe (Figure 10E).

The D620 probes were also labeled with biotin-11-UTP and used to probe a northern blot which contained total RNA extracted from human dermal fibroblasts previously separated on a 1% denaturing agarose gel. Transferring the RNA onto a nylon membrane and subsequent probing was done using Ambion kits for RNA labeling/detection and northern blotting. After hybridization and chemiluminescent detection, two bands were detected which corresponded to those normally reported for decorin mRNA (data not shown). These bands were 1.6kb and 1.8kb in length.

G. Optimizing In Situ Hybridization with D620 Probes

Five initial separate attempts at performing *in situ* hybridization (protocol #5) using D620 probes on different strains of hypertrophic and normal dermal fibroblasts grown on APTEX-coated slides failed to produce convincing positive results. Cell strains which were used as targets were N19 (18 hours), H/N14 (27 hours), N20 (18 hours), and N20

(48 hours). The number of hours indicate how long the cells were grown on the slides after subculturing before they were fixed with 4% paraformaldehyde. In each experiment, different concentrations of proteinase K were tested, usually 0µg/mL, 0.5µg/mL, and 1.0µg/mL. Only two of the five experiments revealed any staining; however, in one experiment the signal was predominantly nuclear and in the other it was barely detectable. Proteinase K enhanced the staining; however, at concentrations above 0.5µg/mL, some cells detached from the slides.

Finally, using protocol #5 in a time-course experiment on H/N 8 grown on APTEX-coated slides and fixed at 4, 17, 36, and 100 hours after subculturing, significant staining appeared (Figure 11). Proteinase K was used in this experiment at a concentration of 0.5µg/mL. Interestingly, the amount of signal increased with the number of hours the cells were cultured on the slides until 100 hours when the intensity of cytoplasmic staining decreased. Also of interest was that normal fibroblasts displayed more intense staining for decorin mRNA than hypertrophic cells up to 36 hours. The fact that normal human dermal fibroblasts produce more decorin than cells from hypertrophic scar was shown by northern analysis and western blotting (Scott et al., submitted for publication). In a subsequent experiment using H/N20 fibroblasts which were similarly grown on slides but fixed at 12, 28, 60, and 98 hours after subculturing, decorin mRNA expression rose up to 60 hours and then decreased at 98 hours. Again, staining in the hypertrophic cells always had lower intensity than in the normal cells. The increase in decorin expression with time after subculturing was explained by Mauviel and co-workers (1995) who demonstrated that decorin expression was transcriptionally up-regulated during quiescence. Therefore, cells that were grown for longer and in a denser environment, so that their growth and rate of division was slowed, had an increased expression of decorin mRNA.

In addition to the change in the template used to produce the probes, the *in situ* hybridization procedure was changed in that RNase A was incorporated into the procedure in an effort to increase the specificity of the signal and therefore wash out some background binding of the probes which occurred in tissue sections. These objectives were fulfilled (data not shown). Additionally, previous results which were obtained in hypertrophic scars, mature scars, and normal skin using the D600 probes were validated with the D620 probes by performing *in situ* hybridization with D620 probes on tissue which had been previously probed with D600. Patterns of staining observed with D620 in the dermis of such tissues resembled very closely those seen with the D600 probes. Therefore, the results obtained with the D600 probes in hypertrophic scar, mature scar, and normal skin were considered accurate and were quantitated along with those obtained with D620 probes.

H. In Situ Hybridization on Hypertrophic Scar, Mature Scar, and Normal Skin with D620 Probes

The pattern of expression of decorin at the transcriptional level was compared between a total of 20 scar specimens and 6 normal skin specimens using *in situ* hybridization (protocol #5) with either D600 or D620 probes which were labeled with digoxigenin-11-UTP. Hypertrophic scar sections differed in the number of cells which were positive for decorin mRNA. Three examples of *in situ* hybridization on hypertrophic scar tissue sections are shown in Figure 12. A specimen taken only five months post-burn showed very few positive cells for decorin mRNA (Figure 12A). In contrast, in a specimen obtained at 12 months post-burn there were a large number of cells expressing decorin mRNA (Figure 12C). In a scar specimen taken very late (216 months) after injury, very few cells expressed decorin mRNA, although those cells which appeared positive usually had intense staining (Figure 12E). Normal skin usually had very few positive cells if any.

I. Decorin mRNA expression shows a time course of appearance during hypertrophic scar

After examining all of the scar and normal skin specimens, a correlation between decorin expression and time after injury became apparent. Specimens which were collected early after injury displayed a low frequency of cells expressing decorin mRNA. Specimens which were collected later than one year post-burn had many cells which were positive. However, those samples which were obtained after three years displayed, once again, very few positive cells. A method to quantitate the data was established next to determine if the apparent differences between the number of positive cells in different scar samples, based on time after injury, was significant. All of the scar and normal tissue specimens studied were evaluated as a function of the depth of the dermis, since injuries that lead to hypertrophic scar are often partial thickness. The number of positive cells were counted in ten randomly chosen fields (400x magnification) in three evenly divided regions of the dermis of a section of each specimen (Chapter 2, I; Figure 13). The three regions of each section were called papillary, middle, and reticular dermis. The number of positive cells in each region were totaled and these totals were plotted as a function of time after injury on a scatter plot (Figure 14A). In addition, the total numbers of positive cells were also plotted. This demonstrated the trend in total cells positive for decorin over time after injury without discriminating against any particular region of the dermis (Figure 14B).

An interesting correlation became apparent in each region of the dermis. At early times after injury, decorin expression appeared suppressed. Its levels increased dramatically between one and three years post-burn. This was followed by a decrease during later stages of healing. The specimens were then grouped into three groups according to time after injury: early (0-11 months), intermediate (12-36 months), and late (more than 36 months); the groups contained 8, 7, and 5 samples, respectively. Scatter plots which organized the data into these three groups demonstrate more dramatically the shift in the abundance of positive cells at different times (Figure 15A & B).

Using the same quantitation method outlined in Figure 13, the total number of connective tissue cells was counted using sections stained with hematoxylin and eosin. Ten randomly chosen high power (40x objective power) fields in each third of each section were counted. The numbers from each region of the dermis were totalled and plotted against time after injury (Figure 16A) . The total numbers, which were the sums of the numbers in each region of the dermis for each sample, were also plotted (Figure 16B). Whereas the number of cells do not differ remarkably between the early and intermediate time points after injury, a significant decrease was observed in the late time point. To determine the percentage of positive cells over time, the number of positive cells in each region of the dermis for each sample was divided by the corresponding total number of cells. These numbers were also plotted on scatter plots and expressed either as a function of the individual time points (Figure 17) or as a function of the early, intermediate, and late periods (Figure 18). Regardless of the manner in which they are expressed, the graphs of the percentage of positive cells displays a 'tighter' distribution of data than the raw data. Therefore, the difference between the expression of decorin mRNA between the three major time points appears more significant; as well, the calculation of percentage positive cells eliminates the possibility of the dramatic changes in decorin expression being the result of a change in cell number over time.

The average numbers of positive cells in each region of the dermis at either early, intermediate, or late times after injury as well as in the normal samples are presented in Table 2. Similarly, the total number of connective tissue cells in each region of the dermis at each time period, as well as in normal samples, are presented in Table 3. And, finally, the percentage of positive cells at each time period, as well as in normal samples, are presented in Table 4. Decorin expression shows a significant increase in all regions of the dermis, papillary, middle and reticular, from early to intermediate time periods. These levels decreased significantly in all regions from intermediate to late time periods. Comparisons by one-way analysis of variance (ANOVA) revealed a statistically significant difference ($p<0.01$) between the mean number of positive cells in the early and the intermediate time periods and between the mean number of positive cells in the intermediate and the late time periods ($p<0.01$) for all regions of the dermis (Table 2). In the whole dermis, the difference in the mean number of positive cells between the early and the intermediate time periods and between the intermediate and the late time periods are significant ($p<0.001$). The differences between the early and late time periods in each region of the dermis or in the whole dermis were not significant.

Interestingly, when the percentage of positive cells were considered (Table 4), the significance of the differences between the early and intermediate time periods and between the intermediate and the late were maintained ($p<0.01$). Furthermore, for the papillary and reticular dermis between the early and the intermediate periods, and for the reticular dermis between the intermediate and the late periods, the significance was even greater ($p<0.001$).

J. Immunohistochemical staining levels correlate with decorin mRNA expression except in late hypertrophic scar

Serial sections to those shown for *in situ* hybridization were stained using a monoclonal antibody for decorin, 6D6. Decorin is detected mainly as an extracellular protein (Figure 19). In the early specimens, very little staining can be found for this proteoglycan, as is seen in the 5 month scar specimen. In contrast, a dramatic increase in staining is seen in the specimens of the intermediate time point as shown in the 12 month scar specimen. This intensity of staining stays high and in some cases increases in late samples in which the organization of collagen into fibre and fibre-bundles now closely resembles that of normal skin, as seen in the 216 month specimen. In all of the normal skin samples studied, abundant decorin was found.

K. Decorin expression displays regional variation during the course of hypertrophic scar

The time course of decorin expression during hypertrophic scar, detected either by *in situ* hybridization or immunohistochemistry, was made more interesting by the observation that nodular- or whorl-like areas within the dermis were usually devoid of any decorin mRNA (Figure 20A) or protein expression (Figure 20B). Such regions within the dermis had collagen fibrils which were very thin and loosely-packed. However, where the collagen appeared to be gaining the qualities of mature scar or normal skin, which was sometimes apparent within the whorl-like areas, staining for decorin was seen.

II. TGF-ß1 Expression in Hypertrophic Scar

The pattern of expression of TGF-ß1 was investigated in sections of hypertrophic scar, mature scar, and normal skin using a series of cRNA probes which were generated off different templates that incorporated cDNA fragments of rat and human TGF-ß1. The attempts made to establish a working protocol to detect TGF-ß1 mRNA in our scar and normal skin samples with a satisfactory degree of sensitivity and specificity were numerous and the task itself, very challenging. This work was started before that on decorin and was conducted alongside the decorin studies. Therefore, many of the conditions which were optimized for the decorin studies were done also during the TGF-ß work. The probe templates were changed in an effort to produce more specific probes and to increase transcription efficiency as discussed below; therefore, these changes were made to optimize the *in situ* hybridization protocol for the detection of TGF-ß1 mRNA in our human skin samples.

Previous reports have demonstrated that TGF-ß levels do increase during the proliferative phase of wound healing. Regarding the local production levels of this cytokine in hypertrophic scar, TGF-ß1 mRNA levels were found by dot blot analysis to be 61% higher in three samples of the scar tissue compared to normal skin from the same patients respectively (Ghahary et al., 1993). In this same study, however, northern analysis of samples from three other patients revealed a 250% increase in a 4.9 kb transcript for TGF-ß1 compared to a normal skin control. Cultured fibroblasts explanted from hypertrophic and normal skin tissue displayed two transcripts (4.9 kb and 2.5 kb) which did not significantly differ in quantity between HSc and NSk samples. Immunohistochemical analysis (Ghahary et al., 1995) using a rabbit polyclonal antibody which is supposed to recognize extracellular TGF-ß1 revealed staining in HSc tissue but no staining in normal skin.

The specific pattern of expression of mRNA for TGF-ß1 has not been previously investigated in HSc tissue. The geographic localization and temporal expression of the TGF-ß1 mRNA transcript during the progression of wound healing that leads to HSc may help us understand the etiology of the scar. As well, we know from previous immunohistochemical studies (Scott et al., 1995) that TGF-ß1 and decorin have similar temporal expression patterns, i.e. they are scarce in HSc but more prevalent in MSc sections. Also, both localized to the deep dermis in HSc tissue. Therefore, it would be valuable to know if TGF-ß1 and decorin are both being actively produced, locally, in HSc. If this is true, it would also be worthwile to find out if they are both produced in the same location. Alternatively, if this cytokine is not being produced locally, it may be deposited by the circulatory system and bound to decorin until needed.

A. Rat TGF-ß1(287)/pGEM 3Z as a Template for cRNA Probes

1. Establishing cRNA Probes From Rat TGF-ß1(287)/pGEM 3Z

The first template that was used to generate cRNA probes for TGF-ß1 consisted of a 287bp cDNA fragment of rat TGF-ß1 (rTGF-ß1) cloned into the PCS of the plasmid vector pGEM 3Z at restriction sites *Pst* I and *Bam* H I. The PCS of this vector is flanked by a T7 promoter on one end and by an SP6 promoter on the other. Sequencing using the Sanger method (DNA Sequencing Lab) and the T7 primer revealed a sequence that was identical to 287 nucleotides in rat TGF-ß1 mRNA between nucleotides 601 and 886 (Genbank accession #X52498). Therefore, a cRNA probe generated using this template and T7 RNA polymerase has the same sequence as rat TGF-ß1 mRNA and is considered sense. Considering the high degree of homology of the TGF-ß1 gene between species (>90%), this template was used to generate riboprobes for probing human dermal fibroblasts and skin.

The template was digested with *Pst* I and *Bam* H I which liberated the 287bp rTGF-ß1 cDNA fragment from the plasmid (Figure 21A). The template was then used directly after linearizing with either *Pst* I or *Bam* H I (Figure 21B) which digested the template on either side of the insert cDNA. The *Pst* I digest was used with the T7 polymerase and the *Bam* H I digest with SP6 polymerase. The labeling reactions were conducted with 500ng of template DNA for anywhere between five and twelve hours and produced only small quantities of probes, especially using SP6 polymerase; T7 polymerase was able to produce 6.25µg of probe but SP6 polymerase, only between 250pg and 65ng per labeling reaction (Figure 21C). And while the sensitivity of the T7 probes was 10pg, that of the SP6 probes was only 50 - 100pg (Figure 21D). These probes were used in *in situ* hybridizations on cultured dermal fibroblasts as well as on paraffin sections of HSc and normal skin.

2. Optimizing *in situ hybridization* protocol with TGF-ß1(287)/pGEM 3Z cRNA probes

The *in situ* hybridizations (protocol #1) performed on the paraffin-embedded tissues resulted in a loss of most of the tissues. This was probably a result of too high concentrations of proteinase K which was tested later. As well, overstaining of tissue which were stained with both sense and antisense probes was seen which was probably due to a combination of excessive quantities of proteinase K and probe (data not shown). Quantitation of the probes revealed that the amount of T7 probe used per slide was up to 10000X more than that of the SP6 probe. When the procedure failed with the tissues, human dermal fibroblasts which were explanted from HSc and patient matched NSk were tested as positive controls with which to establish different parameters of the *in situ* hybridization protocol, considering that similar fibroblasts have been previously demonstrated by northern analysis to produce TGF-ß1 mRNA and especially in high quantities soon after subculturing (Varedi, et al., 1995).

The cells which were initially used were H/N15 (P5) which were cultured on APTEX-coated glass slides for twelve hours before fixing and storing them under 4% paraformaldehyde (PFA) for three days. In situ hybridization (protocol #1) on these cells was performed with different concentrations of proteinase K and various hybridization temperatures. Concentrations of proteinase K above 1µg/mL and hybridization temperatures above 52°C obliterated any staining (data not shown). Most of the staining seen was obtained with the T7/sense probe but this may have been due to that fact that even though equal volumes of probe were used in the hybridization solution, later quantitation of the probes revealed that the T7 probe was 1250X more concentrated than the SP6 probe.

At this point, numerous problems were recognized with, and corrections made to, the labeling and *in situ* hybridization protocols. Firstly, the cDNA templates used in the labeling reactions had not been purified after restriction digestions; this was corrected by extracting the digested products with phenol/chloroform (1:1) to inactivate and remove all proteins, especially the enzymes in the DNA solutions. Secondly, after precipitating the labeled probes, the pellets were resuspended at room temperature in sterile deionized water by repeatedly pipetting the water over the wall of the microfuge tubes. This resulted in a relatively low yield of the probes due to inadequate resuspension. The yield was improved considerably by resuspending the pellets in DEPC-treated water at 37°C for 15 minutes with regular vortexing. The DEPC was used to inactivate RNases in the water and the warmer temperature assisted in dissolution. Thirdly, the amount of labeled RNA that was trancribed off the template DNA using SP6 polymerase was consistently much lower than that transcribed using the T7 polymerase. The efficiency of transciption by T7 and SP6 RNA polymerases may be different and factors that affect this efficiency were sought. It has been reported that SP6 polymerase is not able to efficiently incorporate digoxigenin-labeled nucleotides into newly synthesized RNA strands and that altering the ratio of unlabeled to labeled nucleotides in a labeling reaction such that the concentration of the unlabeled nucleotide is increased beyond that recommended by Boehringer Mannheim in an effort to decrease the level of steric hindrance improves the rate of incorporation. This was attempted in two experiments where in addition to the labeling mixture provided by Boehringer Mannheim which contained digoxigenin-labeled UTP at a ratio of 35:65, labeled UTP at a ratio of 15:85 was also used. The lower ratio of labeled UTP resulted in either smaller amounts of labeled cRNA or no difference at all. Therefore, the labeling mixture provided by Boehringer Mannheim continued to be used. The discrepancy between the amount of probe produced using these two polymerases was further confirmed through spectrophotometric determination of the concentration of total RNA transcribed in a labeling reaction. Equal volumes of RNA transcribed by both T7 and SP6 RNA polymerases in the presence of digoxigenin-labeled UTP were diluted to the same ratio and read by spectrophotometry to determine the concentration of total RNA. The concentraton of RNA in the T7 sample (1.15µg/uL) was six times that in the SP6 sample (0.192µg/uL) Fourthly, the amount of template used in the labeling reactions (500ng) was found to be too low; increasing this amount by at least three-fold yielded anywhere between a 10- and 100-fold increase in the amount of labeled probe (Figure 22). However, SP6 polymerase still gave less probe than T7 polymerase. The fifth problem was that of maintaining an RNase-free environment throughout the labeling and *in situ* hybridization procedures. Considering the widespread presence of RNases and therefore the strong possibility of degradation of probes and target RNA, it was necessary to treat whatever reagents possible with diethylpyrocarbonate (DEPC) which destroys RNases. Certain solutions, such as those containing amines (eg: Tris buffers) which react rapidly with DEPC and are therefore not treatable with DEPC, were made in DEPC-treated water. Plasticware, such as the containers used to perform the *in situ* hybridizations, were treated with chloroform to eliminate RNases. Glassware such as beakers and graduated cylinders were baked at 180°C - 200°C for at least 12 hours.

3. Re-evaluating cRNA Probes Produced From TGF-ß1(287)/pGEM 3Z

To characterize the probes further, equal quantities of SP6 and T7 probes were analyzed by pseudonorthern analysis. This was performed to visualize the homogeneity of the probe fragments, to compare the sizes of the probes with each other, to possibly detect degradation of the probe which would appear as smaller fragments or a smear below the main band, and to potentially visualize the effects of different storage conditions on the probe, ie. -20°C vs -70°C and storage of probe in hybridization mix vs in DEPC-treated water.

In the first attempt at running rTGF-ß1 probes, those stored at -20°C were run beside those kept at -70°C. The results indicate bands of very close to the same size for SP6 and T7 probes and no difference between the quality of the probes stored at the different temperatures; however, the results were ambiguous since the lanes contained more than just one band and a heavy smear through its entire length which obscured the bands (data not shown). Problems identified with this experiment include the samples not being adequately denatured before running on the gel, overloading the lanes, degradation of the samples, and the absence of a marker to allow the estimation of the size of transcripts in the samples.

In the next attempt, samples were denatured using heat, formaldehyde and formamide; as well, one tenth the amount of sample was loaded and a 100bp DNA ladder in addition to total RNA was added as a reference marker. In this run, samples which were stored in hybridization mix at -20°C were also included to compare them with those stored in DEPC-treated water. The results (not shown) indicate a drastic improvement in the clarity and resolution of the final bands seen compared to the initial attempt. However, it is hard to estimate the size of the bands since none of the markers are labeled with digoxigenin and this large molecule retards the mobility of nucleic acids through a gel. As well, multiple bands are seen in single lanes indicating that either more stringent conditions are necessary in which to run the gel or with which to pre-denature the samples; this could also indicate that the labeled cRNA samples are not homogeneous and contain very large labeled products which may have resulted from some undigested template DNA. Samples which were stored in hybridization mix appear degraded.

All of the corrections listed above for problems associated with the preparation of the cRNA probes and their usage resulted in improvements in the amounts of probes produced. In three labeling reactions, about 5ug of each of T7 and SP6 products were observed. These probes, however, did not display very good sensitivity levels; usually the least amount of immobilized target DNA that they were able to detect was about 10 to 50pg. As well, a problem with the specificity of the probes was noticed when conducting dot blot hybridizations as the probes would often bind to all of the serial dilutions of the target DNA with equal intensity as well as the control dot (salmon sperm DNA). The cDNA templates were later purified from 1% agarose gels to ensure the purity of the linearized template. Subsequent to this added procedure in preparing the templates, the T7 product increased from 5μg of labeled cRNA to 25μg; however, the amount of SP6 product was only about 20ng at best and problems with sensitivity and specificity still persisted. Clearly, with a pure template, and similar conditions between the labeling reactions involving T7 RNA polymerase and SP6 RNA polymerase, SP6 is less efficient at producing cRNA products which are labeled with digoxigenin-11-UTP.

4. In Situ Hybridization on Human Dermal Fibroblasts with TGF-ß1(287)/pGEM 3Z cRNA Probes

The process of identifying the above-mentioned problems associated with probe production and function involved, in addition to the many labeling procedures, eighteen separate *in situ* hybridizations (protocol #'s 1 to 3), fourteen of which involved cultured human dermal fibroblasts. As mentioned above, the fibroblasts provided a valuable control environment to test the different variables of the *in situ* hybridization protocols used. Indeed, valuable lessons were learned about probe labeling conditions and conditions for the *in situ* hybridizations which were later applied to paraffin-embedded tissue. Through all of these experiments, equal amounts of T7 and SP6 probes, or sense and antisense probes respectively, were used on each target slide (between 10ng and 20ng per slide); this helped to rule out any effect of probe quantity on the results.

Initially, both sense and antisense probes gave positive results in H/N15 and H5/N5 cells (using protocol #1). However, the hybridization temperatures used were about 35°C - 45°C below the T_m calculated for a hybrid involving the probe and its complement and the post-hybridization washes were not stringent enough as the temperature of the most stringent wash was 57°C below the T_m. When the stringencies of the hybridization and post-hybridization reactions were increased such that the temperature of the hybridization was about 37°C below T_m and that of the post-hybridization washes was 18°C to 25°C below T_m (protocol #2), clear positive staining was obtained with the antisense probe (Figure 23) while no staining was seen with the sense probe. When the temperature of the washes, however, approached 12°C below T_m, all staining was obliterated.

The problem that persisted at this point was the loss of cells; in fact, in a few of the *in situ* hybridizations no staining was seen in any of the cells and most of the cells had been lost during the procedure. Alteration of the fixation and storage conditions of the cells as well as the proteinase K digestion conditions during the *in situ* hybridization protocol remedied the problem. Fibroblasts were being grown on glass slides and fixed under 4% paraformaldehyde for 16 - 18 hours at 4°C followed by rinsing and storage under phosphate-buffered saline (PBS). An extended incubation under PFA such as this could lead to over-fixation which can prevent access of probe to its target; as well, this could inhibit adherence of cells to the slides. This was then altered to a fixation time of 10 minutes at 4°C followed by rinsing with PBS and storage under 70% ethanol at 4°C. Under these conditions, the cells can be dependably stored, and the target preserved, for about three months.

The conditions of the proteinase K digestion also seemed too harsh. The cells were exposed to 10μg/mL of proteinase K for 30 minutes at 37C. This was investigated in an *in situ* hybridization experiment where cells received 1, 5, 10, 50, and 100μg/mL of proteinase K at room temperature for 10 minutes, no probe, and the same conditions between all of them with regards to the rest of the variables. As the concentration of the enzyme increased, more cells were lost and the morphology of those remaining deteriorated. The optimum concentration appeared to be 1µg/mL with relatively good results at 5µg/mL. Therefore, for cultured cells, the protocol was changed so that proteinase K digestion was used at 1µg/mL for 10 minutes at room temperature. In one of the experiments in which different proteinase K concentrations (1 and 5µg/mL) were tested, the effect of postfixation with 4% PFA after proteinase K digestion was also analyzed. At the high concentration of proteinase K, the postfixation was necessary to ensure the cells remained intact since only nuclei remained without any postfixation. However, at the low concentration of proteinase K, cells and staining were intact without any postfixation. Therefore, high levels of this enzyme appear to destabilize the attachment of cells to the glass slides and this attachment is again secured by fixation with 4% PFA. This information was critical in evaluating the optimal concentration of enzyme necessary to study the valuable and rare paraffin-embedded HSc sections.

5. In Situ Hybridization on Hypertrophic Scar, Mature Scar, and Normal Skin with TGF-ß1(287)/pGEM 3Z cRNA Probes

Of the eighteen *in situ* hybridizations mentioned above, thirteen involved paraffin-embedded tissue which consisted of a mixture of HSc, MSc, and NSk. The initial experiment (protocol #2) was carried out to test the effects of two concentrations of proteinase K (10 and 100µg/mL) as well as three different stringencies of post-hybridization washes (T_m-12°C, T_m-18°C, and T_m-25°C), specifically with regards to tissue morphology and degree of specific staining including the level of background staining. At both concentrations of proteinase K, the closer the temperature of the post-hybridization washes to the T_m of the expected hybrid, the lower the intensity of staining and the density of positive cells. At the strongest or highest stringency (T_m-12°C), no staining whatsoever was observed.

When comparing the level of staining obtained with the two concentrations of proteinase K, a dramatic reduction was observed at the higher concentration. Using the lowest stringency post-hybridization wash mentioned above, the high concentration of proteinase K resulted in higher amounts of staining; however this increase in staining was mostly associated with the extracellular matrix. In addition to the increase in background staining, very high concentrations of proteinase K were also detrimental to the morphology of the tissue; such was observed with the loss of tissue, especially epidermal tissue, and sometimes large portions of dermal tissue with the use of proteinase K above 50µg/mL. Other later experiments (protocol #3) which tested different concentrations of proteinase K confirmed that specific staining increased with the increase in concentration of this enzyme until 50µg/mL. Higher concentrations led to a deterioration in morphology and staining.

Therefore, this concentration of proteinase K was considered to be optimal to use on paraffin-embedded skin samples for this study. These experiments also used different conditions for the application of the proteinase K; the enzyme was applied in a more controlled fashion than in previous experiments: for about one third of the time and at room temperature instead of at 37°C. As a part of these *in situ* hybridizations, the use of casein blocking buffer (Cambridge; "superblocker") was introduced and found to reduce background staining considerably.

Interestingly, within this series of *in situ* hybridizations, it was found that under the same conditions and using serial sections of the same tissue block, a change in the batch of probe changed the results significantly. This could also be attributed to a phenomenon which appeared only in certain tissue sections. As indicated above, the antisense probe produced strong and specific staining throughout the dermis (Figure 24A) and in the suprabasal layer of keratinocytes in the epidermis of a sample of HSc tissue. In serial sections of the same sample of tissue, the staining was lost when a different batch of antisense probe was used (Figure 24C). Upon decreasing the stringency of the post-hybridization washes in one experiment, however, specific staining reappeared, although faintly (Figure 24E). Intriguingly, in this experiment, the staining appeared more intensely with the sense probe (Figure 24F). At the time, this was considered a nonspecific phenomenon and a technical problem with the probes; efforts were, therefore, directed at elucidating the reason behind the peculiar behavior of the probes and strategies were designed to eventually obtain staining only with the antisense probe if any staining were to occur at all.

Another peculiar occurrence at this time involved serial sections of the same HSc tissue which demonstrated intense and specific staining with the sense probe only in some of the sections but not in others. This phenomenon also involved the antisense probe. The possibility of the sense probe hybridizing to a specific target was considered but dismissed at this time. However, if a specific target did exist which the sense probe recognized, the idea that it only appears in some sections because it might be concentrated in only specific and confined localizations within the dermis is intriguing; when sectioning through a tissue block, it is possible that such a localization may appear in relatively few sections if it covers a very small area.

This series of experiments also included three samples of HSc, two samples of normal skin, and one sample of MSc. References to the origins of the samples are provided in Table 1; henceforth, the patients from whom the samples were acquired will be referred to as PT followed by their number as described in Table 1. Tissue that was obtained at regular intervals from four HSc patients who had undergone treatment with

IFN-α2b was also studied in two experiments. An interesting pattern of staining was found in the HSc sections in addition to the expected positive keratinocytes in the suprabasal layer of the epidermis.

In sections of active HSc (Figure 25A-B), the collagen is not organized as it is in normal skin ; unlike the normal collagen fibre bundles, the collagen appears as thin and loosely packed fibrils. These fibrils appear disorganized throughout the ECM and appear as "bands" of straight collagen fibrils which originate from, and stretch out between, different focal points, thereby forming whorl-like structures. Within these whorl-like structures, the collagen fibrils often appear to regain some organization which approximates collagen fibers. It is in these regions where most of the staining for TGF-ß1 mRNA is found. This occurrence is not an absolute one as positive cells within the straight bands of collagen fibrils are also seen but usually they are not as abundant, and their staining not as intense, as the cells within the 'whorl-like' regions. There are some regions within the dermis that also appear completely negative for TGF-ß1 mRNA and this can be seen in the region just below the immediate papillary dermis of PT#8's tissue (data not shown). This is not an artifact considering the similar occurrence in many serial sections studied in different experiments.

One of the HSc samples studied in this series (PT#15), which presented this same regional variation in staining for TGF-ß1, displayed a large area of negative staining in the dermis which spanned the papillary and middle dermis (Figure 26). This region of the dermis did not appear different from its surroundings. The collagen throughout the section contained disorganized and loosely arranged fibrils (see also Figure 25B) as in PT#8's tissue (Figure 25A) but the disorganization, the whorls, and the banding did not appear as prominently as in other samples. The dermis in PT#15's tissue appeared to be resolving since in many areas in the dermis collagen fibers are present that look more like the normal bundles than anything seen in PT#8's tissue.

The MSc section that was probed twice in this series of *in situ* hybridizations was largely negative except for positive cells throughout the suprabasal keratinocytes (Figure 27A) and a few positive cells in the middle dermis (not detectable in Figure 27). In contrast, a hematoxylin/eosin stain of this section (Figure 27B) shows the many cells, presumably fibroblasts, which are present throughout the dermis. If indeed the excessive local production of TGF-ß1 is a major cause of the complications leading to HSc, then the much lower levels of mRNA for this cytokine in MSc are consistent. As well, the persisting levels of TGF-ß1 protein in MSc (Scott et al., 1995) may be due to its being bound up in the matrix by PGs such as decorin. As reported earlier (Scott et al., 1995), TGF-ß1 protein was only seen in concentrated focal regions in the dermis in HSc tissue.

This contrasted with its widespread but low abundance in MSc and its scarcity in NSk. In agreement with these results, the production of TGF-ß1 appears to decrease substantially in MSc and all together in NSk (Figure 27). In the two samples of NSk studied in this series of *in situ* hybridizations, the appearance of a positive cell was very rare except for some endothelial cells and suprabasal keratinocytes.

Throughout this series of *in situ* hybridizations, four of the thirteen experiments resulted in some samples that stained with both the sense and antisense probes (data not shown). In some of the experiments, the staining with the sense probe was even more intense than that with the antisense probe. The staining seen with the sense probe seemed to colocalize with that of the antisense probe where it was observed except in one sample of NSk where some dermal keratinocytes stained with the sense probe but appeared negative in a serial section probed with the antisense probe. As noted above, this staining was thought at the time to be nonspecific and efforts were directed at cleaning up this 'background' by a number of means, for example, making cleaner probes and increasing the stringency of the hybridization reactions and post-hybridization washes as much as possible .

6. In Situ Hybridization Using TGF-ß1(287)/pGEM 3Z cRNA Probes on Hypertrophic Scar From Patients Treated with IFN-α2b

The final set of tissues probed in this series of *in situ* hybridizations (protocol #3) were HSc samples obtained from four patients (Table 1, #s 7, 17, 20, 18) who had been treated with IFN-α2b. Each patient had one biopsy taken of their scar before treatment (H1) and a series of biopsies taken during the course of their treatment (H2, H3, etc.). Normal skin biopsies taken before treatment were denoted N1, and those after treatment N2. Two experiments were conducted on serial sections of these biopsies where one section of each was placed together on the same slide. Therefore, PT #7 had 4 sections of scar and 2 of NSk on one slide, PT#17 5 sections of scar and 2 sections of NSk, PT#20 7 sections of scar, and PT#18 5 sections of scar and 2 of NSk. Both experiments were conducted using exactly the same conditions except that the sense probe in the first experiment was a mixture of two batches since one batch was finishing up and a new batch was starting to be used. In the second experiment, sense probe was used only from the fresh batch. Only results of PT#7 (probed with antisense probe) are presented in the figures since it was not feasible to include pictures from all sections of all patients studied. In general, almost all of the sections from all biopsies displayed mRNA for TGF-ß1 in the suprabasal keratinocytes.

In the tissue sections obtained from PT#7, the first experiment resulted in staining with only the antisense probe (Figure 28). In the second experiment, however, many sections displayed staining with the sense probe in a pattern similar to that seen for the antisense probe (data not shown). This was sometimes in conjunction with or without staining with antisense probe. In both experiments, mRNA for TGF-ß1 was found throughout the dermis in the first scar tissue; sense staining was similarly found in the second experiment. The second section displayed no TGF-ß1 mRNA except in the epidermis; in the second experiment it was interesting to see only the sense probe staining throughout the dermis. The third section had cells throughout the dermis expressing this cytokine; in the second experiment, staining with the sense probe was also found in the epidermis and in the deep dermis. In the fourth section, mRNA for TGF-ß1 was found only in the dermis; interestingly, the second experiment revealed staining with only the sense probe in the epidermis and in the middle dermis. Both sections of normal skin had mRNA for TGF-ß1 in the epidermis and staining with the sense probe was detected in both sections as well.

The abundance of mRNA for TGF-ß1 did vary between patients. The first section of PT#17 contained TGF-ß1 mRNA throughout the dermis; staining also occurred with the sense probe in the second experiment but only in the keratinocytes and the papillary dermis. The second, third, and fourth sections contained almost no TGF-ß1 mRNA; staining with both sense and antisense probes did occur, however, in the second experiment. The fifth biopsy is interesting since in the first experiment there was no staining obtained whatsoever; in the second experiment, however, staining was obtained in the epidermis and throughout the dermis but only with the sense probe. In the NSk sections, TGF-ß1 mRNA was detected in both sections in the first experiment. In the second experiment, staining with both probes occurred in the first section but only with the sense probe in the second section. The activities of the probes indicate that the batch of the sense probe used in the second experiment, which was fresher, seemed to be more sensitive.

PT#20 had no mRNA for TGF-ß1 in either the first or seventh biopsies. The second, third, fourth, and fifth biopsies contained positive cells in the epidermis only. Additionally, the fifth biopsy also stained with the sense probe. The sixth biopsy was the only biopsy of PT#20 which contained some sparse and faintly stained positive cells distributed throughout the dermis; this was seen with both sense and antisense probes.

In the tissue sections from PT#18, very little staining was obtained with any of the probes. The first scar section demonstrated TGF-ß1 mRNA mainly in the epidermis and a few cells in the middle dermis. In the second section, TGF-ß1 mRNA was also found in the papillary and middle dermis but only in the second experiment; this experiment also revealed staining with the sense probe in the middle and deep dermis. The rest of the sections (third, fourth, and fifth) demonstrated very little TGF-ß1 mRNA and only in the keratinocytes. The first section of NSk demonstrated TGF-ß1 mRNA only in the epidermis whereas the papillary and middle dermis had positive cells as well in the second experiment. Sense staining was only found in the second experiment in the epidermis.

The staining that was obtained with the sense probe was found only in the second experiment except for one section of tissue in PT#20's series of biopsies. The only difference between the two experiments was that the batch of sense probe was entirely new in the second experiment but the mixture used in the first experiment contained sense probe which was about four months old.

To summarize the staining obtained for these tissues: PT#20 and PT#18 demonstrated almost no TGF-ß1 mRNA in their first HSc section; corresponding sections from PT#7 and PT#17 contained this message throughout the dermis and epidermis. Regarding the series of tissue for PT#17, PT#20, and PT#18, TGF-ß1 mRNA was found in only one section during their treatment, H3 for PT#17, H6 for PT#20, and H2 for PT#18. And in these sections, staining was usually obtained with both sense and antisense probes. In H5 of PT#17, however, sparse staining was found throughout the dermis with only the sense probe. For PT#7, cells positive for TGF-ß1 mRNA were seen throughout H3 and H4; as well, some cells in the middle and deep dermis stained with the sense probe. The H2 for this patient stained only with the sense probe in the dermis. From these samples, only PT#17's tissue gives indication of the ability of IFN-α2b to inhibit the production of TGF-ß1. The problem with using the data from PT#20 and RF to support this hypothesis is that their non-treated HSc sections did not display any TGF-ß1 mRNA and therefore cannot be used to assess the effect of agents which might have an inhibitory effect on the TGF-ß1 expression. The tissue from PT#7 shows a reduction in TGF-ß1 expression with therapy but this expression reappears in H3 and H4.

B. Rat TGF-ß1(287)/pT7T3 as a Template for cRNA Probes

1. Establishing cRNA Probes From Rat TGF-ß1(287)/pT7T3

The persistently poor labeling efficiency obtained using SP6 RNA polymerase eventually led to subcloning of the rTGF-ß1 cDNA fragment from pGEM 3Z into the PCS of pT7T3α-18 between the restriction sites*Hind* III and *Eco* RI. Restriction digestion with both *Hind* III and *Eco* RI liberated the rTGF-ß1 cDNA insert which is just short of 300bp (Figure 29). Since sense and antisense probes used for *in situ* hybridization needed to be produced in quantities which were typically within one order of magnitude, another promoter system besides SP6 was needed to generate the antisense probe. The use of pT7T3 eliminates the use of SP6 polymerase. As its name suggests, the PCS of pT7T3 is flanked by T7 and T3 promoter sites. Using either the restriction enzyme *Hind* III or *Eco* RI to linearize this recombinant vector (Figure 29), the use of either T7 or T3 RNA polymerase respectively, led to the production of either sense or antisense probes respectively. Before the linearized vector was used as a template for *in vitro* transcription, it was cleaned up by extracting the solution of DNA with phenol/chloroform (1:1) followed by chloroform alone and precipitation.

Throughout the course of using this template for *in vitro* transcription, seven labeling reactions were conducted using digoxigenin-11-UTP as the labeled nucleotide. Normally, between 1 and 10µg of labeled cRNA product was produced in each labeling reaction; however, when the reaction is scaled up such that all components of the reaction, except for the amount of template DNA, are increased by 2.5 or 5.0 times, then the amount of product was between 2 and 20µg. The sensitivity of the probes, as measured by dot blot hybridization to unlabeled rTGF-ß1 cDNA of the same sequence as the labeled probe, was between 1 and 50pg. Their specificity was usually acceptable; occasionally, however, they did bind to salmon sperm DNA.

The labeling reactions were all conducted with a reaction time of 9 hours. The extended length of the reaction was found to be unnecessary as the RNA polymerases work very quickly to produce the optimum amount of cRNA product; usually in 1 to 2 hours. Therefore, the incubation time was changed and an additional 3 labeling reactions were performed with a reaction time of only 2 hours. This seemed to stabilize the variation in the product as all three reactions resulted in 5µg of labeled product which had a sensitivity between 1 and 10pg; as well, their specificity was acceptable.

2. In Situ Hybridization on Human Dermal Fibroblasts with TGF-ß1(287)/pT7T3 cRNA Probes

These cRNA probes, which were all generated off the pT7T3 vector, were used to perform 24 *in situ* hybridizations (protocol #'s 3 and 4). Of these 24 experiments, 23 included human dermal fibroblasts that were cultured on glass slides. In all of these experiments, different conditions were tested to enhance staining in the tissue with the antisense probe and decrease background binding of the probes. If the fibroblasts were not the only target in these experiments, then they were included as a standard control since we can depend on their expression of TGF-ß1 at 10 to 12 hours after subculturing. The strains of fibroblasts used were H16/N16, H15/N15, H2/N2, and H11/N11.

The H16/N16 fibroblasts were included in eight experiments as biological controls. In seven of the eight *in situ* hybridizations, staining was observed with both sense and antisense probes (for example see Figure 30). Of these seven, the results from two displayed clear and strong staining with both probes whereas five demonstrated very faint staining with the sense probe compared to that with antisense. One experiment of the eight demonstrated staining with the antisense probe only. In two experiments, hypertrophic fibroblasts displayed more staining than normal fibroblasts and this occurred with the antisense probe only. Certain conditions that were tested had an influence on the level of staining. Increasing the amount of probe as well as heat denaturing the probes before hybridization intensified the signal. Increasing the proteinase K concentration, however, led to nuclear staining and eventually to loss of cells, as shown before.

The H15/N15 cells were included in five *in situ* hybridizations. In three of these, they served as controls and in all three staining was observed with both sense and antisense probes. One experiment was particularly interesting in that the signal obtained in the hypertrophic fibroblasts was much more intense than that of the normal fibroblasts when the antisense probe was used; this result was also obtained, even though the difference was not as marked, with the sense probe (Figure 31). The other two *in situ* hybridizations which used this strain of fibroblasts were time-course studies. H15/N15 fibroblasts were subcultured onto glass slides such that each slide contained hypertrophic and normal fibroblasts. Thereafter, batches of these slides were fixed at 6, 12, 18, 24, 48, and 72 hours and stored under 70% ethanol. In the first of these two experiments, staining was obtained with both sense and antisense probes; a new batch of probes was then made in an effort to produce more "specific" staining with the antisense probe. In the first experiment (data not shown), staining with the sense probe decreased at 24 and 48 hours but increased again at 72 hours whereas that with the antisense probe was almost constant at all times. Differences between hypertrophic and normal fibroblasts did not appear significant. In the second experiment (data not shown), in which a fresh batch of probes was used, hypertrophic cells contained more signal than normal cells at 6, 12, and 48 hours when treated with the antisense probe. At 6, 12, 18, and 24 hours, the same phenomenon occurred with the sense probe. At 72 hours, however, normal cells expressed more signal than hypertrophic cells with both probes.

The H2/N2 fibroblasts were used in 6 *in situ* hybridizations of which in three, these fibroblasts were utilized as positive controls. In two of the three experiments, TGF-ß1 mRNA in the hypertrophic cells was significantly more abundant than in the normal cells; the cells from the third experiment dried up and were therefore destroyed. The other three experiments which involved H2/N2 fibroblasts were performed to test the effect of TGF-ß1 on the expression of TGF-ß1; more importantly, the answer to whether an autoinduction of this cytokine, if in fact it occurred, can be detected by our methodology. In one of these three experiments, the level of signal for TGF-ß1 mRNA was dramatically more intense in those treated with TGF-ß1; this result was only obtained in hypertrophic cells. As for the other two *in situ* hybridizations conducted on TGF-ß1-treated cells, no differences between treated and non-treated cells were seen in one of them and in the other, a severe loss of cells occurred possibly due to poor preservation.

The H/N11 fibroblasts were similarly used to check if the possible effects of autoinduction of TGF-ß1 *in vivo* were detectable by our method of *in situ* hybridization. However, the results displayed no differences in staining between treated and nontreated cells.

3. In Situ Hybridization on Hypertrophic Scar Used to Optimize Variables of the Protocol

As noted above, the 24 *in situ* hybridizations (protocol #'s 3 and 4) conducted with probes transcribed off a rTGF-ß1 cDNA fragment that is contained in the pT7T3α-18 vector were largely performed to optimize different conditions of the protocol. The hypertrophic tissue of PT#8 was included in almost all of the experiments (16 of 24). PT#8's tissue is classically hypertrophic in that the dermis and epidermis are excessively thick, the dermis is infiltrated with many cells of which fibroblasts probably make up a large portion, the dermis is mostly avascular, the collagen fibrils in the dermis are loosely arranged in a disorganized fashion which in some areas appear 'whorl-like', and, throughout this disorganized matrix, bands of collagen also appear to be stretched out between "pressure" points. This being the case, PT#8's tissue was included in all of these experiments to optimize background levels and tissue integrity considering that our main focus was HSc tissue. As well, having serial sections from the same tissue block helped to provide valuable comparisons of the effects of different variables in our protocol. Serial sections of the same block of normal skin were also included on the same slides as PT#8's tissue.

The variables that were tested were higher concentrations of the DIG-blocking solution, heat denaturing of the probes before hybridization, incorporation of RNase A treatment after hybridization, acetylation of free amino groups, different concentrations of proteinase K, different probe quantities during hybridization, relabeling the probe, different stringencies of hybridization and post-hybridization washes, and the incorporation of bovine testicular hyaluronidase in the preteatment of the tissues before hybridization. The changes which contributed most to the reduction of background binding of the probe to the extracellular matrix was the increase in the concentration of DIG-blocking solution to 5%, post-hybridization treatment with RNase A, acetylation of free amino groups before hybridization, using lower probe quantities, and decreasing the salt concentration (increasing the stringency) of the hybridization and post-hybridization washes. All of these changes were incorporated into protocol #5.

Increasing the proteinase K concentration helped to strengthen the cytoplasmic signal; however, above a certain concentration, excessive background and a loss of tissue integrity did occur. Therefore, a compromise was made between the strength of the signal and preservation of tissue morphology; also an excessive level of this enzyme (above 40µg/mL) led to a reduction in signal.

Heat denaturing the probes before hybridization also seemed to increase the final signal intensity obtained. Heating the probes in this way helps to eliminate the secondary structure that RNA is prone to assume and allows the probes to hybridize to their target more efficiently.

The inclusion of hyaluronidase also increased the final signal intensity. This enzyme digests hyaluronic acid as well as some chondroitin sulfate and dermatan sulfate chains and therefore removes GAGs which could interfere with access of the probes to their target. As well, fewer obstacles means fewer chances of the probe to bind nonspecifically to an element of the extracellular matrix.

The RNase A treatment was only effective at eliminating background signal in the matrix at low concentrations. High concentrations of RNase A entirely obliterated any staining. The large structure of the digoxigenin molecule may offer steric hindrance that interrupts the formation of tight and stable hybrids. In turn, the possible inclusion of 'bubbles' in the hybrids may render the resulting single-stranded RNA strands susceptible to degradation by RNase A.

Regardless of the conditions tested, in 15 of the 16 *in situ* hybridizations, staining was obtained with both sense and antisense probes in PT#8's tissue. This signal appeared specific as it was only found in the cytoplasm of keratinocytes in the epidermis and in what are presumably fibroblasts in the dermis. In 4 of these 15 experiments, the signal obtained with the sense probe was more intense than that with the antisense probes. Hyaluronidase was included in two of these four experiments. In one of these 4, an experiment in which hyaluronidase was included, the signal appeared almost entirely from the sense probe (Figure 32). Interestingly, in this experiment, the normal skin section, which was on the same slide as PT#8's tissue, displayed almost no staining with the sense probe and only minimal signal with the antisense probe. As well, the H16/N16 fibroblasts which were included in this experiment displayed strong staining with the antisense probe but very faint, if any, staining with the sense probe. As for the other three, one displayed staining with sense in NSk only with hyaluronidase pretreatment, one had no signal at all in the NSk, and the last one demonstrated more staining with the sense probe than the antisense probe in the NSk section. Hyaluronidase was eliminated from the protocol after these experiments since it appeared to contribute to high levels of background staining in many of the tissue sections studied.

4. Regional Variation in the Expression of TGF-ß1 mRNA in Hypertrophic Scar

The pattern of staining obtained in PT#8's tissue was interesting in that it presented a regional variation in the expression of TGF-ß1 mRNA. This pattern was consistently obtained in 15 of the 16 experiments conducted on PT#8's tissue; as well, this pattern was seen in the results of both the antisense and sense probes (Figure 33). In the epidermis, TGF-ß1mRNA was found mostly in the suprabasal keratinocytes. In the immediate papillary dermis, an obvious zone of negative staining was observed below which the frequency of positive cells increased. In the middle and deep dermis, TGF-ß1 mRNA was localized to regions which appeared most disorganized with respect to the collagen arrangement. Where the collagen appeared to assemble into bands of thin fibrils, the expression of TGF-ß1 was much weaker in comparison. This expression intensified in regions between these bands where the collagen appeared most loosely arranged and disorganized. Once again, of interest, is the colocalization of signal obtained with the sense and antisense probes and the variation in relative intensities of both.

5. In Situ Hybridization on Normal Skin with rTGF-ß1(287)/pT7T3 cRNA Probes

As noted above, serial sections of the same block of normal skin were included on the same slides as PT#8's tissue. In 4 of these 16 experiments, signal was obtained with only the antisense probe; and in one of these four, signal was only detected after pretreating the tissue with hyaluronidase. Signal was obtained with both sense and antisense probes in 8 of the 16 experiments; in one of these, the sense probe contributed to the results only after predenaturing the probes. In another, sense 'hybridization' was only detected after the sections were pretreated with hyaluronidase. In two of these 8 experiments, more intense staining was observed with the sense probe than with the antisense probe; in both of these experiments, acetylation of the tissues was carried out before hybridization. Four experiments were conducted where no staining was found whatsoever with either sense or antisense probes (data not shown).

6. In Situ Hybridization on Other Samples of Hypertrophic Scar, Mature Scar, and Normal Skin with rTGF-ß1(287)/pT7T3 cRNA Probes

In addition to PT#8's tissue and the NSk mentioned above, several other HSc, MSc, and NSk samples were studied in 10 *in situ* hybridizations (protocol #4). Specifically, 9 samples of post-burn scar were analyzed of which 5 appeared to be mature scars or scars beginning to mature, based on the organization of the collagen fibers. The other 4 scar samples appeared unquestionably hypertrophic based on qualities described above. Additionally, 4 normal skin samples were analyzed; however, one of these samples was taken from a patient who had HSc and his NSk sample appeared somewhat abnormal as the epidermis and dermis were thicker than that usually found in NSk.

The 4 HSc samples stained with both the sense and antisense probes; however, the intensities varied between tissue samples. The sample that was obtained at 5 months post-burn (PT#5) displayed very little TGF-ß1 mRNA but pockets of fairly strong postitivity were found in the papillary and middle dermis with the sense probe. At 12 months post-burn (PT#12) this individual's scar expressed higher levels of TGF-ß1 mRNA but this staining was concentrated only in certain regions of the papillary and middle dermis. The staining with the sense probe appeared to colocalize with that of TGF-ß1 mRNA except it also spread to the deep dermis. The samples obtained at 14 and 36 months post-burn (PT#15 and PT#25, respectively) also displayed strong positive cells with both probes that were abundant throughout the dermis; as well, the distribution of these cells demonstrated some regional variation as observed in Figure 33.

The samples that appear mature in this set of scars also demonstrate staining with both sense and antisense probes. In the scars obtained at 14 months (PT#14), 15 months (PT#16), and 27 months (PT#23) post-burn, strong staining appeared with both probes and these levels varied between experiments. This may have been purely the result of the variability in staining between tissue sections. Nonetheless, the important fact is that with the antisense probe, specific cytoplasmic staining was observed; however with the sense probe, similar levels or stronger or weaker levels of staining were observed when compared to that of the antisense probe. A very intriguing result was found in 2 sections of MSc, obtained at 36 months (PT#26) and 45 months (PT#27) post-burn: staining was obtained with only the sense probe (Figure 34) whereas serial sections in the same experiment revealed no TGF-ß1 mRNA (data not shown). This recurring phenomenon of strong and specific staining with the sense probe at high stringency, even when no mRNA was observed with the antisense probe in the same experiment and in different experiments, tempted us to later explore whether, in fact, the sense rTGF-ß1 probe is finding, and hybridizing to a specific target (see Chapter 3, II, D).

7. In Situ Hybridization on Hypertrophic Scar From Patients Treated with IFN-α2b with rTGF-β1(287)/pT7T3 cRNA Probes

Sections from serial biopsies of two hypertrophic scar patients (PT#s 4 and 21) who underwent therapy with IFN-α2b were analyzed (protocol #3). The results from both of these patients indicate that during the course of treatment with this agent, the level of TGF-β1 mRNA decreases. In the case of PT#4 (Figure 35), this is demonstrated more dramatically since more signal for TGF-β1 mRNA is readily detectable through most of the dermis in the H1 than for PT#21. Also of interest is the regional variation in the expression of this cytokine which is analogous to that found in HSc sections from PT#8. A progressive decrease then occurs until H4 in which mRNA for TGF-β1 was almost absent. Thereafter, in H5 (not shown), positive cells reappeared, mostly in the papillary dermis. Two normal skin biopsies were also taken from these patients, one before treatment and the second one after treatment had started. Results on normal skin are not presented here. The N1 from PT#4 contained many positive cells for TGF-β1 mRNA; these positive cells included endothelial cells and fibroblasts. The level of staining decreased in N2 as fewer fibroblasts were positive and no positive endothelial cells were found. Specific staining was also found with the sense probe in most of the endothelial cells and dermal fibroblasts of N1; this occurrence decreased in N2.

Although the reduction in mRNA for TGF-β1 is not as drastic across all of the hypertrophic tissue collected for PT#21 as seen in PT#4, a decrease in the degree of positivity is clearly discernible from H1 to H2 (not shown). Furthermore, a significant decrease was seen between H2 and H6 at which time almost no positive cells could be detected in the dermis except for a few in the papillary dermis. Again, the pattern of appearance of positive cells in many of the scar sections was interestingly reminiscent of that found in PT#8's tissue. The number of positive cells was seen to also decrease from N1 to N2 for this patient.

Staining with the sense probe also revealed many positive cells in H1 of PT#21 and PT#4 (Figure 36 for PT#4; PT#21 not shown) throughout the dermis which colocalized with staining obtained with the antisense probe. The density of positive cells obtained with the sense probe also appeared to decrease with the progression of treatment. In scars H3-6 (only H1-4 are shown), very few cells appeared positive. No change appeared to occur in the NSk sections (not shown) when stained with the sense probe; few cells were positive in either N1 or N2.

C. Human TGF-ß1 cDNA as a Template for cRNA Probes

1. Establishing cRNA Probes Using a 420bp Fragment of Human TGF-ß1 cDNA

While the rTGF-ß1/pT7T3 template was being used to generate the probes used to perform the experiments discussed above, a human TGF-ß1 cDNA template was acquired which was ready to use to transcribe cRNA probes. Even though TGF-ß isoforms are extremely conserved across species, the use of a probe that was specific for a human sequence was still desired since all our target samples are human. This template consisted of a 420bp cDNA fragment of human TGF-ß1 cloned into the *Bam* HI and *Eco* RI sites of pGEM 3 plasmid vector DNA (this construct will be referred to as pT420 and any probes transcribed off it as T420); and the PCS of this vector is flanked by SP6 and T7 promoter sites. Upon double digestion with *Bam* HI and *Eco* RI two bands (about 3kb and about 450bp) are visible by gel electrophoresis which approximately correspond to the expected sizes of the plasmid and insert cDNA (2.9kb and 420bp, respectively) (Figure 37A).

After linearizing the plasmid at either end of the insert DNA using either *Bam* HI or *Eco* RI (Figure 37B), digoxigenin-labeled sense and antisense probes were transcribed off the template and quantitated using the standard dot blot quantitation method. About 5µg of transcript was produced with T7 RNA polymerase but absolutely no labeled RNA was detected for the transcript produced using SP6 RNA polymerase (Figure 37C). In light of the aforementioned concerns about the inefficient functioning of the SP6 promoter, especially with regards to incorporating digoxigenin-11-UTP during *in vitro* transcription, cloning was attempted to transfer this 420bp TGF-ß1 cDNA fragment from pGEM 3 to pBS. Once this was complete, the information about the previously discussed GC rich region of the PCS of pBS possibly contributing to non-specific hybridization of probes produced from this vector was discovered. This led to the subsequent cloning of this cDNA fragment into the *Hind* III and *Bam* HI sites of pT7T3.

Linearization of this construct was followed again by synthesizing digoxigenin-labeled sense and antisense probes. In situ hybridization was conducted with these probes on H/N8 and H/N20 fibroblasts grown on glass slides for 17 and 12 hours, respectively and revealed a lot of staining with the T7 probe but almost nothing with the T3 probe. Upon sequencing this template construct using the T3 primer, a 47bp-long stretch of uninterrupted thymidines was found (Figure 37D). This indicated that this fragment of TGF-ß1 cDNA was the 3' end of the molecule and included the poly-A tail of the molecule. As probes, the cRNAs generated off this template were invalidated as a stretch of homopurines such as poly-T would be too susceptible to binding indistinguishably to all mRNA strands. Another important factor to consider is the possible inhibition or termination of transcription that this poly-A region may have caused and hence the completely undetectable amount of probe produced by SP6 polymerase.

2. Establishing T112 Probes

To prepare a functional probe template, a 112bp fragment from the 5' end of the cDNA insert of T420/pT7T3 was digested out of this plasmid using *Sma* I and *Xba* I and cloned into these sites in pT7T3. This clone was verified by sequencing before proceeding with any other experiments. Sequencing using the T7 primer yielded a product that was complementary to TGF-ß1 mRNA; therefore, the use of T7 polymerase to transcribe off this template should yield antisense probe. The template was linearized with *Pst* I so that T7 polymerase could be used to generate the antisense probe. Conversely, *Eco* R I was used to generate a linearized template which could be used with T3 polymerase to produce sense probes (Figure 38). These linearized templates were purified by phenol:chloroform (1:1) followed by precipitation. Double digestion with both *Pst* I and *Eco* R I liberated the 112bp cDNA fragment from its vector (Figure 38). This construct is henceforth referred to as pT112, and all probes transcribed off it as T112 probes.

Four labeling reactions were performed using these templates of which 3 involved the use of digoxigenin-11-UTP as the label and 1 utilized ^{35}S-UTP. Quantitation of the digoxigenin-labeled probes revealed quantities between 2μg and 3μg using the T3 polymerase and between 15μg and 50μg using the T7 polymerase. Clearly either the template containing the T7 promoter or the T7 polymerase, or a combination of both, generated labeled probe more efficiently than similar components in the T3 system. Even the radioactively labeled probes demonstrated a 44% higher quantity of T7 probe than T3 probe. Dot blot hybridizations were used to test the sensitivity and specificity of the probes and found that the T3 probes detected down to about 50pg of complementary non-labeled template DNA; the T7 probes, however, could detect down to about 5pg of target. Therefore, the T7 probes were more sensitive as well. Both T7 and T3 probes looked specific.

3. In Situ Hybridization on Human Dermal Fibroblasts with T112 Probes

A total of 11 *in situ* hybridizations (protocol #5) were performed using T112 probes all of which included cultured dermal fibroblasts of different strains. Results were unobtainable in five of these experiments because the cells either dried up and therefore were disrupted, there was simply too much background throughout the slides, or the staining was too faint to make any conclusions. In the remaining experiments, strong staining was observed in three of them and this staining was only obtained with the sense probe (data not shown). The antisense probe seemed to find very little if any target in the cells. These results were all found in H/N20. In two of these three experiments, a separate batch of cells were also treated with human TGF-ß1 (75pM) and we found that in one experiment the treated cells expressed more staining with the sense probe than the untreated cells; staining with the antisense probe was non-existent.

Another cell strain, H/N14, was also probed (data not shown) and, once again, only the T3 probe produced any staining and this was only at the edges of the population of cells where their density was low. In one experiment, both the T3 and T7 probes stained faintly with no difference in intensities. In only one of this series of experiments was the T7 probe found to produce a stronger signal than the T3 probe.

To test whether the labeling system was contributing to the apparently anomalous results, ie. intense staining with the sense probe and almost no staining with the antisense probe, T112 was labeled with ^{35}S-UTP and used on two sets of H/N20 cells. The results were similar to those found with the digoxigenin-labeled probes. The same degree of positivity was found with both probes in one set of slides; however, in the other set, only the T3 probe revealed some positive cells.

4. In Situ Hybridization on Hypertrophic Scar, Mature Scar, and Normal Skin with T112 Probes

In this series of 11 *in situ* hybridizations, paraffin-embedded HSc, MSc, and NSk tissue sections were included in 5 experiments; in 2 of these 5, both digoxigenin-labeled and ^{35}S-UTP-labeled probes were used. Once again, radioactively labeled probes were used to compare their functioning with that of the digoxigenin-labeled probes to see if the labeling system had any effect. In one of these 2 experiments, which included 4 HSc sections and 2 NSk sections, an even 'mat' of black grains was seen over all of the tissue sections which received the ^{35}S-UTP-labeled probes and was therefore considered as background staining. Only one HSc section displayed regions in the epidermis which contained a higher density of grains; this was obtained with only the sense probe. This result was also seen with digoxigenin-labeled T112 probes indicating that the type of label does not affect the result of the experiment. A problem that was experienced, however, in this experiment was the occurrence of large crystals that precipitated throughout the tissue sections which received the digoxigenin-labeled probes. This was probably the effect of heating (75°C to 90°C) the hybridization mix, which contains dextran sulfate, to denature the probes. Considering the very large size of dextran sulfate (500 000 Da), upon denaturation it is possible that fragments may form that incorporate small amounts of the probe. These fragments may stick randomly to the tissue section resulting in an appearance of large crystals and thus high levels of background. Washing with ethanol and xylene removed these crystals.

In a second attempt to use ^{35}S-UTP-labeled T112 probes on HSc, MSc, and NSk, a high concentration of grains were seen throughout the tissue sections but these were not specifcally located. The only 'hot spots' were in the basal keratinocytes.

From the three other experiments conducted which included tissue, one was inconclusive due to very high levels of background. In the other two experiments in which were analyzed 5 samples of HSc, 1 sample of MSc, and 3 samples of NSk using digoxigenin-labeled T112 probes, staining was seen with both T3 and T7 probes. The levels of positivity changed between samples from being present only with the T3 probe to occurring almost equally with both probes to occurring only with the T7 probe. Interestingly, PT#19's tissue displayed a pattern of staining similar to that of PT#8's tissue; therefore, certain regions of negativity are present in the dermis which are adjacent to focal areas of positivity. These two regions display significantly different morphologies. Background levels, in the form of punctate dots and large patches of blue precipitate, in many of the tissue samples made it difficult to assess those tissue sections.

D. The Possibility of an Antisense TGF-ß1 Transcript

The persistent appearance of staining with sense probes, which occurs very specifically in the cytoplasm of cells at high stringencies, at different intensities, in the absence of any staining with the antisense probe, with regional variation within the same tissue section, and selectively in only some tissue sections in one experiment, suggests that these probes are hybridizing to RNA sequences that are complementary to these sense probes and thus complementary to a portion of mRNA for TGF-ß1. Therefore, attempts were made to confirm that a specific target did exist for the sense TGF-ß1 probes which were used.

1. Northern Analysis Using T112 Probes

Northern analysis was next attempted using the T112 probes to determine if indeed the sense probe was hybridizing to a different RNA species than the antisense probe. To avoid the problem of the probe binding to ribosomal RNA species, poly(A)$^+$ RNA was enriched from total RNA extracted from human dermal fibroblasts (explanted from hypertrophic (H) and normal (N) tissue) using oligo (dT) cellulose (Type 2; Collaborative Research, Inc.) and a batch enrichment protocol. The only problem with studying poly(A)$^+$ RNA is that we do not know whether the RNA species that the sense probe is recognizing is polyadenylated; if indeed this species is antisense RNA then it may be transcribed off the opposite strand of the gene as the sense probe. Therefore, it is not known if signals for polyadenylation exist in the opposite strand in an orientation and sequence which may be used for polyadenylating the antisense RNA species. For this reason, the poly(A)$^+$ enrichment was only attempted once.

Initially, total RNA was extracted from H/N18, H/N20, and NIH 3T3 cells. Seventy micrograms of total RNA from the dermal fibroblasts and 41µg from the NIH cells were enriched for poly(A)$^+$ RNA before running on a denaturing gel while 40µg of each sample (except 20µg of NIH cells) were run directly without prior treatment (20µg/lane; 2 lanes each; NIH cells: 10µg/lane). The poly(A)$^+$ enriched samples were divided evenly into two batches before gel electrophoresis. After electrophoresis, the RNA was transferred to nitrocellulose and probed with ^{32}P-UTP-T112 riboprobes. The results from the H/N18 blots were patchy probably due to the membranes strips sticking to each other in the hybridization bag. As well, they contained a lot of background and the only discernible bands are those of 28S rRNA which decrease in intensity with poly(A)$^+$ enrichment. These two problems made the results from the H/N18 RNA inconclusive. The background on the H/N20 blots was lighter and the results were not patchy (Figure 39); these two factors facilitated the identification of the band corresponding to TGF-ß1 mRNA in an N20 (poly(A)$^+$) blot probed with the antisense probe as well as another band which is larger and is found in N20 blots probed only with the sense probe. Binding to 28S RNA is still a problem.

One possible cause of these extraneous levels of background is that the probes may have contained unincorporated labeled nucleotides or very short fragments of labeled cRNA. Therefore, T112 probes were subsequently purified by polyacrylamide gel elecrophoresis (PAGE) before being used to probe northern blots. Initially, a 6% nondenaturing gel was used on which multiple bands were seen for the T3 probe but only one for the T7 probe. These bands were cut out of the gel and the eluted cRNAs were used to reprobe the H/N20 blots mentioned above. A band corresponding to TGF-ß1 mRNA was found in the N20 blot containing total RNA and probed with antisense probe. As well, similar bands were detectable in the H20 total RNA and poly(A)$^+$ blots probed with antisense.

The gel purification of the probes seemed to clean up background binding since the blots do not appear so black as they did before. However, a few problems remain. Firstly, large spots appear on the blots which indicate probe precipitation and subsequent random adherence to the membrane. As well, the band corresponding to TGF-ß1 mRNA is not clearly seen on all blots which are probed with antisense; this is with 20µg of total RNA loaded per lane. And finally, binding to the 28S rRNA band is still occurring.

The next attempt at northern analysis involved total RNA from H/N4, H/N11, H/N14, and H/N20. Two identical gels were run; 25µg of each sample was used (except for 6.5ug of H14) on each gel. After transferring these gels to nitrocellulose, one was probed with T112 sense and the other with antisense; the probes were labeled with ^{32}P-CTP instead of ^{32}P-UTP since there is a higher ratio of GC than AT in T112 and therefore labeled CTP yielded probes with higher specific activity. The antisense probe hybridized to a band corresponding to TGF-ß1 mRNA (2.5kb) in all samples except H14 (Figure 40). The bands were faint and binding to 28S rRNA was still prevalent in all samples. The blot that was hybridized to the sense probe also displayed specific bands; these transcripts corresponded to RNA of larger size than TGF-ß1 mRNA. In H20 and N20, two bands are visible and they appear in the same location for both samples. In H4, N4, and N14, only the smaller of these two bands is visible. Nonetheless, the location of this band is the same as that of the smaller of the two bands which appear in the lanes of H20 and N20. The problem of binding to 28S rRNA also exists for the sense probe.

These results verify that the antisense T112 probe does, in fact, hybridize to TGF-ß1 mRNA. The sense probe, however, also finds a specific and complementary target in the total RNA pool of human dermal fibroblasts. The fact that this same target appears consistently in different experiments and in different samples in the same experiment indicates that its specificity for T112 sense is high. The occurrence of more than one band is preliminary evidence for splice variants of a particular transcript. This data takes us closer to accepting the concept of an antisense RNA species for TGF-ß1 that binds to the mRNA to control or regulate the production of this cytokine.

These blots revealed some background throughout the membranes; as well, the bands that appeared were faint. Therefore, the membranes were rehybridized to freshly labeled probe. These probes were, once again, purified from a denaturing gel (Figure 41) during which it was noticed that the T7 probe migrated very slowly through the gel and almost hung just below the well. Before hybridization, the membranes were pre-incubated in old hybridization mix (containing old probe) that was predenatured in a boiling water bath.

Very high levels of background resulted from this rehybridization which was denoted by the overall dark color of the blots and the high density of spots and dark regions on the blots especially around the edges (not shown). On the antisense membrane the

TGF-ß1 mRNA band appeared much stronger this time but at the expense of higher background levels. On the sense membrane, no bands could be seen.

In yet another attempt to improve the quality of the results from northern analysis, two identical Hybond N^+ membranes containing 20ug each of H20 and N20 RNA transferred from a denaturing gel were hybridized to ^{32}P-CTP-T112 probes. The hybridization mixture was changed for this experiment to the same one used for *in situ* hybridization plus DTT and without SDS and N-lauroylsarcosine. When the probes which were used on these membranes were gel purified, the T7 probe hung up again just below the well whereas the T3 probe migrated into the gel. The results clearly demonstrate TGF-ß1 mRNA with the antisense probe in addition to 28S rRNA background. There were absolutely no results obtained with the sense probe initially; after exposing the membranes for 5 days, however, faint bands appeared which would correspond to the smaller band found previously using the sense probe. Background problems were still prevalent especially with the T7 probe as the blots appeared very dark.

A possible explanation for these high and spotty background levels is the denaturation of dextran sulfate which, upon boiling, may become particulate and stick randomly to the membranes along with the probes. Another recurring problem was the lack of mobility of the T7 probe during PAGE. This could be due to the self-aggregation of the probe due to short repeats within the sequence, especially G or C repeats.

2. Attempted Ribonuclease Protection Assay Using T112 Probes

To ensure a reasonable degree of complementarity between the sense probe and the targets being identified by northern analysis, ribonuclease protection assay (RPA) was also attempted using the same probes as those used to probe the northern blots. In an RPA, if the target sequence hybridizes to and protects the probe from digestion by a cocktail of RNases specific for single-stranded RNA, then a band should appear on a denaturing gel that is of the same size as the probe.

RNA that was extracted from H/N4, H/N11, and H/N20 for northern analysis was also used for RPA. *E. coli* tRNA was also included as a negative control as we do not expect the T112 probes to hybridize to, and therefore be protected by, the tRNA. After hybridizing total RNA from these cell strains to ^{32}P-CTP-T112 probes (not gel purified), an RNase cocktail was added and the resulting mixture after incubation was extracted with phenol/chloroform (1:1) and precipitated. Denaturing PAGE was then used to separate the precipitated product and analyze for protected fragments. A technical problem with the gel prevented the proper mobility of the samples and therefore the samples did not separate well enough to be able to identify any protected fragments and their sizes. Problems that led to this may include the salt concentration of the samples and of the gel, not pre-running the gel, and the abnormal porosity of the gel possibly due to improper preparation.

The protocol for the preparation of the gel was changed; subsequent to this, the next gel included only size markers to test for their proper migration. The markers appeared to migrate well through this gel as the separation was clean and the different bands clearly discernible. Therefore, the RPA was repeated but with RNA from only two cell strains, H20 and N20 (Figure 42). The protocol was changed to include the incorporation of RNase T1, in addition to RNase A, in the ribonuclease digestion mix. Also included in this RPA were the probe-only controls which when digested with the RNases should yield no bands. This did occur for the T3 probe but the T7 probe, upon digestion, displayed a ladder of bands. An identical ladder appeared in all samples hybridized with the T7 probe including the tRNA. Therefore, this experiment showed that this probe was binding to itself and, in the case of RPA, was protecting itself. No bands were seen in any of the lanes in which T3 protected by total RNA or tRNA were run except for one very small band which appears in all lanes including that of tRNA.

Taken together, the results from these RPAs are inconclusive. The template used for transcribing TGF-ß1 riboprobes (pT112) needs to be remade. The inclusion of a broader region of the cDNA sequence around the T112 region is necessary to provide the resulting probe with more specificity and less tendency to contribute to background by sticking to non-specific sites.

Figure 1A **Gel electrophoresis of pD150.** pD150 undigested (lane 2) and linearized with either *Pst I* or *Eco* R I (lane 3 or lane 5, respectively) were analyzed by gel electrophoresis on a 1% agarose gel. Double digestion of pD150 was also carried out with *Pst* I and *Eco* R I (lane 4 and 6) and liberated the 150bp decorin cDNA insert from pD150. The standard marker DNA in lane 1 is λ DNA digested with *Hind* III; the sizes of the fragments in lane 1 are indicated.

Figure 1B **Dot blot quantitation of digoxigenin-labeled cRNA probes transcribed off pD150.** Serial dilutions (1/10, 1/100, 1/1000, $1/10^4$, $1/10^5$, $1/10^6$, $1/10^7$) of sense (SP6) and antisense (T7) D150 probes were spotted onto a nylon membrane along with serially smaller quantities (1ng, 0.1ng, 10pg, 1.0pg, 0.1pg, 10fg) of digoxigenin-labeled control RNA. Concentrations were calculated as 1.0μg/μL for the T7 probe and 50ng/μL for the SP6 probe.

Figure 1C **Dot blot hybridization of sense and antisense D150 probes to serially diluted pD150.** Serially diluted amounts of pD150 (top row: 1ng, 0.1ng, 10pg, 1.0pg, 0.10pg, 10fg, 50ng salmon sperm DNA; bottom row: 0.50ng, 50pg, 5.0pg, 0.50pg, 50fg, 5.0fg, 70ng yeast tRNA) fixed to nylon by U.V. crosslinking served as the target.

Figure 1

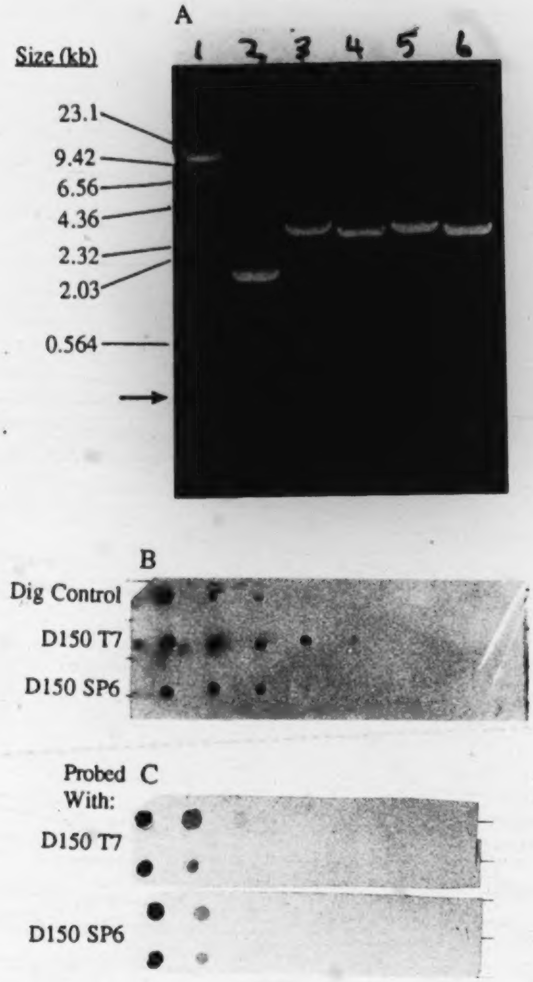
A
Size (kb)
1
2
3
4
5
6
23.1
9.42
6.56
4.36
2.32
2.03
0.564
B
Dig Control
D150 T7
D150 SP6
Probed With:
C
D150 T7
D150 SP6

Figure 2A **Gel electrophoresis of linearized pD600.** pD600 was digested with *Eco* R I (lane 1), *Cla* I (lane 2), or *Apa* I (lane 3) and analyzed by gel electrophoresis on a 1% agarose gel. Sizes of the digested fragments were compared with λ/*Hind* III (lane 4).

Figure 2B **Gel electrophoresis of double digested pD600.** Undigested pD600 (lane 2) and pD600 digested with *Apa* I and *Cla* I (lanes 3 and 5) were analyzed by gel electrophoresis on a 1% agarose gel. Sizes of the digested fragments were compared with λ/*Hind* III (lane 1).

Figure 2C **Pseudonorthern analysis of sense and antisense D600 transcripts.** The following samples were studied by pseudonorthern analysis: total RNA extracted from human dermal fibroblasts (10-15μg; lane 1); digoxigenin-labeled RNA molecular weight marker III (100ng; lane 2); D600/T7 (250ng; lane 3); D600/SP6 (25ng; lane 4); D600/T7 (500ng; lane 5); D600/T7 (1000ng; lane 6); D600/T3 (100ng; lane 7); D600/T3 (400ng; lane 8).

Figure 2D **Dot blot quantitation of D600 sense (T7) and antisense (T3) probes as described for Figure 1B above.** Concentrations were calculated as 300ng/μL for the T7 probe and 100ng/μL for the T3 probe.

Figure 2E **Dot blot hybridization of sense and antisense D600 probes to serial dilutions of unlabeled D600 as described for Figure 1C.**

Figure 2

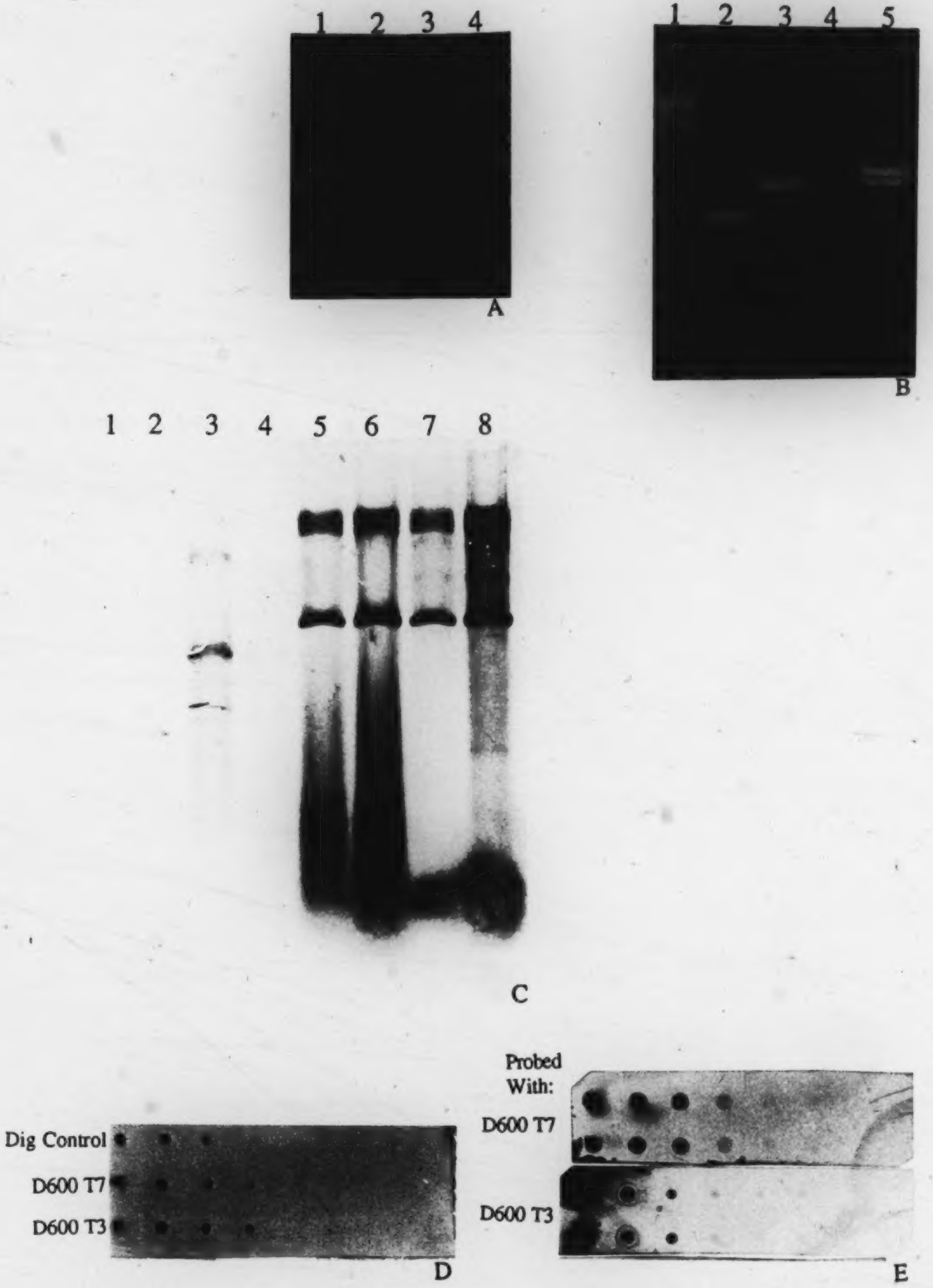
1
2
3
4
A
1
2
3
4
5
B
1
2
3
4
5
6
7
8
C
Dig Control
D600 T7
D600 T3
D
Probed With:
D600 T7
D600 T3
E

Figure 3 **In situ hybridization with antisense D600.** Human dermal fibroblasts explanted from hypertrophic scar (H16; A and C) and normal skin (N16; B and D) and cultured onto APTEX-coated slides served as target. Post-hybridization washes were conducted at two stringencies, T_m-19°C (A and B) and T_m-28°C (C and D). Staining with the sense probe was negligible (data not shown).

Figure 3

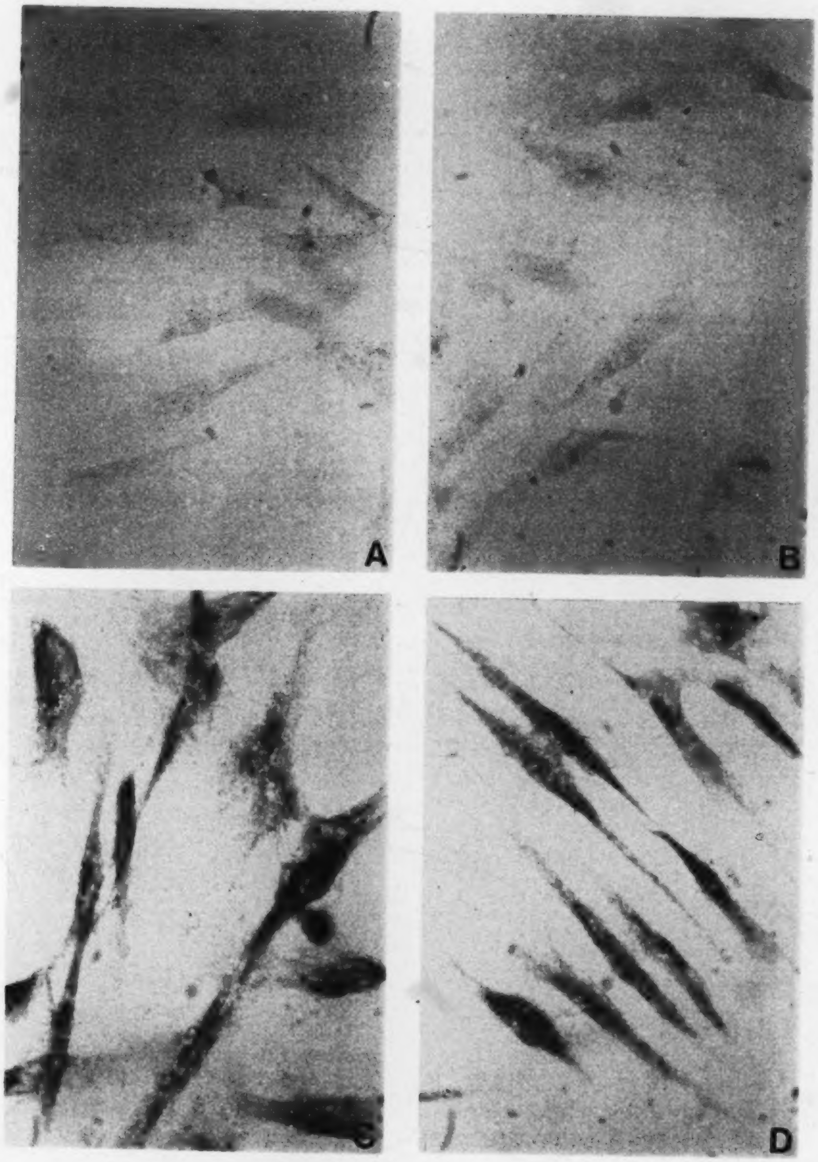

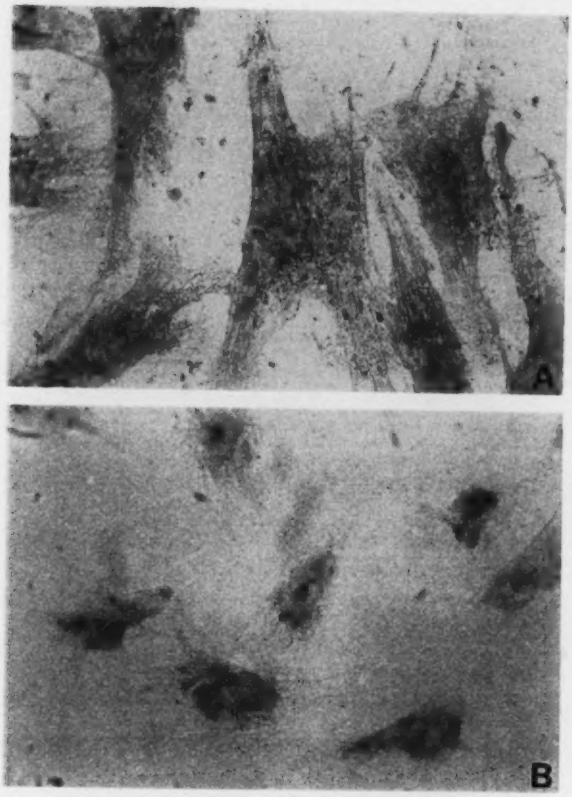

Figure 4 **In situ hybridization with antisense D600.** Human dermal fibroblasts explanted from hypertrophic scar (H2) and cultured onto APTEX-coated slides served as target. The stringency of hybridization was altered by changing the salt concentration from 1X SSC (0.17M Na^+; A) to 5X SSC (0.83M Na^+;B) in the hybridization mixture.

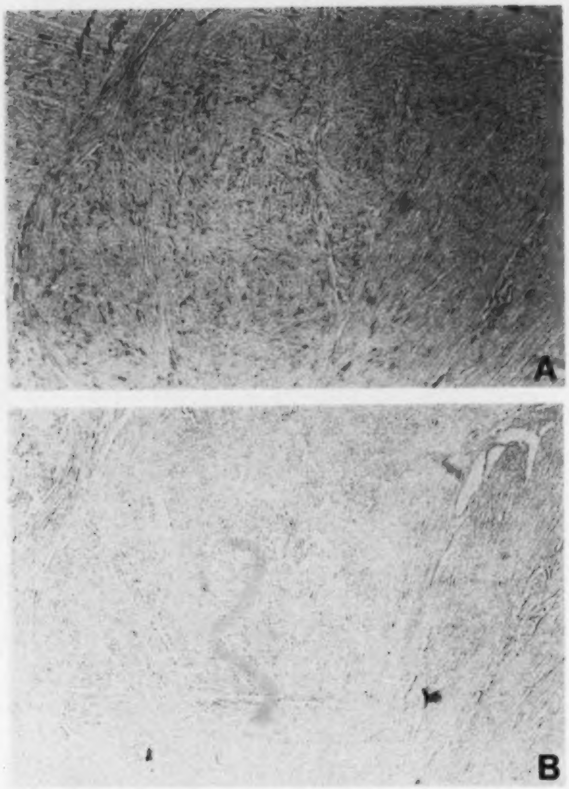

Figure 5 **In situ hybridization with antisense (A) and sense (B) D600 probes on 4 - 5μm sections of paraffin-embedded hypertrophic scar from PT#8.** Pictures were taken at 2x objective power.

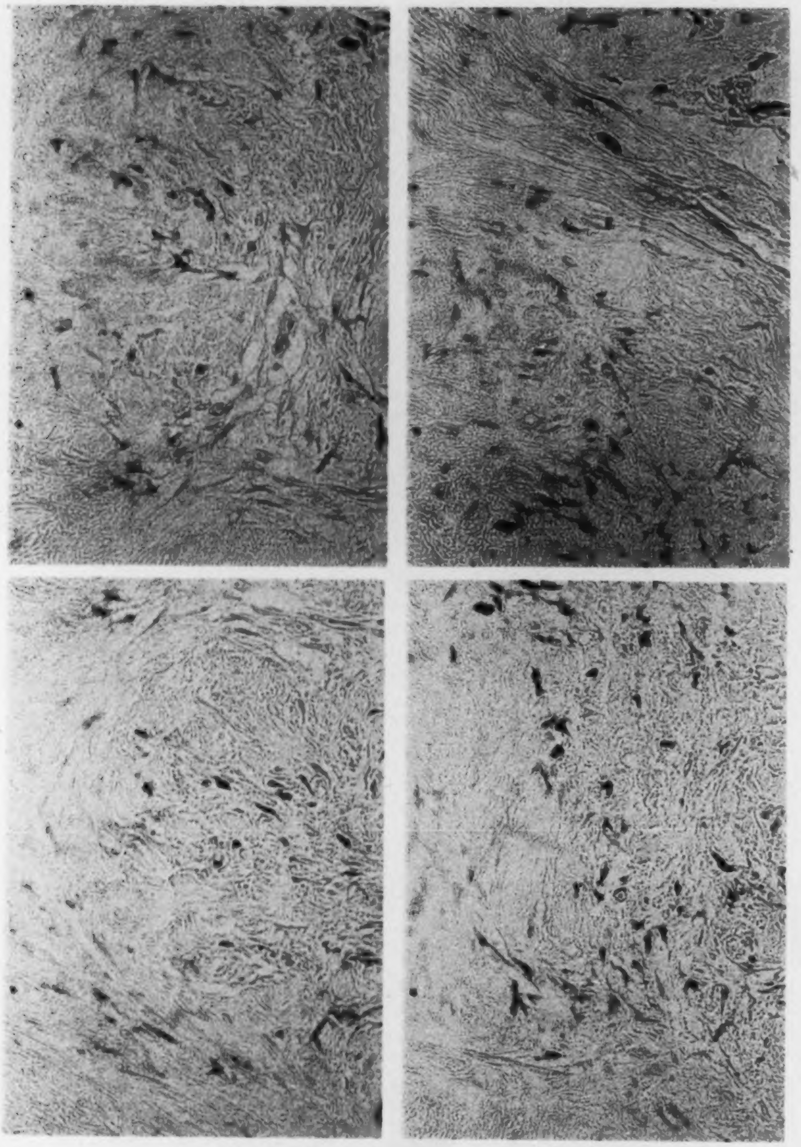

Figure 6 **In situ hybridization with antisense D600 probes on 4 - 5um sections of paraffin-embedded hypertrophic scar.** Sections presented here are serial sections of the same sample of HSc presented in Figure 5. Pictures were taken at 40x objective power.

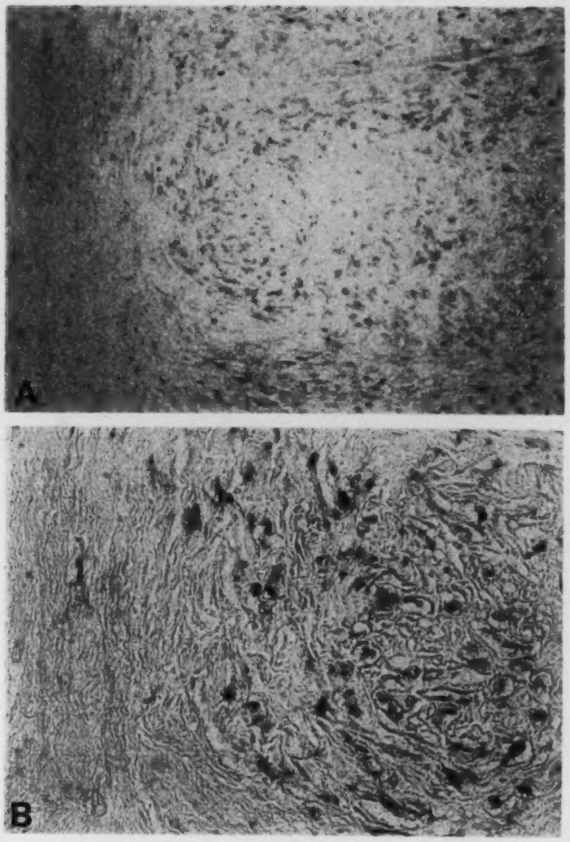

Figure 7 **In situ hybridization with antisense D600 probes on 4 - 5μm sections of paraffin-embedded hypertrophic scar from PT#15.** Pictures were taken at 10x (A) and 40x (B) objective power.

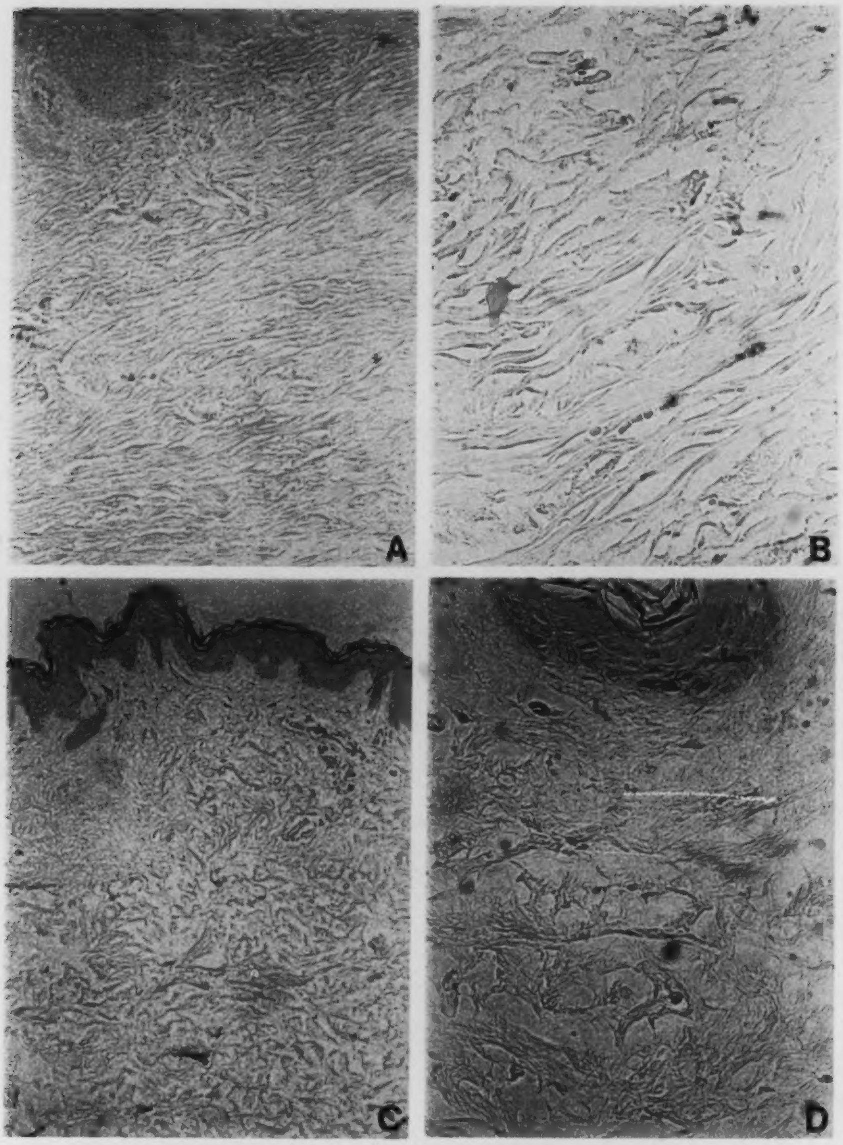

Figure 8 **In situ hybridization with antisense D600 probes on 4 - 5μm sections of paraffin-embedded mature scar from PT#27(A, B) and normal skin (C, D).** Pictures were taken at 10x (A, C) and 40x (B, D) objective power.

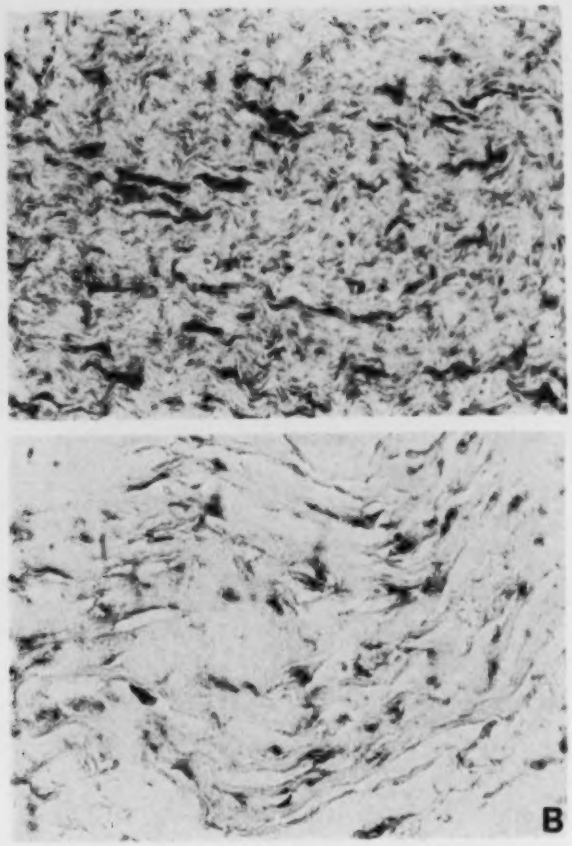

Figure 9 **In situ hybridization using antisense D600 on 4 - 5µm thick sections of paraffin-embedded HSc tissue from PT#12.** Different conditions for incubation of probed sections with the sheep polyclonal anti-digoxigenin antibody during the detection procedure were tested: room temperature for 30 minutes (A) and 4C for 20 hours (B).

Figure 10A **Gel electrophoresis pD620.** pD620 undigested (lane 1) and digested with restriction enzymes *Kpn* I (lane 2) or *Kpn* I and *Pst* I (lane 3) were analyzed by gel electrophoresis in a 1% agarose gel. Digestion with *Eco* R I (lane 4) liberated the decorin cDNA fragment from the pT7T3 vector as indicated by the arrow. DNA size marker was λ/*Hind* III and *Eco* R I (lane 5).

Figure 10B **Dot blot quantitation of digoxigenin-labeled cRNA probes transcribed off pD620 as described for 1B.**

Figure 10C **Dot blot hybridization of antisense (T3) and sense (T7) D620 probes to serially diluted amounts of pD620 as described for 1C.**

Figure 10D **Pseudonorthern analysis of D620 and T112 probes as described for 2C.** Lane 1 digoxigenin-labeled marker III (100ng); lane 2 labeled control RNA (100ng); lane 3 labeled control RNA (200ng); lane 4 blank; lane 5 D620/T3 (100ng); lane 6 D620/T7 (500ng); lane 7 D620/T3 (100ng); lane 8 D620/T7 (500ng); lane 9 T112/T3 (100ng); lane 10 T112/T7 (500ng); lane 11 T112/T3 (from hybridization mixture); lane 12 T112/T7 (from hybridization mixture). Labeled control RNA served as a size marker (760bp) against which to compare samples in the other lanes.

Figure 10E **Pseudonorthern analysis of D620 and T112 probes as described for 2C.** Lane 1 digoxigenin-labeled marker III (100ng); lane 2 blank; lane 3 labeled control RNA (100ng); lane 4 D620/T3 (100ng); lane 5 D620/T7 (500ng); lane 6 D620/T3 (100ng); lane 7 D620/T7 (500ng); lane 8 T112/T3 (100ng); lane 9 T112/T7 (500ng). Samples run on this gel were the same as those in Figure 10D, however, more stringent conditions were used to denature them before electrophoresis, ie. heating to 85°C in 80% formamide.

Figure 10

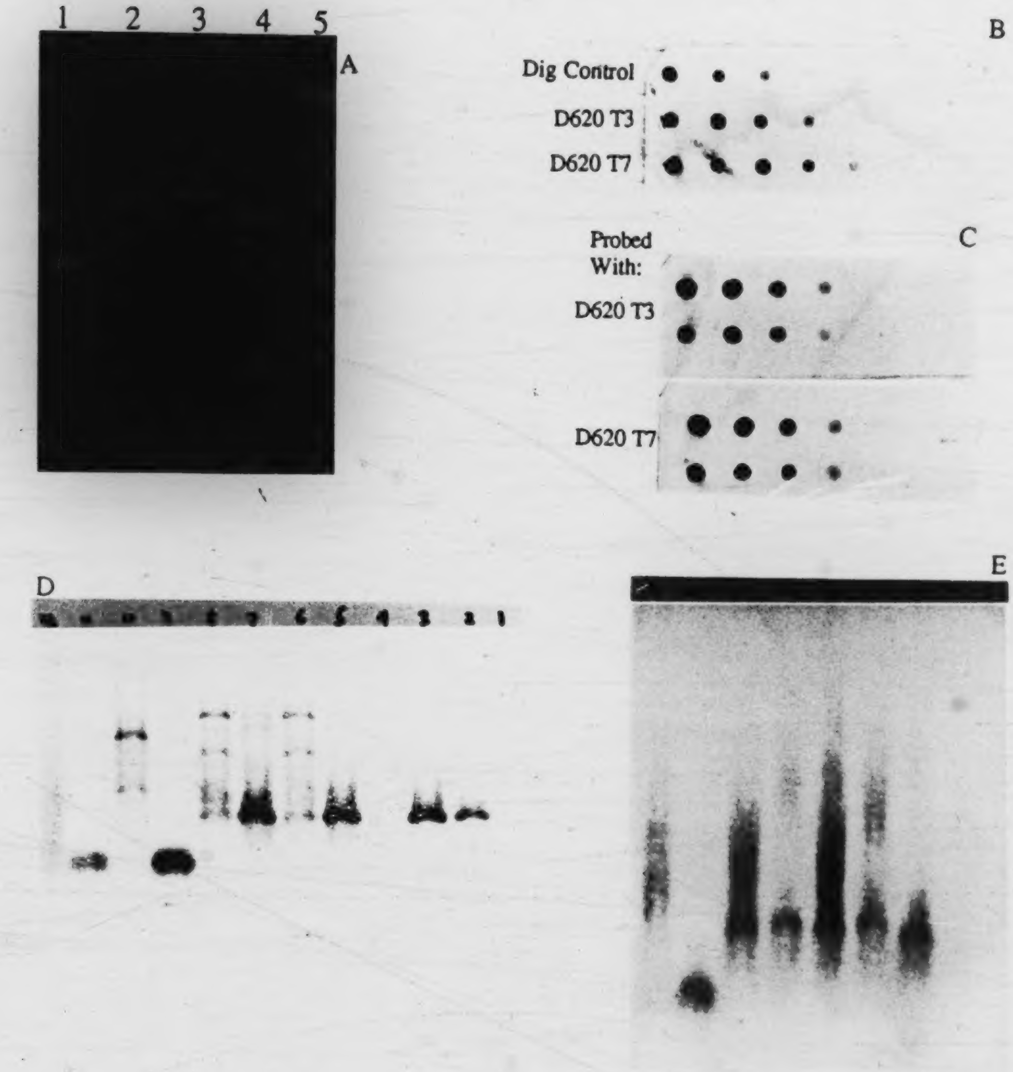
1 2 3 4 5
A
B
Dig Control
D620 T3
D620 T7
C
Probed With:
D620 T3
D620 T7
D
8 7 6 5 4 3 2 1
E

Figure 11 **In situ hybridization with antisense D620.** Human dermal fibroblasts explanted from HSc (H8; A, C, E, G) and NSk (N8; B, D, F, H) and grown on APTEX-coated slides for 4 (A and B), 17 (C and D), 36 (E and F), and 100 (G and H) hours served as target. The sense probe produced negligible staining.

Figure 11

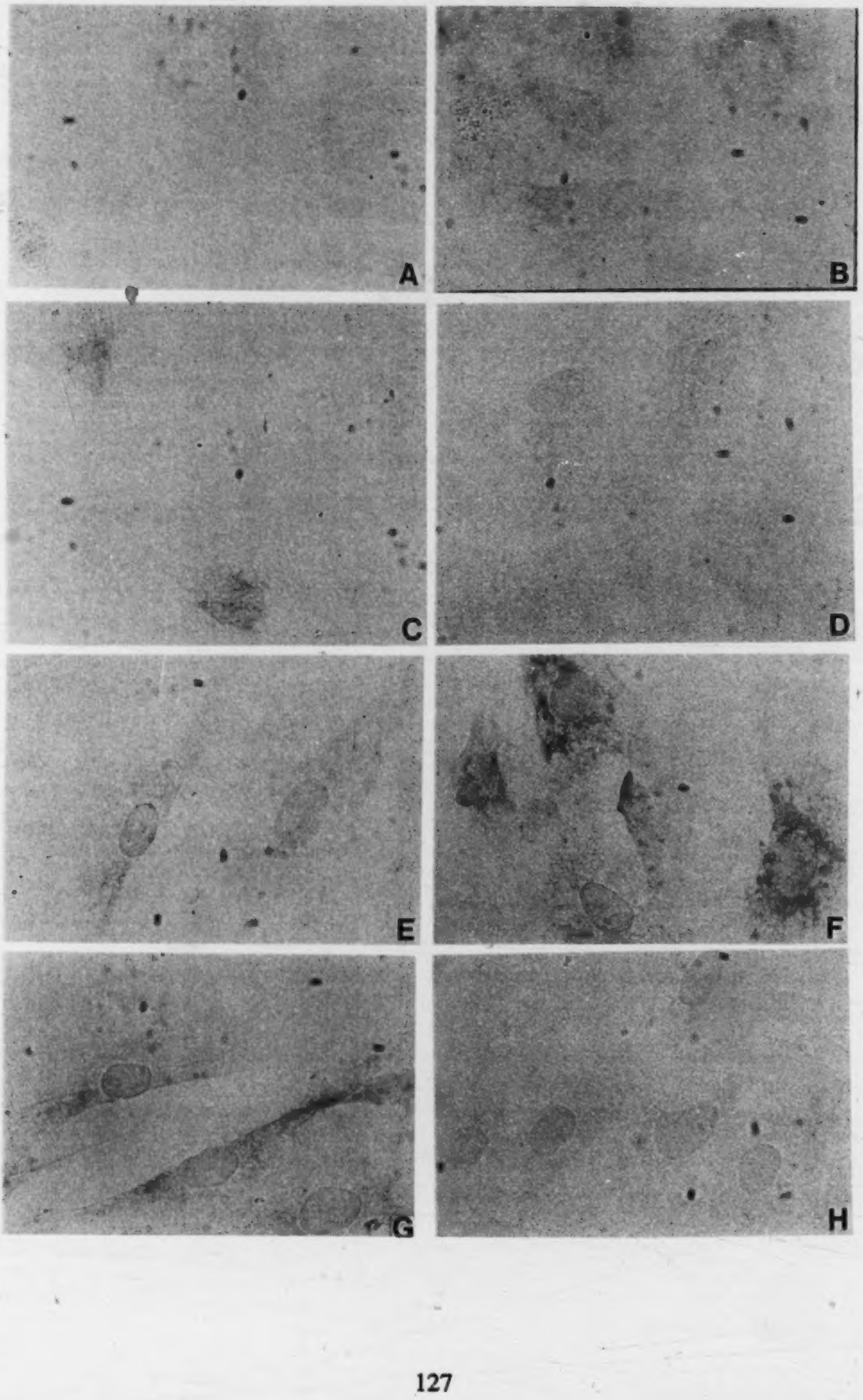

Figure 12 **In situ hybridization with sense (S) and antisense (AS) D620 probes on 4 - 5μm sections of different samples of paraffin-embedded HSc.** Specimens presented were obtained from PT#5 at 5 months (A, B), PT#12 at 12 months (C, D), and PT#30 at 216 months (E, F) post-burn.

Figure 12

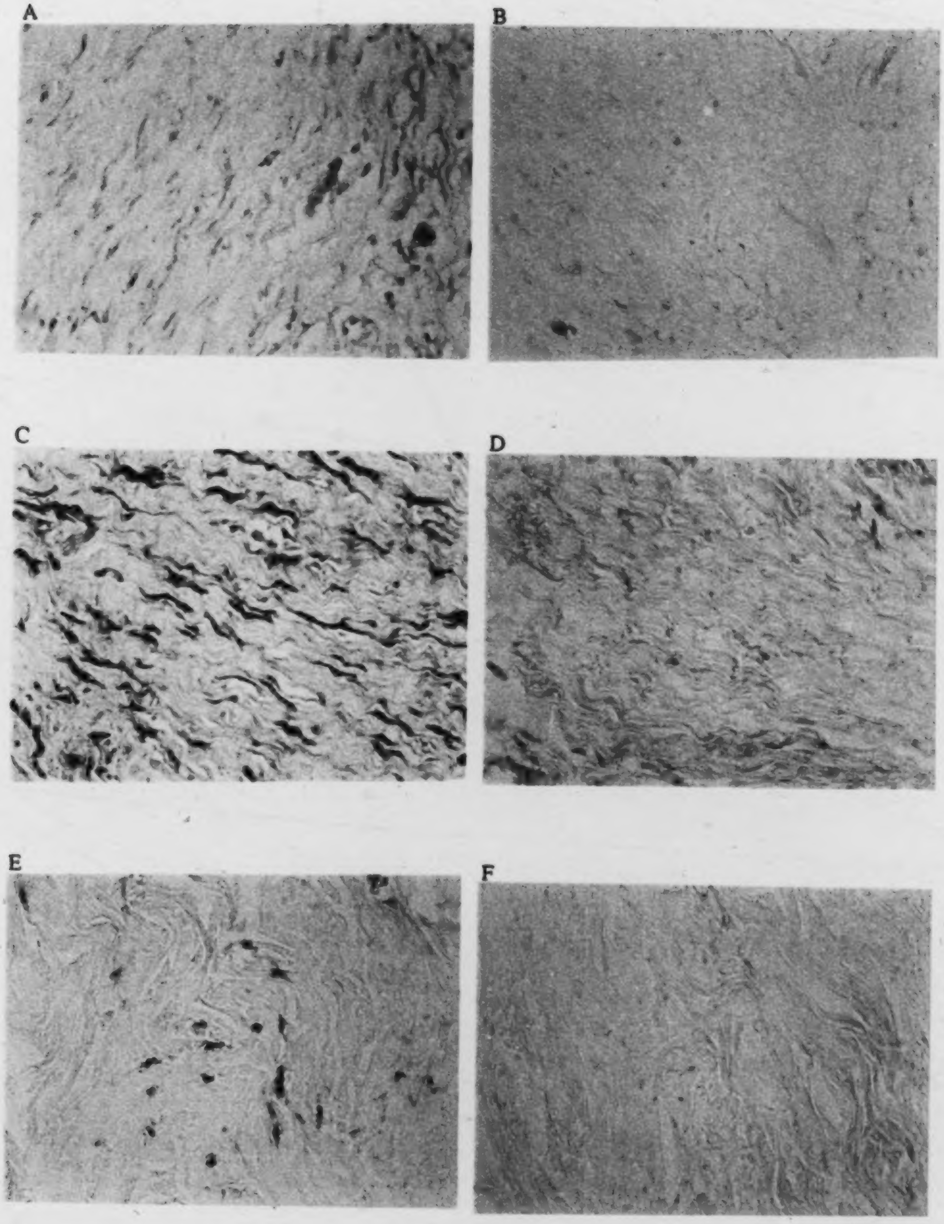

7

Figure 13 **Low power (2x objective) view of a section of HSc to illustrate the methodology employed to quantitate the *in situ* hybridization results.** The depths of the sections were measured under 40x objective power from epidermis to dermis using a marked ocular lens. The depth was divided into thirds by counting the total number of fields from the epidermis to the bottom of the deep dermis ("x") and dividing this value by 3 ("y").The one-third segment closest to the epidermis was termed the papillary dermis; below that was the next one-third of the dermis which was called the middle dermis and the lowest third was called the reticular dermis. In each third of the dermis, the number of fields across its width was referred to as "z". Multiplying y and z resulted in the total number of fields in that third of the dermis. Ten randomly chosen fields were selected within each third of each section using a table of 1000 random digits (Rosner, 1990, p. 540). The number of positively stained cells was counted in each of the randomly chosen fields and then summed for each third of each section

Figure 14 **Scatter plot of decorin expression with time after injury.** The total number of positive cells for decorin mRNA, by *in situ* hybridization, within each region of the dermis (A) and totalled for each section (B) were plotted against time after injury.

Figure 14

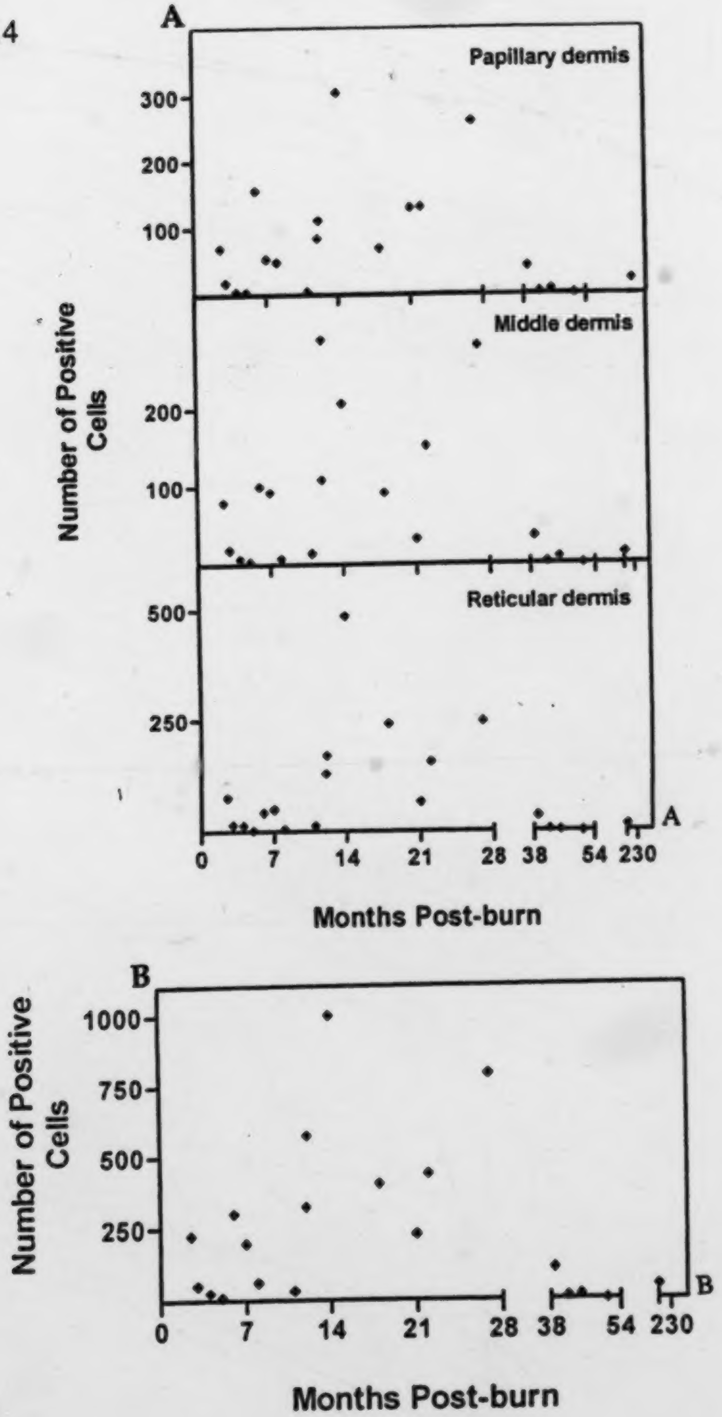
A
Papillary dermis
300
200
100
Middle dermis
200
100
Reticular dermis
500
250
Number of Positive Cells
A
0
7
14
21
28
38
54
230
Months Post-burn
B
1000
750
500
250
Number of Positive Cells
B
0
7
14
21
28
38
54
230
Months Post-burn

Figure 15 **Grouped scatter plot of decorin expression with time after injury.** Numbers of positive cells within each region of the dermis (A) and in each entire section (B) were plotted on a grouped scatter plot according to the different time points, early, intermediate, and late, after injury.

Figure 15

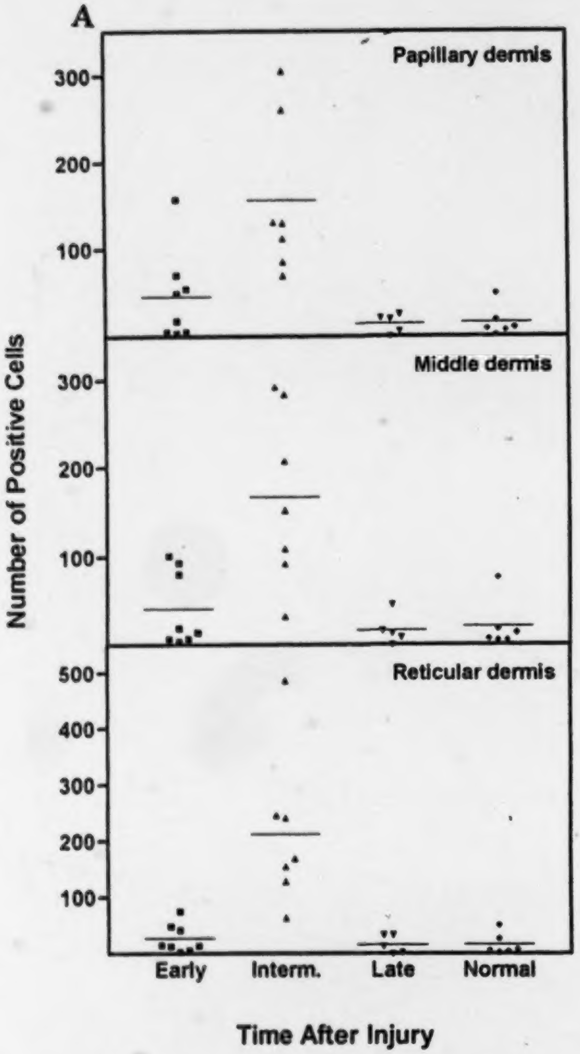
A
Papillary dermis
Middle dermis
Reticular dermis
Number of Positive Cells
300
200
100
300
200
100
500
400
300
200
100
Early
Interm.
Late
Normal
Time After Injury

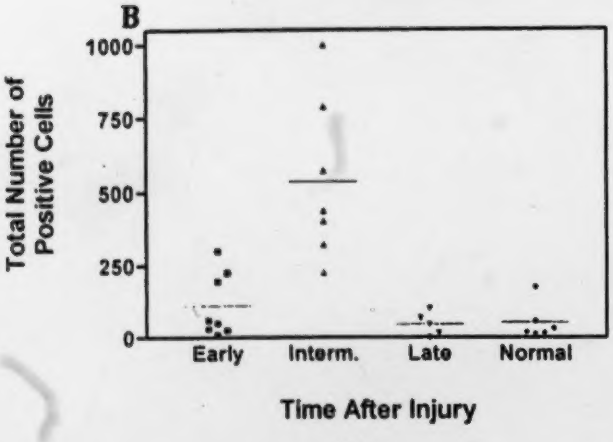
B
Total Number of Positive Cells
1000
750
500
250
0
Early
Interm.
Late
Normal
Time After Injury

Figure 16 **Scatter plot of cell number with time after injury.** The total number of connective tissue cells within each region of the dermis (A) for all sections studied and within each entire section (B) were counted in hematoxylin-stained sections and were plotted against time after injury on a scatter plot.

Figure 16

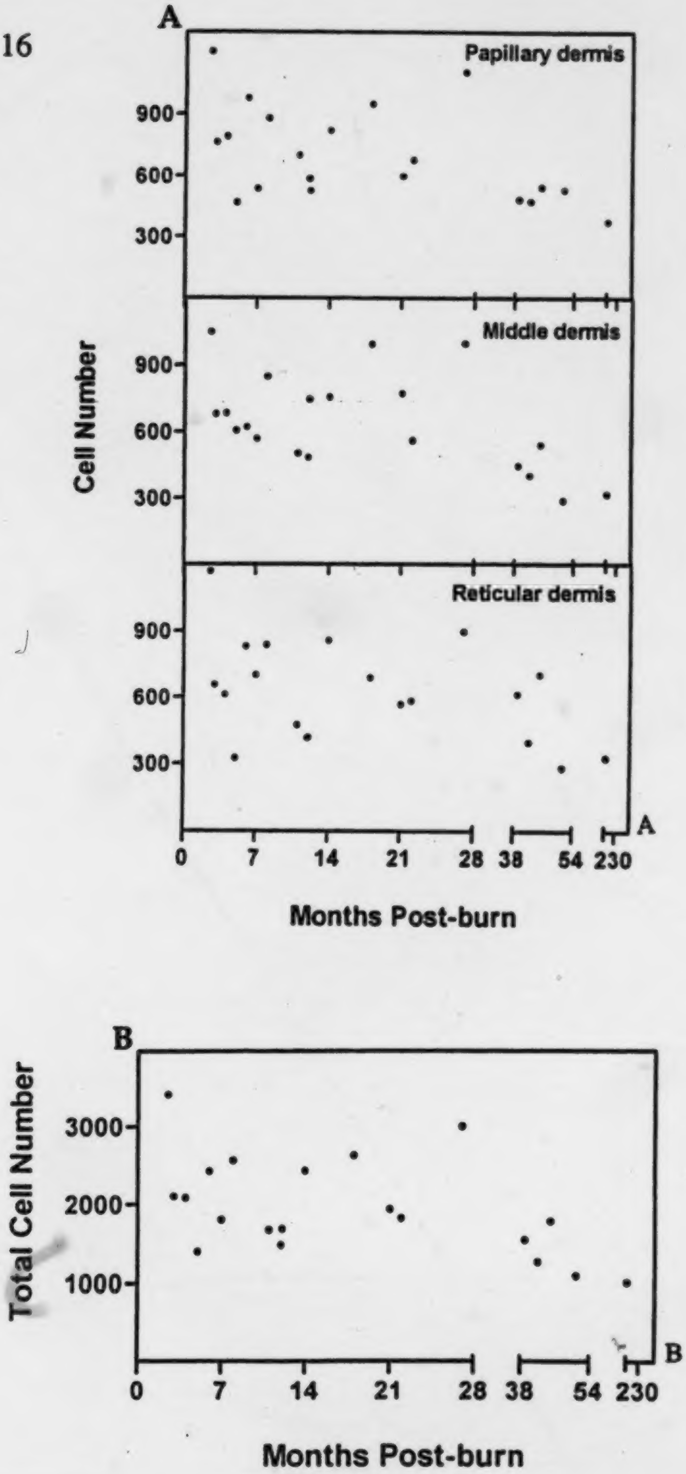
A
Papillary dermis
Middle dermis
Reticular dermis
Cell Number
900
600
300
0
7
14
21
28
38
54
230
A
Months Post-burn
B
Total Cell Number
3000
2000
1000
0
7
14
21
28
38
54
230
B
Months Post-burn

Figure 17 **Scatter plot of percent decorin expression with time after injury.** The percent number of positive cells for decorin mRNA in each region of the sections studied (A) and within each entire section (B) were plotted against time after injury on a scatter plot.

Figure 17

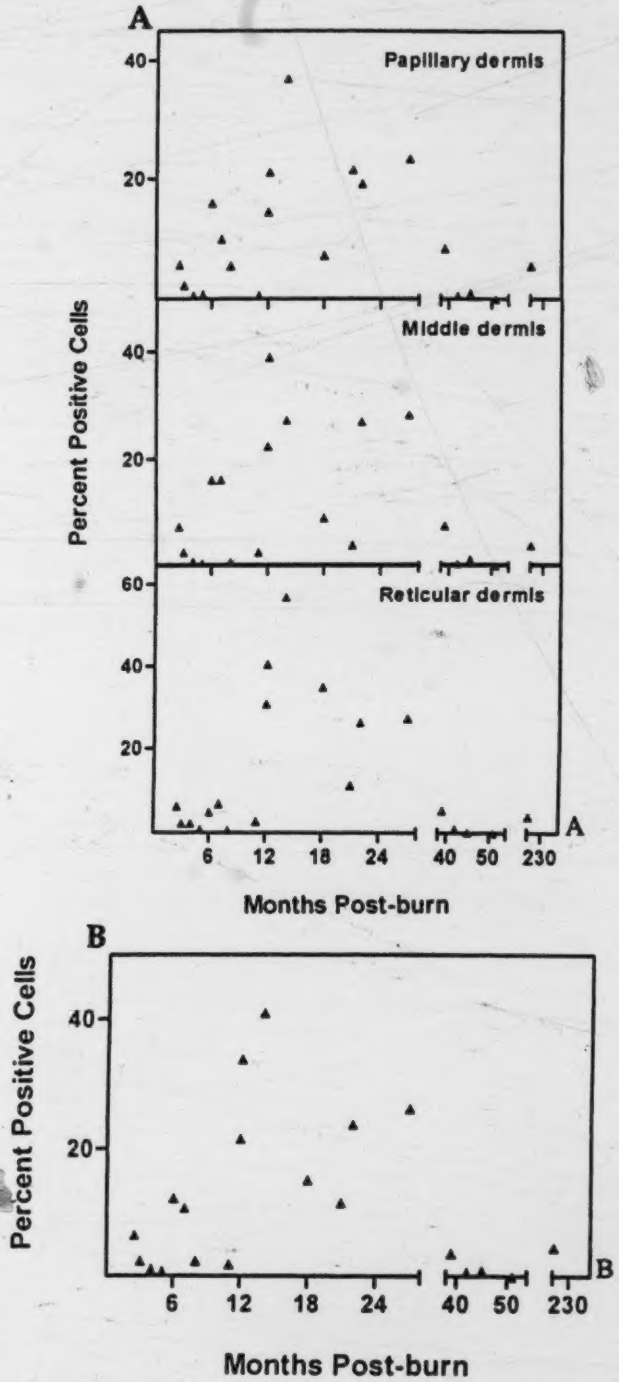
A
Papillary dermis
Middle dermis
Reticular dermis
40
20
40
20
60
40
20
Percent Positive Cells
6
12
18
24
40
50
230
Months Post-burn
A
B
40
20
Percent Positive Cells
6
12
18
24
40
50
230
Months Post-burn
B

Figure 18 **Grouped scatter plot of percent decorin expression with time after injury.** The percent number of positive cells within each region of the dermis (A) and in each entire dermis (B) were plotted on a grouped scatter plot according to the different time points, early, intermediate, and late, after injury.

Figure 18

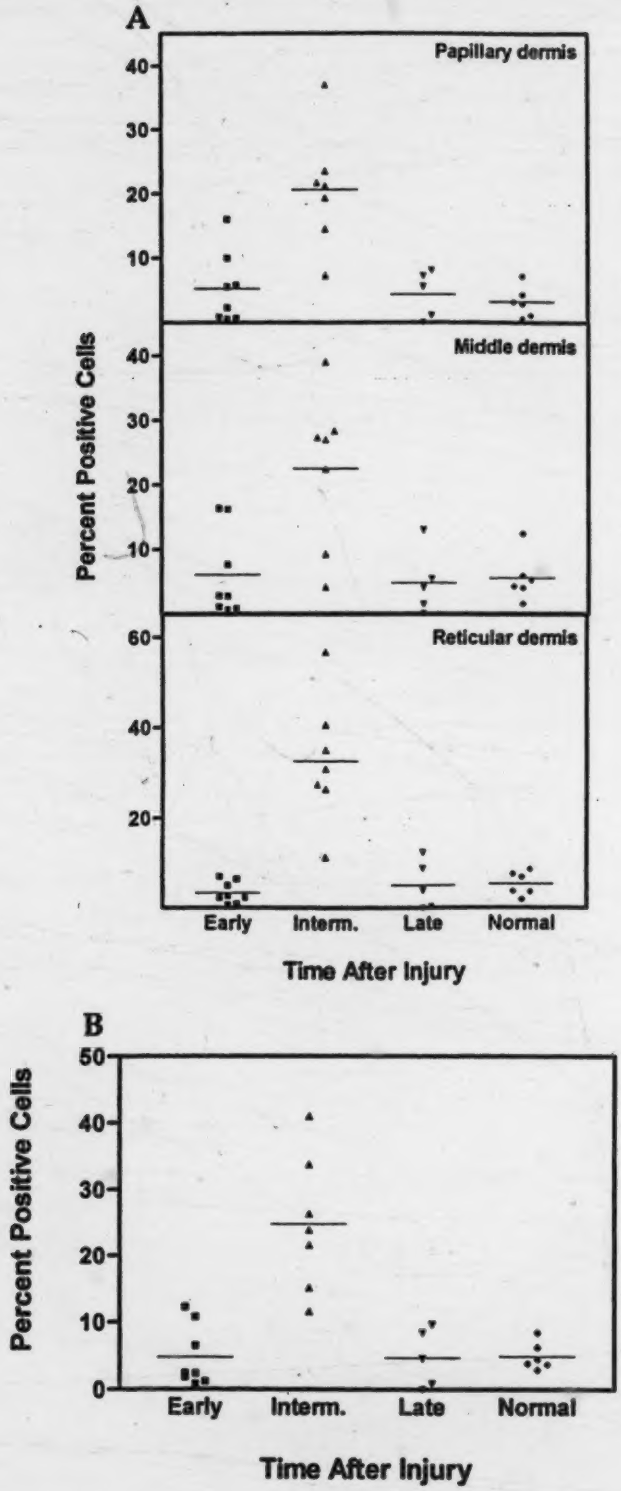
A
Papillary dermis
Middle dermis
Reticular dermis
Percent Positive Cells
40
30
20
10
60
Early
Interm.
Late
Normal
Time After Injury
B
50
0
Percent Positive Cells
Time After Injury

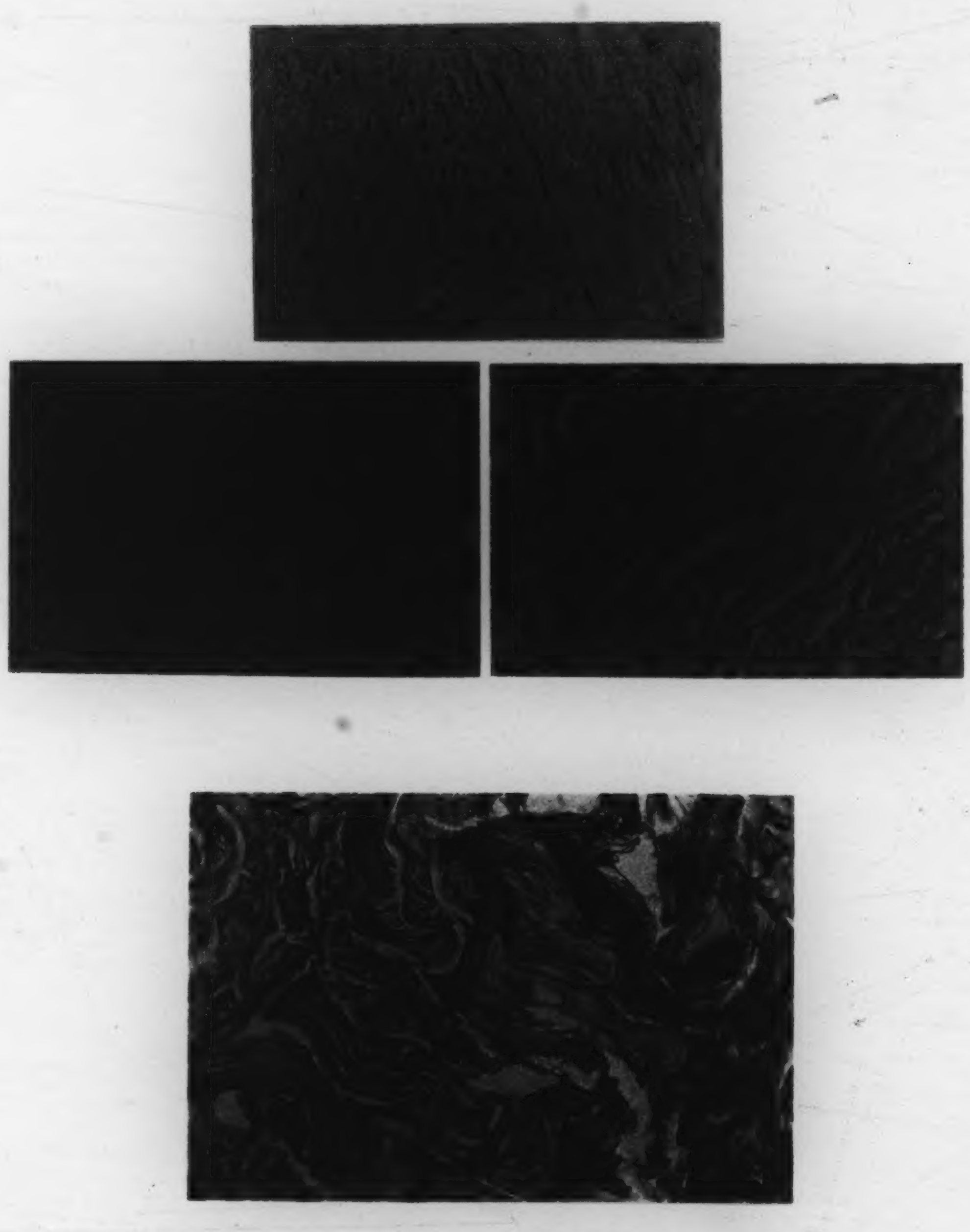

Figure 19 **Immunolocalization of decorin in early (5 mo.; PT#5), intermediate (12 mo.; PT#12), and late (216 mo.PT#30) hypertrophic scar and normal skin (NSk).**

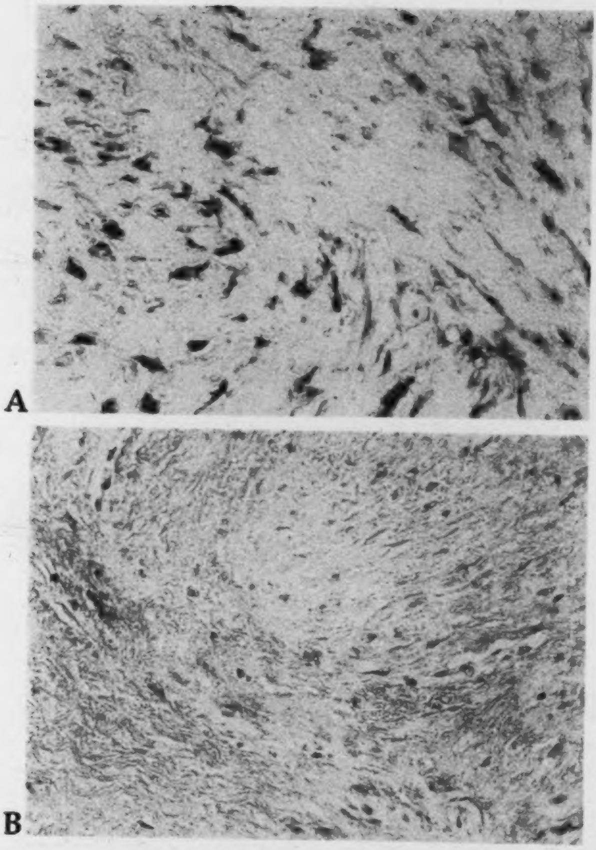

Figure 20 **Regional variation in decorin expression in HSc by *in situ* hybridization and immunoperoxidase staining.** Serial sections of the same sample of HSc (PT#19) were stained either for decorin mRNA (A) or for decorin protein (B).

Figure 21A **Analysis of rat TGF-ß1(287)/pGEM.** TGF-ß1(287)/pGEM 3Z uncut (lane 2) and digested with *Pst* I and *Bam* HI (lane 3), which liberated the TGF-ß1 cDNA fragment (287bp) from the plasmid, were analyzed by gel electrophoresis in a 1% agarose gel. Lane 1: λ/*Hind* III.

Figure 21B **Analysis of rat TGF-ß1(287)/pGEM.** TGF-ß1(287)/pGEM 3Z (lane 2) uncut and linearized with either *Pst* I (lane 3) or *Bam* HI (lane 4) were analyzed by gel electrophoresis in a 1% agarose gel. Fragment size was compared against the size marker λ/*Hind* III (lane 1).

Figure 21C **Dot blot quantitation of digoxigenin-labeled sense and antisense rTGF-ß1/pGEM 3Z probes.** Serial dilutions of probe and control labeled RNA were performed as described for 1B. Concentrations of the probes are: for T7, 0.125µg/uL; for SP6 probe, 1.25ng/uL.

Figure 21D **Dot blot hybridization of sense and antisense rTGF-ß1/pGEM 3Z probes to unlabeled rTGF-ß1/pGEM 3Z.** Serially diluted amounts of rTGF-ß1/pGEM 3Z (top row: 10ng, 1ng, 0.1ng, 10pg, 1.0pg, 0.1pg, 10fg, 50ng salmon sperm DNA; bottom row: 5ng, 0.50ng, 50pg, 5.0pg, 0.50pg, 50fg, 5.0fg, 70ng yeast tRNA) served as target. The sensitivity of the probes was about 10pg for the T7 or sense probe and 100pg for the SP6 or antisense probe.

Figure 21

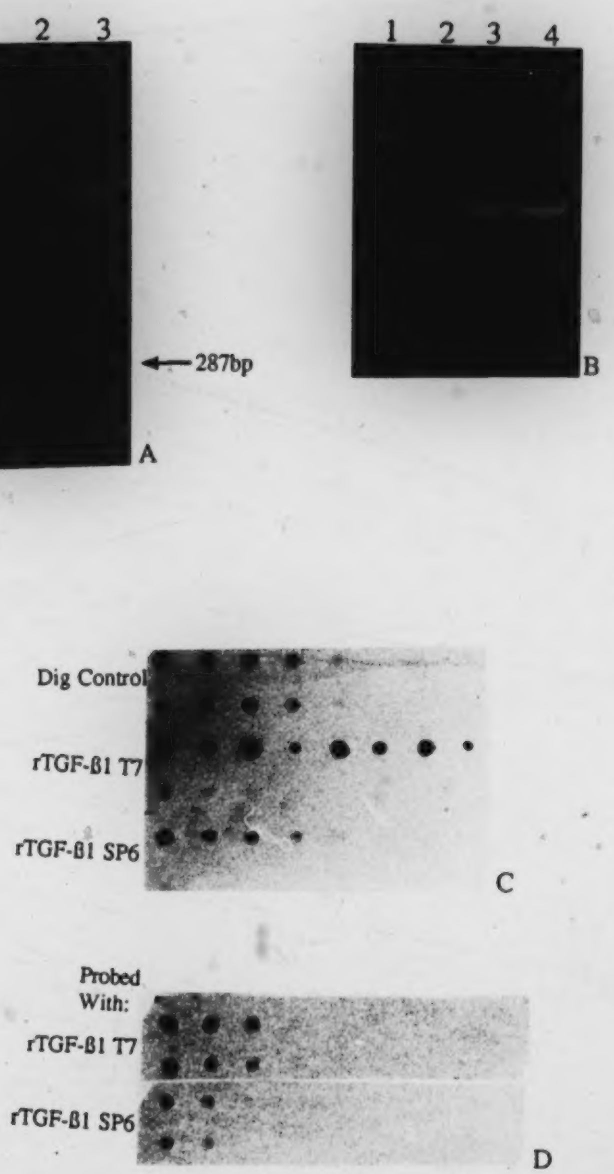
1
2
3
287bp
A
1
2
3
4
B
Dig Control
rTGF-ß1 T7
rTGF-ß1 SP6
C
Probed With:
rTGF-ß1 T7
rTGF-ß1 SP6
D

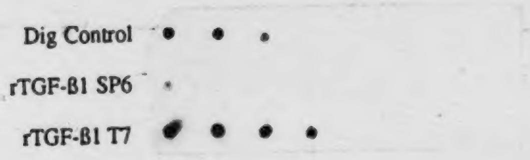

Figure 22 **Dot blot quantitation of digoxigenin-labeled sense and antisense rTGF-ß1/pGEM 3Z probes.** Serial dilutions of probe and control labeled RNA were performed as described for 1B. Concentrations of the probes are: for SP6, 100pg/uL; for T7, 500ng/uL.

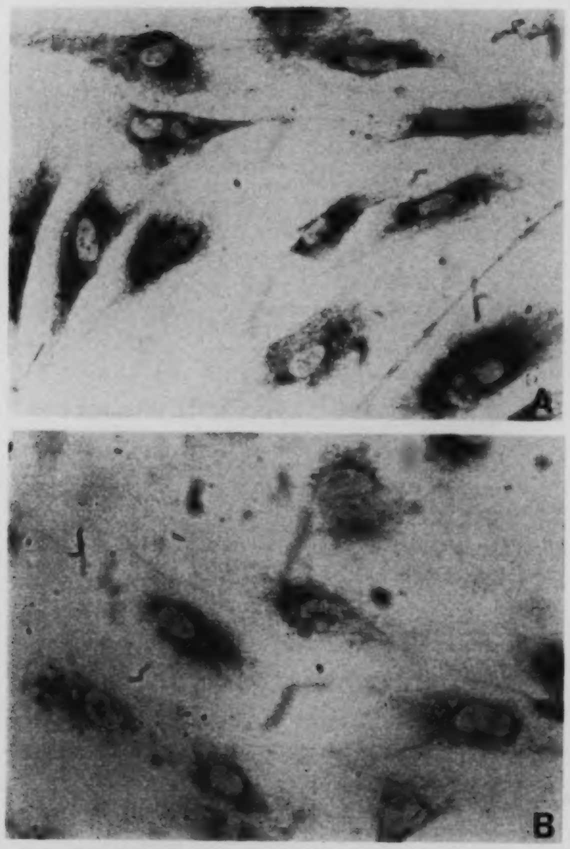

Figure 23 **In situ hybridization with antisense rTGF-ß1/pGEM 3Z probes on human dermal fibroblasts.** Fibroblasts were explanted from HSc (H15; A) and NSk (N15; B) and cultured on APTEX-coated slides. Staining from sense probes was negligible.

Figure 24 **Variation in *in situ* hybridization results with different batches of sense (B, D, and F) and antisense (A, C, and E) rTGF-ß1/pGEM 3Z probes on serial sections of HSc from PT#8.** One batch of probes (A and B) produced strong and specific staining. The same quantity of a different batch of probes (C and D) resulted in no staining whatsoever. The second batch of probes was used with lower stringency post-hybridization washes (E and F) to allow signal to return. Pictures were taken at 40x objective power.

Figure 24

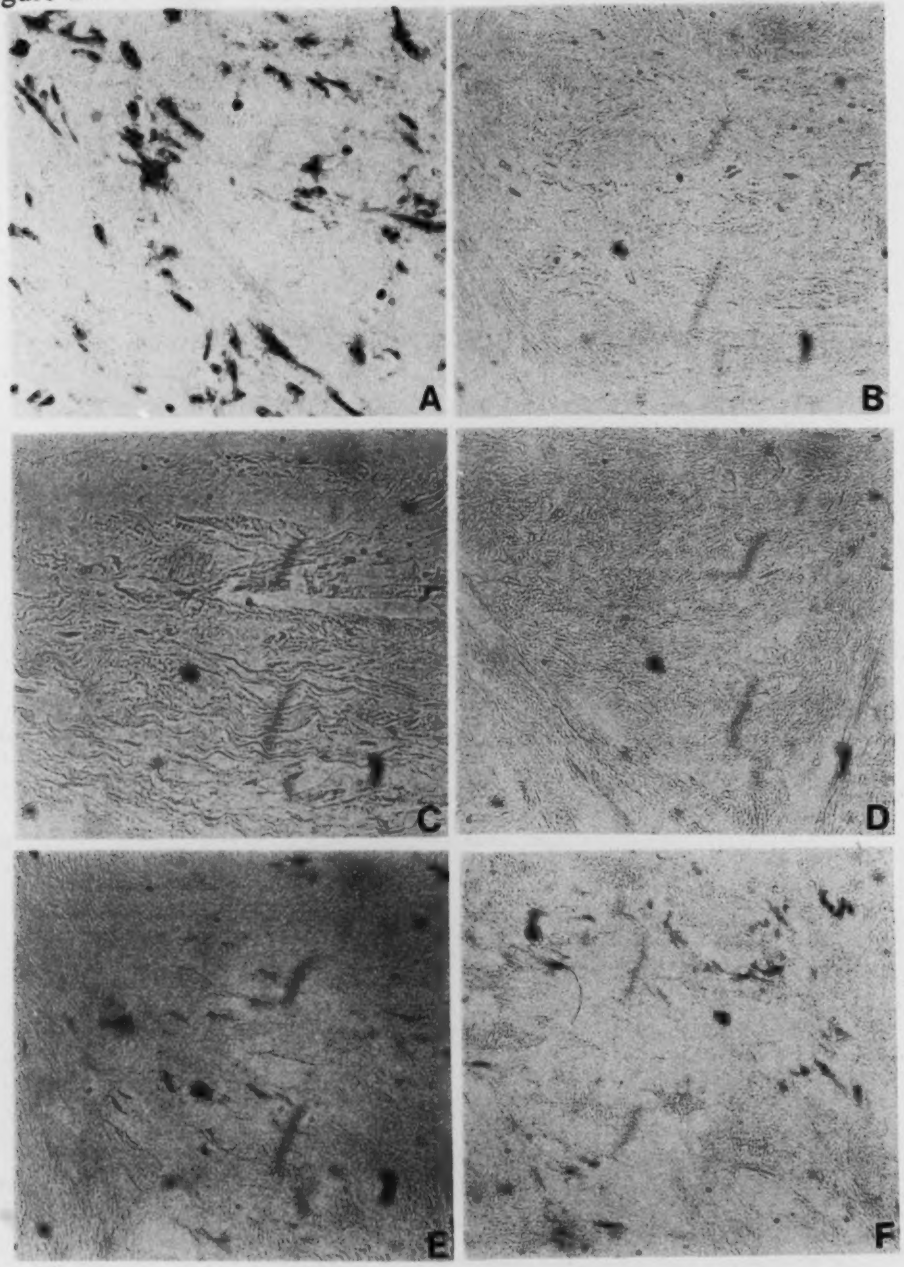

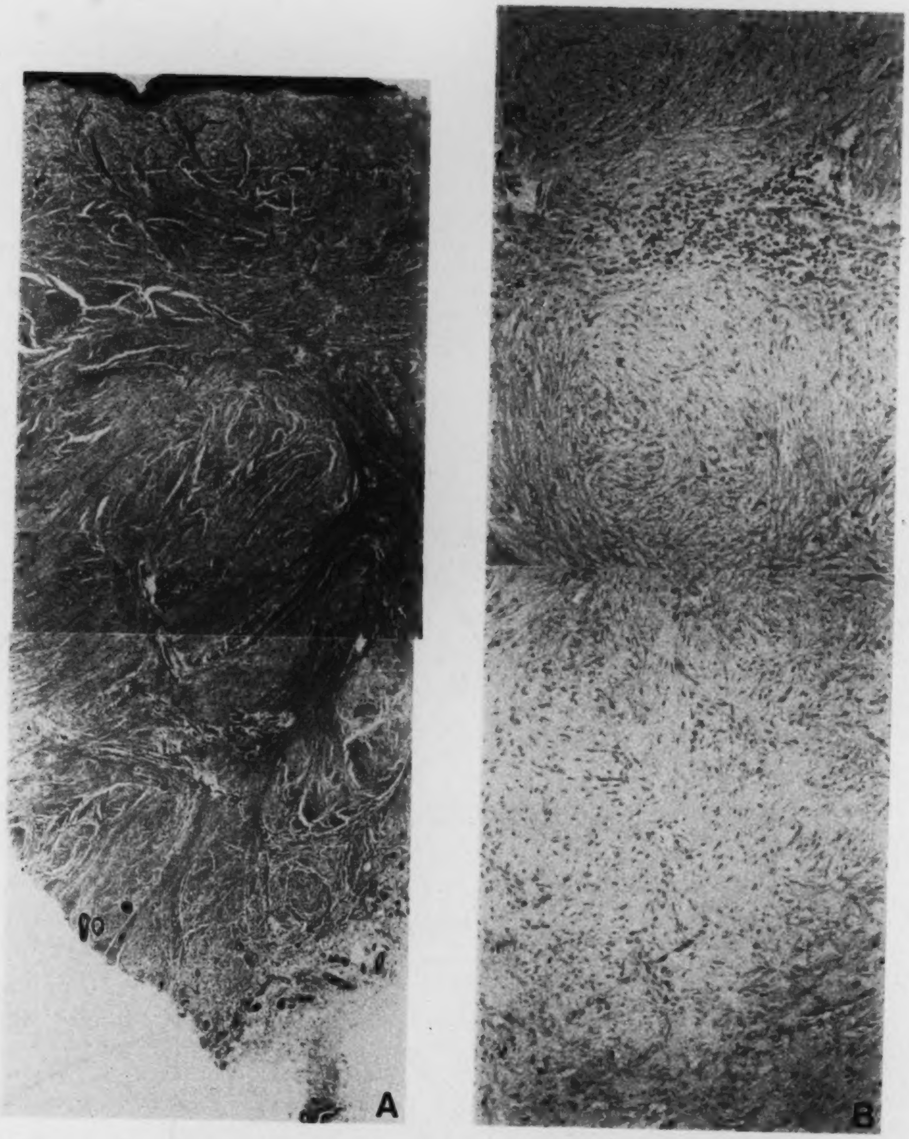

Figure 25 **Sections of paraffin-embedded HSc from PT#8 stained with hematoxylin and eosin (A) or hematoxylin alone (B).** Pictures were taken at 2x objective power (A) and at 10x objective power (B)

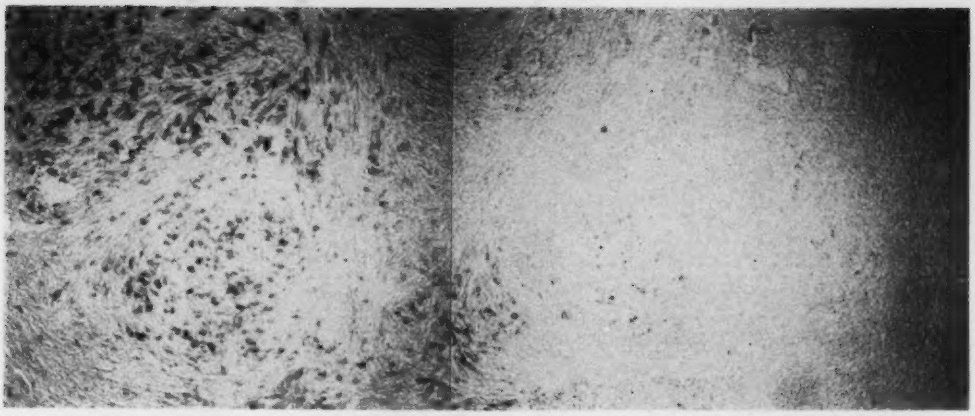

Figure 26 **In situ hybridization using antisense rTGF-ß1/pGEM 3Z probe on a section of paraffin-embedded HSc from PT#15.** 10x objective power.

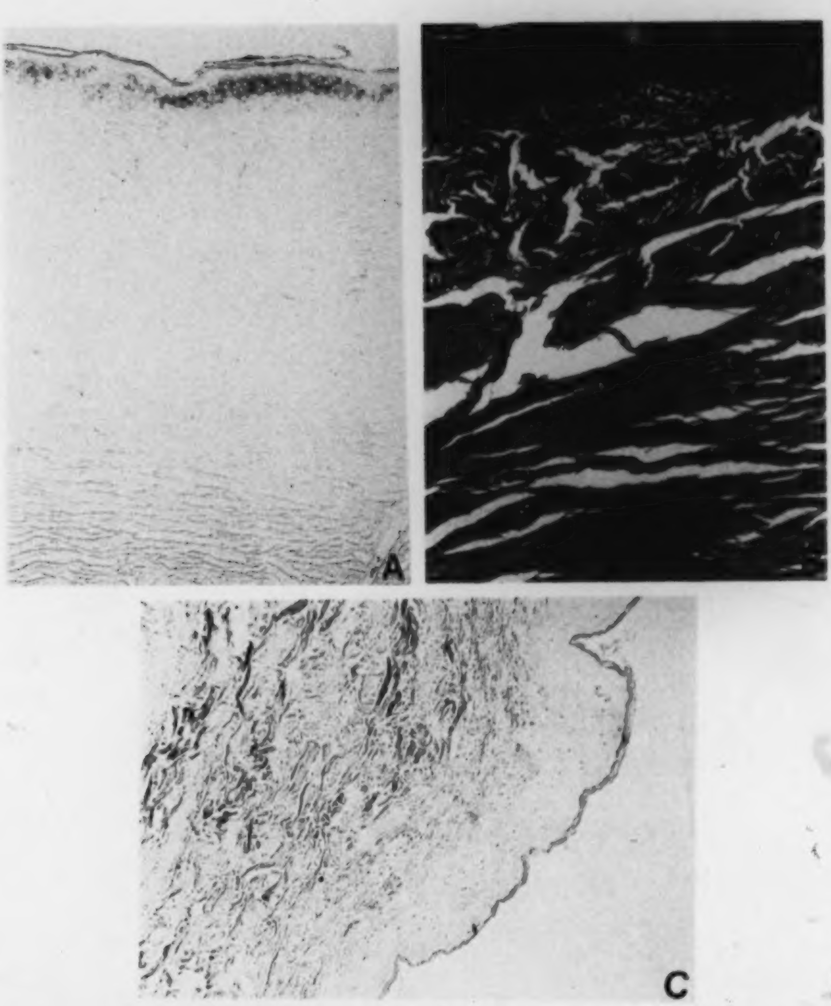

Figure 27 **In situ hybridization for TGF-ß1 in mature scar.** A section of paraffin-embedded MSc (PT#26) was probed with antisense rTGF-ß1/pGEM 3Z (A) and stained with hematoxylin and eosin (B). A normal skin sample (C) from the same experiment as the MSc shown here and probed with antisense rTGF-ß1/pGEM 3Z is also presented. Pictures were taken at 10x objective power.

Figure 28 **In situ hybridization using antisense rTGF-ß1/pGEM 3Z probe on sections of paraffin-embedded HSc and NSk samples received from PT#7 during the course of treatment with IFN-α2b.** H1 was biopsied at 6 months post-burn just before the start of IFN-α2b treatment; H2 was biopsied at 8 months post-burn or 2 months of treatment; H3 was biopsied at 10 months post-burn or 4 months of treatment; H4 was biopsied at 14 months post-burn or 8 months of treatment. The first NSk sample (N1) was obtained at the same time as H1; the second (N2) was obtained at the same time as H4. Pictures were taken at 2x objective power.

Figure 28

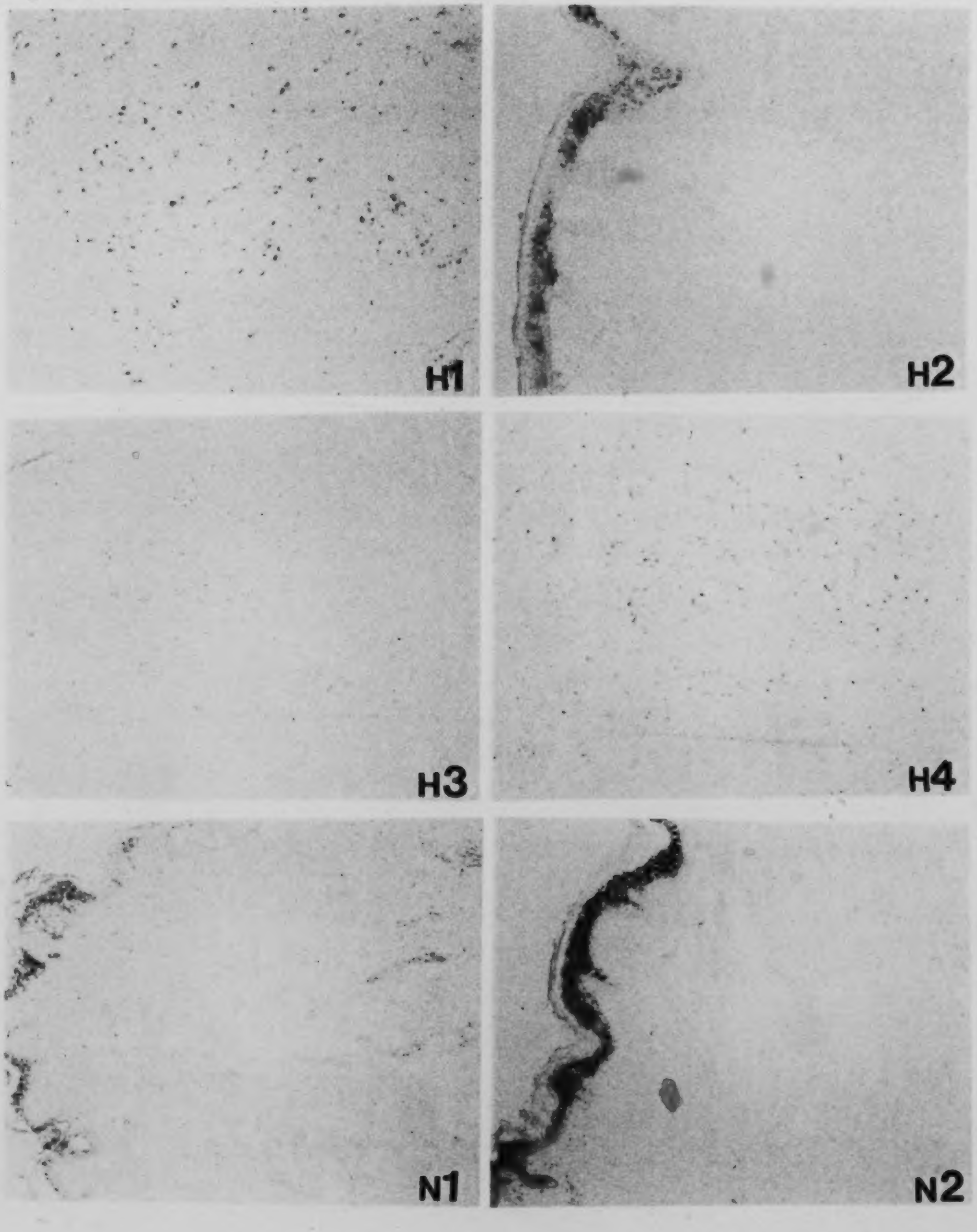

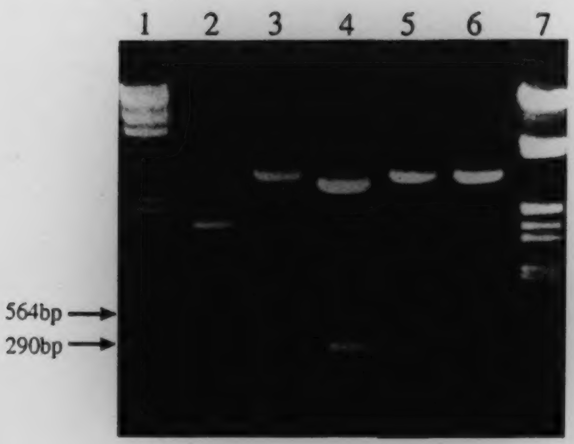

Figure 29 **Gel electrophoresis of rTGF-ß1/pT7T3.** rTGF-ß1/pT7T3 undigested (lane 2; 287ng) and digested with *Hind* III (lane 3; 290ng), *Hind* III and *Eco* R I (lane 4; 500ng), *Hind* III (lane 5, 290ng), and *Eco* R I (lane 6, 290ng). Fragment sizes were compared with the size markers λ/*Hind* III (lane 1) and λ/*Hind* III and *Eco* R I (lane 7).

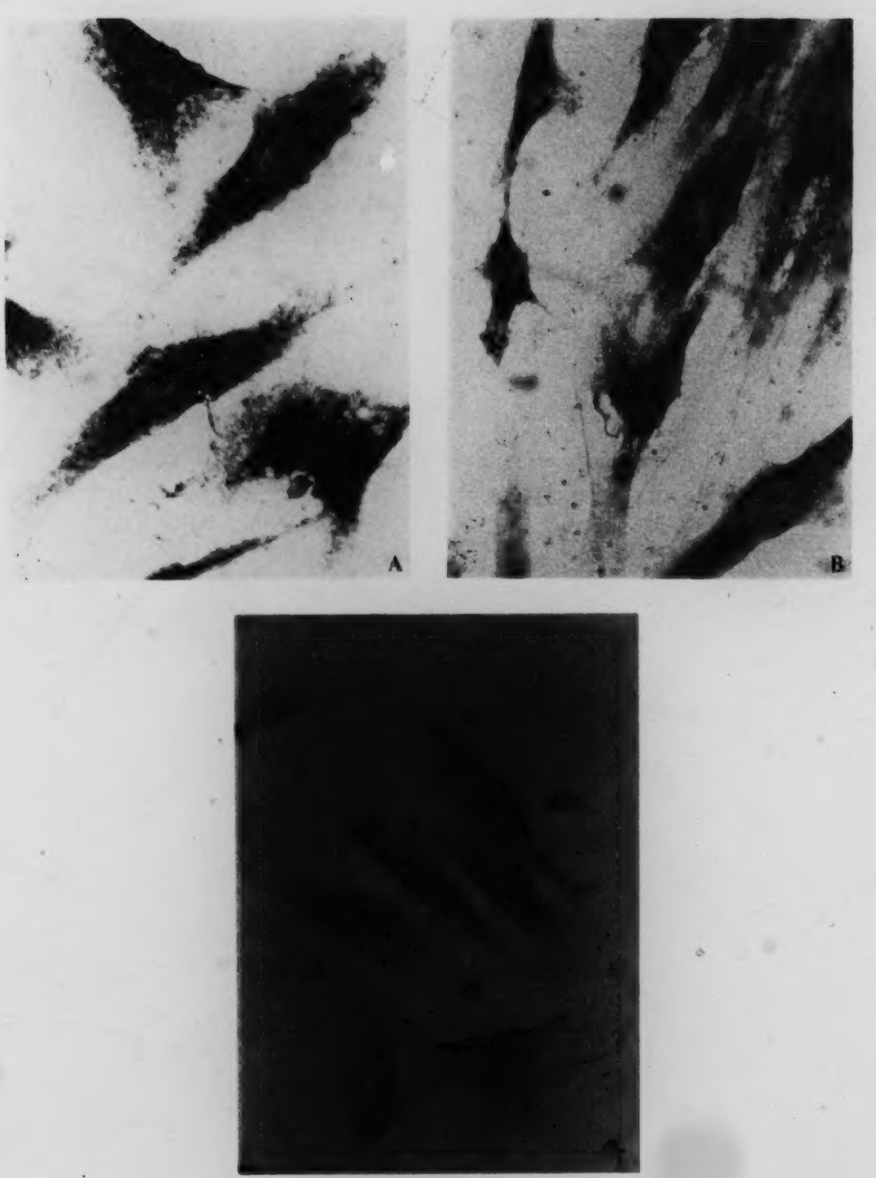

Figure 30 **In situ hybridization with antisense (A and B) and sense (C) rTGF-β1/pT7T3 probes.** Human dermal fibroblasts explanted from HSc (H16; A and C) and NSk (N16; B) and cultured on APTEX-coated slides for 10 - 12 hours served as target. Pictures were taken at 40x objective.

Figure 31 **In situ hybridization with antisense (A and B) and sense (C and D) rTGF-ß1/pT7T3 probes.** Human dermal fibroblasts explanted from HSc (H15; A and C) and NSk (N15; B and D) and cultured on APTEX-coated slides for 10 - 12 hours served as target. Pictures were taken at 40x objective power.

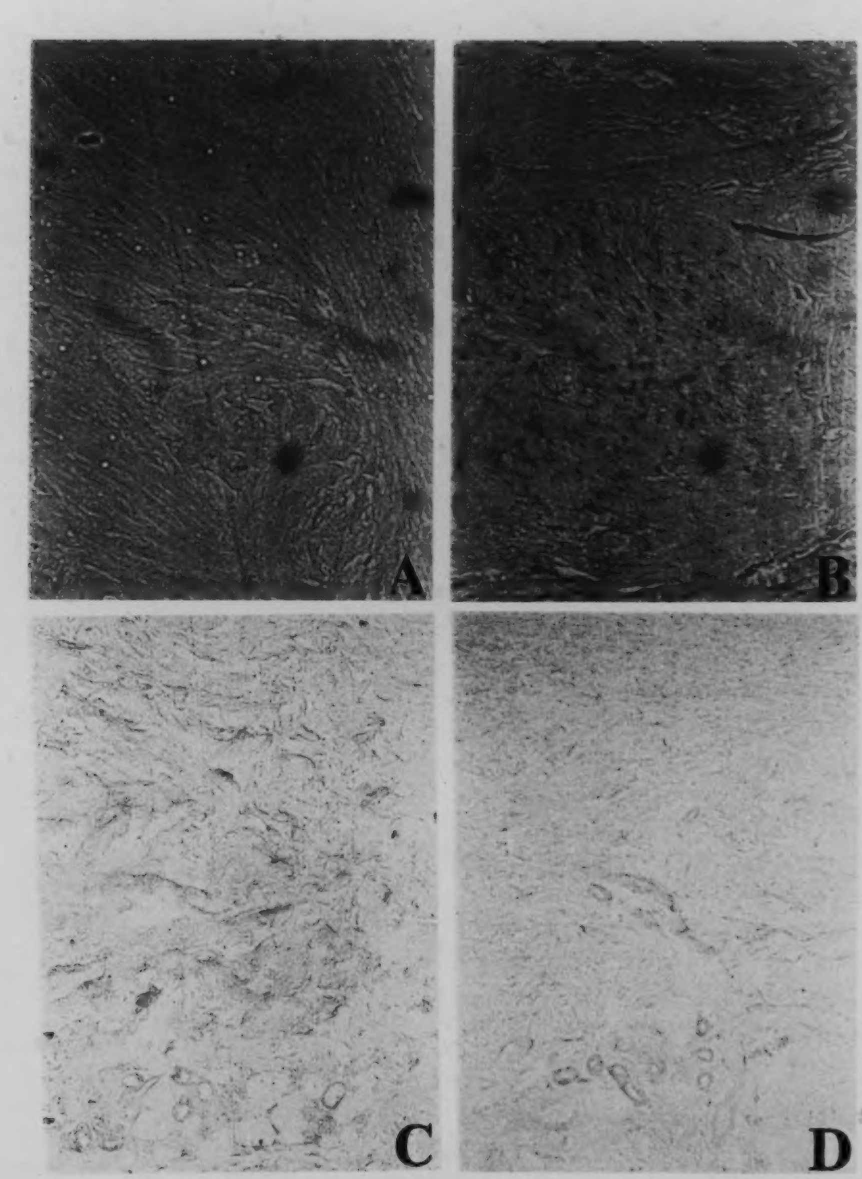

Figure 32 **In situ hybridization with antisense (A and C) and sense (B and D) rTGF-ß1/pT7T3 probes on serial sections of paraffin-embedded HSc from PT#8 (A and B) and NSk (C and D).** Pictures were taken at 10x objective power.

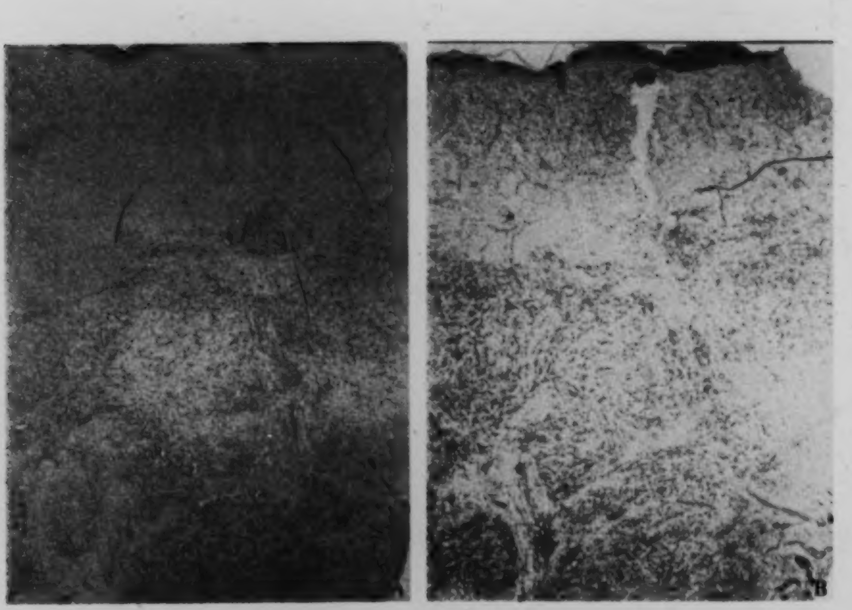

Figure 33 **Regional expression of staining obtained with both the antisense (A) and sense (B) rTGF-ß1/pT7T3 probes by *in situ* hybridization on serial sections of paraffin-embedded HSc from PT#8.** Pictures were taken at 2x objective power.

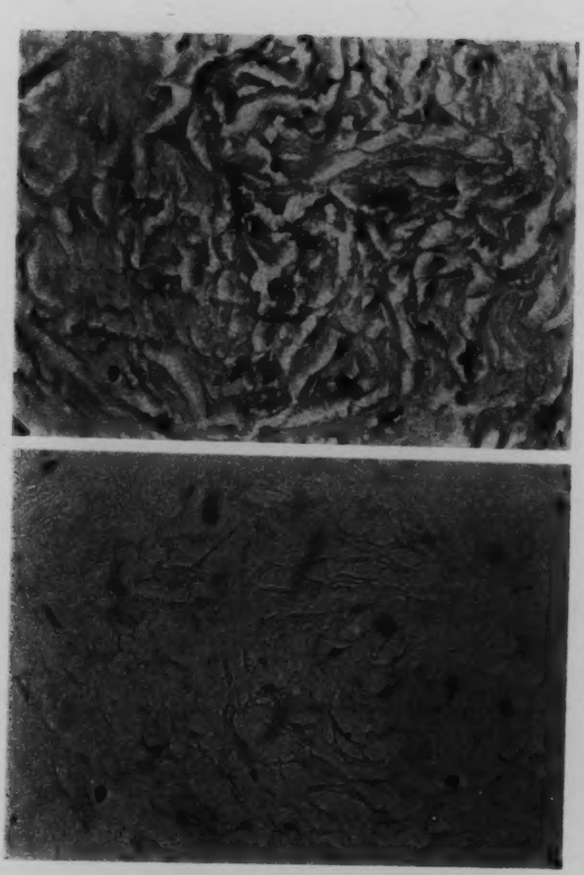

Figure 34 **In situ hybridization with the sense rTGF-ß1/pT7T3 probe on sections of different samples of paraffin-embedded MSc.** Results from the antisense probe were negligible. A:PT#27; B:PT#26. Pictures were taken at 40x objective power.

Figure 35 **In situ hybridization using antisense rTGF-ß1/pT7T3 on sections of paraffin-embedded HSc samples received from PT#4 during the course of treatment with IFN-α2b.** H1 was biopsied at 4 months post-burn just before the start of IFN-α2b treatment; H2 was biopsied at 6 months post-burn or 2 months of treatment; H3 was biopsied at 8 months post-burn or 4 months of treatment; H4 was biopsied at 10 months post-burn or 6 months of treatment; H5 (not shown) was biopsied at 12 months post-burn or 8 months of treatment. Pictures were taken at 2x objective power.

Figure 35

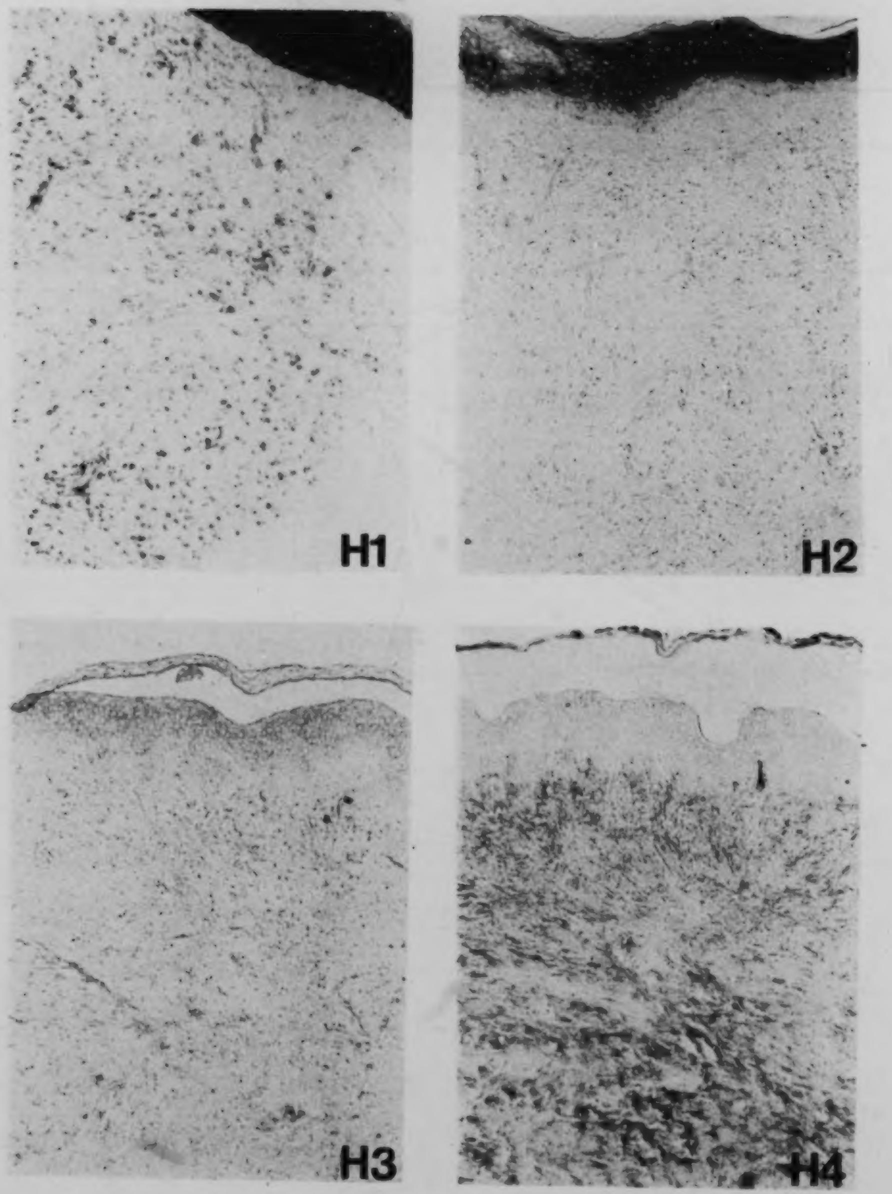

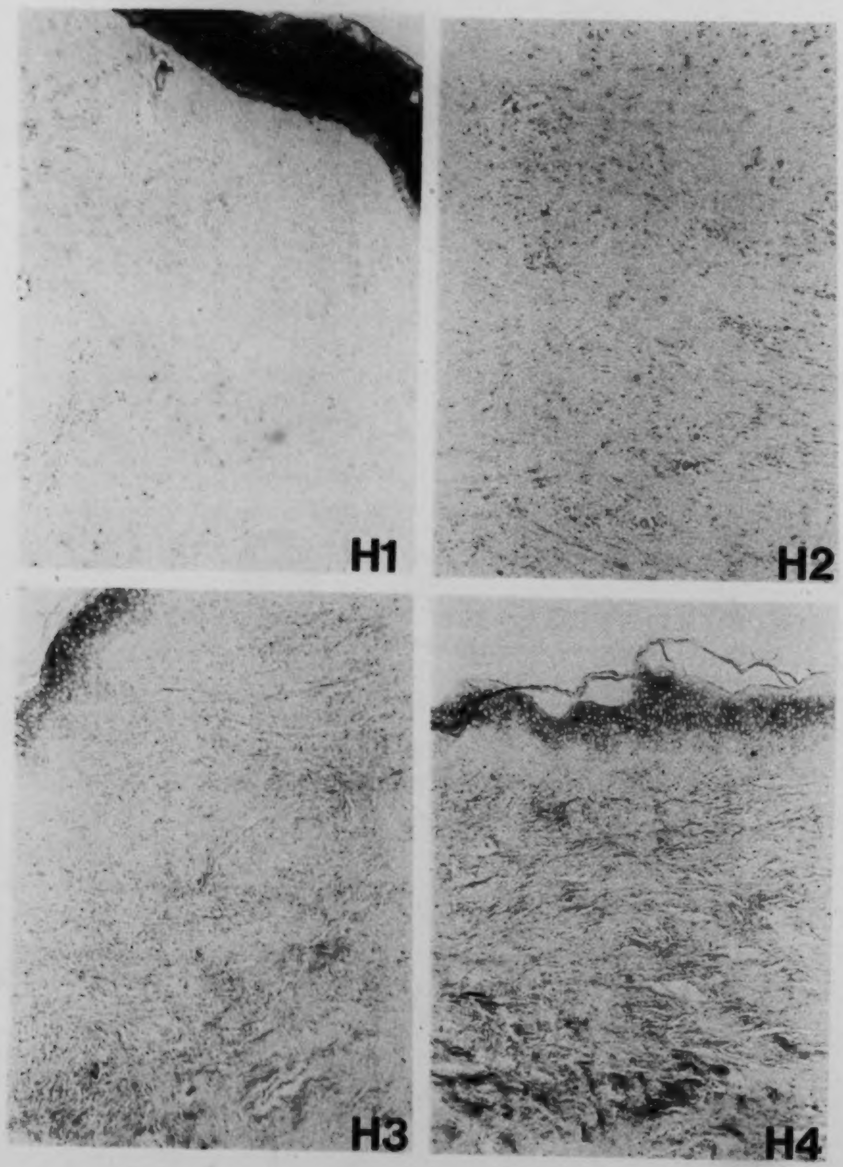

Figure 36 **In situ hybridization using sense rTGF-β1/pT7T3 on sections of paraffin-embedded HSc samples received from PT#4 during the course of treatment with IFN-α2b.** Sections in this figure are serial sections of those presented in Figure 35. Pictures were taken at 2x objective power.

Figure 37A **Gel electrophoresis of pT420.** pT420 digested with *Bam* H I and *Eco* R I (lane 3; 500ng) which liberated the TGF-ß cDNA insert (420bp) from the plasmid was analyzed by gel electrophoresis in a 1% agarose gel. Other lanes include the size marker λ/*Hind* III and *Eco* R I (lane 1; 800ng) and pBluescript digested with *Bam* H I and *Eco* R I (lane 2; 500ng).

Figure 37B **Gel electrophoresis of pT420.** pT420 linearized with *Bam* H I (lane 3; 300ng) or *Eco* R I (lane 4; 300ng) was analyzed using gel electrophoresis in a 1% agarose gel. Other lanes include the size markers λ/*Hind* III (lane 1; 800ng) and λ/*Hind* III and *Eco* R I (lane 2; 800ng).

Figure 37C **Dot blot quantitation of digoxigenin-labeled cRNA probes transcribed off pT420 as described for 1B.**

Figure 37D **Sequencing of TGF-ß1(420)/pT7T3 using the Sanger method and a primer with the T3 promoter sequence (Biochemistry Sequencing Laboratory, University of Alberta)**

Figure 37

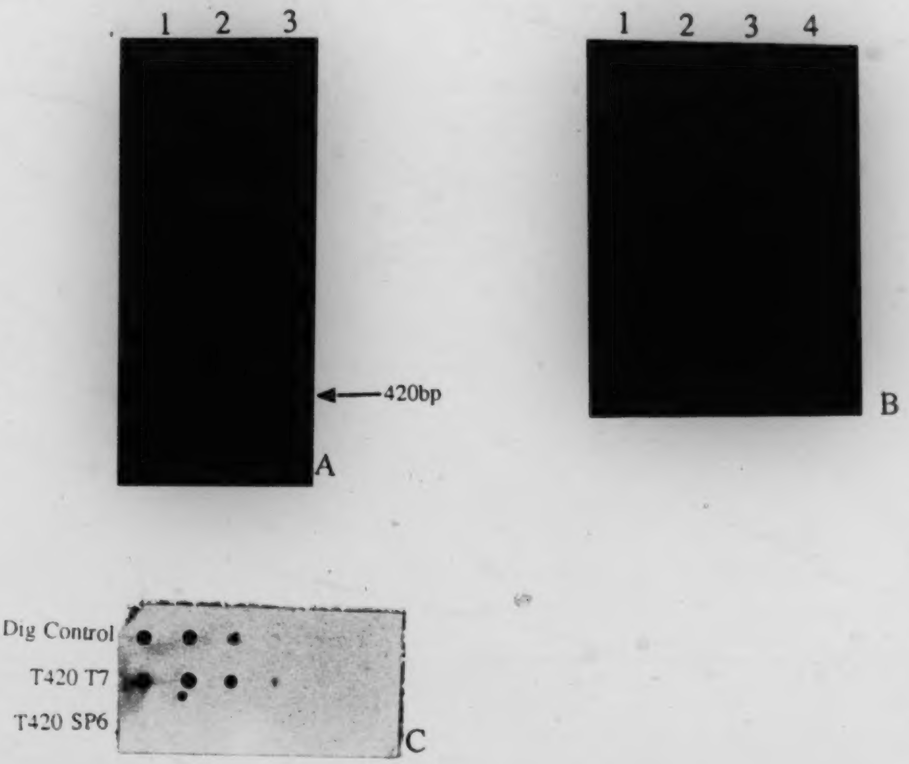

```
Applied                 Sample 12                       Points 804 to 8032   Base 1  804
Biosystems              DyeTerminator{AnyPrimer}        336 MATRIX FILE
Model 373A              Lane 12                         SCOTT-1
Version 1.2.0           Signal: G:169 A:135 T:108 C:70  T420/T3
  1   GNAGAGACNA  GCTTNATATC  GAATTCGGGT  TTTTTTTTTT  TTTTTTTTTT
 51   TTTTTTTTTT  TTTTTTTTTT  TTTTTTTCCC  NCNCNCCATC  TTNAATGGGG
101   CCCCAGTTGG  GCTTGGGGCA  CGGNTTTCCT  NAAATACACC  CCCCATGGGC
151   AAGGCACCGG  GGGCGGGGCG  GGGTGGGGCC  GGGCCTCCCG  GGGCGGGGCG
201   GGGCGGGGCG  GAACCN
```

D

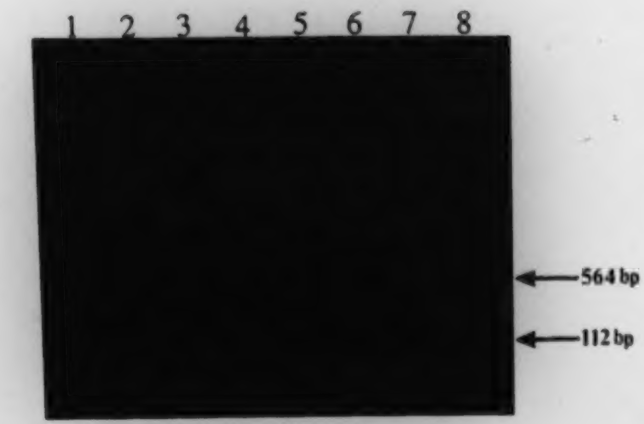

Figure 38 **Gel electrophoresis of pT112.** Uncut pT112(lane 3; 500ng) and pT112 digested with the restriction enzymes*Pst* I (lane 4; 694ng), *Eco* R I (lane 5; 637ng), and *Pst* I and *Eco* R I (lane 6; 500ng) which liberated the 112bp TGF-ß1 cDNA insert from the vector. Fragment sizes were compared with the size marker λ/*Hind* III and *Eco* R I(lane 1 and 8; 800ng). Lanes 2 and 7 are blank.

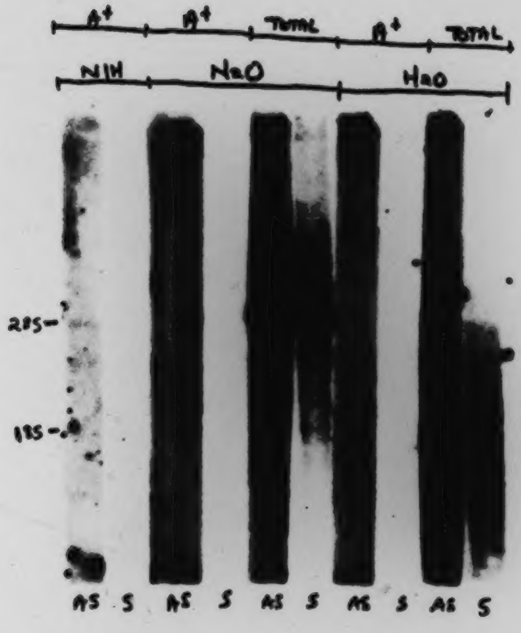

Figure 39 **Northern blot hybridization of total (20ug/lane) and poly (A)$^+$-enriched RNA (35ug [before enrichment]/lane) from HSc (H20) and NSk (N20) using ^{32}P-labeled T112 sense (S) and antisense (AS) probes.** Poly (A)$^+$ RNA (20.5ug [before enrichment]/lane) from confluent NIH 3T3 cells was also included in this experiment. Ethidium bromide staining of the RNA (except the poly (A)$^+$ RNA which is not detected by this method) in the gel before blotting displayed equal amounts of RNA between samples (data not shown).

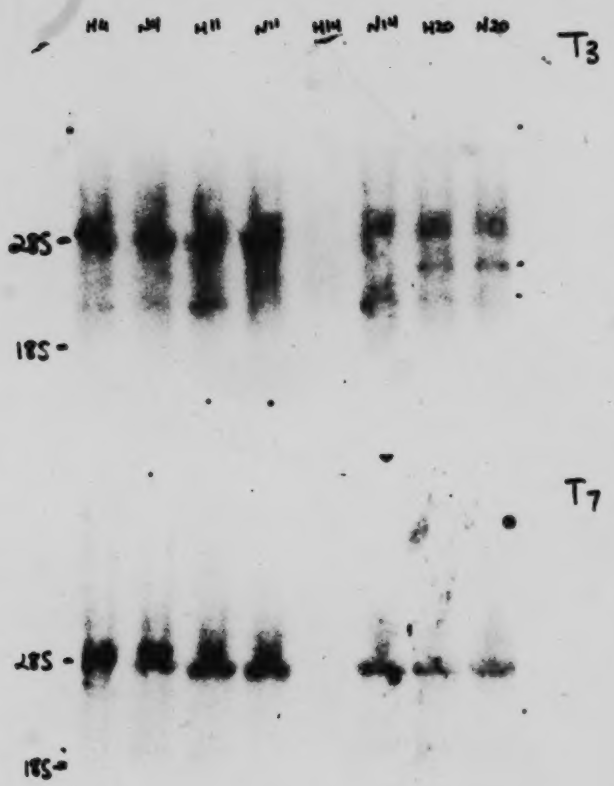

Figure 40 Analysis of total RNA (25µg/lane except for 6.5µg of H14) from HSc (H4, H11, and H20) and NSk (N4, N11, and N20) by Northern blot hybridization using gel purified ^{32}P-labeled sense (S; T3) or antisense (AS; T7) T112 probes.

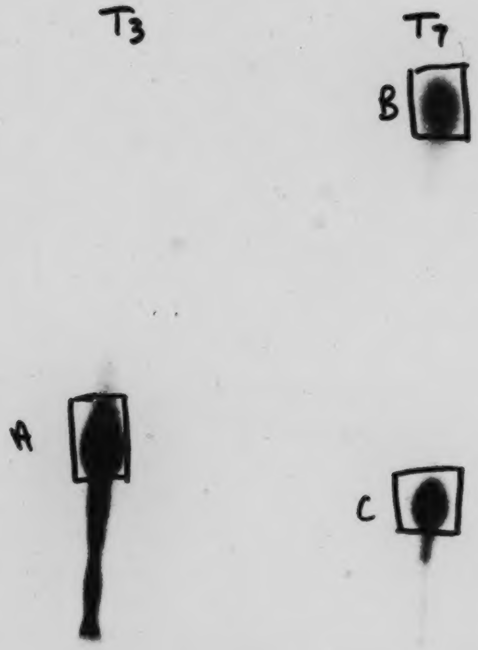

Figure 41 **Polyacrylamide gel electrophoresis of ^{32}P-labeled sense (T3) and antisense (T7) T112 probes.** Boxes indicate the bands that were cut out off the gel and eluted for purification. In the case of T112/T7, a very large labeled species indicated by "B" consistently appeared when T112 was labeled; this was also the case when labeling was carried out using digoxigenin (Figure 6d lane 10 and 6e lane 9). This band may correspond to aggregated probe.

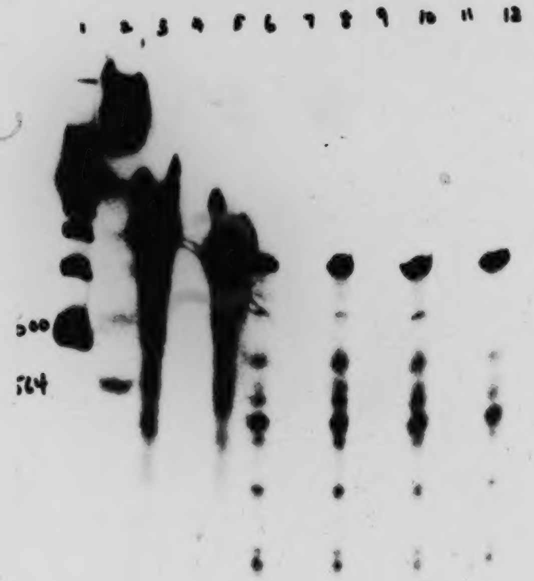

Figure 42 **Ribonuclease protection assay of total RNA from H20 and N20 with ^{32}P-labeled sense and antisense T112 probes.** Between 25ug and 35ug of each of H20 and N20 as well as *E. coli* tRNA were hybridized to either sense (T3) or antisense (T7) probes after which RNase A and T1 was used to digest all single stranded RNA species. Protected probe fragments were then detected on a 8% acrylamide/7M urea gel. Lanes 7, 9, and 11 contain protected T3 or sense probe whereas lanes 8, 10, and 12 contain protected T7 or antisense probe. RNA in lanes 7 and 8 were protected by H20 total RNA; RNA in lanes 9 and 10 were protected by N20 total RNA; RNA in lanes 11 and 12 were protected by *E. coli* tRNA. Sense and antisense probes alone were run in lanes 3 and 5, respectively. Sense and antisense probes digested with RNase A/T1 were run in lanes 4 and 6, respectively. Lanes 1 and 2 contained the γ-dATP-end labeled markers 100bp marker and λ/*Hind* III, respectively.

Table 1. **Source of Burn Tissues**

Pt. #	Age at burn (yr)	Sex	Biopsy site	TBSA (%)[a]	Months post-burn
1	67	M	Calf	5	2
2[c]	41	M	Calf	40	3
3[c]	41	M	Foot	3	3
4[c]	36	M	Shoulder	65	4
5[b,c]	4	M	Neck	55	5
6[c]	49	M	Forearm	25	5.5
7	25	M	Left Arm	45	6
8[c]	46	F	Hand	1	7
9[c]	29	M	Chest	85	8
10[c]	36	M	Chin	35	11
11	35	M	Hip	18	12
12[b,c]	4	M	Chest	55	12
13[c]	27	M	Lip	85	13.75
14	9	M	Leg	11	14
15[c]	6	M	Neck	35	14
16	2	M	Left Arm	30	15
17	46	F	Right Arm	20	16
18	49	M	Back	32	17
19[c]	1	M	Neck	15	17
20	49	M	Left Thigh	30	17
21[c]	32	M	Thigh	60	21
22[c]	2	M	Leg	9	22
23	4	F	Face	15	27
24[c]	9	M	Leg	11	27
25	13	M	Neck	35	36
26[c]	28	F	Chin	45	36
27[c]	30	M	Hand	7	45
28[c]	30	F	Neck	50	51
29[c]	5	F	Neck	20	63
30[c]	4	F	Neck	20	216

[a] Percentage of total body surface area affected

[b] Patients 5 and 12 are the same individual biopsied at different times after injury

[c] Patients used in decorin study

Table 2. **Average Number of Cells Expressing Decorin mRNA in Early, Intermediate, and Late Hypertrophic Scars and in Normal Skin**

Months Post-Burn	Papillary Dermis	Middle Dermis	Reticular Dermis	Whole Dermis
Early[*] (0-11 months)	45.25[a] ±18.4	40.63 ±15.1	27.13 ±9.00	113.1 ±39.0
Intermediate[*,#] (12-35 months)	156.1 ±34.2	166.7 ±37.2	212.6 ±51.5	535.6 ±103
Late[#] (≥36 mnths)	14.40 ±4.82	16.40 ±7.65	16.20 ±7.21	47.00 ±18.4
Normal Skin	16.00 ±6.98	20.83 ±11.24	16.83 ±7.70	53.67 ±25.4

[a] Values are expressed as mean # positive cells/10 microscope fields (40x) ± S.E.M. (n=8 for early, 7 for intermediate, 5 for late, and 6 for normal)

[*] Differences between early and intermediate in all regions are significant by one-way ANOVA ($p<0.01$).

[#] Differences between intermediate and late in all regions are significant by one-way ANOVA ($p<0.01$).

Table 3. **Average Number of Connective Tissue Cells in Early, Intermediate, and Late Hypertrophic Scars and in Normal Skin**

Months Post-Burn	Papillary Dermis	Middle Dermis	Reticular Dermis	Whole Dermis
Early (0-11 months)	792.8* ±84.1	696.1 ±62.0	700.9 ±90.6	2190 ±223
Intermediate (12-35 months)	695.2 ±66.0	760.6 ±73.4	631.7 ±73.0	2147 ±209
Late (≥36 mnths)	409.6 ±56.7	359.0 ±47.0	391.0 ±76.7	1160 ±165
Normal Skin	290.2 ±83.3	246.0 ±89.6	277.8 ±99.2	914.0 ±272.8

*Values are expressed as mean number of connective tissue cells/10 microscope fields (40x) ± S.E.M. (n=8 for early, 7 for intermediate, 5 for late, and 6 for normal)

Table 4. **Average Percentage of Cells Expressing Decorin mRNA in Early, Intermediate, and Late Hypertrophic Scars and in Normal Skin**

Months Post-Burn	**Papillary Dermis**	**Middle Dermis**	**Reticular Dermis**	**Whole Dermis**
Early[*] **(0-11 months)**	5.234[a] ±1.93	6.024 ±2.37	3.425 ±0.855	4.818 ±1.60
Intermediate[*,#] **(12-35 months)**	20.62 ±3.44	22.48 ±4.53	32.60 ±5.28	24.77 ±3.85
Late[#] **(≥36 mnths)**	4.386 ±1.62	4.786 ±2.261	5.071 ±2.41	4.725 ±1.942
Normal Skin	3.203 ±0.968	5.547 ±1.50	5.405 ±1.09	4.957 ±0.833

[a] Values are expressed as the mean of the percentage of positive cells/10 microscope fields (40x) ± S.E.M. (n=8 for early, 7 for intermediate, 5 for late, and 6 for normal)

[*] Differences between early and intermediate are significant by one-way ANOVA ($p<0.01$) for middle dermis and are more significant ($p<0.001$) for papillary and reticular dermis.

[#] Differences between intermediate and late are significant by one-way ANOVA ($p<0.01$) for papillary and middle dermis and are more significant ($p<0.001$) for reticular dermis.

CHAPTER 4. DISCUSSION

I. Establishing an *in situ* hybridization protocol to study scar and normal skin tissue

The establishment of an *in situ* hybridization protocol for the analysis of hypertrophic scar, mature scar, and normal skin samples was a challenging and technically demanding experience. There are potentially many variables involved with this method which need to be manipulated and optimized according to the environment in which the *in situ* hybridization is being conducted. This environment has two major components, the characteristics of which affect the number and type of variables used in the procedure. These components are the target sample and the probe which is used to search for the target.

The critical target used in this study was paraffin-embedded human skin tissue. The test sample was comprised of hypertrophic and mature scars from different patients as well as normal skin. The processing involved in preparing such tissue samples is rigorous and involves replacing the water in the tissue with paraffin wax. Therefore, the tissue is put through various aqueous and organic solvents; as well molten wax whose melting point is about 53°C is perfused through the tissue under vacuum. Thereafter, the tissue is handled to embed it in the right orientation in a tissue block. This is followed by sectioning of the tissue block into 4-5um thin sections which are laid out on a hot water bath and then mounted onto glass slides; sections are then heated at about 53°C overnight to properly adhere them to the slides. In situ hybridization on these sections then requires them to be exposed to yet another series of organic and aqueous solutions before the hybridization mix containing the probe. Such an involved procedure allows many opportunities for degradation of target RNA species by RNases. Without even considering the limitation placed on the penetration of the probes imposed by fixation and processing of the tissue, the rigorous procedure identified above supports various reports of an approximately 25% reduction in the amount of target detected in paraffin-embedded tissue compared to frozen tissue (Dijkman, et al., 1996; Lucassen, et al., 1996; Wilcox, 1993). To protect against such degradation, many steps had to be incorporated into the preparation for and the execution of the *in situ* hybridizations including the treatment of solutions, glassware, and plasticware.

Another fundamental factor that needs consideration is the source of our target tissue. The many layers and components of skin make it a difficult tissue to probe. The epidermis is notorious for binding antibodies and nucleic acid probes nonspecifically. As well, the dermis of normal skin is made up mostly of extracellular matrix comprising collagen, proteoglycans, and other proteins with very few cells present. The abundance of these proteins, and in turn, many charged surfaces, allows probes many nonspecific sites to bind to and sometimes very strongly.

The high concentration of extracellular matrix in hypertrophic scar also presents a barrier between the probes and their targets in the cytoplasm of cells. Because the cells are surrounded by matrix, the cRNA probes, which are highly charged and which assume considerable secondary structure, can easily bind nonspecifically to components of the matrix thereby reducing the specific cytoplasmic signal and increasing the background. For this purpose, proteinase K and hyaluronidase are used to digest proteins and other matrix components and to permeabilize cell membranes to allow better accessibility of the probes to their cytoplasmic targets. The use of such enzymes requires optimization of the conditions to maximize specific signal but also to minimize any damage to the tissue and to prevent tissue loss.

Background staining is a major problem encountered with *in situ* hybridization and besides proteolytic enzymes, many other approaches are utilized to prevent binding of probe to nonspecific sites within the dermis of skin tissue. Such methods include acetylation of free amino groups. In addition to prevention strategies, procedures are also employed to remove nonspecifically bound probes from tissue after hybridization; for example, RNase A and T1 can digest single stranded RNA but leave double stranded RNA hybrids intact. All of these different steps require optimization to maximize specific signal. Conditions which are too weak permit excessive background but very harsh conditions prevent development of specific signal.

The preparation of probes as well as the optimization of conditions required considerable work. The most common method of generating cRNA probes requires the cloning of a cDNA of interest into a plasmid vector which harbors, at the ends of its PCS, RNA promoter regions for the *in vitro* transcription of cRNA probes off the template. Clones are then sequenced to identify the sense and antisense strands. After linearizing the template, it must be purified to an acceptable level before transcription.

Before the transcribed probe can be hybridized to its target, many variables need to be adjusted which affect the melting temperature or T_m of the hybrid of the probe with its desired target. Such variables include the salt and formamide concentrations of the hybridization mixture as well as the proportion of GC in the probe sequence. After the T_m is calculated, the stringency of the hybridization reaction and the washes that follow can be established. All of these variables and conditions need to be tested before an optimized protocol can be established. During the entire procedure, steps must be employed to protect the cRNA probes from degradation by RNases.

This list of tasks for establishing *in situ* hybridization in human skin using cRNA probes is far from complete. But, nonetheless, it provides a good overview of how involved and time-consuming the set-up of such a procedure was before it could be used to gather the data in this study. Additionally, expectations can be misleading when establishing this protocol for regular use. In other words, the antisense probe is expected to always provide the signal whereas the sense probe should not bind any RNA sequence, considering it has an identical sequence to the mRNA under study. This means any staining with the sense probe is automatically considered "background" and should be washed out more rigorously. This had an effect on when to finally decide to pursue the identity of what the TGF-ß1 sense probes were hybridizing to throughout my study and made it a very long process.

The results obtained with *in situ* hybridizations using non-radioactive probes, such as those labeled with digoxigenin, are essentially qualitative. Deriving numerical data manually was tedious and time-consuming. Another option which was available was to automate the quantitation by digitizing images of probed skin sections and assigning the color value which the computer should count. This option was not chosen since the variable background levels in the tissues made it very difficult to optimize the program to assign clear values to the specific staining only.

In addition to all of the manipulations stated above which are needed to make such a procedure work, other methods were also employed to establish the protocol. For example, different molecular methods were used to clone different probe templates. As well, northern analysis, dot blot hybridization and pseudonorthern analysis were all used to verify the functioning and integrity of labeled probes.

In summation, the above mentioned rigorous procedures were the reason for the extra time consumed in completing this study. However, the experience, knowledge, and technical skill gained are invaluable.

II. The Time Course Expression of Decorin mRNA During Hypertrophic Scar

Previous immunohistochemical (Scott, PG., 1995) and biochemical (Scott, PG., 1996) analyses of hypertrophic scar, mature scar, and normal skin have established lower levels of decorin protein in the former as compared to normal skin and mature scar. Except for the deep dermis and a narrow zone below the epidermis, decorin is virtually absent in HSc but reappears in the scar during maturation. In contrast, decorin is found abundantly in normal skin. It was not known at the commencement of this study whether the altered expression of decorin in HSc is due to regulatory mechanisms at the transcriptional, translational, or post-translational level, ie. whether there is deficient production, incomplete production, or enhanced degradation of the PG.

In this study, *in situ* hybridization revealed an interesting time course of expression of decorin mRNA through the development and resolution of post-burn hypertrophic scar. In this time course of expression, decorin mRNA levels changed significantly depending on time after injury. Fibroblasts in early hypertrophic scar were deficient in the production of decorin as the scar tissue which was collected before one year post-burn had very few cells which expressed decorin mRNA even though many fibroblasts had infiltrated the wound site. The number of positive cells rose dramatically in samples of scar collected between 12 and 36 months post-burn but dropped significantly in samples obtained after 36 months. Therefore, decorin mRNA expression follows a characteristic time course in the wound healing process which leads to hypertrophic scar and its subsequent resolution.

This observation became more significant when the total number of cells was counted in the same samples and used to calculate the percentage of positive cells. The average number of total cells in the early and intermediate samples did not change but seemed to decrease somewhat for the late samples. Nonetheless, the percentage of positive cells seemed to follow the same time course of expression of decorin mRNA as that described above. Therefore, the phenomenon was not merely a consequence of the changing number of cells in HSc. The decrease in the number of cells, however, in the late samples is an intriguing observation which needs to be followed up on with further studies. The mechanism responsible for this decrease should be investigated since it may be important in the maturation process of the scars.

Early in the course of HSc, up to 11 months post-burn, decorin mRNA expression, on average, appeared suppressed in scar samples obtained from 8 patients. Immunohistochemical analysis revealed very little decorin protein. In contrast, two burn patients whose afflicted sites did not turn hypertrophic appeared to express above average levels of decorin mRNA and protein. Although one of these patient's biopsies was taken at approximately 12 months after the burn date, the percentage of cells expressing decorin mRNA was well above the average for the intermediate time range. As well, compared to another patient's biopsy also taken at 12 months, this patient expressed twice as much decorin mRNA. The suppression of decorin expression appears even more significant when compared to data obtained by Yeo and co-workers (1991) who found abundant levels of decorin early after wounding from day 2 to day 49 in normal healing guinea pig wounds. Also important to consider about our early scars is that their collagen arrangement was not of the fiber and fiber-bundle morphology of normal skin but instead fibrils appeared thinner, more loosely spaced and arranged in whorls and nodules.

The association between collagen and proteoglycans has been examined in fibrous connective tissues of many vertebrate and invertebrate species (Scott, JE., et al., 1981; Scott, JE., 1988; Van Kuppevelt et al., 1987; Trotter and Koob, 1989). This evolutionarily conserved phenomenon demonstrates the importance of PGs in the collagen network. Decorin, in particular, has been demonstrated to be of potential importance in maintaining the proper morphology of collagen fibers. Electron microscopy studies have shown the presence of dermatan sulphate chains in regular orthogonal arrays on collagen fibrils (Scott and Haigh, 1985); moreover, it has been proposed from such studies that antiparallel dermatan sulphate duplexes may form between pairs of protein cores on adjacent fibrils to strengthen the interaction between fibrils (Scott, JE., 1993). As well, binding studies have revealed specific binding sites on fibrillar collagens for decorin (Hedbom and Heinegard, 1993). Furthermore, studies which examined fibrillogenesis of collagen, *in vitro*, by measuring the turbidity of soluble collagen upon warming found an inhibition of fibrillogenesis in the presence of decorin (Vogel et al., 1984), although turbidity levels in the presence of this PG did eventually reach the same levels as the controls (Vogel and Trotter, 1987). And recently, a binding site for type I collagen has been mapped to leucine-rich repeats 4-5 of the core protein of decorin (Svensson et al., 1995). The presence of decorin early in the wound healing process, therefore, seems vitally important to establish the proper conditions for collagen fiber regeneration. When bound to the fibrils, decorin may allow for proper spacing and regular interaction of collagen fibrils through protein-protein and GAG-GAG interactions during fiber growth and assembly. The absence of this PG, therefore, early after severe burn injury may result in the assembly of collagen fibrils into the whorls and nodules seen in HSc.

A recent study that provides fundamental support for this hypothesis involved the development of a mouse model in which was harbored a targeted disruption of the decorin gene (Danielson, et al., 1997). The genomic locus containing the decorin gene was targeted with a vector which was partly comprised of the decorin gene with a neomycin resistance cassette interrupting exon 2. Heterozygous mice were mated to homozygosity and mRNA and protein analyses of different organ types including skin from homozygous animals revealed a complete obliteration of decorin production. Using probes for lumican and biglycan, proteoglycans classified in the same small leucine-rich proteoglycan (SLRP) family as decorin, on the same blots used to probe for decorin, no changes were detected. Therefore, neither of these two other SLRPs were upregulated to compensate for the deficient production of decorin.

Detailed analysis of the skin of decorin-deficient mice revealed six major observations. On macroscopic and histological levels, the skin appeared thinner and more fragile as it was more prone to rupture during cervical dislocations. When skin fragility was measured more objectively by measuring the maximal force the tissue could bear using a Comten tensile machine, skin from decorin-deficient animals could withstand only 25% of the force as that of wild-type animals.

An in-depth analysis using electron microscopy revealed a disordered arrangement and abnormal structure of collagen fibrils. For example, packing of collagen fibrils appeared less orderly in the decorin-deficient animals. Essentially, the fibrils appeared more loosely packed than those of the wild-type animals. Also, a great variability in shape and size of the fibrils was observed: whereas fibrils which were from wild-type animals and prepared in cross-section appeared circular, those of the mutant mice were irregular and oblong with a larger range of diameters and sometimes had edges that appeared 'scalloped'. Finally, this disordered arrangement included a mixture of thin and large fibrils sharing the same area whereas the fibrils of wild-type animals have a more uniform size and distribution.

Lastly, mass mapping of dermal fibrils along their axes was measured to determine the changes in mass per unit length of individual fibrils and revealed dramatic changes along the length of the collagen fibrils of decorin-deficient mice whereas those of the wild-type mice were relatively constant. The authors of this study concluded that the abnormal morphology of collagen found in their decorin-deficient mice was due to a reduction in collagen-bound proteoglycans.

The histological observations of collagen structure and arrangement in hypertrophic scar bear close resemblance to those of the decorin-deficient mice mentioned above. Collagen fibrils appear thinner, more loosely arranged, and disorganized than in normal skin (Scott et al., 1994; Linares et al., 1972). A significant difference however is that while the skin of decorin-deficient mice is thinner and more fragile than normal skin, that of hypertrophic scar appears more resilient and is substantially thicker than normal skin. The complicating factor that makes the direct comparison between these two conditions difficult is that hypertrophic scar results from a prolongation of the inflammatory and fibroproliferative phases of wound healing following injury. Therefore, even though decorin production may be deficient in the early stages of wound healing which lead to HSc, excessive levels of other extracellular matrix components such as collagen and the proteoglycans versican and biglycan are produced. These PGs can increase the turgor of the healing tissue while the absence of decorin is causing a disarray in the organization of the newly forming collagen fibrils. The result is thicker, more disorganized and less pliable skin tissue than normal skin.

What is silencing the expression of the decorin gene early in hypertrophic scar? It has been reported by immunohistochemistry that HSc specimens contain elevated levels (qualitative data only) of the growth factor TGF-ß-1 as compared to normal skin (Ghahary et al., 1993). As well, elevated levels of this growth factor have been found in the serum of hypertrophic scar patients as compared to normal individuals (Tredget et al., submitted). TGF-ß is an autoinductive (Van Obberghen-Schilling et al., 1988) fibrogenic and inflammatory cytokine (Roberts and Sporn, 1990) that differentially regulates the production and accumulation of extracellular matrix components by fibroblasts. For example, TGF-ß has been shown to upregulate the production of collagen and fibronectin (Ignotz and Massague, 1986) and the PGs biglycan and versican while decreasing the production of decorin (Kahari et al., 1991). As well, TGF-ß has been found to suppress the production of collagenase while upregulating the production of TIMP (tissue inhibitor of metalloproteinases) (Edwards et al., 1987). In the rat model of glomerulonephritis TGF-ß1 has been linked to the occurence of fibrosis (Border et al., 1990) and decorin was shown to be a natural inhibitor of this pathology (Border et al., 1992).

Characterization of the decorin gene promoter revealed a TGF-ß negative regulatory element (Santra et al., 1994). Excessive TGF-ß in HSc may, therefore, inhibit the production of decorin which then results in the excessive and uncontrolled activity of this growth factor in HSc, since decorin can bind to TGF-ß and selectively inactivate it (Hausser et al., 1994). As well, this PG may act as a reservoir for this growth factor in the extracellular matrix. A negative regulatory loop may function whereby TGF-ß inhibits decorin production leading to lower levels of decorin and more uncontrolled activity of TGF-ß. The combination of the absence of decorin to integrate into newly forming collagen fibrils and the excessive levels of TGF-ß which can upregulate the production of many extracellular matrix components and inhibit the degradation of others, leads to an overall unregulated environment such as the fibrotic condition of hypertrophic scar.

Another mechanism which may play a role in the down-regulation of the decorin gene is its degree of methylation. The degree of hypomethylation of the decorin gene in human colon carcinoma tissue was estimated to be three-fold higher than in normal colon tissue (Adany et al., 1990). This finding was used to explain why decorin was highly expressed in human colon cancer. Conversely, hypermethylation of the decorin gene in hypertrophic scar victims may predispose these patients genetically to a situation where they are not able to produce enough of this PG to allow for efficient regeneration of their wounds. Such a possibility needs further investigation since such findings could influence the understanding and treatment of hypertrophic scar.

Later in the course of HSc, between 12 and 36 months post-burn, the number and percentage of cells expressing decorin mRNA increases significantly. Decorin protein was found, immunohistochemically, to increase as well. Through an undefined mechanism, possibly high cell density (Mauviel et al., 1995), the suppression of decorin production is relieved and cells within the scar begin to upregulate their production of this PG. This increase may be a response to the need for controlling the fibrosis. Decorin is able to bind collagen monomers and pre-formed fibrils. The introduction of this PG onto newly forming fibrils as well as pre-formed fibrils may initiate the regular spacing and assembly of collagen fibers needed for maturation of the scar tissue. This is demonstrated in Figure 13 where the areas of the scar in which cells are positive for decorin mRNA are those which appear to be gaining a morphology more closely resembling normal skin.

The increase of decorin expression at approximately one year after injury correlates with other reports which claim that the onset of maturation or permanent remodelling of hypertrophic scar occurs at about one year after injury (Reid et al., 1987). Such observations support the hypothesis that decorin expression is essential for the progressive maturation of hypertrophic scar.

An increase in decorin levels was also observed in other fibrotic conditions such as liver fibrosis (Krull et al., 1993). Such an increase may serve to bind and inactivate fibrogenic growth factors such as TGF-ß and TNF-alpha. This would be beneficial in HSc due to the abundant levels of TGF-ß present in the scar. Inactivation of this growth factor may relieve the suppression of decorin production and therefore the negative regulatory loop.

As decorin binds collagen, it's stability in the matrix is likely to increase. As well, while bound, it's uptake by decorin receptors on the surface of cells such as fibroblasts (Gotte, et al., 1995) may decrease. This may lead to an increased half-life of decorin in the matrix. This is evident in late HSc specimens. Decorin mRNA levels fall dramatically at time points later than three years post-burn but immunohistochemically, decorin appears to remain abundant. As the tissue matures due to controlled levels of growth factors and ample decorin protein on collagen fibers, the need for high production of decorin decreases.

The insufficient expression of decorin, therefore, in early wound samples which become hypertrophic may be due to transcriptional silencing of decorin production. The cells, most probably fibroblasts, in samples of HSc collected early after wounding are deficient in decorin production. This PG is needed for proper collagen fiber growth and assembly. Therefore, HSc serves as a human fibrotic model in which there is a greatly reduced or absent level of decorin production early in wound healing, which has prolonged inflammatory and fibroproliferative phases. This model has allowed us to further establish the vital roles of decorin in controlling fibrosis as well as in producing novel collagen fibres with proper morphological characteristics. Upregulating decorin production by gene delivery (Isaka et al., 1996) early in the course of HSc may help prevent the progression of such a fibrotic disorder.

III. The Regulation of TGF-ß1 Expression in Hypertrophic Scar is Complex

The process of establishing a protocol to detect TGF-ß1 mRNA in paraffin-embedded human skin and hypertrophic scar tissue by *in situ* hybridization was a rigorous one. Signal obtained with sense probes was the main recurring problem and sometimes the level of this signal exceeded, or was observed in the absence of, any staining with the antisense probes.

The impetus behind establishing this protocol was to investigate the expression of TGF-ß1 mRNA in hypertrophic scar samples and compare this to expression patterns in normal skin and mature scar. Considering that TGF-ß1 protein is rarely found in normal skin (Scott et al., 1995) and that it is upregulated sporadically in HSc and MSc, its source of production was keenly sought. Serum TGF-ß levels were recently found to increase significantly in some HSc patients (Tredget, et al., submitted). With knowledge of the local expression patterns of TGF-ß in HSc, it would be possible to start addressing issues such as whether circulating TGF-ß upregulates local TGF-ß1 production in fibroproliferative hypertrophic scar tissue; whether TGF-ß1 mRNA is being expressed locally with decorin mRNA, considering their colocalization at the protein level in MSc (Scott et al., 1995); whether it is possible that TGF-ß1 is not being produced locally but is coming from the circulation and is being bound by other proteins in the dermis, such as decorin; and whether the local expression of TGF-ß1 in HSc follows a time course similar to that for decorin because of its reported association with this PG.

Interesting questions were asked during the study about the regulation of expression of TGF-ß1; their relevance was only appreciable because of the results obtained from the experiments which utilized sense and antisense TGF-ß1 cRNA probes on dermal fibroblasts as well as on HSc, MSc, and NSk. Many reports have enlightened us on the different potential mechanisms which upregulate TGF-ß1 expression. However, very few insights have been offered into how the expression of TGF-ß1 is down-regulated or even shut off.

One possible mechanism is the production of antisense RNA which is produced off the opposite strand of DNA used for the transcription of mRNA. This phenomenon is well-studied and established in prokaryotes (Nellen and Lichtenstein, 1993) especially in the case of plasmid DNAs. The regulation of the steady-state copy number of plasmids in their hosts is finely controlled and this control is negative (Nordstrom and Wagner, 1994). This can occur via a repressor protein as well as an antisense RNA which would be involved in controlling the synthesis of a rate-limiting replication (Rep) protein. For example, in the R1 plasmid (Nordstrom and Wagner, 1994) which is a member of the IncFII class, initiation of replication requires the binding of many copies of RepA protein (encoded by R1) to the origin of replication or *oriR1*. Rep A is the rate-limiting factor and its production is controlled post-transcriptionally by an antisense RNA (CopA) which is encoded by a region upstream of the *repA* gene. The result is the hybridizing of CopA to its complement CopT which is the leader region of the RepA mRNAs and this, in turn, makes the double-stranded RNA susceptible to degradation by RNase III (Nordstrom and Wagner, 1994; Nellen and Lichtenstein, 1993) and thus the inhibition of translation of RepA protein from its mRNA.

In eukaryotes, 'antisense RNA' primarily denoted a technology that was developed to knock out expression of specific genes either for experimental or, more recently, therapeutic purposes. It makes sense, intuitively, that eukaryotic systems must produce endogenous antisense RNAs, considering that so many studies have introduced antisense RNA fragments into living cells without having the cells either reject, ignore, or degrade the fragments. Instead, the fragment comfortably finds its complement and the targeted gene gets down-regulated.

Recently, a number of reports have revealed different species of endogenous antisense RNAs in different eukaryotic systems. For example, analysis of the eukaryotic initiation factor (eIF) 2α gene revealed a sequence with homology to the "initiator sequence" or Inr sequence 450bp downstream of the eIF-2α promoter which was situated to allow it to produce antisense transcripts to eIF-2α (Silverman, et al., 1992). Later, it was found that sense and antisense eIF-2α transcripts were being produced in opposite directions off the eIF-2α gene (Noguchi, et al., 1994). Also, a protein was found to bind to a region immediately upstream of the Inr that was implicated in the access of RNA polymerase II transcription complexes to the transcription initiation site.

Another interesting study reported, using northern analysis and RT-PCR, the presence of basic fibroblast growth factor (bFGF) sense and antisense transcripts in unfertilized human oocytes and postnatal differentiated tissues (Knee et al., 1994). The concentration of the antisense bFGF transcript was found to vary relative to the sense transcript in different tissues with its expression exceeding the sense strand in heart, liver, skeletal muscle, and testis. It was suggested that antisense bFGF plays a role in the regulation of bFGF expression. Antisense transcripts for type I collagen were also found in chick embryo chondrocytes and their presence was found to correlate with the down-regulation of the α1(I) collagen gene (Farrell and Lukens, 1995).

An antisense RNA transcript was also found for TGF-ß3, which was thought to function in the regulation of this cytokine during cardiac valve induction in the chick heart (Potts et al., 1992). Of more interest was that this study was able to derive, through expression quantities, a function for this antisense transcript during the epithelial-mesenchymal transformation in the heart. Cells in the atrioventricular canal were found to express 5 times more TGF-ß3 mRNA during transformation than the adjacent endothelial cells of the ventricle but only a minor increase in the antisense transcript. During time course studies of the different stages of this transformation, TGF-ß3 was found to increase but then return to initial levels at late stages. The antisense transcript also increased during the period of development examined; this increase coincided with the loss of the ability of the myocardium of the atrioventricular canal to induce the transformation.

Considering that TGF-ß1 is highly conserved across species, that it belongs to the same family as TGF-ß3, that a 120bp region at the 3' end of its cDNA is 80% GC which indicates possible promoter activity, and that probing for its transcript using sense and antisense cRNA transcripts yielded specific, intense, and differentially expressed signal in human dermal fibroblasts and normal human skin and hypertrophic scar, it is not unlikely that an antisense transcript is also employed to regulate its expression. Therefore, attempts to confirm and identify this transcript were made and need to be followed up. The results could have a considerable impact on the manner in which the regulation of this cytokine is studied.

The fate of the double-stranded (ds) RNA species is an important issue although one that is beyond the scope of this study. However, it is of interest that the presence of a dsRNA molecule can activate a dsRNA-dependent protein kinase (DDPK) (Nellen and Lichtenstein, 1993) which can then trigger a complex signal transduction pathway. Additionally, dsRNases are being found, such as the one in *Dictyostelium* (Nellen and Lichtenstein, 1993), which can degrade sense-antisense duplexes and has a minimal substrate length which, therefore, protects short intramolecular structures. This enzyme is inactivated when dephosphorylated. Therefore, if the presense of dsRNA molecules activates DDPK and this kinase, in turn, phosphorylates and thus activates dsRNases, then this could be a potential mechanism which deals with dsRNAs. Other mechanisms have been discussed by Nellen and Lichtenstein (1993).

The results obtained with the antisense probes for TGF-ß1 in sections of HSc, MSc, and NSk are not extensive enough to suggest a pattern of expression in these tissues. These results were derived from the many attempts made to establish an *in situ* hybridization protocol for the detection of TGF-ß1 mRNA in these tissues. Therefore, as explained above, a restricted number of samples were analyzed to reduce the number of variables. In the HSc sections studied, the abundance of TGF-ß1 mRNA seemed to vary. However, it appeared that the expression of this cytokine was greater in HSc sections than in MSc and NSk sections. Also, regardless of the sample studied, those which displayed TGF-ß1 mRNA also stained with a sense probe. Often, the signal obtained with the sense probe was many times more intense than that with the antisense probe. Intriguingly, this was found in three of the four mature scars probed; and in two of these mature scars, staining was obtained only with the sense probe.

Also of particular interest is the finding in one experiment that while one patient's tissue stained strongly and specifically with the sense probe, its staining with the antisense probe was almost negligible; as well, in that same experiment, the normal tissue included on the same slide demonstrated very little TGF-ß1 mRNA and no staining with the sense probe and the dermal fibroblasts expressed abundant amounts of mRNA and no staining with the sense probe. These results lend support to the possible existence of an endogenous antisense TGF-ß1 mRNA species.

Another interesting observation was the regional expression of TGF-ß1 mRNA. The pattern observed in many of the scars was similar to that seen in sections probed with the decorin probes. In sections which displayed architectural similarities to PT#8's tissue (Figure 18), expression was concentrated in those regions which appeared to be gaining the qualities of normal skin. Therefore, where the collagen appeared as thin, loosely-packed fibrils arranged in whorls and nodules, expression of TGF-ß1 was weak. But in areas which appeared to be regaining some organization of NSk, TGF-ß1 mRNA was more abundant. The intriguing correlation to this finding was that the staining with the sense probe in such tissues colocalized to that with the antisense. If indeed the sense probe was detecting a TGF-ß1 antisense RNA species and if this RNA species was responsible for controlling the activity of TGF-ß1 mRNA, it makes intuitive sense that TGF-ß1 mRNA and its complement sense RNA species colocalize.

The colocalization of TGF-ß1 mRNA and decorin mRNA within some of the scars analyzed is also an interesting finding. The interaction between these proteins have been demonstrated to control the fibroproliferative activities of TGF-ß1 (Border et al., 1992; Isaka et al., 1996). Decorin may act as one component in the regulation of the activities of TGF-ß1 in hypertrophic scar. Therefore, their proximal production could mean that freshly produced decorin is able to bind freshly produced TGF-ß1 and this association may inhibit the otherwise uncontrolled activity of this cytokine.

The results obtained from the biopsies taken from HSc patients who were treated with IFN-α2b suggest that this agent inhibits TGF-ß1 production. The first scar sample (taken before treatment) from four of six patients analyzed contained abundant levels of TGF-ß1 mRNA which was significantly reduced with treatment. This was demonstrated by an abrogation in staining in all of the second biopsies (or first biopsy after treatment). Positive cells did reappear in subsequent biopsies for some of the patients.

It appears from the results stated above that in the early phase of the scar, less than one year after injury, decorin production is suppressed. The absence of this PG may contribute to the dysregulation of TGF-ß1. Without sufficient amounts of decorin, pools of unbound TGF-ß1, either produced locally or transported to the site of injury through the vascular system, could be accessible to bind to activating factors such as proteases in the extracellular environment. The result could be an excessive amount of activated cytokine which can trigger the abnormal events associated with hypertrophic scar. The early phase of HSc is therefore the time of greatest need for an antiinflammatory and antifibrogenic factor such as IFN-α2b. Such a factor which down-regulates TGF-ß1 may then, in turn, help to relieve the down-regulation of decorin by TGF-ß1 which occurs through the TGF-ß1 negative regulatory element in the decorin promoter.

This sequence of events could then allow for faster wound healing which is characterized by a healed wound of better quality. In some preliminary attempts at probing for decorin mRNA in serial biopsies of scar taken from HSc patients who underwent treatment, one patient demonstrated an increase in decorin expression during the course of treatment after expressing very low amounts of this PG before treatment (data not shown). More data are needed to establish this course of events as a real occurrence which can be generally expected.

The other concept which was serendipitously encountered in this study and needs further work to establish it is that of endogenous antisense TGF-ß1 RNA. In an attempt to confirm and identify the target of the sense TGF-ß1 probes used in the study, T112 probes were used in northern analyses and ribonuclease protection assays (RPAs) to try and find this target and characterize its size as well as to try and see if it protected the probe and therefore, indeed, was hybridizing to the sense probe and not just non-specifically binding to it. Although background levels were high and bands were somewhat faint, northern analyses did consistently reveal two bands, one about 3kb and the other about 4kb, when blots containing RNA from dermal fibroblasts were probed with TGF-ß1 sense probes. The antisense probes hybridized to a 2.5kb band which is the expected length of TGF-ß1 mRNA. The RPAs were inconclusive as technical problems prevented the proper functioning of the antisense probe and overall, bands were not clearly resolved. It is, therefore, necessary to repeat both the northern analyses and the RPAs to establish preliminary evidence for the existence of TGF-ß1 antisense RNA. Furthermore, other techniques such as anchored PCR and large batch RNA extraction from fibroblasts followed by sequencing of a reverse transcribed product would establish the presence of such an RNA species and rule-out any doubts about its non-specificity.

Taken together, the findings of this study in relation to other reports on hypertrophic scar suggest that TGF-ß1 introduced to the site of a burn, early after injury, has two fundamentally important effects which predispose the injury to heal with hypertrophic scar as the outcome. First, this autoinductive cytokine up-regulates the local expression of TGF-ß1 by infiltrating fibroblasts, and second, high amounts of sytemic TGF-ß1 silence the decorin gene through its TGF-ß negative regulatory element in its promoter.

Regeneration of the collagen, therefore, occurs in the absence of an essential structural component, decorin. We know that HSc contains 30% less hydroxyproline (and therefore collagen) than NSk (Scott et al., 1996); therefore, the gross abnormalities in the architecture of the skin in HSc are most likely due in large part to the temporary down-regulation of decorin expression. To complicate matters, the absence of this PG early after injury leaves high amounts of locally-produced and systemically-provided TGF-ß1 unbound, and therefore, uncontrolled. Compounding factors include the abnormally high levels of biglycan and versican (Scott et al., 1995) in HSc tissue which are probably upregulated by TGF-ß1 and are responsible for the hydration of the scar giving it its bulkiness and turgor.

The eventual upregulation of both decorin expression as well as antisense TGF-ß1 RNA control the fibroproliferative and fibrogenicity of this cytokine by inactivating it or inhibiting its further production, respectively. The onset of resolution of the scar is probably governed by the ability to achieve control of the dysregulated environment with such factors while the components of the scar are actively turning over. The presence of antisense TGF-ß1 RNA may assist in controlling TGF-ß1 production levels to the level needed to relieve the suppression on decorin expression. With this sequence of events, decorin can begin to settle on newly-forming collagen fibrils and allow them to assemble into the fibers characteristic of normal skin and normal scar. Additionally, with TGF-ß1 levels under control, versican and biglycan levels probably approximate normal levels and thus relieve the healing wound of the added stress of extra-hydration which abundant levels of these PGs probably cause.

BIBLIOGRAPHY

Adany, R., Heimer, R., Caterson, B., Sorrell, J.M., Iozzo, R.V. (1990). Altered expression of chondroitin sulfate proteoglycan in the stroma of human colon carcinoma. J. Biol. Chem., *265*, 11389-11396.

Adany, R., Iozzo, R.V. (1991). Hypomethylation of the decorin proteoglycan gene in human colon cancer. Biochem. J., *276*, 301-306.

Alexander, S. A., Donoff, R. B. (1980). The histochemistry of glycosaminoglycans within hypertrophic scars. Journal of Surgical Research, *28*, 171-181.

Allen, J. B., Wong, H. L., Guyre P. M., Simon, G. L., Wahl, S. M. (1991). Association of circulating receptor Fc gamma RIII-positive monocytes in AIDS patients with elevated levels of transforming growth fator-beta. J. Clin. Invest., *87*, 1773-9.

Andres, J. L., Stanley, K., Cheifetz, S., Massague, J. (1989). Membrane-anchored and soluble forms of betaglycan, a polymorphic proteoglycan that binds transforming growth factor-beta. J. Cell Biol., *109*, 3137-45.

Angerth, T., Huang, R., Aveskogh, M., Pettersson, I., Kjellen, L., Hellman, L. (1990). Cloning and structural analysis of a gene encoding a mouse mastocytoma proteoglycan core protein; analysis of its evolutionary relation to three cross hybridizing regions in the mouse genome. Gene, *93*, 235-240.

Antoniades, H. N., Owen, A. J. (1982). Growth factors and regulation of cell growth. [Review]. Annual Review of Medicine, *33*, 445-63.

Antoniades, H. N., Galanopoulosk T., Neville-Golden, J., Kiritsy, C. P., Lynch, S. E. (1991). Injury induces in vivo expression of platelet-derived growth factor (PDGF) and PDGF receptor mRNAs in skin epithelial cells and PDGF mRNA in connective tissue fibroblasts. Proc. Natl. Acad. Sci. USA, *88*, 565-569.

Anzano, M. A., Roberts, A. B., De Larco, J. E., Wakefield, L. M., Assoian, R. K., Roche, N. S., Smith, J. M., Lazarus, J. E., Sporn, M. B. (1985). Increased secretion of type beta transforming growth factor accompanies viral transformation of cells. Mol. Cell. Biol., *5*, 242-7.

Ausubel, F., Brent, R., Kingston, R. E., Moore, D. D., Seidman, J. G., Smith, J. A., Struhl, K. (Ed.). (1995). Short Protocols in Molecular Biology (3 ed.). John Wiley & Sons, Inc.

Bailey, A. J., Baxin, S., Sims, T. J., LeLous, M., Nicoletis, C., DeLaunay, A. (1975). Characterization of the collagen of human hypertrophic and normal scars. Biochim. Biophys. Acta, *405*, 412-421.

Baird, A., Mormede, P., Bohlen, P. (1985). Immunoreactive fibroblast growth factor in cells of peritoneal exudate suggests its identity with macrophage-derived growth factor. Biochem. Biophys. Res. Comm., *126*, 358-364.

Bassols, A., Massague, J. (1988). Transforming growth factor beta regulates the expression and structure of extracellular matrix chondroitin/dermatan sulfate proteoglycans. J. Biol. Chem., *263*, 3039-45.

Battaglia, C., Aumailley, M., Mann, K., Mayer, U., Timpl, R. (1993). Structural basis of beta 1 integrin-mediated cell adhesion to a large heparan sulfate proteoglycan from basement membranes. Eur. J. Cell Biol., *61*, 92-9.

Beavan, L. A., Quentin-Hoffmann, E., Schonherr, E., Snigula, F., Leroy, J. G., Kresse, H. (1993). Deficient expression of decorin in infantile progeroid patients. J. Biol. Chem., *268*, 9856-62.

Bianco, P., Fisher, L.W., Young, M.F., Termine, J.D., Robey, G.P. (1990). Expression and localization of the two small proteoglycans biglycan and decorin in developing human skeletal and non-skeletal tissues. J. Histochem. Cytochem., *38*, 1549-1563.

Birchenall-Roberts, M. C., Ruscetti, F. W., Kasper, J., Lee, H. D., Friedman, R., Geiser, A., Sporn, M. B., Roberts, A. B., Kim, S. J. (1990). Transcriptional regulation of the transforming growth factor beta 1 promoter by v-*src* gene products is mediated through the AP-1 complex. Mol. Cell. Biol., *10*, 4978-83.

Bird, A.P. (1986). CpG-rich islands and the function of DNA methylation. Nature, *321*, 209-213.

Blochberger, T. C., Vergnes, J. P., Hempel, J., Hassell, J. R. (1992). cDNA to chick lumican (corneal keratan sulfate proteoglycan) reveals homology to the small interstitial proteoglycan gene family and expression in muscle and intestine. J. Biol. Chem., *267*, 347-352.

Border, W.A., Okuda, S., Languino, L.R., Sporn, M.B., Ruoslahti, E. (1990). Suppression of experimental glomerulonephritis by antiserum against transforming growth factor ß1. Nature, *346*, 371-374.

Border, W.A., Noble, N.A., Yamamoto, T., Harper, J.R., Yamaguchi, Y., Pierschbacher M.D., Ruoslahti, E. (1992). Natural inhibitor of transforming growth factor-ß protects against scarring in experimental kidney disease. Nature, *360*, 361-364.

Buckley, A., Davidson, J. M., Klamerath, C. D., Wolt, T. B., Woodworth, S. C. (1985). Sustained release of epidermal growth factor accelerates wound repair. Proc. Natl. Acad. Sci. USA, *82*, 7340-7344.

Butzow, R., Fukushima, D., Twardzik, D. R., Ruoslahti, E. (1993). A 60-kD protein mediates the binding of transforming growth factor-beta to cell surface and extracellular matrix proteoglycans. J. Cell Biol., *122*, 721-7.

Castagnoli, C., Peruccio, D., Stella, M., Magliacani, G., Mazzola, G., Amoroso, A., Richiardi, P. (1990). The HLA-DRß16 allogenotype constitutes a risk factor for hypertrophic scarring. Human Immunology, *29*, 229-232.

Chen, R. H., Derynck, R. (1994). Homomeric interactions between type II transforming growth factor-beta receptors. J. Biol. Chem., *269*, 22868-74.

Chiang, C. P., Nilsen-Hamilton, M. (1986). Opposite and selective effects of epidermal growth factor and human platelet transforming growth factor-beta on the production of secreted proteins by murine 3T3 cells and human fibroblasts. J. Biol. Chem., *261*, 10478-81.

Chirgwin, J. M., Przybyla, A. E., MacDonald, R. J., Rutter, W. J. (1979). Isolation of biologically active ribonucleic acid from sources enriched in ribonuclease. Biochemistry, *18*, 5294-9.

Chomczynski, P., Sacchi, N. (1987). Single-step method of RNA isolation by acid guanidinium thiocyanate-phenol-chloroform extraction. Analytical Biochemistry, *162*, 156-9.

Chopra, R.K., Pearson, C. H., Pringle, G. H., Fackre, D. S., Scott, P. G. (1985). Dermatan sulphate is located on serine-4 of bovine skin proteodermatan sulphate. Biochem. J., *232*, 277-279.

Chung, L. P., Bentley, D. R., Reid, K. B. (1985). Molecular cloning and characterization of the cDNA coding for C4b-binding protein, a regulatory protein of the classical pathway of the human complement system. Biochem. J., *230*, 133-141.

Cohen, I.R., Grassel, S., Murdoch, A.D., Iozzo, R.V. (1993). Structural characterization of the complete human perlecan gene and its promoter. Proc. Natl. Acad. Sci. USA, *90*, 10404-10408.

Cox, K. H., DeLeon, D. V., Angerer, L. M., Angerer, R. C. (1984). Detection of mRNAs in sea urchin embryos by *in situ* hybridization using asymmetric RNA probes. Developmental Biology, *101*, 485-502.

Cunningham, B. A., Hemperly, J. J., Murray, B. A., Prediger, E. A., Brackenbury, R., Edelman, G. M. (1987). Neural cell adhesion molecule: structure, immunoglobulin-like domains, cell surface modulation, and alternative RNA splicing. Science, *236*, 799-806.

Dallas, S. L., Park-Snyder, S., Miyazono, K., Twardzik, D., Mundy, G. R., Bonewald, L. F. (1994). Characterization and autoregulation of latent transforming growth factor beta (TGF beta) complexes in osteoblast-like cell lines. Production of a latent complex lacking the latent TGF beta-binding protein. J. Biol. Chem., *269*, 6815-21.

Danielson, K. G., Fazzio, A., Cohen, I., Eichstetter, I., Iozzo, R. V. (1993). The human decorin gene: intron-exon organization, discovery of two alternatively spliced exons in the 5' untranslated region, and mapping of the gene to chromosome 12q23. Genomics, *15*, 146-160.

Danielson, K. G., Baribault, H., Holmes, D. F., Graham, H., Kadler, K. E., Iozzo, R. V. (1997). Targeted disruption of decorin leads to abnormal collagen fibril morphology and skin fragility. J. Cell Biol., *136*, 729-43.

De Larco, J. E., Todaro, G. J. (1978). Growth factors from murine sarcoma virus-transformed cells. Proc. Natl. Acad. Sci. USA, *75*, 4001-5.

Dean, D. C., Newby, R. F., Bourgeois, S. (1988). Regulation of fibronectin biosynthesis by dexamethasone, transforming growth factor beta, and cAMP in human cell lines. J. Cell Biol., *106*, 2159-70.

Deitch, E. A., Wheelahan, T. M., Rose, M. P. (1983). Hypotrophic burn scars: Analysis of variables. Journal of Trauma, *23*, 895-899.

Derynck, R., Jarrett, J. A., Chen, E. Y., Eaton, D. H., Bell, J. R., Assoian, R. K., Roberts, A. B., Sporn, M. B., Goeddel, D. V. (1985). Human transforming growth factor-beta complementary DNA sequence and expression in normal and transformed cells. Nature, *316*, 701-5.

DiCorleto, P. E., and Bowen-Pope, D. (1983). Cultered endothelial cells produce a platelet-derived growth factor-like protein. Proc. Natl. Acad. Sci. USA, *80*, 1919-1923.

Dyne, K. M., Valli, M., Forlino, A., Mottes, M., Kresse, H., Cetta, G. (1996). Deficient expression of the small proteoglycan decorin in a case of severe/lethal osteogenesis imperfecta. [Review]. American Journal of Medical Genetics, *63*, 161-6.

Ebner, R., Chen, R. H., Lawler, S., Zioncheck, T., Derynck, R. (1993). Determination of type I receptor specificity by the type II receptors for TGF-beta or activin. Science, *262*, 900-2.

Edwards, D. R., Murphy, G., Reynolds, J. J., Whitham, S. E., Docherty, A. J., Angel, P., Heath, J. K. (1987). Transforming growth factor beta modulates the expression of collagenase and metalloproteinase inhibitor. EMBO Journal, *6*, 1899-904.

Esch, F., Ueno, N., Baird, A., Hill, F., Deneroy, L., Ling, N., Gospodarowicz, D., Guillemin, R. (1985). Primary structure of bovine brain acidic fibroblast growth factor (FGF). Biochem. Biophys. Res. Comm., *133*, 554-562.

Esch, F., Baird, A., Ling, N., Ueno, N., Hill, F., Deneroy, L., Klepper, R., Gospodarowski, D., Boheln, P., Guillemin, R. (1985). Primary structure of bovine pituitary basic fibroblast growth factor (FGF) and comparison with the amino-terminal sequence of bovine brain acidic FGF. Biochem. Biophys. Res. Comm., *82*, 6507-6511.

Farrell, C. M., Lukens, L. N. (1995). Naturally occurring antisense transcripts are present in chick embryo chondrocytes simultaneously with the down-regulation of the alpha 1 (I) collagen gene. J. Biol. Chem., *270*, 3400-8.

Fischer, G., and Boedeker, C. (1861). Kunstliche Bildung von Zucker aus Knorpel (Chondrogen), und uber die Umsetzung des genossenen Knorpels im menschlichen Korper. Ann. Chem. Pharm., *117*, 111-118.

Fisher, L. W., Termine, J. D., Young, M. F. (1989). Deduced protein sequence of bone small proteoglycan I (biglycan) shows homology with proteoglycan II (decorin) and several nonconnective tissue proteins in a variety of species. J. Biol. Chem., *264*, 4571-6.

Franzen, P., ten Dijke, P., Ichijo, H., Yamashita, H., Schulz, P., Heldin, C. H., Miyazono, K. (1993). Cloning of a TGF beta type I receptor that forms a heteromeric complex with the TGF beta type II receptor. Cell, *75*, 681-92.

Fukushima, D., Butzow, R., Hildebrand, A., Ruoslahti, E. (1993). Localization of transforming growth factor ß binding site in betaglycan. J. Biol. Chem., *268*, 22710-22715.

Geiser, A. G., Busam, K. J., Kim, S. J., Lafyatis, R., O'Reilly,M. A., Webbink, R., Roberts, A. B., Sporn, M. B. (1993). Regulation of the transforming growth factor-beta 1 and -beta 3 promoters by transcription factor Sp1. Gene. *129*, 223-8.

Ghahary, A., Shen, Y. J., Scott, P. G., Gong, Y., Tredget, E. E. (1993). Enhanced expression of mRNA for transforming growth factor-ß1, type I and type III procollagen in human post-burn hypertrophic scar tissues. J. Lab. Clin. Med., *22*, 465-473.

Ghahary, A., Shen Y. J., Nedelec, B., Scott, P. G., Tredget, E. E. (1995). Enhanced expression of mRNA for insulin-like growth factor-1 in post-burn hypertrophic scar tissue and its fibrogenic role by dermal fibroblasts. Mol. Cell. Biochem., *148*, 25-32.

Ghahary, A., Shen, Y. J., Scott, P. G., Tredget, E. E. (1995). Immunolocalization of TGF-beta 1 in human hypertrophic scar and normal dermal tissues. Cytokine, *7*, 184-90.

Gospodarowicz, D., Neufeld, G., Schweigerer, L. (1986). Fibroblast growth factor (Review). Mol. Cell. Endocrinol., *46*, 187-204.

Gotte, M., Kresse, H., Hausser, H. (1995). Endocytosis of decorin by bovine aortic endothelial cells. Eur. J. Cell Biol., *66*, 226-233.

Gougos, A., kSt Jacques, S., Greaves, A., O'Connell, P. J., d'Apice, A. J., Buhring, H. J., Bermabeu, C., van Mourik, J., A., Letarte, M. (1992). Identification of distinct epitopes of endoglin, an RGD-containing glycoprotein of endothelial cells, leukemic cells, and syncytiotrophoblasts. International Immunology, *4*, 83-92.

Guiot, Y., Rahier, J. (1995). The effects of varying key steps in the non-radioactive *in situ* hybridization protocol: a quantitative study. Histochemical Journal, *27*, 60-68.

Haaparanta, T., Uitto, J., Ruoslahti, E., Engvall, E. (1991). Molecular cloning of the cDNA encoding human laminin A chain. Matrix, *11*, 151-160.

Halberg, D. F., Proulx, G., Doege, K., Yamada, Y., Drickamer, K. (1988). A segment of the cartilage proteoglycan core protein has lectin-like activity. J. Biol. Chem., *263*, 9486-9490.

Hames, B. D. and Higgins, S. J. (Ed.). (1988). Nucleic acid hybridization. A practical approach. Oxford: IRL Press Limited.

Hardingham, T. E., and Bayliss, M. T. (1990). Proteoglycans of articular cartilage changes in aging and in joint disease. Semin. Arth. Rheum., Suppl. 1, 12-33.

Hardingham, T.E., Fosang, A.J. (1992). Proteoglycans: many forms and many functions. FASEB Journal, *6*, 861-870.

Hascall (1986). Functions of the Proteoglycans. In Ciba Foundation Symposium Great Britain: John Wiley & Sons.

Hata, R., Sunada, H., Arai, K., Sato, T., Ninomiya, Y., Nagai, Y. (1988). Regulation of collagen metabolism and cell growth by epidermal growth factor and ascorbate in cultured human skin fibroblasts. Eur. J. Biochem., *173*, 261-267.

Hausser, H., Groning, A., Hasilik, A., Schonherr, E., Kresse, H. (1994). Selective inactivity of TGF-ß/decorin complexes. FEBS Letters, *353*, 243-245.

Hayashi, K., Madri, J. A., Yurchenco, P. D. (1992). Endothelial cells interact with the core protein of basement membrane perlecan through beta 1 and beta 3 integrins: an adhesion modulated by glycosaminoglycan. J. Cell Biol., *119*, 945-59.

Hedbom, E., Heinegard, D. (1993). Binding of fibromodulin and decorin to separate sites on fibrillar collagens. J. Biol. Chem., *268*, 27307-27312.

Heino, J., Kahari, V. M., Mauviel, A., Krusius, T. (1988). Human recombinant interleukin-1 regulates cellular mRNA levels of dermatan sulphate proteoglycan core protein. Biochem. J., *252*, 309-12.

Hildebrand, A., Romaris, M., Rasmussen, L.M., Heinegard, D., Twardzik, D.R., Borders, W.A., Ruoslahti, E. (1994). Interaction of the small interstitial proteoglycans biglycan, decorin and fibromodulin with transforming growth factor ß. Biochem. J., *302*, 527-534.

Huber, S., Winterhalter, K. H., Vaughan, L. (1988). Isolation and sequence analysis of the glycosaminoglycan attachment site of type IX collagen. J. Biol. Chem., *263*, 752-756.
Ignotz, R. A., Massague, J. (1986). Transforming growth factor-beta stimulates the expression of fibronectin and collagen and their incorporation into the extracellular matrix. J. Biol. Chem., *261*, 4337-45.

Ignotz, R. A., Endo, T., Massague, J. (1987). Regulation of fibronectin and type I collagen mRNA levels by transforming growth factor-beta. J. Biol. Chem., *262*, 6443-6.

Iozzo, R.V., Wight, T.N. (1982). Isolation and characterization of proteoglycans synthesized by human colon and colon carcinoma. J. Biol. Chem., *257*, 11135-11144.

Iozzo, R.V., Bolender, R.P., Wight, T.N. (1982). Proteoglycan changes in the intercellular matrix of human colon carcinoma - an integrated biochemical and stereologic analysis. Laboratory Investigation, *47*, 124-138.

Iozzo, R.V., Cohen, I.R., Grassel, S., Murdoch, A.D. (1994). The biology of perlecan: the multifaceted heparan sulphate proteoglycan of basement membranes and preicellular matrices. Biochem. J., *302*, 625-639.

Iozzo, R. V. and Hassell, J. R. (1989). Identification of the precursor protein for the heparan sulfate proteoglycan of human colon carcinoma cells and its post-translational modifications. Arch. Biochem. Biophys., *269*, 239-249.

Isaka, Y., Brees, D. K., Ikegaya, K., Kaneda, Y., Imai, E., Noble, N. A., Border, W. A. (1996). Gene therapy by skeletal muscle expression of decorin prevents fibrotic disease in rat kidney. Nature Medicine, *2*, 418-423.

Jakowlew, S. B., Kondaiah, P., Flanders, K. C., Thompson, N. L., Dillard, P. J., Sporn, M. B., Roberts, A. B. (1988). Increased expression of growth factor mRNAs accompanies viral transformation of rodent cells. Oncogene Research, *2*, 135-48.

Kahari, B., Larjava, H., Uitto, J. (1991). Differential regulation of extracellular matrix proteoglycan (PG) gene expression. J. Biol. Chem., *266*, 10608-10615.

Kerr, L. D., Miller, D. B., Matrisian, L. M. (1990). TGF-beta 1 inhibition of transin/stromelysin gene expression is mediated through a Fos binding sequence. Cell, *61*, 267-278.

Kim, S. J., Glick, A., Sporn, M. B., Roberts, A B. (1989). Characterization of the promoter region of the human transforming growth factor-beta 1 gene. J. Biol. Chem., *264*, 402-8.

Kim, S. J., Jeang, K. T., Glick, A. B., Sporn, M. B., Roberts, A. B. (1989). Promoter sequences of the human transforming growth factor-beta 1 gene responsive to transforming growth factor-beta 1 autoinduction. J. Biol. Chem., *264*, 7041-5.

Kim, S. J., Kehrl, J. H., Burton, J., Tendler, C. L., Jeang, K. T., Danielpour, D., Thevenin, C., Kim K. Y., Sporn, M. B., Roberts, A. B. (1990). Transactivation of the transforming growth factor beta 1 (TGF-beta 1) gene by human T lymphotropic virus type 1 tax: a potential mechanism for the increased production of TGF-beta 1 in adult T cell leukemia. J. Exp. Med., *172*, 121-9.

Kim, S. J., Lee, H. D., Robbins, P. D., Busam, K., Sporn, M. B., Roberts, A. B. (1991). Regulation of transforming growth factor beta 1 gene expression by the product of the retinoblastoma-susceptibility gene. Proc. Natl. Acad. Sci. USA, *88*, 3052-6.

Kischer, C. W., Shetlar, M. R. (1974). Collagen and mucopolysaccharides in the hypertrophic scar. Connect. Tissue Res., *2*, 205-213.

Kischer, C. W. (1974). Fibroblasts of the hypertrophic scar, mature scar and normal skin: a study by scanning and transmission electron microscopy. Texal Reports on Biology & Medicine, *32*, 699-709.

Knee, R. S., Pitcher, S. E., Murphy, P. R. (1994). Basic fibroblast growth factor sense (FGF) and antisense (gfg) RNA transcripts are expressed in unfertilized human oocytes and in differentiated adult tissues. Biochem. Biophys. Res. Comm., *205*, 577-83.

Kohler, A., Lipton, A. (1974). Platelets as a source of fibroblast growth-promoting activity. Exp. Cell Res., *87*, 297.

Kovacs, E. J. (1991). Fibrogenic cytokines: the role of immune mediators in the development of scar tissue. [Review]. Immunology Today, *12*, 17-23.

Kovacs, E. J., and DiPietro, L. A. (1994). Fibrogenic cytokines and connective tissue production. FASEB J., *8*, 854-861.

Kresse, H., Hausser, H.,Schonherr, E., Bittner, K. (1994). Biosynthesis and interactions of small chondroitin/dermatan sulphate proteoglycans. Eur. J. Clin. Chem. Clin. Biochem., *32*, 259-264.

Kresse, H., Hausser, H., Schonherr, E. (1994). Small proteoglycans. EXS, *70*, 73-100.

Krueger, R.C. Jr., Fields, T.A., Hildreth, J. IV, Schwartz, N.B. (1990). Chick cartilage chondroitin sulfate proteoglycan core protein. I. Generation and characterization of peptides and specificity for glycosaminoglycan attachment. J. Biol. Chem., *265*, 12075-12087.

Krull, N.B., Zimmerman, T., Gressner, A.M. (1993). Spatial and temporal patterns of gene expression for the proteoglycans biglycan and decorin and for transforming growth factor-ß1 revealed by *in situ* hybridization during experimentally induced liver fibrosis in the rat. Hepatology, *18*, 581-589.

Krusius, T., Ruoslahti, E. (1986). Primary structure of an extracellular matrix proteoglycan core protein deduced from cloned cDNA. Proc. Natl. Acad. Sci. USA, *83*, 7683-7.

Krusius, T., Gehlsen, K. R., Ruoslahti, E. (1987). A fibroblast chondroitin sulfate proteoglycan core protein contains lectin-like and growth factor-like sequences. J. Biol. Chem., *262*, 13120-13125.

Kulozik, M., Hogg, A., Lankat-Buttgereit, B., Krieg, T. (1990). Co-localization of transforming growth factor ß2 with a1(I) procollagen mRNA in tissue sections of patients with systemic sclerosis. J. Clin. Invest., *86*, 917-922.

Laiho, M., DeCaprio, J. A., Ludlow, J. W., Livingston, D. M., Massague, J. (1990). Growth inhibition by TGF-beta linked to suppression of retinoblastoma protein phosphorylation. Cell, *62*, 175-85.

Lehnert, S. A., Akhurst, R. J. (1988). Embryonic expression pattern of TGF beta type-1 RNA suggests both paracrine and autocrine mechanisms of action. Development, *104*, 263-73.

Linares, H. A., Kischer, C. W., Dobrkovsky, M., Larson, D. L. (1972). The histiotypic organization of the hypertophic scar in humans. J. Invest. Dermatol., *59*, 323-31.

Logel, J., Dill, D., Leonard, S. (1992). Synthesis of cRNA probes from PCR-generated DNA. Biotechniques, *13*, 604-10.

Lopez-Casillas, F., Cheifetz, S., Doody, J., Andres, J. L., Lane, W. S., Massague, J. (1991). Structure and expression of the membrane proteoglycan betaglycan, a component of the TGF-beta receptor system. Cell, *67*, 785-95.

Lucassen, P. J., Goudsmit, E., Pool, C. W., Mengod, G., Palacios, J. M., Raadsheer, F. C., Guldenaar, S. E., Swaab, D. F. (1996). In situ hybridization for vasopressin mRNA in the human supraoptic and paraventricular nucleus; quantitative aspects of formalin-fixed paraffin-embedded tissue sections as compared to cryostat sections. Journal of Neuroscience Methods, *64*, 133.

Lund, P. K., Moats-Staats, B. M., Hynes, M. A., Simmons, J. G., Jansen M., D'Ercole, A. J., Van Wyk, J. J. (1986). Somatomedin-C/insulin-like growth factor-I and insulin-like growth factor-II mRNAs in rat fetal and adult tissues. J. Biol. Chem., *261*, 14539-44.

Lynch, S. E., Nixon, J. C., Colvin, R. B., Antoniades, H. N. (1987). Role of platelet-derived growth factor in wound healing: Synergistic effects with other growth factors. Proc. Natl. Acad. Sci. USA, *84*, 7696-7700.

MacDonald, I. M., Pannu, R., Kovithavongs, K., Peters, C., Tredget, E. E., Ghahary, A. (1995). Effect of retinoic acid on expression of transforming growth factor-ß by retinal pigment epithelial cells in culture. Can. J. Ophthalmol., *30*, 301-305.

Maddox, P. H., Jenkins, D. (1987). 3-Aminopropyltriethoxysilane (APES): a new advance in section adhesion. J. Clin. Path., *40*, 1256-7.

Madri, J. A., Pratt, B. M., Tucker, A. M. (1988). Phenotypic modulation of endothelial cells by transforming growth factor-beta depends upon the composition and organization of the extracellular matrix. J. Cell Biol., *106*, 1375-84.

Makower, A. M., Wroblewski, J, Pawlowski, A. (1988). Effects of IGF-I, EGF, and FGF on proteoglycans synthesized by fractionated chondrocytes of rat rib growth plate. Exp. Cell. Res., *179*, 498-506.

Mann, D. M., Yamaguchi, Y., Bourdon, M. A., Ruoslahti, E. (1990). Analysis of glycosaminoglycan substitution in decorin by site-directed mutagenesis. J. Biol. Chem., *265*, 5317-5323.

Matrisian, L. M., Leroy, P., Ruhlmann, C., Gesnel, M. C., Breathnach, R. (1986). Isolation of the oncogene and epidermal growth factor-induced transin gene: complex control in rat fibroblasts. Mol. Cell. Biol., *6*, 1679-86.

Mauviel, A., Santra, M., Chen, Y.Q., Uitto, J., Iozzo, R. (1995). Transcriptional regulation of decorin gene expression. J. Biol. Chem., *270*, 11692-11700.

Meyer, D. H., Krull, N., Dreher, K. L., Gressner, A. M. (1992). Biglycan and decorin gene expression in normal and fibrotic rat liver: Cellular localization and regulatory factors. Hepatology, *16*, 204-216.

Meyer, K., and Palmer, J. W. (1934). The polysaccharide of vitreous humour. J. Biol. Chem., *107*, 629-634.

Meyer, K., Dubos, R., Smythe, E. M. (1937). The hydrolysis of the polysaccharide acids of vitreous humour, of umbilical cord, and of streptococcus by the autolytic enzyme of pneumococcus. J. Biol. Chem., *118*, 71-78.

Meyer, K., and Chaffee, E. (1941). The mucopolysaccharides of skin. J. Biol. Chem., *138*, 491-499.

Meyer, K., Linker, A., Davidson, E. A., Weissmann, B. (1953). The mucopolysaccharides of bovine cornea. J. Biol. Chem., *205*, 611-616.

Meyer, K., Davidson, E. A., Linker, A., Hoffman, P. (1956). The acid mucopolysaccharides of connective tissue. Biochim. Biophys. Acta. *21*, 506-518.

Mihara, K., Cao, X. R., Yen, A., Chandler, S., Driscoll, B., Murphree, A. L., T'Ang, A., Fung, Y. K. (1989). Cell cycle-dependent regulation of phosphorylation of the human retinoblastoma gene product. Science. *246*, 1300-3.

Millar, M. R., Sharpe, R. M., Maguire, S. M., Gaughan, J., West, A. P., Saunders, P. T. (1994). Localization of mRNAs by in-situ hybridization to the residual body at stages IX-X of the cycle of the rat seminiferous epithelium: fact or arefact? International Journal of Andrology. *17*, 149-60.

Mirkin, S. M., Lyamichev, V. I., Drushlyak, K. N., Dobrynin, V. N., Filippov, S. A., Frank-Kamenetskii, M. D. (1987). DNA H form requires a homopurine-homopyrimidine mirror repeat. Nature. *330*, 495-7.

Mitchell, P.J., Tjian, R. (1989). Transcriptional regulation in mammalian cells by sequence-specific DNA binding proteins. Science. *245*, 371-378.

Moren, A., Olofsson, A., Stenman, G., Sahlin, P., Kanzaki, T., Claesson-Welsh, L., ten Dijke, P., Miyazono, K., Heldin, C. H. (1994). Identification and characterization of LTBP-2, a novel latent transforming growth factor-beta-binding protein. J. Biol. Chem., *269*, 32469-78.

Morgelin, M., Paulsson, M., Malmstrom, A., Heinegard, D. (1989). Shared and distinct structural features of interstitial proteoglycans from different bovine tissues revealed by electron microscopy. J. Biol. Chem., *264*, 12080-12090.

Murdoch, A. D., Liu, B., Schwarting, R., Tuan, R. S., Iozzo, R. V. (1994). Widespread expression of perlecan proteoglycan in basement membranes and extracellular matrices of human tissues as detected by a novel monoclonal antibody against domain III and by in situ hybridization. J. Histochem. Cytochem., *42*, 239-249.

Nakayama, H., Ichikawa, F., Andres, J.L., Massague, J., Noda, M. (1994). Dexamethasone enhancement of betaglycan (TGF-ß type III receptor) gene expression in osteoblast-like cells. Exp. Cell Res., *211*, 301-306.

Neame, P. J., Choi, H. U., Rosenberg, L. C. (1989). The primary structure of the core protein of the small, leucine-rich proteoglycan (PG I) from bovine articular cartilage. J. Biol. Chem., *264*, 8653-61.

Nellen, W., Lichtenstein, C. (1993). What makes an mRNA anti-sense-itive? [Review]. Trends in Biochemical Sciences, *18*, 419-23.

Noguchi, M., Miyamoto, S., Silverman, T. A., Safer, B. (1994). Characterization of an antisense Inr element in the eIF-2 alpha gene. J. Biol. Chem., *269*, 29161-7.

Noonan, D. M., Fulle, A., Valente, P., Cai, S., Horigan, E., Sasaki, M., Yamada, Y., Hassell, J. R. (1991). The complete sequence of perlecan, a basement membrane heparan sulfate proteoglycan, reveals extensive similarity with laminin A chain, low density lipoprotein-receptor, and the neural cell adhesion molecule. J. Biol. Chem., *266*, 22939-22947.

Nordstrom, K., Wagner, E. G. (1994). Kinetic aspects of control of plasmid replication by antisense RNA. [Review]. Trends in Biochemical Sciences, *19*, 294-300.

Okadome, T., Yamashita, H., Franzen, P., Moren, A., Heldin, C. H., Miyazono, K. (1994). Distinct roles of the intracellular domains of transforming growth factor-beta type I and type II receptors in signal transduction. J. Biol. Chem., *269*, 30753-6.

Overall, C. M., Wrana, J. L., Sodek, J. (1989). Independent regulation of collagenase, 72-kDa progelatinase, and metalloendoproteinase inhibitor expression in human fibroblasts by transforming growth factor-beta. J. Biol. Chem., *264*, 1860-9.

Pannu, R (1995) In vitro and in vivo antagonism of transforming growth factor-beta production by interferon alpha-2b. Masters, University of Alberta.

Paetkau, V (1994), Biochemistry 530 Lecture Notes, University of Alberta

Pelton, R. W., Nomura, S., Moses, H. L., Hogan, B. L. (1989). Expression of transforming growth factor beta 2 RNA during murine embryogenesis. Development, *106*, 759-67.

Penttinen, R. P., Kobayashi, S., Bornstein, P. (1988). Transforming growth factor beta increases mRNA for matrix proteins both in the presence and in the absence of changes in mRNA stability. Proc. Natl. Acad. Sci. USA, *85*, 1105-8.

Potts, J. D., Vincent, E. B., Runyan, R. B., Weeks, D. L. (1992). Sense and antisense TGF beta 3 mRNA levels correlate with cardiac valve induction. Developmental Dynamics, *193*, 340-5.

Price, L. K., Choi, H. U., Rosenberg, L., Stanley, E. R. (1992). The predominant form of secreted colony stimulating factor-1 is a proteoglycan. J. Biol. Chem., *267*, 2190-2199.

Pringle, G. A., Dodd, C. M., Osborn, J. W., Pearson, C. H., Mosmann, T. R. (1985). Production and characterization of monoclonal antibodies to bovine skin proteodermatan sufate. Collagen & Related Research, *5*, 23-39.

Rapraeger, A.C., Krufka, A., Olwin, B.B. (1991). Requirement of heparan sulfate for bFGF-mediated fibroblast growth and myoblast differentiation. Science, *252*, 1705-1708.

Rapraeger, A.C. (1993). The coordinated regulation of heparan sulfate, syndecans and cell behavior. Current Opinion in Cell Biology, *5*, 844-853.

Reed, M. J., Vernon, R. B., Abrass, I. B., Sage, E. H. (1994). TGF-beta 1 induces the expression of type I collagen and SPARC, and enhances contraction of collagen gels, by fibroblasts from young and aged donors. Journal of Cellular Physiology, *158*, 169-79.

Reid, W. H., Evans, J. H., Naismith, R. S., Tully, A. F., Sherwin, S. (1987). Hypertrophic scarring and pressure therapy. Burns, *13*, 529-532.

Reiser, K., Summers, P., Medrano, J. F., Rucker, R., Last, J., McDonald, R. (1996). Effects of elevated circulating IGF-1 on the extracellular matrix in "high-growth' C57BL/6J mice. Am. J. Physiol., *271*, R696-703.

Robbins, P. D., Horowitz, J. M., Mulligan, R. C. (1990). Negative regulation of human c-fos expression by the retinoblastoma gene product. Nature, *346*, 668-71.

Rockwell W. B., Cohen, I. K., Ehrlich, H. P. (1989). Keloids and hypertrophic scars: a comprehensive review. [Review]. Plastic & Reconstructive Surgery, *84*, 827-37.

Roitsch, T., Lehle, L. (1989). Requirements for efficient in vitro transcription and translation: a study using yeast invertase as a probe. Biochim. Biophys. Acta, *1009*, 19-26.

Rosner, B (1990). Fundamentals of Biostatistics (3 ed.). Boston, Massachusetts: PWS-Kent.

Ross, R., Glomset, J. A., Kariya, B., Harber, L. (1974). A platelet-dependent serum factor that stimulates the proliferation of arterial smooth muscle cells *in vitro*. Proc. Natl. Acad. Sci. USA, *71*, 1207-1210.

Rossi, P., Karsenty, G., Roberts, A. B., Roche, N. S., Sporn, M. B., de Crombrugghe, B. (1988). A nuclear factor 1 binding site mediates the transcriptional activation of a type I collagen promoter by transforming growth factor-beta. Cell, *52*, 405-14.

Roughley, P.J., Melching, L.I., Recklies, A.D. (1994). Changes in the expression of decorin and biglycan in human articular cartilage with age and regulation by TGF-ß. Matrix Biology, *14*, 51-59.

Santra, M., Danielson, K.G., Iozzo, R.V. (1994). Structural and functional characterization of the human decorin gene promoter. J. Biol. Chem., *269*, 579-587.

Santra, M., Skorski, T., Calabretta, B., Lattime, E.C., Iozzo, R.V. (1995). *De novo* decorin gene expression suppresses the malignant phenotype in human colon cancer cells. Proc. Natl. Acad. Sci. USA, *92*, 7016-7020.

Schmid, P., Cox, D., Bilbe, G., Maier, R., McMaster, G. K. (1991). Differential expression of TGF beta 1, beta 2 and beta 3 genes during mouse embryogenesis. Development, *111*, 117-30.

Schmitt-Graff, A., Desmouliere, A., Gabbiani, G. (1994). Heterogeneity of myofibroblast phenotypic features: an example of fibroblastic cell plasticity. [Review]. Virchows Archiv., *425*, 3-24.

Schonherr, E., Beaven, L.A., Hausser, H., Kresse, H., Culp, L.A. (1993). Differences in decorin expression by papillary and reticular fibroblasts *in vivo* and *in vitro*. Biochem. J., *290*, 893-899.

Scott, J. E., Orford, C. R., Hughes, E. W. (1981). Proteoglycan-collagen arrangements in developing rat tail tendon. Biochem. J., *195*, 573-581.

Scott, J. E., Haigh, M. (1985). Proteoglycan-type I collagen fibril interactions in bone and non-calcifying connective tissues. Bioscience Reports, *5*, 71-81.

Scott, J. E. (1988). Proteoglycan-fibrillar collagen interactions. Biochem. J., *252*, 313-323.

Scott, J. E. (1995). Extracellular matrix, supramolecular organisation and shape. [Review]. Journal of Anatomy, *187*, 259-69.

Scott, P. G., Dodd, C. M. (1989). The *N*-linked oligosaccharides of bovine skin proteodermatan sulphate. Biochemical Society Transactions, *17*, 1031-2.

Scott, P. G., Dodd, C. M. (1990). Self-aggregation of bovine skin proteodermatan sulphate promoted by removal of the three *N*-linked oligosaccharides. Connective Tissue Research, *24*, 225-35.

Scott, P. G., Dodd, C. M., Pringle, G. A. (1993). Mapping the locations of the epitopes of five monoclonal antibodies to the core protein of dermatan sulfate proteoglycan II (Decorin). J. Biol. Chem., *268*, 11558-11564.

Scott, P. G. (1993). Structures of the protein cores of the small dermatan sulphate proteoglycans. In J. E. Scott (Eds.), Dermatan Sulphate Proteoglycans (pp. 81-101). London and Chapel Hill: Portland Press Ltd.

Scott, P.G., Ghahary, A., Chambers, M.M., Tredget, E.E. (1994). Biological Basis of Hypertrophic Scarring. In Advances in Structural Biology (pp. 157-202). JAI Press Inc.

Scott, P.G., Dodd, C.M., Tredget, E.E., Ghahary, A., Rahemtulla, F. (1995). Immunohistochemical localization of the proteoglycans decorin, biglycan and versican and transforming growth factor-ß in human post-burn hypertrophic and mature scars. Histopathology, *26*, 423-431.

Scott, P.G., Nakano, T., Dodd, C.M. (1995). Small proteoglycans from different regions of the fibrocartilaginous temporomandibular joint disc. Biochim. Biophys. Acta, *1244*, 121-128.

Scott, P. G., Dodd, C. M., Tredget, E. E., Ghahary, A., Rahemtulla, F. (1996). Chemical characterization and quantification of proteoglycans in human post-burn hypertrophic and mature scars. Clinical Science, *90*, 417-425.

Segarini, P. R., Rosen, D. M., Seyedin, S. M. (1989). Binding of transforming growth factor-beta to cell surface proteins varies with cell type. Molecular Endocrinology, *3*, 261-72.

Seppa, H., Grotendorst, G., Seppa, S., Schiffmann, E., Martin, G. R. (1982). Platelet-derived growth factor is chemotactic for fibroblasts. J. Cell Biol., *92*, 584-8.

Shah, M., Foreman, D. M., Ferguson, M. W. (1992). Control of scarring in adult wounds by neutralising antibody to transforming growth factor beta. Lancet, *339*, 213-4.

Shetlar, M. R., Dobrkovsky, M., Linares, H., Villarante, R., Shetlar, C. L., Larson, D. L. (1971). The hypertrophic scar. Glycoprotein and collagen components of burn scars. Proceedings of the Society for Experimental Biology & Medicine, *138*, 298-300.

Shetlar, M. R., Shetlar, C. L., Chien, S. F., Linares, H. A., Dobrkovsky, M., Larson, D. L. (1972). The hypertrophic scar. Hexosamine containing components of burn scars. Proceedings of the Society for Experimental Biology & Medicine, *139*, 544-7.

Shetlar, M. R., Shetlar, C. L., Linares, H. A. (1977). Burns, *4*, 14-19.

Shetlar, M. R., Shetlar, C. L., Kischer, C. W. (1981). Burns, *8*, 27-31.

Shimokado, K., Raines, E. W., Madtes, D. K., Barrett, T. B., Benditt, E. P., Ross, R. (1985). A significant part of macrophage-derived growth factor consists of at least two forms of PDGF. Cell, *43*, 277-86.

Silverman, T. A., Noguchi, M., Safer, B. (1992). Role of sequences within the first intron in the regulation of expression of eukaryotic initiation factor 2 alpha. J. Biol. Chem., *267*, 9738-42.

Sporn, M. B., Roberts, A. B., Wakefield, L. M., de Crombrugghe, B. (1987). Some recent advances in the chemistry and biology of transforming growth factor-beta. [Review]. J. Cell Biol., *105*, 1039-45.

Sporn, M. B., Roberts, A. B. (1990). TGF-beta: problems and prospects. [Review]. Cell Regulation, *1*, 875-82.

Stryer, L. (1981). Biochemistry, 2nd Edition (2 ed.). New York: W. H. Freeman and Company.

Sudhof, T. C., Goldstein, J. L., Brown, M. S., Russell, D. W. (1985). The LDL receptor gene: a mosaic of exons shared with different proteins. Science, *228*, 815-822.

Suzu, S., Ohtsuki, T., Yanai, N., Takatsu, Z., Kawashima, T., Takaku, F., Nagata, N., Motoyoshi, K. (1992). Identification of a high molecular weight macrophage colony-stimulating factor as a glycosaminoglycan-containing species. J. Biol. Chem., *267*, 4345-4348.

Svensson, L., Heingard, D., Oldberg, A. (1995). Decorin-binding sites for collagen type I are mainly located in leucine-rich repeats 4-5. J. Biol. Chem., *270*, 20712-20716.

Tan, E.M.L., Hoffren, J., Rouda, S., Greenbaum, S., Fox IV, J.W., Moore, Jr, J.H., Dodge, G.R. (1993). Decorin, versican, and biglycan gene expression by keloid and normal dermal fibroblasts: differential regulation by basic fibroblast growth factor. Exp. Cell Res., *209*, 200-207.

Trotter, J. A., Koob, T. J. (1989). Collagen and proteoglycan in a sea urchin ligament with mutable mechanical properties. Cell & Tissue Research, *258*, 527-39.

Tsuji, T., Okada F., Yamaguchi, K., Nakamura, T. (1990). Molecular cloning of the large subunit of transforming growth factor type beta masking protein and expression of the mRNA in various rat tissues. Proc. Natl. Acad. Sci. USA, *87*, 8835-9.

Upholt, W.B., Chandrasekaran, L., Tanzer, M.L. (1994). Molecular cloning and analysis of the protein modules of aggrecans. EXS, *70*, 37-52.

Van Kuppevelt, T. H., Janssen, H. M., van Beuningen, H. M., Cheung, K. S., Schijen, M. M., Kuyper, C. M., Veerkamp, J. H. (1987). Isolation and characterization of a collagen fibril-associated dermatan sulphate proteoglycan from bovine lung. Biochim. Biophys. Acta, *926*, 296-309.

Van Obberghen-Schilling, E., Roche, N. S., Flanders, K. C., Sporn, M. B., Roberts, A. B. (1988). Transforming growth factor beta 1 positively regulates its own expression in normal and transformed cells. J. Biol. Chem., *263*, 7741-6.

Vlodavsky, I., Folkman, J., Sullivan, R., Fridman, R., Ishai-Michaeli, R., Sasse, J., Klagsbrun, M. (1987). Endothelial cell-derived basic fibroblast growth factor: Synthesis and deposition into subendothelial extracellular matrix. Proc. Natl. Acad. Sci. USA, *84*, 2292-2296.

Vogel, K.G., Paulsson, M., Heinegard, D. (1984). Specific inhibition of type I and type II collagen fibrillogenesis by the small proteoglycan of tendon. Biochem. J., *223*, 587-597.

Vogel, K.G., Trotter, J.A. (1987). The effect of proteoglycans on the morphology of collagen fibrils formed in vitro. Collagen Rel. Res., *7*, 105-114.

Wakefield, L. M., Smith D. M., Flanders K. C., Sporn, M. B. (1988). Latent transforming growth factor-beta from human platelets. A high molecular weight complex containing precursor sequences. J. Biol. Chem., *263*, 7646-54.

Westergren-Thorsson, G., Antonsson, P., Malmstrom, A., Heinegard, D., Oldberg, A. (1991). The synthesis of a family of structurally related proteoglycans in fibroblasts is differently regulated by TGF-ß. Matrix, *11*, 177-183.

Westergren-Thorsson, G., Schmidtchen, A., Sarnstrand, B., Fransson, L., Malmstrom, A. (1992). Transforming growth factor-ß induces selective increase of proteoglycan production and changes in the copolymeric structure of dermatan sulphate in human skin fibroblasts. Eur. J. Biochem., *205*, 277-286.

Westergren-Thorsson, G., Hernnas, J., Sarnstrand, B., Oldberg, A., Heinegard, D., Malmstrom, A. (1993). Altered expression of small proteoglycans, collagen, and transforming growth factor-$ß_1$ in developing bleomycin-induced pulmonary fibrosis in rats. J. Clin. Invest., *92*, 632-637.

Wight, T.N., Mecham, R.P., (Ed.). (1987). Biology of the Proteoglycans. Orlando, Florida: Academic Press, Inc.

Wilcox, J. N. (1993). Fundamental principles of in situ hybridization. J. Histochem. Cytochem., *41*, 1725-33.

Wrana, J. L., Attisano, L., Wieser, R., Ventura, F., Massague, J. (1994). Mechanism of activation of the TGF-beta receptor. Nature, *370*, 341-7.

Yamaguchi, Y., Ruoslahti, E. (1988). Expression of human proteoglycan in Chinese hamster ovary cells inhibits cell proliferation. Nature, *336*, 244-246.

Yamaguchi, Y., Mann, D.M., Ruoslahti, E. (1990). Negative regulation of transforming growth factor-ß by the proteoglycan decorin. Nature, *346*, 281-284.

Yanagishita, M. (1994). A brief history of proteoglycans. EXS, *70*, 3-7.

Yeo, T-K., Brown, L., Dvorak, H. F. (1991). Alterations in proteoglycan synthesis common to healing wounds and tumors. Am. J. Path., *138*, 1437-1450.

Zimmermann, D.R., Dours-Zimmerman, M.T., Schubert, M., Bruckner-Tuderman, L. (1994). Versican is expressed in the proliferating zone in the epidermis and in association with the elastic network of the dermis. J. Cell Biol., *124*, 817-825.

Zimmermann, D. R. and Ruoslahti, E. (1989). Multiple domains of the large fibroblast proteoglycan, versican. EMBO Journal, *8*, 2975-2981.